Drug Recovery in Paediatric Tuberculous Meningitis

Mvuwo Phophi Tshavhungwe

(TSHPHO001)

Thesis presented in fulfilment of the requirement for the degree:

Doctor of Philosophy in Neuroscience

in the Division of Paediatric Neurosurgery

UNIVERSITY OF CAPE TOWN

30 December 2023

Supervisor: Prof. Anthony A. Figaji

Co-supervisor: Assoc. Prof. Ursula K. Rohlwink

DECLARATION

I, Phophi Tshavhungwe, hereby declare that the work on which this thesis is based is my original work (except where acknowledgements indicate otherwise) and that neither the whole work nor any part of it has been, is being, or is to be submitted for another degree in this or any other university. I empower the University to reproduce the whole or any portion of the contents for research in any manner whatsoever.

Signature: Signed by candidate Date: 30 December 2023

DEDICATION

To my dad, Itani Z. Tshavhungwe, and late mom, Thivhakoni R. Tshavhungwe, I am empowered to be who I am because of your unwavering love and support.

To fellow Women in Science, who passed away during the last stretch of their PhD journeys: Ms Ndoni Mcunu and Ms Cleopatra Kopaopa. May your bright lights that shone immensely continue to inspire future generations.

ACKNOWLEDGEMENTS

To God Almighty - my sure foundation, thank you for your grace that has carried and sustained me throughout my PhD journey.

To my supervisors, Prof Anthony Figaji and co-supervisor Assoc. Prof. Ursula Rohlwink, infinite thanks for all your thorough project guidance and support. This work would not be possible without your enduring input and encouragement. What a thrilling privilege of a best-of-both-worlds experience!

To the Neurosurgery team: Nico, Ncedile, Sean, Nqobile, Lindizwe, Jill, Lisarae, Christel, Byron, Lizet, Andrew, Dan, Tomson, Rene, Thembani, Jed, Henco, Stefan, Luxwell and students; Nicholas, Joshua, Gabriela, Claudia, Andrew, Rentia and Kate, thanks, for all your support. It's been an absolute pleasure working with such brilliant minds. A special thanks to all the Neurosurgery registrars who helped with most of the patient sampling, my colleague Lindizwe who was my tag team partner for microdialysis monitoring and Jill who was incredibly helpful with the data analysis process and additional analysis for data enrichment of time-linked samples.

To the UCT pharmacology team: Prof. Helen, Assoc. Prof. Lubbe and Prof. Paolo, a tremendous thank you for kindly welcoming me to learn and grow through pharmacology courses in your department and providing expert input for my research project. A special thanks to Noha and Paolo for lending their pharmacometrics expertise. I have deep gratitude for your generous support through my PhD journey.

To Dr. James Nuttall, for his invaluable input during my project's early days.

To Sister Prins for her invaluable input in PK sampling consumables and approach.

To my siblings, sister Phuluso, and my brothers, Rudzani, Hangwelani, Vhutshilo and Mpho, a special thank you for your continued collective support, including finances, prayers, breathing space and encouragement. I am blessed to have kind and thoughtful family, very grateful for you guys.

To all my nephews and nieces, a special thank you for the gift each of you is and for bringing joy and laughter in challenging times. I'm grateful to be your aunt.

To Lewis, a special thank you for all your love and support and for inspiring me through your diligence and determination to keep going. I am very grateful for you.

To Dr. Lloyd for lending fresh eyes to one of my literature review chapters. Thank you for your insightful and kind comments.

To Uncle Alu, thank you for helping me identify gaps in one of my literature review chapters.

To my friend Dr. Caroline, thank you for lending fresh eyes to two of my literature review chapters. your thorough edits are highly appreciated.

I am deeply grateful to all my friends and extended family members for their encouragement. A special thanks to Precious for our long phone calls and catch-ups, which have encouraged me to keep pushing in our PhD journeys.

To the ladies in the lab, Raquel, Wonita and Anthenette. Thank you for your encouraging words and lab chats.

To Noorunisa, thank you for helping me secure a place to stay during the last stretch of my PhD. I am deeply grateful for your kindness.

Many thanks to the nursing staff at Red Cross War Memorial Children's Hospital (RCWMCH)'s intensive care unit for assisting with vial changes by the bedside and to all the clinical staff who alerted me to sample collection times and were helpful in assisting me with patient dosing schedules.

To the Staff at Records office at RCWMCH, thank you for all your help in assisting with patient folders.

To the NHLS team thanks for all your help in assisting with protein analysis of our samples.

Many thanks to Nombeko and Dilshaad at the Institute of Child Health library who were a joy to work with and who provided a serene library space where most of my pre-covid PhD work was done.

Many thanks to Dr. Tanya and Prof. Vivienne whom I met early on in my PhD and who were pivotal in my growth in the field of Neuroscience through opening doors of opportunities.

To my connect/life group mates whom I have had the pleasure of doing life with through my PhD journey, thank you for all your encouraging words and prayers.

To our HOD, Prof. Graham Fieggen, thank you for your encouragement and for opening doors of opportunities to diversify my skills as a student. Grateful for your inclusive and supportive leadership that has enabled me to be myself as I navigate academia.

A tremendous thank you to the Oppenheimer Memorial Trust for your very generous financial support through my PhD journey. You came through in very tight and uncertain times.

To the National Research Foundation, thank you for your generous financial support.

A special thank you to all the patients and parents/guardians at RCWMCH who without them, this project would not be possible.

Isiah 55: 12 (NIV)

You will go out in joy,

And be led forth in peace,

The mountains and hills will burst into song before you,

And all the trees of the field will clap their hands.

ABSTRACT

BACKGROUND Tuberculosis (TB) remains the single leading infectious disease killer across the world. Infection of the central nervous system (CNS) is the most lethal form of the disease. There has been little adjustment to the standard drug regimens over several decades, but there remain many unknowns about their effectiveness, especially because penetration across the blood-brain barrier (BBB) has been difficult to study. Rifampicin (RIF) is a leading drug in the management of TBM but concentrations in ventricular cerebrospinal fluid (VCSF) have not been studied in TBM patients, and emerging evidence suggests that lumbar spinal CSF (LCSF) concentrations of substances may not fully reflect brain concentrations. Finally, there are no data on brain extracellular fluid (ECF) concentrations of TB drugs in humans.

AIMS AND OBJECTIVES The aim was to produce the first pilot data of RIF concentrations in VCSF in children with TBM and to explore the use of microdialysis (MD) to detect RIF in brain ECF. The primary objective was to measure RIF total concentrations in multiple compartments, namely plasma, LCSF, VCSF, and brain ECF. The secondary objectives were 1) to examine RIF concentrations in paired, time-linked L- and VCSF of TBM patients (samples taken at the same time), and 2) to determine total protein concentrations in time-linked L-and VCSF.

METHODS This study prospectively recruited children with definite or probable TBM in a descriptive cross-sectional study design at a university-affiliated paediatric hospital in Cape Town. Patients were treated with standard TB drug regimens. Sampling was performed after standard drug administration. Blood samples were taken from routine procedures or long lines or arterial lines. LCSF was sampled from scheduled clinically indicated procedures. VCSF was accessed from external ventricular drains (EVD) or CSF shunt insertion. In a subgroup of patients, VCSF and LCSF were taken at the same time (usually from clinically indicated column tests). A subgroup of patients underwent bedside MD monitoring of brain chemistry for clinical purposes. Remnant fluid was stored and examined offline for RIF concentrations in brain ECF.

RESULTS A total of 61 children who fulfilled the definition of definite or probable TBM and who had samples analysed for RIF were recruited to the study; the median age was 2.3 years and 7% were human immunodeficiency (HIV) positive. All patients had hydrocephalus (HCP) and most presented in stage 2 and 3. Plasma concentrations peaked at 2 hours (hrs) post-dose while CSF values peaked after 4 hrs. Below level of quantification percentages were 8%, 15%, 16% and 22% respectively for plasma, LCSF,

VCSF, and ECF respectively. The median peak concentration in plasma was 5.2 µg/mL. By comparison, LCSF concentrations at 4 and 6 hrs were 0.23 and 0.14 µg/mL and VCSF concentrations were 0.15 µg/mL and 0.14 µg/mL respectively. CSF concentrations were at most 5% of peak plasma concentrations. RIF was detectable in MD samples (n=74) but showed the lowest concentrations. ECF concentrations ranged from 0.01-0.04 µg/mL. In the first 10 hrs of sampling, brain ECF RIF concentrations were 13-26% of corresponding VCSF concentrations. In a subgroup of patients with time-linked LCSF and VCSF samples (n=28), median RIF concentrations were significantly lower in the VCSF:133 ng/mL (range, 7.40-937 ng/mL) versus LCSF: 299 ng/mL (range, 5-1080 ng/mL) as were protein concentrations: 1.3 g/L (0.17-7.44 g/L) and 6.0 g/L (range, 0.68-51.8 g/L). LCSF showed higher RIF concentrations in 64% of paired samples, and higher protein concentrations in all paired samples. There were no apparent differences in the time-to-peak drug concentrations in the two CSF compartments.

CONCLUSION Our data adds to the limited knowledge of CNS distribution of RIF, an important drug in TBM management. We report RIF concentrations in VCSF for the first time in patients with TBM. Intriguingly, the paired sample analysis shows higher concentrations in LCSF, which may reflect a sump effect or differential permeability in the spinal blood vessels. Given that the current knowledge of RIF in TBM patients is largely based on spinal CSF studies, it is important to note that this may overestimate concentrations in VCSF. We also demonstrated for the first time the capacity to serially sample RIF directly from brain ECF, where concentrations were lower than in VCSF. This may be technical but also may reflect a difference between total and free drug concentrations, given the differential barrier properties of the BBB (former) and the blood-CSF barrier (BCSFB) (latter). This study contributes timely and important data in an era of focus on maximising RIF exposure by increasing drug dosing.

LIST OF ABBREVIATIONS

%	Percent
°C	Degree Celsius
µg	Micrograms
ADIH	Anti-TB drug-induced hepatotoxicity
ADH	Antidiuretic hormone
ADME	Absorption, distribution, metabolism and excretion
AEG	Air encephalogram
AFB	Acid fast bacilli
AIDS	Acquired immune deficiency syndrome
AMK	Amikacin
ANP	Atrial natriuretic peptide
ART	Antiretroviral therapy
ATP	Adenosine triphosphate
AUC	Area under the curve
BBB	Blood-brain barrier
BCA	Bicinchoninic acid
BCG	Bacillus Calmette-Guérin
BCRP	Breast cancer resistance protein
BCSFB	Blood cerebrospinal fluid barrier
BDQ	Bedaquiline
bp	Base pair
BSCB	Blood-spinal cord barrier
Ca	Calcium

CAP	Capreomycin
Cec	Residual calibrator concentration
C_{ECF}	Concentration of brain extracellular fluid
cells/µL	Cells per microlitre
CFZ	Clofazimine
Cic	Concentration of calibrator
CLp	Plasma clearance
Cm	Centimetre
C_{max}	Maximum concentration
CNS	Central nervous system
CommHC	Communicating hydrocephalus
COMT	Catechol-o-methyltransferase
$C_{perfusate}$	Concentration of perfusate
CPP	Cerebral perfusion pressure
CPX	Ciprofloxacin
CS	Cycloserine
CSF	Cerebrospinal fluid
CSWS	Cerebral salt wasting syndrome
CT	Computed Tomography
CYP	Cytochrome
DILI	Drug-induced liver injury
DLM	Delamanid
DNA	Deoxyribonucleic acid
DR	Drug resistance

DUSP	Dual specificity phosphatase
EC	Endothelial cells
ECF	Extracellular fluid
EDTA	Ethylenediaminetetraacetic acid
ELISA	Enzyme-linked immunosorbent assay
EMB	Ethambutol
ESAT	Early secretory antigenic target
ESX	Secretion system 1
ETH	Ethionamide
ETV	Endoscopic third ventriculostomy
EVD	External ventricular drain
FQs	Fluoroquinolones
g/L	Gram per litre
GBP	Guanylate binding protein
GCS	Glasgow coma score
G-CSF	Granulocyte colony-stimulating factor
GFAP	Glial fibrillary acid protein
GFX	Gatifloxacin
GIT	Gastrointestinal tract
GM-CSF	Granulocyte-macrophage colony-stimulating factor
GST	Glutathione-s-transferase
H_20	Water
HCP	Hydrocephalus
HIV	Human Immunodeficiency virus

hrs	hours
IBM	International Business Machines
ICP	Intracranial pressure
IFNγ	Interferon-γ
IL-1β	Interleukin 1-β
INH	Isoniazid
IRIS	Immune reconstitution inflammatory syndrome
IV	Intravenously
K	Potassium
KAN	Kanamycin
kDa	Kilodalton
kg	Kilogram
KLF	Krüppel-like factor
LAM	Lipoarabinomannan
LC-MS/MS	Liquid chromatography-tandem mass spectrometry
LCSF	Lumbar cerebrospinal fluid
LFA	Lateral flow assay
LFX	Levofloxacin
LogP	Logarithm of partition coefficient
LP	Lumbar puncture
LPR	Lactate pyruvate ratio
LZD	Linezolid
M^2	Square metre
MD	Microdialysis

MDR	Multi-drug resistance
Mg	Magnesium
mg	Milligrams
MGIT	Mycobacteria Growth Indicator Tube
MHC	Major histocompatibility complex
MIC	Minimum inhibitory concentration
min	Minute
miRNAs	MicroRNAs
mL	Millilitre
mmol	Millimole
MMPs	Matrix metalloproteinases
MODS	Microscopic observation drug susceptibility
MOX	Moxifloxacin
MPO	Myeloperoxidase
MRC	Medical Research Council
MRI	Magnetic Resonance Imaging
mRNA	Messenger ribonucleic acid
MRP1	Multidrug resistance protein 1
Mtb	*Mycobacterium tuberculosis*
NAATs	Nucleic acid amplification tests
NAT	N-acetyltransferases
NCHC	Non-communicated HCP
ng	Nanograms
NGT	Nasogastric tube

NHLS	National Health Laboratory Service
NLME	nonlinear mixed-effects
nm	Nanometre
NPV	Negative predictive value
OAT	Organic anion transporters
OATP	Organic anion-transporting peptide
OFX	Ofloxacin
ORD	Other respiratory diseases
PAMPs	Pathogen-associated molecular patterns
PAS	Para-aminosalicylic acid
PBMCs	Peripheral blood mononuclear cells
PBPK	Physiologically based pharmacokinetics
PCR	Polymerase chain reaction
PD	Pharmacodynamic
PGLA	Poly (lactic-co-glycolic-acid)
P-gp	P-glycoprotein
pH	Measurement of hydrogen ion concentration
PK	Pharmacokinetics
PKa	A measure of the strength of an acid
PMD	Pretomanid
PPRs	Pattern recognition receptors
PPV	Positive predictive value
PST	Phenol sulfotransferase
PTB	Pulmonary tuberculosis

PTH	Prothionamide
PZA	Pyrazinamide
RIF	Rifampicin
RPHA	Reverse passive hemagglutination immunoassay
rpm	Rates per minute
RR	Relative recovery
RRDR	Rifampicin resistance determining region
SA	South Africa
SAH	Subarachnoid haemorrhage
SARChI	South African Research Chairs Initiative
SIADH	Syndrome of inappropriate antidiuretic hormone
SLC	Solute carrier family
STR	Streptomycin
SULTs	Sulfotransferase
$T_{1/2}$	Half-life
TAZ	Thioacetazone
TB	Tuberculosis
TBI	Traumatic brain injury
TBM	Tuberculous meningitis
TLR	Toll-like receptor
T_{max}	Maximum time
TNFα	Tumour necrosis factor-α
TPP	Target product profile
TRD	Terizidone

UCT	University of Cape Town
UDP	Uridine diphosphate
UGT	Uridine diphosphate-glucuronosyltransferase
ULOQ	Upper limit of quantification
VCSF	Ventricular cerebrospinal fluid
VEGF	Vascular endothelial growth factor
VM	Viral meningitis
VPS	Ventriculoperitoneal shunt
WC	Western Cape
WHO	World Health Organization
XDR	Extensively drug-resistant
ZN	Ziehl-Neelsen

TABLE OF CONTENTS

LIST OF TABLES

Page number

LIST OF FIGURES

Page number

LIST OF APPENDICES

CHAPTER 1: GENERAL INTRODUCTION

In 2021, an estimated 10.6 million people became ill with TB, 1.6 million of these died from TB [1]. This report highlighted an increase in the TB incident rate by 3.6% in 2021 when compared to 2020 partly affected by the COVID-19 pandemic [2]. TBM, the most lethal form of TB, remains one of the most common cause of paediatric bacterial meningitis in the Western Cape (WC), South Africa (SA) [3]. The non-specific symptoms at the early stage of the disease makes it difficult to diagnose and children are usually diagnosed when irreversible neurologic damage has already occurred [4].

Furthermore, HIV co-infection with TBM is associated with mortality approaching 50% [5,6]. Even though the antibiotics used to treat TBM have been available for more than 60 years, there remains limited pharmacokinetics (PK) data in children [7].

Therefore, appropriate treatment regimens that reach the target site of infection are essential. Research on drug recovery of anti-TB drugs has relied on blood and LCSF samples as a surrogate for drug concentrations in the brain. However, the brain ECF is closest to the target site of infection. Hence measurement of this site using MD, a technique that enables continuous sampling of the drug directly in the tissue of interest would provide more useful information [8–10].

Rationale

There is limited knowledge of the distribution and concentration of RIF in the brain. This has important clinical implications for the dosing regimen of this key bactericidal drug. Arguably, brain ECF is closest to the site of disease, and as such MD enables a unique opportunity to examine these concentrations. However, there is also limited knowledge on the penetration of RIF in VCSF, which is closer to the site of disease than LCSF and is known to be different from LCSF. Furthermore, VCSF is more commonly accessible than brain ECF.

Therefore, the primary objective of this research was to measure RIF total concentrations in blood, CSF (lumbar and ventricular) and brain ECF samples in paediatric patients diagnosed with definite or probable TBM. Given that RIF is highly protein-bound, and the total concentration of RIF is routinely measured and reported, the secondary objective was to examine RIF and total protein concentrations in time-linked L- and VCSF.

The thesis is structured as follows:

Chapter 2: begins with the pathogenesis of TBM from primary exposure to the establishment of infection in the brain, followed by intracerebral manifestation of TBM. This chapter gives an overview of TBM as a disease and management thereof and forms the basis for subsequent chapters in this thesis.

Chapter 3: describes the drug target site PK, which includes: the differences between children and adults that need to be taken into consideration when administering drugs and system and drug properties that affect the PK of the drug in the brain. The purpose is to track the drug from oral administration in a dynamic system that is developing, to account for factors that affect the distribution of the drug to the brain, expanding on the complexity of the brain and varying TBM disease severity and introduce implications for the drug reaching the target site and eliciting optimal therapeutic effect.

Chapter 4: Reviews literature on the treatment of TBM in the context of paediatrics with a focus on RIF, an important drug in the treatment of TBM owing to its sterilizing properties and highlights factors that influence the PK of RIF. This chapter also reviews PK literature of anti-TB drugs in systemic circulation and CNS compartments and highlights knowledge gaps in target site PK data and introduces MD as a clinical tool for drug recovery in the brain.

Chapter 5: describes the use of intracerebral MD as a clinical tool for drug recovery. The topics in this chapter include the use of MD as a technique, clinical application of MD with an introduction to markers of secondary brain injury, methodological considerations, the application of MD in PK studies in general, analysis methods of MD samples and a conclusion.

Chapters 6 and 7: describe the methodological approach of the research project and patient admission and clinical characteristics.

Chapter 8: describes the results of patient admission and clinical characteristics and discussion thereof.

Chapter 9: describes PK methods from the collection of samples to analysis and results. Analysis of RIF was done in a stepwise approach. Section A reports overall RIF results across multiple compartments and section B reports time-linked analysis of RIF and total protein.

CHAPTER 2: AN OVERVIEW OF TBM

Pathogenesis of TBM: a brief description

Primary infection

TB is an airborne disease caused by *Mycobacterium tuberculosis* (*Mtb*) bacteria [11]. *Mtb* bacilli are transmitted to a host through an airborne spread of nuclei droplets from an individual with active TB [11]. When an individual inhales *Mtb* bacillus, usually from a host with active pulmonary TB (PTB), it crosses the lung epithelium, resulting in infection of lung alveolar macrophages, neutrophils [12,13] and dendritic cells [14,15].

The mechanisms through which the host mounts an immune response to TB infection is through recognition of the invading pathogen, followed by the activation of innate host immune responses and subsequent initiation of an adaptive immune response [16]. The innate immune response is initiated by pattern recognition of microbial structures known as pathogen-associated molecular patterns (PAMPs) [16]. PAMPs are recognised by germ-line encoded receptors mainly expressed on immune cells called pattern recognition receptors (PPRs) [17]. Therefore, PAMPs of *Mtb* are recognised by specific PRRs of the host, which elicit an immune response, followed by ingestion and killing of mycobacteria [16].

The activated alveolar macrophages, ingest the bacilli, which then reside within their intracellular phagosomes and also initiate an adaptive T-cell immune response [16]. Following development of T-cell immunity, proinflammatory cytokines such as interleukin 1-β (IL-1β), tumour necrosis factor-α (TNFα) and interferon-γ (IFNγ) activate macrophages to kill intracellular bacteria. This results in the formation of granulomas with a caseous necrotic centre [18]. TNFα is important for the formation of granuloma and serves as an important mechanism for containing and restricting the replication of bacilli [18,19]. IL-1β, a cytokine of the IL-1 family, is important, given that IL-1 mediated signals that are essential components of the host defence to mycobacteria [20–22]. IFNγ, secreted by activated T cells and natural killer cells during infection [23], also improves macrophages' expression of major histocompatibility complex (MHC) class II molecules, resulting in improved antigen presentation to T cells [16]. In addition, various receptors have been implicated in the recognition and uptake of *Mtb*, these include: mannose receptors, Toll-like receptor (TLR) 2 and TLR4, surfactant protein A receptors, CD14, scavenger receptors, complement receptors and immunoglobulin receptors [16,24].

Infection with *Mtb* may result in a dormant state in some individuals or progress in the lung and in some cases result in haematogenous spread to distant sites of the body [11,16]. The state in which the *Mtb* remains dormant is referred to as latent infection where the host has no symptoms but the bacteria persist in a non-transmissible form [25]. However, there is a 2-8% probability of reactivation of infection even many years after of primary infection [26]. This could occur as a result of malnutrition,

immunosuppression, steroid use, anti-tumour necrosis factor therapy or HIV infection which initiates a switch to high metabolic activity of bacteria and disease reactivation [25,27]. Aside from latent infection, two additional TB disease states have been proposed, namely incipient TB and subclinical TB [28]. Incipient TB is defined as an infection with *Mtb* that is likely to progress to active disease in the absence of further intervention but has not yet caused clinical symptoms, radiographical abnormalities, or microbiologic evidence of active TB disease [28]. Subclinical TB is defined as disease owing to viable *Mtb* bacteria that does not cause clinical TB-related symptoms but causes other abnormalities that are detectable using radiological and microbiological assays [28]. These proposed definitions of disease states are to aid in dividing active and latent TB along the clinical disease spectrum [28].

In approximately 20-50% of individuals exposed to TB bacilli, the bacteria can override the innate immune response resulting in multiplication of bacteria in alveolar macrophages, dendritic cells, epithelial cells and interstitial macrophages (19, 20). The bacteria within the macrophages have been shown to spread from cell to cell through the apoptosis of macrophages resulting from the secretion system 1 (ESX-1) type VII also known as early secretory antigenic target (ESAT6) secretion system [31–33]. In mycobacteria, ESX systems function as specialised secretion systems that enable the transport of selected substrates across complex mycobacterial cell envelope that form a structural barrier to protein transport [34]. Thereafter, the high burden of mycobacteria at the primary site of infection can spread to other parts of the body such as the CNS, infecting different cells through lymphatics and the bloodstream [26].

CNS infection

The brain is separated from peripheral blood circulation by the blood-brain barrier (BBB) and the brain-cerebrospinal fluid barrier (BCSFB) [35–37]. The BBB is composed of microvascular endothelial cells with tight junctions lining the walls of blood vessels and is responsible for protecting the brain from toxins and pathogens present in systemic circulation [36,38]. In contrast, the BCSFB is a monolayer of epithelial cells consisting of tight junctions at the vascularised choroid plexus where CSF is produced [39]. This BCSFB also prevents entry of exogenous and some endogenous compounds [39].

Modification of the BBB resulting from infection of brain tissue by TB bacteria may cause leakage of both exogenous and endogenous substances, including proteins into the ECF. Vascular endothelial growth factor (VEGF), a 46-kDa glycosylated homodimeric protein, is a potent inducer of vascular permeability and angiogenesis, and has been implicated in disruption of the BBB following TBM [40]. Inhibition of VEGF has been suggested to result from adjuvant corticosteroid therapy that is normally administered in TBM treatment [40,41] .

Furthermore, Matrix metalloproteinases (MMPs) which include MMP-2 and MMP-9 which are upregulated in TBM, have been implicated in the disruption of BBB and BCSFB through breakdown of the extracellular matrix that constitutes the barriers [42]. MMPs are an enzyme family of zinc-dependent endopeptidases responsible for the degradation of the extracellular matrix [43]. The influx of serum proteins into the brain through a leaky BBB may result in seizure activity, activation of glia, and cell damage [44,45]. Crossing of albumin from plasma into the brain has been associated with astrocytic activation, activation of the innate immune system and modification of brain networks leading to epilepsy [46,47]. Brain barriers will be discussed in more detail in chapter 3.

CNS inflammatory response

Historically it has been suggested that the haematogenous spread of *Mtb* into the brain results in the formation of a sub-pial granuloma named Rich focus [48]. The Rich focus was described by Arnold Rich and Howard McCordock based on clinical and experimental observations in rabbits and guinea pigs and also post-mortem dissections in children [48]. Findings from Rich and McCordock have been revisited to describe the close association between TBM pathogenesis and miliary TB [49]. The rupture of the Rich focus releases *Mtb* in the subarachnoid space enabling the spread of bacilli in the CSF and the manifestation of basal meningitis [50,51]. Meningitis in children usually occurs as part of this disseminated primary disease rather than a later reactivation [52]. As such, the time from primary infection to onset of TBM is less than 12 months in 75% of children [53]. This process of disease dissemination is graphically represented in Figure 2.5. Infected macrophages and neutrophils have also been implicated in disseminating *Mtb* through the choroid plexus via a trojan horse mechanism whereby pathogenic mycobacteria utilize several strategies to avoid lysosomal delivery ensuring their intracellular survival [54].

Microglia

Microglia are often referred to as the brain's resident macrophages [11]. They serve as the brain's main line of defence past the BBB and play an important role in the immune response and regulation in the CNS [14,55]. Microglia are the main CNS cells infected by *Mtb* [56–58]. Once activated, microglia can destroy invading microorganisms, remove potentially harmful debris, and promote tissue repair by removing growth factors and enabling the return of tissue homeostasis [59].

When an individual develops TBM, activation of microglia leads to a release of several proinflammatory cytokines (TNF-α, INF-γ and IL-6) and chemokines. These cytokines are important in the host defence towards infection with *Mtb* but also mediate inflammation [14]. TNF has been implicated in contributing, in part to the extent of disease pathogenesis in TBM [60]. Studies have also highlighted other cytokines released by microglia following *Mtb* stimulation, these include IL-1α, IL-

10, IL12p40, granulocyte colony-stimulating factor (G-CSF), and granulocyte-macrophage colony-stimulating factor (GM-CSF) [61,62].

CNS pathology of TBM

Exudate

TBM infection leads to formation of a thick exudate at the base of the brain (Figure 2.1) [63]. This exudate can extend to the basal cisterns, sylvian fissure, brain stem and cerebellum [63]. The exudate is characterised by a thick gelatinous consistency and consists of polymorphonuclear leukocytes, macrophages, lymphocytes and erythrocytes with increasing quantities of fibrin [64]. Inflammatory exudate can also extend to the subarachnoid space around the spine and can surround the spinal roots (Figure 2.4) [64,65]. Brain tissue underlying tuberculous exudate has been shown to display varying degrees of oedema, perivascular infiltration and a microglial response process known as border-zone encephalitis [63]. This thick gelatinous inflammatory exudate disturbs the normal flow of CSF resulting in HCP and consequent raised intracranial pressure (ICP) [63].

HCP

Exudate may spread to the lateral ventricles resulting in blockage in the flow of CSF at the cerebral aqueduct or the outflow of CSF at the fourth ventricle. This blockage in brain compartments results in the accumulation of CSF known as HCP (Figure 2.2) [52]. HCP commonly occurs in 75-80% of TBM patients [66–68]. In addition, the outward pressure imposed by expanding ventricles and the opposite pressure of brain oedema owing to TBM pathological processes can have implications on the grey and white matter, resulting in pallor and diffuse loss of myelin [64].

Vasculitis and cranial nerve palsies

Exudate also causes inflammation of the small and large blood vessels in the brain; also known as vasculitis. Vasculitis may eventually lead to cerebral ischaemia, resulting in infarction (Figure 2.3) [69]. The blood vessels involved include the blood vessels of the circle of Willis: most commonly the middle cerebral artery and its perforating vessels to the basal ganglia [66,69–72]. Exudate in the interpeduncular cistern can compromise the vessels supplying the hypothalamic region and precipitate hypothalamic symptoms in these patients [65]. Other common sites of infarction include the thalami and brainstem [73]. The dense basal exudate around the base of the brain can affect cranial nerves, particularly II, III, IV and VI resulting in cranial nerve palsies [69,74].

Tuberculomas

Intracranial tuberculomas are described as lesions that are typically granulomatous and consist of a necrotic centre surrounded by epithelial cells, lymphocytes, and a border of astrocytes [75]. They commonly develop as solitary lesions but multiple tuberculomas are also seen [11,76–79]. Tuberculomas are associated with peripheral oedema and vascular proliferation (Figure 2.5) [64]. They may occur in various parts of the brain including the cerebrum, cerebellum and the brain stem [64,66]. Tuberculomas are predominantly found in infratentorial regions in children in contrast to supratentorial regions in adults [80,81]. They may develop early on or late during TBM treatment, highlighting the importance of follow-up brain imaging during the treatment course [66,82–85]. Rare cases of development of tuberculomas after anti-TB treatment have been described [86].

A less frequent occurrence is the formation of TB brain abscesses [87] which may occur from TBM or develop independently [88,89]. TB brain abscesses have been reported in the cerebrum [87,89], posterior fossa [89–91] and less commonly in the brain stem [88].

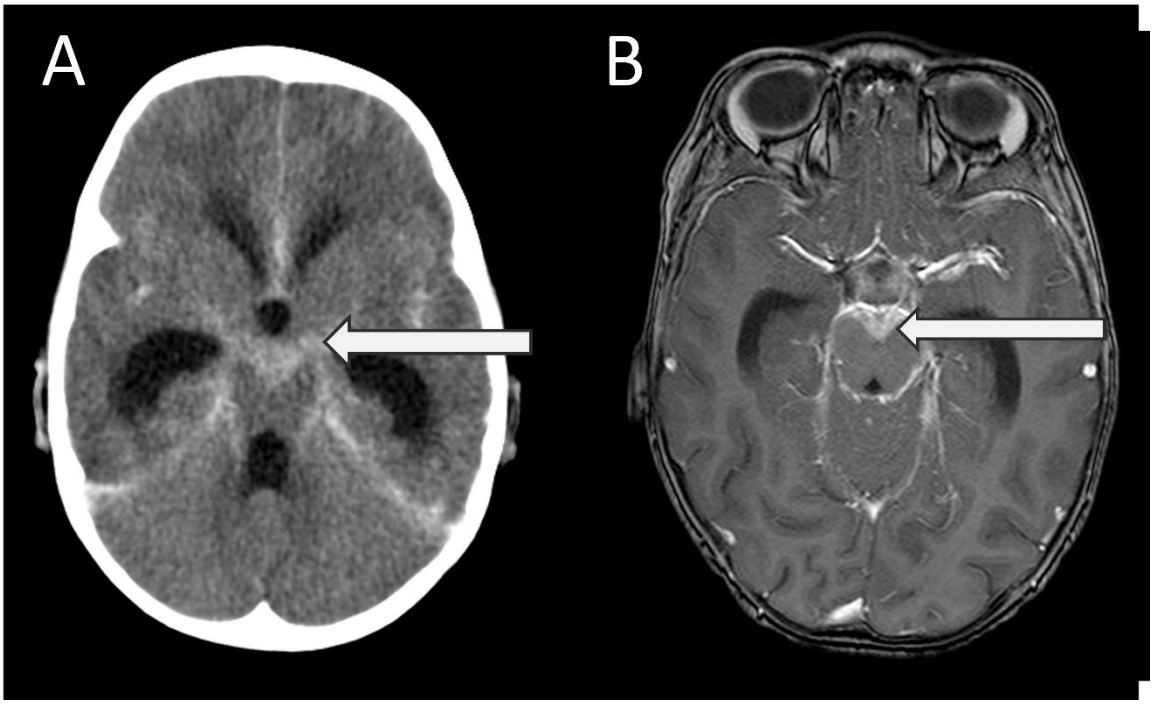

Figure 2.1. Demonstration of exudate in the basal cisterns in TBM. A contrast-enhanced head CT scan; B, contrast-enhanced T1 MRI. The arrows point to the exudate in the interpeduncular and ambient cisterns around the midbrain.

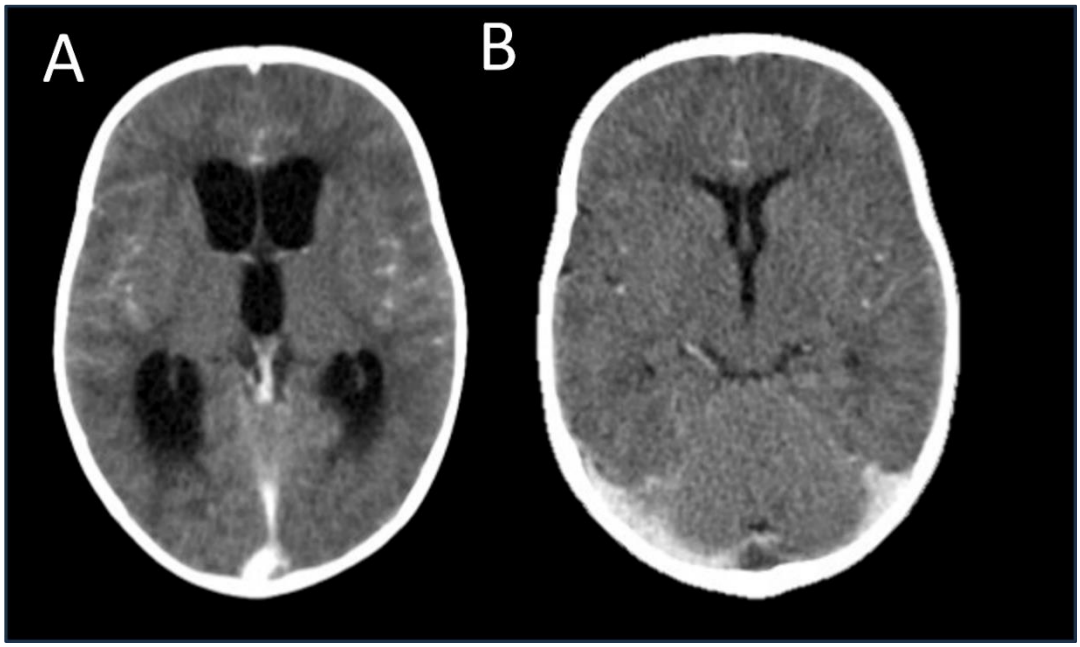

Figure 2.2. Demonstration of hydrocephalus and resolution. A CT scan of a patient with TBM on admission demonstrating hydrocephalus. B, CT scan of the same patient showing resolution of hydrocephalus after successful medical management.

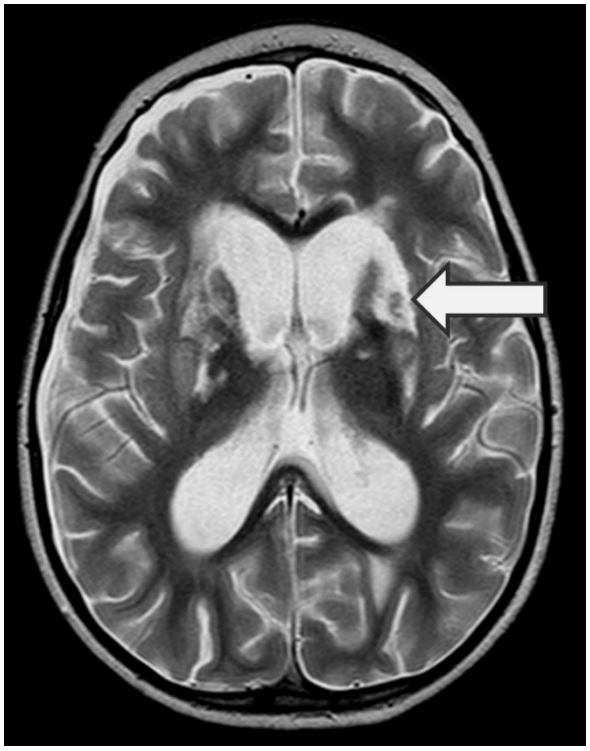

Figure 2.3. Cerebral infarction in TBM: T2 MRI scan image showing ventriculomegaly with atrophy and infarction in the basal ganglia (arrowed).

Spinal TB

TB may manifest in the spine as a result of a primary tuberculous lesion or the intracranial spread of TBM to the spine or secondary to vertebral TB infection [64,92,93]. Spinal TB involves the spinal cord, meninges and nerve roots and manifests as spinal arachnoiditis, intradural (extramedullary) tuberculomas, or rarely as intramedullary tuberculomas [66,94–96]. Exudate that accumulates in the lower lumbar segments of the spine causes difficulty in performing LP and correlates with high CSF protein levels (Figure 2.4) [64,66]. A study in a paediatric TBM cohort, found spinal pathology in 76% of patients, highlighting common occurrence and implications for diagnosis and treatment [66]. Pathology in TBM is summarised in Figure 2.5.

Figure 2.4. T1 with contrast MRI showing enhancement of cord and nerve roots with exudate in the lumbar subarachnoid space (arrowed) in a patient with TBM.

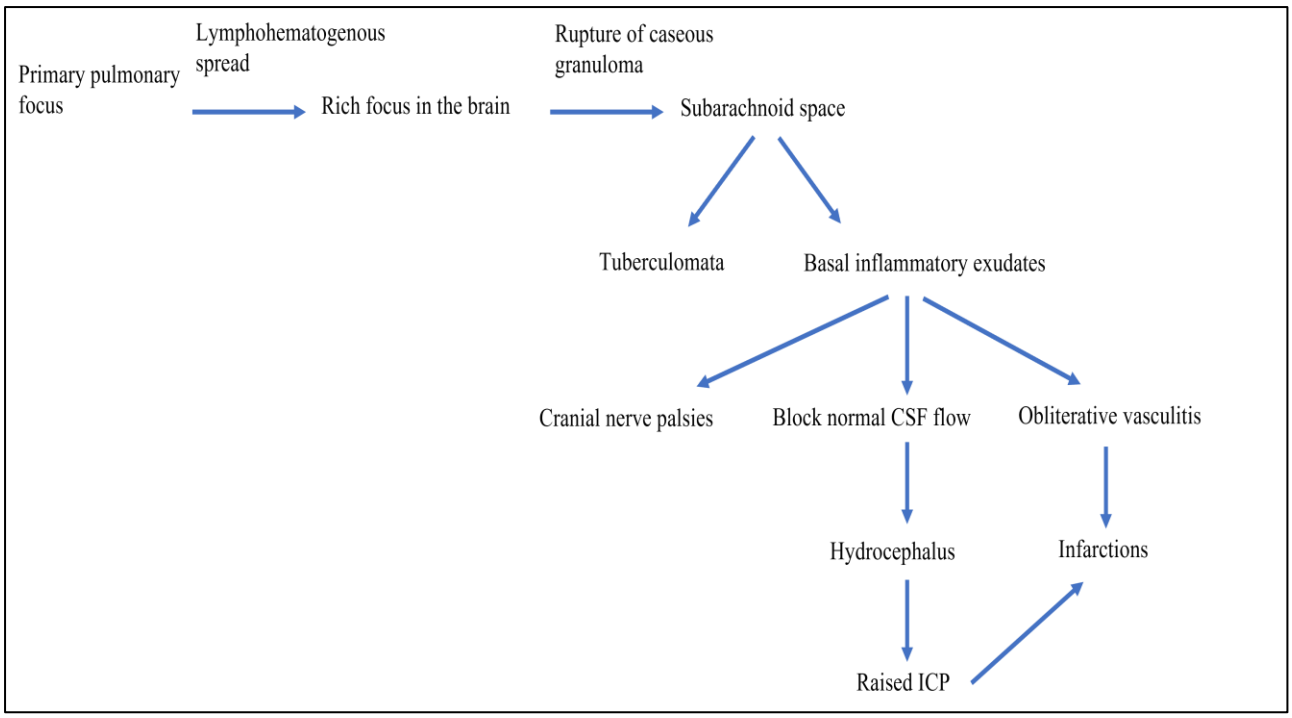

Figure 2.5. Summary of pathology of TBM

Epidemiology of TBM in the WC, South Africa

An increase in the number of people infected with TB and rising drug resistance to TB treatment has led to higher reports of TBM, especially in geographical areas with existing high TB prevalence [53]. A distinguishing feature of TBM in populations with high TB prevalence is the age group. In these populations, TB occurs most commonly in children aged 0-4 years [67,97]. TB incidence at young ages (<5 years) has been predicted to make up 58% of the total paediatric TB with 25% having extrapulmonary TB [98].

BCG vaccination

Bacillus Calmette-Guérin (BCG), an attenuated strain of *Mycobacterium bovis* is the currently available vaccine against TB. However, vaccination with BCG only has a protective effect of 64% against TBM [99]. BCG vaccine is given in most high TB burden countries immediately after birth as recommended by the World Health Organization (WHO) [100]. From 2013, the global supply of BCG was limited, this affected the WC province of SA from 2015 [101]. This resulted in a significant increase in the number of admissions due to TBM, from a mean of 32.7 in 2014-2016 to 70 in 2017. Furthermore, over a period of 10 years, the lowest median age (2.2 years) of children with TBM was observed in 2017 [102].

New vaccines are required to enhance the protective effect against TB [31,103–107]. A phase II clinical trial suggested that revaccination with BCG in adolescents can enhance protection from *Mtb* infection

by reducing the rate of sustained QuantiFERON-TB Gold In-tube assay conversion, with an efficacy of 45.4% [108]. Another study, an ongoing phase IIb controlled trial conducted in adults from SA, Kenya and Zambia, showed that candidate vaccine M72/AS01$_E$ provides protection against progression to bacteriologically confirmed pulmonary active disease in *Mtb-infected* adults by 54.0% [109]. Furthermore, a subsequent final analysis of the phase IIb controlled trial showed that the M72/AS01$_E$ vaccine provides protection against progression to active TB for at least 3 years, with an efficacy of 49.7% at month 36 [110].

TBM diagnostic criteria

The International TBM Consortium developed a consensus statement providing diagnostic criteria for case definition of TBM [111]. This uniform case definition breaks down TBM patients into 4 diagnostic categories based on a combined score of clinical findings, CSF findings, neuroimaging, evidence of TB elsewhere, and exclusion of an alternative diagnosis [111]. As such, patients are classified as, definite, probable, possible and not TBM (see Appendix 3) [111].

A definite diagnosis of TBM is through detection of *Mtb* from CSF through culture, acid-fast bacilli (AFB) smear in CSF or detection of *Mtb* using molecular-based tests including Xpert MTB/RIF® assay (Xpert; Cepheid, Sunnyvale CA, USA) [111,112]. In addition, a definite diagnosis can also be made if AFB is seen in the context of histological changes consistent with TB in the brain or spinal cord in combination with suggestive symptoms and signs and CSF changes and visible meningitis (on autopsy) [111].

The diagnosis of possible or probable TBM is determined by a diagnostic scoring system that requires a combination of symptoms or signs indicative of meningitis plus clinical, CSF or imaging criteria with exclusion of the most likely alternative diagnoses [111].

Clinical findings

Clinical Presentation

Children infected with TBM present with non-specific symptoms which make it difficult to diagnose [113]. Symptoms include cough, fever, failure to thrive, irritability and fatigue which may be followed by loss of consciousness and focal neurological signs [114]. Children are often diagnosed when brain damage has already occurred [115]. Furthermore, younger children (less than 3 years of age) are more likely than older children and adults to develop TBM [116].

Glasgow Coma Scale

The Glasgow Coma Scale (GCS) is used to measure the level of consciousness in children with TBM and determine the severity of disease. Visual (fixation and following), motor (localisation to pain) and verbal responses contribute to the GCS scoring [115,117].

British Medical Research Council staging

The British Medical Research Council (MRC) staging is used to evaluate the severity of disease and may be associated with the prognosis of TBM [118]. The British MRC scale uses GCS scores to define level of consciousness by categorising patients into three clinical stages, 1 to 3, where Stage 1: GCS 15 without focal neurological deficit, stage 2: GCS 10-14, with or without neurological deficits or GCS 15 with neurological deficit and stage 3: GCS less than 10, with or without neurological deficits [117]. When used to evaluate patients 1 week after admission, this staging system has been shown to be strongly associated with neurological outcomes after 6 months of treatment [117]. The 'refined' MRC staging divided stage 2 into stages 2a and 2b (Table 2.1) [117].

Table 2.1. **'Refined' MRC classification of TBM severity** [117]**.**

'Refined' MRC staging	Description
Stage 1	GCS 15/15 without focal neurological deficit
Stage 2a	GCS 15/15 with neurological deficit or GCS 13-14 with or without neurological deficit
Stage 2b	GCS 10-12 with or without focal neurological deficit
Stage 3	GCS < 10 with or without focal neurological deficit

Cerebral imaging findings

Imaging plays an important role in establishing the presumptive diagnosis in combination with patient history, clinical examination and CSF findings [66,111,119]. Typical radiological features include basal and leptomeningeal enhancement, infarcts (often in the basal ganglia), HCP, tuberculomas and rarely TB abscesses [119]. Spinal disease from TBM occurs commonly in children, highlighting the value of spinal imaging in patients suspected of spinal arachnoiditis [66].

CSF findings

CSF analysis in TBM

LCSF from a lumbar puncture (LP) is predominantly used for clinical and research purposes.

CSF findings in healthy individuals has a lower concentration of protein, glucose and potassium, and a higher concentration of chloride compared to plasma. A deviation in the age-dependent reference range of biochemical values indicates pathology in the brain. CSF is an ultrafiltrate of blood partly produced by the choroid plexus [120]. It has been suggested that a reduction in CSF flow rate will result in an increase in CSF protein concentration such as albumin due to decreased volume turnover without changes in BCSFB and related structures [121].

Raised CSF protein and decreased glucose are commonly reported in TBM cases [122,123]. Furthermore, leukocytosis with lymphocyte predominance is found in TBM CSF analysis [124]. Approximately 80% of CSF parameters of children diagnosed with TBM had a predominance of lymphocytes, elevated protein and reduced glucose concentrations [125].

Previous studies done in adult patients with TBM have shown that CSF changes normalise over time with varying rates ranging from 1-32 months [114]. CSF glucose normalises rapidly [126] in contrast to lymphocytes and protein that gradually change [53]. CSF neutrophils also normalise rapidly [122,127,128]. A study in children diagnosed with TBM reported serial LCSF parameters showing a steady decline in lymphocyte and protein count and a rapid decrease in neutrophil count and CSF glucose concentration which is similar to previous reports in adults [129]. In contrast, a group of paediatric patients with TBM displayed atypical findings of median CSF increase in lymphocytes, neutrophils and protein in the first week [129]. Therefore, the authors concluded that the optimal timing for repeat CSF analysis to differentiate persistently high protein in TBM from other forms of meningitis in the absence of clinical, radiologic and microbiologic features, is two weeks post-admission [129].

Atypical CSF findings have also been reported in definite TBM cases (n=47), in a high HIV prevalence setting which includes, polymorphonuclear cell predominance >50 % (in 13% of patients), glucose >2.2 mmol/L (28%), protein concentration of less or equal to 0.45 g/L (6%) and a total leukocyte count of five or less cells/μL (4%) [130]. Furthermore, atypical CSF findings have also been reported for both HIV positive and HIV negative patients including normal CSF glucose, protein, cell count, or neutrophil predominance [78,131–135]. These studies highlight that a deviation from what is expected in CSF chemistry in TBM patients does not rule out TBM and other features should be considered where available to distinguish TBM from other forms of bacterial meningitis.

L- and VCSF in CNS infections

Notable differences in the composition between L- and V-CSF have been observed in CNS infections showing higher levels of LCSF protein and leukocytes as compared to VCSF and lower glucose in both compartments compared to a healthy non-infected individual [136–138]. A study in experimental pneumococcal meningitis showed that decreased glucose concentrations were accompanied by a markedly increased CSF lactate [139]. Case studies in children diagnosed with TBM have reported discrepancies between L- and V-CSF biochemistry and cell count [140,141]. VCSF often has fewer cells and less protein; therefore, if only a VCSF sample is analysed (as when a patient undergoes an EVD placement as the first procedure), one should be cautious about ruling out TBM if the CSF result is not in keeping with the diagnostic criteria.

Conversely, a study by Kamat *et al*., reported that there were no statistical differences in mean protein concentrations between V- and L-CSF compartments, 2.471 g/L and 2.474 g/L respectively from a group of TBM patients (children and adults) who had ventriculoperitoneal shunt (VPS) obstruction [142]. However, this study did not examine time-linked paired L- and V-CSF samples in the same patients and reported means instead of medians, the latter would likely provide a clearer demonstration of central tendency given the anticipated non-parametric distribution of the data [143].

Therefore, there are contrasting arguments of whether there are differences in i.e. protein concentrations in V- compared to L-CSF in a TBM infected brain. A correspondence by Figaji *et al*. cautioned against suggesting that lumbar can be used as a proxy for VCSF [143]. Furthermore, there is increasing evidence from protein, inflammatory mediator, and transcriptomic data that show that LCSF and VCSF are different [144,145], in part perhaps because of the frequency of spinal disease in TBM patients that may affect CSF dynamics [66] as well as structural differences between the blood-brain versus blood-spinal barriers. Protein dynamics in CNS compartments is discussed in detail in chapter 3.

TBM diagnostic tests

Conventional microbiological tests

Culture, microscopy and Ziehl-Neelsen staining

Diagnosis of TBM is difficult owing to the paucibacillary nature of the disease [112]. Conventional tests to diagnose TBM include Ziehl-Neelsen (ZN) microscopy and culture techniques which have been used as gold standards [146]. Microscopy is based on isolation of *Mtb* bacterium in CSF and presence of AFB confirms disease [11]. However, sensitivity on microscopy for detection of *Mtb* is poor (approximately 10-20%) [147–149]. Mycobacterial culture has a higher sensitivity (50-60%) for diagnosis of TBM but the turn-around time is too slow ≥ 8 weeks, particularly on solid media such as

Lowenstein-Jensen [53,150]. However automated systems such as Bactec Mycobacteria Growth Indicator Tube (MGIT) 960 have improved time to yield results with a mean of 18 days [151]. Furthermore, other methods for detection of *Mtb* in liquid culture, such as the microscopic observation drug susceptibility (MODS) assay have been investigated for the diagnosis of TBM [152]. MODS uses microscopy to detect the early *Mtb-specific* 'cords' of bacterial growth and was found to have a sensitivity of 64.9% with a rapid median time to positivity of 6 days when tested on CSF [152].

Mtb yield of culture has been found to be lower in HIV positive TBM patients when compared to HIV negative patients ($P<0.01$) [146]. However, use of large volumes (10-20 mL) of CSF has been reported to increase the detection rate of TBM bacteria [153]. However, this further depends on the quality of the specimen and the skill and persistence of the lab technician in detection of AFB. This finding is supported by a study done in 1953 that detected AFB in 91 of 100 cases through meticulous microscopy and culture, where large volumes of CSF (10-20 ml) were sampled and centrifuged at a high speed [154]. These were all subsequently confirmed by culture [154]. Similar findings have been reported, where AFB was found in the CSF of 45 of 52 (87%) patients undergoing TBM treatment [155]. A study in 132 consecutive adults with TBM found AFB in CSF of 77 (58%) cases and AFB were cultured in 94 (71%) of cases, using the high CSF volume and high-speed CSF processing approach [156]. As such, these studies highlight that sampling high volume of CSF and centrifugation at a high speed with careful identification of AFB can improve diagnostic yield to confirm TBM, although not practical in most laboratory settings.

Molecular assays

Amplification of mycobacterial deoxyribonucleic acid (DNA) using polymerase chain reaction (PCR) known as nucleic acid amplification tests (NAATs) have rapidly improved TB diagnostics [157]. Use of *Mtb* complex repetitive element, IS*6110* insertion sequence has been reported, with improved sensitivity and specificity [158,159]. In-house IS*6110*-PCR showed a higher sensitivity (64%) when compared to microscopy and culture in suspected adult TBM patients, in Indonesia [146]. However, these tests have not been assessed in wider geographical settings and would be costly to implement in resource-limited settings. A systemic review and meta-analysis on NAATs reported an overall pooled sensitivity of 82% and specificity of 99% against culture and a pooled sensitivity and specificity of 68% and 98% respectively, against a combined reference standard [160]. Other potential NAATs for TBM diagnosis include but are not limited to, the loop-mediated isothermal amplification with a sensitivity between 88-96% and specificity of 80-100% [161,162], the commercially available Amplicor TB PCR test which has a sensitivity of approximately 40% and specificity of approximately 90-100% [163] and the Gen-probe amplified *M. tuberculosis* direct test with a pooled sensitivity of 86% and specificity of 99% when tested on CSF samples [160]. Whilst NAATs have improved diagnosis, more data on the performance of these tests in diagnosis of paediatric TBM is still required [164].

Xpert® MTB/RIF and Xpert MTB/RIF Ultra

Xpert which is endorsed by WHO, has shown improvement in TB diagnosis in some settings with sensitivities of about 60% and close to 100% specificity [149,165,166], although the lack of a standardised pre-treatment of samples has been reported [157,167,168]. Xpert is a cartridge-based assay, based on real-time automated PCR test for the detection of *Mtb* in clinical specimens and also detects mutations associated with RIF resistance within 2 hrs [169].

To improve analytical sensitivity for *Mtb* detection and RIF resistance, a new fully automated and PCR-based Xpert® MTB/RIF Ultra (Ultra; Cepheid) was introduced for the Xpert platform [170]. A Ugandan study in 129 HIV infected adults with suspected TBM reported sensitivity of 70% (47-87) using Ultra, 43% (23-66) using Xpert and 43% (22-66) using culture, suggesting that Ultra could improve the diagnosis of TBM [169]. Findings from two further studies in Uganda and Vietnam are summarised in (Table 2.2) [147,171]. Both studies show that Ultra is slightly more sensitive, particularly in HIV uninfected participants [171]. Another study in adults with TBM reported a sensitivity of 70% using Ultra vs 43% as compared to either Xpert or culture [169]. Furthermore, Ultra diagnosed TBM in HIV infected adults with a sensitivity of 95% when compared to either Xpert or culture [169]. Recently, a study in India assessed the performance of Xpert vs Ultra in a paediatric cohort, the latter showed higher sensitivity (18% vs 50%) and higher negative predictive value (NPV) (99% vs 93%) when compared to Xpert. These findings highlight Ultra as a potential diagnostic tool to improve paediatric TBM diagnosis [172]. As such, given the higher sensitivity when compared to Xpert and culture, the WHO has recommended Ultra as an initial test for TBM [173]. Though Xpert improves TBM diagnosis, an expert consensus review cautioned against using Xpert as a sole diagnostic test as this may lead to missed TBM cases [149] and deaths [174]. Furthermore, a negative Xpert result does not rule out TBM [174].

New diagnostic tools

A recent study did a comparative analysis of Truenat™ (Truenat; Molbio Diagnostics, Verna, India) vs Ultra for TBM diagnosis [175]. Truenat is a portable, battery-operated, semi-automated chip-based PCR assay that is operable in tropical climates and can detect *Mtb* in approximately 1 hr and test for RIF resistance in another 1 hr [175,176]. Findings showed Ultra to be comparable to Truenat, with an overall sensitivity of (67.6% vs 78.7%) respectively in TBM diagnosis [175]. However, Truenat was poor in determining RIF resistance [175]. Whilst Truenat is a promising tool, more studies in wider geographical settings are required to validate those findings.

Table 2.2. Xpert® platform diagnostic sensitivity in Uganda [147] **compared to Vietnam** [171]

	Uganda	**Vietnam**
Number of participants	204	205
Total number of TBM cases	42	99
Percentage (%) with HIV	96%	15%
Xpert® MTB/RIF Ultra (sensitivity)	77% (63-87)	58% (43-72)
Xpert® MTB/RIF (sensitivity)	56% (44-70)	48% (35-63)

Immunoassays

Various immunoassays have emerged such as hemagglutination [177], Enzyme-linked immunosorbent assay (ELISA) [178], and T cell-based gamma-interferon release assay [179,180]. These assays enable detection of foreign markers known as antigens or release of host antibodies in response to antigens. A study by Thwaites *et al*. has argued on the detection of antibodies as it proves difficult to distinguish if infection is recent or recurrent [53]. To improve differential diagnosis in TBM, a study assessed detection of circulating mycobacterial antigens in CSF of TBM patients using a reverse passive hemagglutination (RPHA) immunoassay and circulating mycobacterial antigens characterized by immunoblot assay [177]. RPHA was able to detect mycobacterial antigens in CSF at a sensitivity of 94.11% and a specificity of 99.0% and the presence of antigens of masses 30-32 kDa, 71 kDa and 120 kDa were detected compared to controls through Western Blotting, suggesting a potential diagnostic marker for TBM [177].

Detection of lipoarabinomannan using lateral flow assay

Shortcomings of molecular-based tests have led to the investigation of *Mtb* glycolipid lipoarabinomannan (LAM) as a diagnostic marker in CSF [181]. A study in a Zambian adult TBM population showed potential use of a lateral flow assay (LFA) for detection of CSF LAM as a TBM diagnostic tool and found a low sensitivity of 21.9% and specificity of 94.2% [181]. LAM detection by LFA was compared to LAM detection by ELISA and Xpert in CSF from a cohort of 91 adults diagnosed with TBM and HIV co-infection, a sensitivity of 75%, 43% and 100% was reported respectively [182]. These studies highlighted the potential use of LAM LFA as a TBM diagnostic assay.

Adenosine deaminase in CSF

Determination of adenosine deaminase, an enzyme implicated in pathology that induces a T-cell immune response has been suggested as a TBM diagnostic tool [183,184]. A metanalysis has reported a pooled sensitivity of 89% and a specificity of 91% in diagnosis of TBM using an ADA test [185]. However, the enzyme is reportedly upregulated in various CNS pathologies making it non-specific for TBM [186–188].

Biomarker-based approaches

The WHO has recommended a rapid biomarker-based non-sputum test for the diagnosis of extrapulmonary TB with a target product profile (TTP) in adult patients with a sensitivity of at least 80% and specificity of 98% [189]. As such, various biomarkers have been investigated to improve diagnosis of TBM. Biomarker-based TBM diagnostic tools measure host markers (protein concentrations in biological fluids, transcriptional molecules, and metabolites) as potential biomarkers for TBM [164].

CSF host inflammatory biomarker-based studies

A study in a paediatric cohort in SA identified a specific 3-marker host protein biosignature for TBM comprising IL-13, VEGF and cathelicidin LL-37 with a sensitivity of 52%, specificity of 95%, positive predictive value (PPV) of 91.0% and NPV of 66.0% when compared to other types of meningitis [190]. Subsequently, the previously reported 3-marker biosignature was evaluated plus potential host biomarkers as candidates for TBM diagnosis [191]. Validation of the 3-marker biosignature improved accuracy to a sensitivity of 91.3% (21/23) and up to 100% specificity (24/24) when IL-13 and LL-37 were substituted with INF-γ and myeloperoxidase (MPO) [191]. Furthermore, a potential alternative 4-marker biosignature was also identified (ICAM-1, MPO, IL-8 and IFN-γ [191]. A follow-up study validated the previously identified CSF host 3-marker (VEGF-A, IFN-γ and MPO) and 4-marker (IFN-γ, MPO, ICAM-1 and IL8) protein biomarkers which showed TBM diagnostic potential with a sensitivity of 80.6% and specificity of 86.8% and sensitivity 81.6% of and specificity of 83.7% respectively [192]. The study also identified a new biomarker signature (CC4b, CC4, procalcitonin, and CCL1) which showed potential with an area under the curve (AUC) of 0.98 [192]. A potential 3-marker signature (adipsin, Aβ42, and IL-10) has also been identified in the blood of children with TBM with a sensitivity of 82.6% and specificity of 75.0% [193]. These findings show the potential use of host markers as diagnostic candidates in children with TBM.

Host transcriptional biomarker-based signatures

A transcriptomics approach quantifies shifts in RNA abundance triggered by disease and could help in identifying, diagnostic, disease-associated, and treatment response biomarkers [164]. A study looked at gene expression in brain tissues of patients co-infected with TBM and identified 4 potential gene products- glial fibrillary acid protein (*GFAP*), serpin peptidase inhibitor, clade A member 3 (*SERPINA3*), thymidine phosphorylase (*TYMP/ECGF1*) and heat shock 70 kDa protein 8 (*HSPA8*) as potential candidates [194].

Most recently, a prospective, multi-site study reported interim results using a newly developed finger stick blood test by Cepheid (the Xpert MTB Host Response [MTB-HR] prototype) which generates a TB score based on messenger ribonucleic acid (mRNA) expression of 3 genes (guanylate binding protein 5 [GBP_5], dual specificity phosphatase 3 [$DUSP_3$], and Krüppel-like factor 2 [KLF_2]) [195] as previously reported [196,197]. Xpert MTB-HR prototype quantifies the expression of the 3 transcripts in whole-blood samples which then computes a TB score based on cycle threshold values using an in-built algorithm [196,198,199]. Xpert MTB-HR discriminated between TB and other respiratory diseases (ORD) with a sensitivity of 87% and specificity of 94% against Ultra and a sensitivity of 90% and specificity of 86% for a triage test [195]. Furthermore, Xpert MTB-HR was able to discriminate between TB and ORD with a sensitivity of 80% and a specificity of 94% against a composite microbiological score irrespective of HIV status or geographical location [195]. Whilst interim Xpert MTB-HR prototype fingerstick blood test results show potential in improving point-of-care TB diagnostics, more data is still needed for TBM, specifically in a paediatric TBM cohort.

Host miRNA biosignatures

MicroRNAs (miRNAs) are small, single-stranded, highly conserved, non-coding RNAs which function at the post-transcriptional level to regulate gene expression [200–202]. MiRNAs have been shown to regulate diverse cellular processes such as cell differentiation, proliferation, organ development, apoptosis, immune response, and angiogenesis and also act as biomarkers for infectious diseases [203–205]. Studies have proposed miRNAs as potential biomarkers to differentiate active from latent TB infection [193,197,198] and other microbial infections [206]. A study identified an expression profile of circulating miRNAs as potential diagnostic biomarkers which showed that miR-1, miR-55, miR-31, MiR-146a, miR-10a, miR-125b and miR-150 were downregulated while miR-29 was upregulated in children with PTB vs uninfected children [207]. Another study in paediatric patients with PTB investigated miRNA-31 diagnostic values in peripheral blood mononuclear cells (PBMCs) and reported a low expression of miRNA-31 in paediatric TB patients when compared to normal controls (0.48 ± 0.15 vs 1.23 ± 0.36, $P<0.05$) respectively [208]. However, serum levels of cytokines IL-6, TNF-α, NF-kB and INF-γ were significantly higher in paediatric TB when compared to normal controls [208].

miRNA had a cut-off threshold of 0.835 with a sensitivity of 98.5% and a specificity of 86.7% [208]. These studies gave insight on expression profile of miRNA in children infected with TB. An evaluation of PBMCs and CSF in diagnosis of paediatric TBM reported that miR-29 expression was significantly higher in PBMCs and CSF of children with TBM when compared to the control group and expression of miR-29 in PBMC showed diagnostic potential for TBM with a sensitivity of 62.7% and specificity of 88.5% and a sensitivity of 81.1% and specificity of 90% when evaluated in CSF [209]. The combination of PBMCs and CSF showed a sensitivity of 84.4% and a specificity of 95.38%, suggesting miR-29 as a potential diagnostic biomarker for paediatric TBM [209]. A genome-wide miRNA screening of PBMCs in TBM, viral meningitis (VM) and healthy controls identified 4 miRNAs (miR-126-3p, miR-1301-3p, miR-151a-3p and miR-199a-5p) in PBMCs that distinguish TBM from VM with a sensitivity of 90.6% and specificity of 86.7% and distinguished TBM from healthy controls with a sensitivity of 93.5% and specificity of 70.6% [210]. Three of these (miR-126-3p, miR-130a-3p, miR-151a-3p) were significantly different in distinguishing TBM from VM in CSF [210]. Further validation of the 4 MiRNAs in an independent sample set from the same study showed a sensitivity of 81.8% (9/11) and specificity of 90.0% (9/10) in discriminating TBM and VM and sensitivity of 81.8% (9/11) and specificity of 84.6% (11/13) in discriminating TBM from non-TBM patients [210]. Three exosomal miRNAs (miR-126-3p, miR-130a-3p, miR-151a-3p) showed potential as a TBM diagnostic biomarker in combination when integrated with electronic health records for discriminating TBM from non-TBM disease, diagnosing TBM with a sensitivity of 94% and a specificity of 95% [211]. However, there is still no established MiRNA biomarker thus far [200].

Metabolic biosignatures

Metabolomics involves the study of the metabolome, the total repertoire of small molecules present in cells, tissues, organs, and biological fluids [212]. Studies have identified proteins and metabolites as potential biomarkers in TBM diagnosis [213,214]. A study used a metabolomics approach to identify potential diagnostic and follow-up metabolites in urine of paediatric TBM patients and identified a host biosignature (*SUM-4*), which includes, methylcitric, 2-ketoglutaric, quinolinic and 4-hydroxyhippuric acids as potential indicators for state of disease in TBM patients [215].

Clinical management of TBM

Early detection and treatment of TBM improves outcomes. Three approaches have been highlighted to improve TBM treatment, by enhancing bacterial killing, controlling intracerebral inflammation and critical care [216].

TBM Treatment regimen

The presence of the BBB makes it difficult for anti-TB drugs to penetrate the brain tissue. These anti-TB drugs possess varying physiochemical properties that determine their ability to cross the BBB and achieve efficacious concentrations that enable killing of the TBM bacteria. This is discussed in detail in chapter 4.

Host directed therapy

Corticosteroids

Corticosteroids are used as adjunctive treatment to reduce inflammation in the CNS [217,218]. Dexamethasone has been shown to improve TBM outcomes in an adult Vietnamese cohort, particularly in HIV uninfected participants [217]. Corticosteroids have been described to change the inflammatory mediators balance and decrease CSF MMP-9 resulting in reduction of cerebral, meningeal inflammation, cerebral oedema and raised ICP [57]. Furthermore, Corticosteroids improve medium-term survival in HIV uninfected patients but show no effect on morbidity [218]. A review by Dooley and colleagues based on analysis of clinical trials suggested the use of corticosteroids in patients with moderate to severe forms of CNS-TB to better the treatment outcome [219]. In fact, the use of corticosteroids significantly improved the survival rate and intellectual outcome of children with TBM [220].

Aspirin

Aspirin has been postulated to have an effect on the pathology of TBM at varying doses [221], at a low dose, it may prevent ischaemic infarction through inhibition of thromboxane A2 and platelet aggregation, at a higher dose it may inhibit the expression of proinflammatory eicosanoids and TNF-α and triggers production of molecules that contribute to resolution of inflammation [222]. Adjunctive treatment with aspirin has been investigated in clinical trials at varying doses [222–224] and shows potential clinical benefit and reduction in mortality but requires further studies [222,224]. However, a study showed that aspirin does not reduce the risk of infarcts that tend to develop during treatment [223].

Hyponatremia

Hyponatremia is common in TBM and may result from the syndrome of inappropriate antidiuretic hormone secretion (SIADH) or cerebral salt wasting syndrome (CSWS) and distinguishing them is challenging but important as their management is different based on the underlying cause of hyponatremia [225–227] and the therapy of one may cause harm to the other. The underlying mechanism for CSWS in meningitic disorders is not quite known, but increased levels of atrial

natriuretic peptide (ANP) have been described in TBM which mediates renal sodium loss, whereas in SIADH, secretion of antidiuretic hormone (ADH) occurs independently from effective serum osmolality or circulating volume. It is recognised that clinical conditions that were thought to be SIADH have been misjudged and this has been attributed to the primary secretion of ADH and ANP which leads to secondary factors that complicate the distinction of the causative factor [225,226]. Furthermore, CSWS may result in inhibition of aldosterone secretion. As such, the presence of ADH in the plasma does not confirm the diagnosis of SIADH. Though difficult, an accurate assessment of the patient's intravascular volume is necessary. Fluid restriction is the treatment for SIADH as the underlying problem is inappropriate water retention. in CSWS, patients are volume depleted and fluid restrictions are harmful to these patients as intravascular volume is further reduced and the risk of cerebral ischaemia may increase. Hyponatremia is independently associated with poor outcome [228,229] and CSWS has been indicated as a possible predictor of stroke in TBM [230].

HIV coinfection

HIV co-infection adds to the challenge of treating TBM as patients who have TBM and HIV co-infection have a 2 to 3-fold higher mortality as compared to HIV uninfected patients [52].

Immune reconstitution inflammatory syndrome

Patients who are antiretroviral therapy (ART) naïve with TBM are more at risk of developing pronounced adverse events owing to immune reconstitution inflammatory syndrome (IRIS) [231]. IRIS is a condition resulting from intensified restoration of pathogen-specific immune response to a pathogen resulting from extensive inflammation [232]. The conundrum is well explained in an expert review which states that; if these patients are given ARTs too early, then they develop IRIS. However, a delay in initiation of therapy may lead to opportunistic infections and other complications of acquired immune deficiency syndrome (AIDS) [52].

TBM occurring IRIS presents as a recurrence or deterioration of neurological symptoms and typically occurs within the first 3 weeks and up to 3 months after ART is initiated, recommenced or switched [232,233]. TBM patients with positive CSF cultures have a higher risk of IRIS [132,234–236] as compared to patients with CSF negative cultures. In addition, TBM patients with HIV-coinfection generally have less meningeal inflammation than HIV uninfected patients as shown by lower CSF white blood cell count or protein levels [237]. Furthermore, IRIS in TBM is also characterized by high CSF neutrophil counts [232,238].

Neurosurgical Management of TBM

TBM pathology initiates secondary consequences that may include cerebral ischemia, increased ICP, excitotoxicity and other metabolic disorders [144,239].

HCP

HCP is common in children with TBM and may lead to permanent neurological damage or increased mortality if left untreated due to raised ICP [66,126,129,240,241]. Under normal conditions, the total volume within the skull (intracranial vault) remains constant and is determined by the sum of 3 elements: brain tissue (80%), CSF (10%) and cerebral blood volume (10%) [242,243]. When additional volume is added to the system, certain compensatory mechanisms operate that maintain normal ICP [242,243]. However, once this normal compensatory mechanisms are exhausted, a small increase in intracranial volume will result in a steep increase in ICP [242,243]. Coma in TBM is associated with raised ICP [6]. Raised ICP can severely compromise blood flow [14].

HCP may be categorised into communicating and non-communicating; however, the distinction is not easy on conventional imaging such as head CT and MRI. Different centres have different approaches to this, with some not making the distinction in the management strategy. At our institution, we use a procedure known as an air encephalogram (AEG), where 5-10 ml of air are injected at the level of the lumbar subarachnoid space [244]. If, on the follow-up skull X-ray, air is located in the basal cisterns but not the ventricular system, the system is non-communicating and if air is in the ventricles the system is communicating [244]. Results are captured by a skull X-ray or head computed tomography (CT) scan [245]. If no intracranial air is observed on imaging after an AEG, this may also be due to spinal arachnoiditis preventing the movement of air up the spinal sub-arachnoid space and could be regarded as a failed procedure [244].

In patients with an EVD in situ, a column test can also be used to determine whether HCP is communicating. In this case, the opening pressure at the EVD and LP needle are measured simultaneously prior to the following CSF removal from the LP. If the change in pressure is equal at both sites the system is considered to be communicating [245]. Communicating HCP (CommHC) results from obstruction to CSF flow in the basal subarachnoid cisterns [246] and is medically treated with repeated LPs and diuretics (acetazolamide and furosemide) for 3 weeks or until the ICP has normalised [247]. This approach has been reported to be successful in 75-80% of patients [248,249], with the rest being treated with VPS. Non-communicating HCP (NCHC) results from obstruction to CSF flow at the outlet foramina of the fourth ventricle or at the aqueduct, which may be constricted owing to circumferential compression by meningeal exudate, mesencephalic oedema, or tuberculoma

[250]. NCHC is treated with an EVD or endoscopic third ventriculostomy (ETV) or VPS [245,250]. Management of HCP in children with TBM is discussed in detail in chapter 7.

Outcome

TBM affects children during important neurodevelopmental stages. As such, there is a high risk of developmental sequelae, such as intellectual impairment [251,252] and subsequent neurological deficit including; visual impairment [67,74,253,254], motor deficits [67,74,253] and hearing loss [67,253]. Neurodevelopmental deficits post follow-up in a paediatric TBM cohort include deficits in locomotion, language, co-ordination, personal, social and executive function relative to controls [253]. It is suggested that outcome depends on the extent of disease, immune function and the virulence of the infecting organism [255]. Delayed diagnosis, treatment, severity of disease and HCP contribute to poor outcome [67,74,256–261] and highlight the need for more sensitive rapid diagnostics and effective supportive care [245]. Infarcts have been reported as predictive of poor outcome in a paediatric TBM cohort, particularly if they are large, multiple and/or bilateral [66]. In addition, persistent brainstem dysfunction is a poor prognostic indicator in children with TBM [117].

Certain biochemical markers are associated with TBM outcomes. A study has shown that a relatively low CSF white cell count and a low CSF: blood glucose ratio is a predictor of outcome in TBM patients [217]. Furthermore, recent studies have shown that CSF-glucose, lactate and protein levels are linked to poor outcomes [262,263]. Persistent increase in MMP-9 and MMP-2 is associated with unfavourable outcomes in adults [42]. As such, MMP-9 has been suggested as a target on which steroids (eg. dexamethasone) act to suppress and improve patient outcomes in TBM [264].

However, this was not the case in a paediatric TBM study, which reported no association between MMPs and unfavourable outcomes [265]. Furthermore, an increase in MMP-9 during hospital stay was associated with better outcome [265].

CHAPTER 3: PAEDIATRIC DRUG TARGET SITE KINETICS

Introduction

Drugs targeted at the CNS must be able to cross brain barriers and achieve optimal concentrations at the site of disease. This poses a challenge for most drugs that are delivered orally such as anti-TB drugs. The drug of interest must go through processes that characterise PK which include, absorption, distribution, metabolism, and excretion (ADME). These ADME processes differ in children as compared to adults and can affect the PK profile of a drug [266].

Only the unbound free fraction of the drug can cross membranes, hence the unbound concentration in plasma drives transport in the brain [267]. This implies that variability of protein in the blood of developing children needs to be taken into consideration as the unbound concentration would be higher in younger children as compared to older children who would have reached adult levels of plasma proteins. Furthermore, it is also recognised that there is a lag time from systemic circulation to distribution of the drug into and within the brain. Variability of drug concentrations between plasma and the CNS have been described to arise primarily from the barrier properties of the brain and the processes that drive the distribution of the drug within the brain [268].

Drug development

Drug development for drugs targeting the CNS is a very challenging task for the pharmaceutical industry [269]. The success rate of first-in-human trials is about 8% for CNS drugs as observed over a 10-year period (1991-2000) [269].

It is important that a specific drug of interest undergoes pre-clinical testing in animals and clinical development stages in humans, prior administration to a patient. The clinical development stages are divided into phase I to phase III trials. Phase I studies are conducted to determine the drug's PK properties and toxicity profile. These studies are done in healthy volunteers or patients [270,271]. Phase II studies are conducted to determine the drug candidate's therapeutic efficacy and the patient's response to a range of dose regimens [270]. Lastly, phase III trials are done in a larger population of patients to confirm the therapeutic efficacy of the drug prior to administration to the patient [270]. In addition, clinical development can also get to phase IV where the drug is tested for the first time in the real world after marketing authorization approval per label [272].

High failure rates have been described in phase II and phase III for CNS drugs [269]. The CNS, one of the therapeutic areas with very high attrition rates is also an area in which animal models are not predictive of human physiology [269] .

A recent review described the importance of drug permeation studies during early pre-clinical testing as plasma does not give the overall picture of drug distribution to the target site of infection as observed for TB lesions, a heterogenous TB microenvironment in treatment of PTB [273]. Similarly, the CNS is not just one compartment and target site concentrations would provide an improved understanding of dosing strategies and patient outcome, particularly in the TB disease (pulmonary and CNS).

Adverse effects

Past studies have shown that a drug can cause adverse effects if safety is not established [274]. One example is thalidomide, which resulted in outbreaks of phocomelia, a rare congenital deformity in children in over 46 countries, resulting from ingestion of the drug by pregnant mothers prescribed for the treatment of nausea [274,275]. This horrific event led to the enactment of the Kefauver-Harris amendment in 1962, which required that a drug undergo testing for safety and efficacy prior to reaching the marketplace [275].

Another occurrence is the "grey baby syndrome" in which neonates were administered the antibiotic chloramphenicol as extrapolated from adults which led to very high plasma levels of the active drug resulting from their immature uridine-5'-diphospho-glucuronosyltransferase enzymes [276]. This was a consequence of past exclusion of children in the development of therapeutic drugs. However, as highlighted, children are not small adults, owing to changes in their body composition and size [277]. Furthermore, protein expression and cellular function also change during development [275]. Therefore, it has been proposed that infants and children be included in drug developmental stages "lest they become therapeutic orphans [278]. " These reports highlight the importance of inclusion of children in drug development which in turn aids in establishing safety of the drug prior administering to children thereby limiting adverse events.

Why children cannot be treated as small adults

Despite these tragedies and passing of laws and acts that advocated for inclusion of children in drug clinical trials and expansion of labelling of approved paediatric drugs that did not have adequate labelling, there remains inadequate pharmacological data on drugs that are currently used in clinical paediatric practice [275]. Furthermore, most data is still extrapolated from adult studies, resulting in 50-80% off-label/unlicensed drug use in children [279–282]. This highlights that the differences between children and adults are often underestimated [283] and stresses the need for controlled clinical trials in children.

Factors that affect the PK of a drug during development

An improved understanding of the principles that govern PK is important to prevent drug adverse effects, which have been linked to drug dosage, especially in the vulnerable paediatric population [284]. Furthermore, it has been shown that developmental changes in children and young infants can affect the response to treatment and advocates a need for age-dependent adjustment of dose in order to achieve optimal therapeutic effect [285].

Various factors that are associated with physiological growth have been highlighted, this includes: body size, physiology, isoenzyme maturity in the gut and liver, liver blood flow, plasma protein binding and age. These factors may alter the PK and pharmacodynamics (PD) of a drug [286]. Emphasis in this section will be, on body size and age.

Body size

Body size is the main driver of PK variability after the age of 2 years [287]. Dosing of drugs in the paediatric population has mostly been extrapolated from adults using an allometric scaling approach which references a child's body size to a 70kg adult using a coefficient of 1 for a volume of distribution and an exponent of 0.75 for clearance [287]. Drug clearance is one of the important factors that account for age dependence of PK profiles [288].

Accurate prediction of drug clearance from adults is very important for first-dose-in-children studies and requires prior knowledge of adult clearance mechanisms and age-dependence of physiological and enzymatic development [288]. However, the allometric scaling to a fixed exponent of 0.75 approach has shortcomings that have been found to result in large over-predictions of hepatic metabolic plasma clearance (CLp) in children less than 5 years of age and even higher over-predictions in children less than 2 years of age, particularly when isoenzymes are immature [289–291].

In contrast, a mechanistic approach has been described that is used to predict clearance across different ages, taking into account the physiological developmental processes such as liver size, liver blood flow, plasma protein binding and maturation of isoenzymes in the gut and the liver [292].

Age

Age is an important factor in optimizing drug dosing, as such, a recent study has suggested the use of an age-dependent exponent method which surpasses allometric scaling with a fixed exponent of 0.75 as previously described, in that different allometric exponents are used for different age groups, thus accounting for variability as a function of age [291]. However, this method also has limitations as it does not consider variability in isoenzyme maturation which can affect hepatic metabolic clearance. This was found in a study that investigated a scaling method that combines allometric scaling and maturation function [292].

In addition, the ADE model was recently compared with physiologically based PK (PBPK) modelling to predict drug clearance from neonates to adolescents and there were no significant differences in their predictive power [293]. Other scaling methods have been described which include: bodyweight-dependent exponent model [294–297] and a segmented regression model [289].

Factors affecting the PK of a drug to the brain

Many CNS and drug properties can influence the distribution of a drug to the brain [298]. The main factors that influence the drug kinetics to the brain include: 1) plasma kinetics (absorption, bioavailability, plasma protein binding and drug metabolism), 2) blood-brain transport (BBB and BCSFB) and 3) intracerebral distribution (cerebral blood flow, effective brain surface capillary surface area, BCSFB transport, brain ECF, CSF turnover, extra-intracellular exchange, brain tissue binding and drug metabolism) [298,299]. These will be described within the ADME processes that characterise the PK of a drug in the next section. Furthermore, drug properties also determine the PK of a drug, these include: physiochemical properties such as lipophilicity, size, charge, hydrogen binding potential and polar surface area [300].

Ideally, for effective treatment, the drug should be delivered to the CNS at the right time, in the right concentration and at the right place [298]. This is often challenging owing to different conditions that contribute to inter- and intra-individual variability such as genetic background, age, diet, disease and drug treatment that result in varying CNS effects [298].

1. Plasma kinetics in the developing brain

Absorption

The factors that affect the bioavailability of the drug can be categorised into physiochemical and physiological factors [301,302]. Absorption of drugs by passive diffusion is dependent on the physiochemical properties of the drug which include: molecular size, charge and lipid solubility which can influence drug permeability as described further in the text [303].

Physiological factors that can influence absorption include: gastrointestinal tract (GIT) fluid composition and volume, transit time, microbiota, bile salts, intestinal pH, pancreatic function, drug-metabolizing enzymes, drug transporters, disease state and environmental factors (e.g. food), many of which may vary with age [304–306].

Most drugs that are administered to children are given orally [304]. For an orally given drug to elicit a therapeutic effect, the drug of interest must dissolve in the fluids of the GIT, be stable in the lumen, cross the epithelial membrane and undergo minimal first-pass metabolism [307,308]. Changes during development in the GIT can affect the rate and extent of the drug that will reach systemic circulation [285]. In addition, the changes in the luminal pH at different segments of the GIT can affect the stability

and degree of ionization of the drug which affects the relative amount of the drug available for absorption [285].

Physiological parameters that affect drug absorption

Gastric pH

Gastric pH may play a role in the absorption process, although consensus has not been established. Some studies report that gastric pH is influenced by the developmental process from birth until adulthood resulting in varying pH [309], whereas other studies show that the gastric pH is continually maintained at acidic values from neonates to adults [305,310].

Gastric emptying

Although it has been suggested that gastric emptying varies with age (from preterm neonates as compared with older children and adults) [311], other data show that gastric emptying is influenced by meal type rather than age, with solid meals being the slowest as compared to an aqueous meal [312].

Intestinal transit time

The small intestine is the region where most drug and nutrient absorption occurs [313]. Young children are reported to have shorter intestinal transit times, which may reduce the amount of the drug absorbed, especially for poorly soluble drugs [314].

Gut microbiome

The gut microbiome has been implicated in influencing drug absorption [315]. As such, this presents a physiological source of variability in both individuals and populations which should be taken into consideration [316].

The gut microbiota has been described to contribute to metabolism of drugs, thereby affecting drug stability [307]. Furthermore, of major concern is the possible metabolite toxicity from drugs that are substrates of these bacterial enzymes [307,317]. The GIT microbiota metabolize drugs through reductive and hydrolytic reactions, resulting in non-polar, low molecular weight by-products as compared to the liver which metabolizes via oxidation and conjugation producing high polar molecular weight by-products [307]. These processes constitute the first-pass metabolism and hepato-biliary extraction [308].

Transporters

Active transport is driven by transporters which are categorised into facilitated transport and adenosine triphosphate (ATP)-dependent protein transport. Facilitated transport includes: solute carrier family (SLC), such as organic anion-transporting polypeptide (OATP) and organic anion transporters (OATs), whereas ATP-dependent transport includes the ABC transporters such as P-glycoprotein (P-gp), multidrug resistance protein 1 (MRP1) and breast cancer resistance protein (BCRP) [318,319]. These transporters are minimally expressed during foetal and neonatal ages and increase from the age of 7. Of particular interest is the ABC transporter, P-gp which plays a role in RIF PK.

ATP-dependent transport

P-gp

P-gp is a 170 kilodalton (kDa) transmembrane glycoprotein that has been extensively studied and functions as a biological barrier by excreting toxins and xenobiotics out of cells [320–322]. Furthermore, P-gp also confers multidrug resistance (MDR) in tumours as well as normal tissue and the brain [323].

This transporter plays an important role in the absorption and disposition of a drug [320]. P-gp has been suggested to limit the uptake of drugs from blood circulation to the brain and from intestinal lumen to epithelial cells [320]. However, the activity of P-gp becomes saturated at the intestinal lumen by high concentrations of a drug [324]. Adult levels of P-gp are reached by 2 years of age [318].

Two members of the P-gp gene family (*MDR1 and MDR2*) exist in humans whereas three members of this family have been found in mice (*mdr1a, mdr1b and mdr2*) [325,326]. The human *MDR1* and the mouse *mdr2* genes function as drug efflux transporters [327]. This is achieved through a single integral protein that is able to recognise and transport various drugs with different chemical structures [328,329]. Furthermore, most of the substrates of P-gp are hydrophobic in nature [320]. This is supported by studies that have shown that lipophilicity and number of hydrogen bonds of compounds are determinants for substrates and P-gp interaction [330–332].

Apart from expression of P-gp in tumour cells, it is localised on the canalicular surface of hepatocytes in the liver, the apical surface of epithelial cells of proximal tubules in kidneys, columnar epithelial cells of the intestine (colon and jejunum), epithelial cells of the placenta and the luminal (blood) surface of capillary endothelial cells in the human brain [333,334]. Owing to its localisation, it is believed that P-gp plays a significant role in the processes that govern the PK of a drug in humans and animals [335,336]. As such, many pharmaceutical companies have begun to include the screening for P-gp drug transport in the drug discovery process [320].

Studies have also shown that there is inter- and intra-individual variability in the expression of P-gp in the intestinal mucosa which may contribute to variability of oral absorption of drugs that are substrates of P-gp [337,338]. Furthermore, administration of drugs such as dexamethasone, has been shown to induce the expression of P-gp in a dose-dependent manner [339–341]. P-gp has also been described as a cause of drug interactions for digoxin and RIF, where RIF reduced the bioavailability of digoxin through P-gp-mediated induction [342]. TB treatment with RIF-based regimens was found to modestly increase MDR-1 expression in brain tissues obtained from mice treated with high-or standard dose RIF regimen [343].

First-pass metabolism

Drug metabolism

Although the liver is a major site for drug metabolism, other sites such as the small intestines and kidney may also account for the overall drug metabolism in the body [344]. Drug-metabolizing enzymes can be divided into phase I and phase II enzymes.

Phase I drug-metabolizing enzymes

The cytochrome (CYP) P450 family, which forms part of the phase I drug-metabolizing enzymes, are important for biotransformation of exogenous and endogenous compounds. The CYPs are grouped into families as represented by a number, the subfamily by a letter and each member of the subfamily by a second number e.g. CYP3A1[345]. The most abundant is the CYP3A subfamily, which is involved in approximately 50% of biotransformation of drugs that are administered to children [346].

The CYP3A subfamily consists of at least 3 isoforms: CYP3A4, CYP3A5 and CYP3A7 [347]. Studies have shown varied expression of CYP3A enzymes [315,348]. Developmental changes may influence the expression of these enzymes. To exemplify, CYP3A7 enzymes, a subfamily of CYP3A which is expressed in the foetal liver, peaks at birth followed by a progressive decline to reach adult levels, and CYP1A2 is the last enzyme to be acquired in the liver, with expression at 1-3 months of life [349,350]. Furthermore, diet has been linked to the activity of CYP1A2 and formula-fed infants acquire more function faster than breastfed infants [351].

The CYP3A4 enzymes are the most expressed CYPs and account for approximately 30-40% of the total expression in the human adult liver and small intestine [347]. The total CYP enzymes in the foetal liver are 30-60% that of adults and 100% is only reached in the first 10 years of life [352]. Interindividual variability of drug-metabolizing enzymes has been well-described [353]. This could influence the amount of drug present in systemic circulation which distributes to tissues.

Phase II drug-metabolizing enzymes

Another class of drug-metabolizing enzymes are the phase II enzymes, these include uridine diphosphate (UDP)-glucuronosyltransferase (UGT), N-acetyltransferases (NAT), glutathione-s-transferase (GSTs) and sulfotransferase (SULTs). These enzymes catalyse phase II reactions which result in pharmacological inactivation, activation or detoxification; a change in the expression of these enzymes can have a considerable effect on the PK of the drug [352].

NAT is known to metabolize isoniazid (INH), one of the important drugs in TBM treatment. It consists of various genetic polymorphisms that influence the PK of the drug, particularly in the NAT2 gene locus [354]; including the rapid and slow acetylation status of NAT [355]. A study has shown that the cumulative frequency of fast acetylators increases with age and plateaus at about 4 years of age [356]. As such, it has been suggested that a higher proportion of children less than 2 years of age are phenotypically slow acetylators. The most important families of UGT enzymes are UGT1 and UGT2, which play a role in metabolizing drugs and endogenous molecules such as bilirubin and steroids.

Distribution

Drug distribution of drugs targeted for the CNS is quite complex. As such the following sections will explore factors that influence the distribution of drugs from systemic circulation to the CNS followed by CNS drug distribution from transport through brain barriers to distribution in the brain and factors thereof that affect the distribution of drugs within the brain.

Factors that affect the distribution of drugs from systemic circulation to the brain

The distribution of the drugs is reportedly influenced by body composition, physiochemical properties of the drug and plasma proteins that have the potential to bind the drug of interest [266,275,357–359]. Other factors which influence drug binding and distribution include: variability in regional blood flow, organ perfusion, permeability of cell membranes, changes in acid-base balance and cardiac output [285,360].

Protein binding

The drug of interest can either be bound to proteins and lipids in plasma (namely plasma protein binding [PPB]), or protein and plasma in the tissues or be unbound. As such, this would result in variability of bound vs free drug in the two compartments (plasma vs tissues) [308]. Changes in the composition and amount of plasma proteins, which include albumin and α-acid glycoprotein, can influence the distribution of highly protein-bound drugs [285].

Plasma protein levels are influenced by disease state, age and nutrition [275]. Furthermore, adult plasma protein levels are reached by 1 year of age, therefore, children younger than 1 year would have lower

protein plasma concentrations compared to older children [275,358]. Therefore, plasma proteins are immature in neonates which may affect drug-binding affinity [275].

Total vs free fraction pharmacological effect

Drugs that are targeted to elicit effect in the CNS must be transported through the BBB and be distributed within the brain. It has been suggested that it is the free fraction of the drug that is available for transport to the brain and determines the drug effects [361]. This has been named, the free drug hypothesis.

Part I of this hypothesis states that "at steady state, the free drug concentration is the same on both sides of any biomembrane". Therefore, highly permeable drugs would have the same free drug concentrations in the plasma and biophases [362]. This applies to most drugs regardless of the free fraction in plasma [363–365]. Therefore, this suggests that the unbound plasma concentration is a better predictor of drug effects than other concentration measurements [366]. The exceptions to the first hypothesis are drugs with a slow rate of permeation such as RIF in TBM, which results in a delay to equilibration [367–369], drugs that are substrates for efflux transporters [370], and low blood flow which results in low distribution to the cells [371].

Part II states that "the free drug concentration at the site of action, the therapeutic target biophase, is the species that exerts pharmacological activity". This hypothesis is essentially applied in drug discovery and has been applied in various studies [363,364,372–376]. However, studies have reported that some drugs' total rather than the free drug concentration determines the pharmacological effect [267,377].

Given the low concentration and affinity of albumin and α-1-acid glycoprotein in the blood of neonates, infants and young children, there may be variation in the drug distribution between patients and an increase in the unbound concentration of the drug. This has implications in dosing and supports the argument that extrapolating data from adults to children is not effective [286]. However, Smith *et al*. stated that it is the free drug concentration at the therapeutic target rather than the plasma binding that affects the *in vivo* efficacy of the drug of interest [308]. As such, using plasma as a surrogate in body organs such as the brain where there is a delay in the distribution of the drug requires measuring the free drug closest to the tissue of interest to investigate efficacy.

CNS drug distribution

2. Blood-brain and CSF barrier transport

Anatomy and physiology of the brain barriers

The brain has important roles in cognition, regulating metabolism and coordinating the functions of the peripheral organs and this requires a precise and balanced microenvironment [378]. As such, peripheral blood circulation is separated from the CNS by the presence of brain barriers, namely the BBB and the BCSFB at the level of the choroid plexus. In addition, an arachnoid epithelium has been described which separates the blood from the subarachnoid CSF [379]. Another CNS barrier which is considered as a morphological extension of the BBB to the spine is known as the blood-spinal cord barrier (BSCB). The BBB and the BSCB have similar constituents but have functional differences in their role in disease of the spinal cord [380].

These barriers differ in their morphology and transfer properties [381]. The brain barriers are essential in regulating what goes into and out of the brain compartments. There are four main compartments: the brain intracellular environment, brain ECF and V- and LCSF.

The BBB

The BBB is a vascular structure that separates systemic blood from the brain (ECF) [382,383]. The maturation of the BBB occurs during foetal life and is well-formed by birth [384]. The BBB has a surface area that is approximated at 20 m^2 per 1.3 kg brain and exists in all vasculature of the CNS including the penetrating arteries and arterioles, the dense capillary bed, the postcapillary venules and the draining venules and veins [385,386]. The main functions of the BBB include: maintenance of homeostasis in the brain by regulation of entry of cells of the immune system, chemicals and xenobiotics, and protection of the brain from pathogens and toxins present in systemic circulation [387,388]. The BBB also regulates the brain ECF and prevents secondary injuries during diseases [379,389,390]. Furthermore, the BBB protects the brain from fluctuations in ionic compositions that can occur after a meal or exercise, which would interfere with synaptic and axonal signalling [391]. An intact BBB poses a therapeutic challenge to various aspects of clinical pharmacology, one of which is that the BBB limits the entry of drugs targeted for the CNS [392].

The structure of the BBB

The BBB is made up of cerebrovascular endothelial cells (EC) with tight high electrical resistance cell-cell junction proteins, that are specific to brain vasculature, thereby restricting paracellular movement [378]. Those compounds that enter the BBB are removed by efflux pumps [392]. A study done in mouse, quail and chick embryos suggested that the BBB tightness is not just switched on at a specific time during angiogenesis but rather a gradual process that is independent of vascular proliferation and

initiated late during embryogenesis when angiogenesis is in progress [393]. Transcellular movement of molecules across the EC cells is regulated by specialised transporters, pumps and receptors [379,394,395]. However, the BBB is more permeable in circumventricular organs, specialised regions located around the third and fourth ventricles in the brain, which mediate neuroendocrine functions and the response to systemic toxicants [379]. These organs include the neurohypophysis (posterior pituitary), the median eminence, area postrema (vomiting centre), subfornical organ and the vascular organ of the lamina terminalis [390,396–398].

Brain endothelial cells

The brain EC have many properties, some of which are shared with peripheral EC, including the expression of glycoproteins [399,400], adhesion molecules [401,402] and integrin receptors [402]. Furthermore, the EC also provide a metabolic barrier against potentially penetrating lipophilic substances through the presence of drug-metabolizing enzymes [403]. The EC of the BBB do not possess fenestrae, which are small pores that allow rapid passage of molecules in peripheral EC [404,405]. This makes them unique as compared to EC in other tissues. Furthermore, the brain EC have an increased density of mitochondria as compared to peripheral vasculature, suggesting high metabolic activity and energy requirements for these cells, as well as susceptibility to the formation of reactive oxygen species [406–408]. The brain EC also have 14 fold fewer vesicles known as caveolae relative to peripheral EC [409]. The endothelial caveolae have various functions which include endocytosis, where a molecule is internalised by the EC, and transcytosis where a molecule is transferred across a cell [410]. Endocytosis and transcytosis may either be receptor-mediated or fluid-phase. As such, the EC caveolae possess membrane receptors that play an important role in receptor-mediated transcytosis of molecules that are essential in maintaining cell and tissue homeostasis. These receptors include low- and high-density lipoprotein, epidermal growth factor, TNF, albumin, transferrin, melanotransferrin, lactoferrin, ceruloplasmin, transcobalamin, advanced glycation end products, leptin and insulin [411,412]. Other receptors include p75 and IL-1 which are involved in cell apoptosis [411]. Therefore, the mature brain EC is mainly characterized by their small height, tight junctions, decreased number of caveolae at the luminal surface of the cell and increased number of mitochondria [378,406,407,409].

Adherence junctions

The inter-endothelial space is characterized by adherence junctions, which are cellular contacts formed between a cell and the surrounding extracellular matrix or between two cells [413]. These adherence junctions are spread out in the vasculature and mediate adherence of EC to each other, contact inhibition during vascular growth and remodelling, initiation of cell polarity and partly the regulation of paracellular permeability [414,415].

Tight junctions

Tight junctions consist of transmembrane proteins (junctional adhesion molecule-1, occludin, and claudins 1/3,5 and/or 12) and cytoplasmic accessory proteins (zonula occludens-1 and -2, cingulin, AF-6 and 7H6) that form the primary seal between brain EC and are linked via accessory proteins to the actin cytoskeleton [387,416–422]. The quality of endothelial tight junctions is dependent on the brain microenvironment and basal lamina as well as pericytes, astrocytes and microglia [402]. The occludin and claudin family of transmembrane proteins are reported to be the most important membranous components of the tight junction structure [402]. Occludin is a 60-65 kDa protein with a carboxy (C)-terminal domain, and its main role is tight junction regulation [388,423,424]. The claudin family of proteins are 20-24 kDa and are suggested to contribute to high transendothelial electrical resistance [422,425–428]. Tight junctions are dynamic structures, as such, the proteins of tight junctions are prone to changes in expression, subcellular localization, post-translational modification and protein-protein interactions in response to physiological and pathophysiological changes [429].

Blood-brain barrier formation and integrity

The structure and function of the BBB are maintained by astrocytes, pericytes, and extracellular matrix components [379].

Astrocytes

Astrocytes are glial cells that interact with EC by encircling their end-feet projections on the abluminal (brain) side of cerebral capillaries and play essential roles in homeostasis of extracellular concentrations of transmitters, metabolites, ions and water [379,430–432]. Furthermore, studies have found that astrocytes are also involved in the control of cerebral blood flow [433,434]. Studies have found several effector molecules that are released by astrocytes that are essential in enhancement and maintenance of BBB tightness, which include members of the hedgehog family, the renin-angiotensin hormone system and the cholesterol and phospholipid transporter molecule apolipoprotein E [435–437].

Pericytes

Pericytes are perivascular cells of mesodermal origin, which envelope brain microvessels and capillaries. Recruitment of pericytes is very important in the formation and maturation of the BBB during early development [378,385]. Furthermore, they are important in regulating capillary diameter, cerebral blood flow and extracellular matrix protein secretion levels [438]. As such, the absence of pericytes compromises the integrity of the BBB and regional cerebral blood flow [385,439–441]. Pericytes and EC are enveloped by the basal lamina, a 30-40 nm thick membrane composed of collagen type IV, heparin sulfate proteoglycans, laminin and extrinsic fibronectin [442].

The extracellular matrix

In addition to astrocytes and pericytes, the extracellular matrix of the basal lamina also interacts with the brain EC. As such, disruption of the extracellular matrix is associated with increased permeability of the BBB in pathological conditions [443,444]. Furthermore, the matrix proteins have been suggested to influence the expression of tight junction proteins [445,446].

The connections between neurons, astrocytes, microglia, pericytes and blood vessels and the functional interactions and signalling between them form a dynamic functional unit known as the neurovascular unit [447,448]. Keany *et al*. stated that dysfunction of any of the neurovascular unit members can ultimately lead to dysregulation of transcellular and paracellular pathways across the BBB EC and contribute to pathological BBB breakdown [378].

BBB transport

Essential analytes for energy and transmitter metabolism from the blood are delivered to the brain via transporters [402]. Transport of substances through the BBB results in movement through both the luminal and the abluminal membranes of the endothelium. The brain barriers are permeable to gases such as oxygen, carbon dioxide, helium, xenon, nitrogen and most anaesthetics which diffuse through the lipid membrane [36]. Furthermore, these lipid membranes serve as an entry for small, lipophilic and noncharged drugs which easily diffuse transcellularly [379]. Therefore, transport of drugs through the BBB occurs by active transport or passive diffusion.

BCSFB

The BCSFB is made up of a monolayer of epithelial cells of the choroid plexus separating the blood from the CSF within each ventricle and the subarachnoid epithelial structures facing the CSF space in intracranial and spinal spaces [417]. The choroid plexus is a highly vascularized structure made up of epithelial cells which are abundant in mitochondria, Golgi bodies, endoplasmic reticulum and ribosomes. The plexuses have a leaflike structure and are permeable to polar molecules as compared to the majority of the cerebral vasculature [449]. The BCSFB epithelial cells are fenestrated and have tight junctions at the apical surface [450]. Furthermore, the fenestrated epithelium allows diffusion of blood-borne solutes [417]. The BCSF's epithelial cells have gap junctions and pinocytic vessels, which form a microfilter for proteins. All these constitute the passive characteristics of the BCSFB [449]. All relevant structural differences between the BBB and BCSFB are summarised in Table 3.1.

Table 3.1. Structural differences between the BBB and BCSFB

BBB	BCSFB
Cerebrovascular endothelial cells	Monolayer of epithelial cells of the choroid plexus
Separates blood from brain ECF	Separates blood from CSF
Tight high electrical resistance cell-cell junction proteins	Tight junctions at the apical surface of epithelial cells
No fenestrae	Fenestrated epithelium

Active transporters at BBB and BCSFB

Transporters are present at the BBB and BCSFB and also on the brain parenchyma membrane [300] . Active transport is driven by transporters at the BBB and the BCSFB, which are categorised into facilitated transport and ATP-dependent protein transport as described in the plasma kinetics section [451–458]. Anti-infectives are ligands to active transporters that are responsible for removing toxins from the CNS. Furthermore, these transporters can have variable effects in the CNS compartment [459]. Studies have shown that the expression of the efflux transporters is variable during development [460,461]. Focus will be on ATP-dependent protein transport, specifically P-gp in the CNS.

ATP-dependent transport (P-gp, MRP1)

Various ABC transporters drive the efflux of potentially harmful metabolites that are generated in the CNS and limit accumulation of exogenous compounds such as drugs from systemic circulation [462]. This presents a barrier to treating CNS pathology which includes neuroinfections [462]. In addition, modes of ABC transporters have also been reported at the (BSCB) [463–465]. Members of the ABC family function as ATP-driven transporters on the surface and intracellular membranes, as ion channels and as receptors [462]. In vertebrates, ABC transporters and their subfamilies are highly expressed in barrier and excretory tissues [462]. As such, they have a major influence in the peripheral and CNS PK of various signalling molecules, waste products of normal metabolism, therapeutic drugs, environmental toxicants and drug and toxicant metabolites [462]. ABC transporters can be localized on the luminal (blood-facing) plasma membrane, contributing to the BBB function [462]. Furthermore, ABC transporters are highly expressed on the luminal membrane of EC which contributes to the challenge of delivering small molecule drugs to the brain and enabling CNS disease progression [456,462,466–468].

P-gp is a substrate for broad compounds, particularly, lipophilic compounds [237]. This transporter is made up of an ATP-driven pump that is a carrier for substrates from approximately 300 to 4000 Da

[469]. The P-gp's characteristics, which include a high level of expression, luminal membrane location, multispecificity and high transport potency, make it a primary obstacle in drug delivery to the brain [469,470]. Studies have shown that the P-gp transporter is localised on the luminal side of the EC [452], however, another study suggests that this transporter is mainly localised to astrocyte foot processes [323,471]. This suggests that P-gp may regulate drug transport in the whole BBB at cellular and subcellular levels [472].

Studies have shown that administration of P-gp inhibitors increases transport of drugs across the BBB to the CNS [473,474]. Furthermore, an *in vivo* MD study in moving rats found that co-administration of rhodamine-123, a P-gp substrate with cyclosporin A, a P-gp inhibitor increased its distribution in the brain [475]. This suggests the inhibition of P-gp as an efflux transporter at the level of the BBB as there was no change of rhodamine-123 distribution in plasma [475].

Subfamily C of the ATP-binding cassette transporter in humans (ABCC), consists of 12 members, 9 of which make up the group of MRPs (MRP1-MRP9) [476]. These MRPs are important plasma proteins that mediate the ATP-dependent transport of lipophilic substances conjugated to glutathione, glucuronate or sulfate from cells [456]. The MRP subfamilies also play a role in active efflux of organic anions of toxicological relevance [477,478]. The MRP1 transporter is the most abundant efflux transporter at the level of the BCSFB [479]. Transporter molecules have been suggested to reduce drug exposures within the brain in epilepsy which may have implications in treatment of other drug-resistant pathologic brain conditions [480,481].

The BBB and pathology

The BBB function may vary due to different pathological, chronic and physiological conditions which may influence drug distribution to and within the brain [482]. The breakdown of the BBB can result in impairment of transport processes and flux of various molecules [389]. Furthermore, this can result in changes in permeability, modulation of immune cell transport and trafficking of pathogens into the brain [387,388,483,484]. Two main types of BBB injury have been described; 1) complete breakdown of barrier function e.g. tumours and 2) subtle brain impairment without manifest end organ damage [426]. These BBB changes have been described in various brain diseases, including CNS infections [485–491] .

Compromised BBB tight junctions are a characteristic of a neuroinflammatory disease state such as multiple sclerosis, HIV encephalitis and Alzheimer's disease [492–497]. Furthermore, BBB disruption has been reported as a result of tight junction modulation following infection [498,499].

In circumstances of BBB breakdown, brain EC become activated to release proinflammatory molecules and upregulate cell adhesion molecules like ICAM-1, VCAM-1 and E-selectin [500]. In addition, a recent study analysed the gene expression of brain EC as compared to peripheral EC in mice and found

that their models of brain pathology had similar EC gene expression changes of BBB disruption which suggests that there is a common pathway that could be a potential therapeutic target across neurological disorders [501].

Changes in BBB permeability have important implications for drug penetration into the brain, although other factors are also relevant to cerebral drug delivery [268,502–504]. Physiological and pathological signals can affect the activity and expression of transporters at the BBB [469]. As such, P-gp expression in the brain and brain EC is altered as marked by an increase or decrease following inflammation [505–507]. CNS infections result in increased permeability of the brain barriers which in turn reduces CSF flow and an increase in drug concentrations during inflammation [508].

Physiochemical properties of the drug

The drug physiochemical properties which affect drug absorption and distribution also influence the permeability of the drug through the BBB. As such it has been suggested that they be investigated simultaneously as opposed to past studies that did investigations in isolation [509]. The ideal compound to treat CNS infections has been described as small, moderately lipophilic, with low plasma protein binding, with a volume of distribution of 11/kg and is not a strong ligand for efflux pumps located at the brain barriers [237].

Size

Small, lipophilic molecules can cross the BBB through passive transcellular transport [510,511]. These molecules have been described to have a molecular weight less than 500 Da, log P_{oct} in the range 2-4, and the number of hydrogen bond donors is less than 5 [511,512]. Furthermore, permeability has been suggested to be greater in the developing brain as compared to adults [513].

Lipophilicity

The lipophilicity of a compound enables it to penetrate the CNS membranes and is usually expressed as log *P* [510]. However, compounds that are highly lipophilic tend to bind to the lipid membranes [514]. Furthermore, some highly lipophilic drugs have poor CNS penetration [515]. As such, lipophilicity of a compound does not necessarily make it permeable which highlights the need for an improved understanding of the dynamic BBB and mechanisms that drive transport of drugs targeted in the brain.

Charge

Some compounds can be present in either ionized or unionized form [237]. As such, the penetration of these compounds into the CNS compartments is pH dependent. Furthermore, unionized compounds can penetrate through the lipid membrane barrier more readily than in their ionized form [237]. Under

healthy conditions blood pH is generally higher than CSF, however, the pH of CSF decreases in the presence of bacterial meningitis, as such drugs that are weak acids would readily diffuse from the CNS to the blood [516]. In the presence of bacterial meningitis, the brain barriers become leaky, as such these physiochemical properties become less important as drugs that have poor penetration readily enter the CSF [237].

In summary, physiochemical properties that favour CNS penetration include a log $P \leq$ (octanol/water partition coefficient), a molecular weight $\leq$ 500 Da and a neutral or basic P*K*a (log of the acid ionization constant) [517–519].

Penetration of anti-TB drugs into CSF

Fluoroquinolones, ie, ciprofloxacin (CPX) and moxifloxacin (MOX) are used to treat CNS infections including TBM [520]. This is owing to their physiochemical properties; uncharged, moderate lipophilicity, small size and low protein binding which favours their CSF penetration. Linezolid (LZD), has also been shown to readily cross into the CSF in both inflamed and uninflamed meninges [521–523]. On the contrary, rifamycins, although lipophilic, are 80% protein bound and have a high molecular mass above 800 Da which results in moderate CSF penetration particularly when meningeal inflammation is resolving [8,524–528]. Except in the case of DR, TBM treatment should always include INH and pyrazinamide (PZA), which have moderate lipophilicity and small molecular mass allowing adequate penetration into the CSF [524,527,529,530]. In addition, ethionamide (ETH) has been shown to also readily enter the CSF [524].

3. Intracerebral distribution

Factors that affect intracerebral drug distribution

Cerebral blood flow

Two parameters that influence cerebral blood flow have been described: 1) A change in linear velocity of blood flow through the perfused capillaries and 2) Variations in the total number of perfused capillaries in the brain [299]. An increase in linear velocity of blood flow would result in an increase in transport of highly permeable drugs across the BBB and vice versa whereas BBB transport of impermeable drugs will remain unchanged [299]. Changes in the number of perfused capillaries will in theory affect BBB transport of all drugs [299].

CSF turnover

Production of CSF

The CSF compartments include; intracerebral ventricles, subarachnoid spaces of the brain and spinal, and the central spinal cord canal [381]. The classic hypothesis states that CSF is produced by the choroid

plexus, which is located at the roof of the third and fourth ventricles and the walls of the lateral ventricles. Further, CSF is produced by the interstitium and meninges [381]. Active secretion by the choroid epithelium and filtration of plasma across the endothelial wall of the choroid capillary constitute the VCSF [531]. Over time, findings from various studies have discovered that CSF physiology is much more complex [532–539], furthermore, an updated theory highlights that what is important for CSF formation is the influx and exchange of fluid at the capillary level in the CNS which stresses that CSF is not exclusively formed in the ventricles, suggesting that the whole CSF system participates in formation and absorption of CSF [535,540–544]. This stresses that hydrostatic and osmotic pressure may play the main role in the regulation of the CSF volume and that the imbalance between these forces would result in changes in CSF volumes [532].

The mean CSF production in humans is approximately 0.36 mL/min, 20 mL/hr or 500 mL/day. The hydrostatic pressure within the ventricular system is about 10-15 cm H_20; an increase above 20 cm H_20 is considered abnormal [545]. CSF has various functions which include; mechanical protection of the brain by absorption of shock, metabolic homeostasis by maintaining the electrolytic environment and systemic acid-base balance, and function as a lymphatic system by drainage of degradation products of cellular metabolism and transport hormones, neurotransmitters, releasing factors and other CNS neuropeptides [545,546]. Furthermore, neurotoxic waste products produced during awake or sleep are removed via the CSF [381].

The rate of CSF production is influenced by age, cerebral perfusion pressure (CPP), drugs and compounds including diuretics [547]. CSF is an important diagnostic tool and provides information about the inflammatory response and drug delivery as a surrogate in the injured brain [381].

Dynamics of CSF flow

Once CSF is produced, the classical theory describes that CSF flows out from the lateral ventricles via the foramina of Monro into the third ventricle, through the narrow aqueduct of Sylvius into the fourth ventricle, exits into the various basal cisterns and then into the subarachnoid space through the paired foramina of Lushka and the single foramen of Magendie [531,548]. Furthermore, CSF flowing from the ventricles into the cisterns further divides into the cortical and lumbar subarachnoid space [531]. CSF drains back into the peripheral bloodstream through arachnoid granulations into the superior sagittal sinus and via the spinal nerve roots and olfactory tracts [383]. These serve as exit routes for bulk CSF [549].

CSF flow is stated to be driven by unidirectional bulk flow, pulsatile to-and-fro movement and continuous bi-directional fluid exchange at the BBB and the cell membranes at the borders between CSF and interstitial fluid spaces through the arterio-venous gradient [531,546]. However, new concepts of CSF physiology have emerged as drawn from animal studies which show that CSF does not

unidirectionally move from ventricles to the subarachnoid space and that arachnoid granulations of the dural sinuses are not the dominant site of reabsorption when compared to the big absorptive surface area of the microvessel network of the central nervous tissue [535,542,543]. Furthermore, movement of CSF has been described to differ between cranial subdural space and spinal compartments owing to anatomical and biophysical characteristics [539]. The distribution of a substance in the CSF is suggested to depend on the half-life of that substance inside the CSF and the authors also highlight the importance of distinguishing the CSF movement and distribution of substances within CSF [550–553]. The physiology of CSF movement in the CNS is complicated, in particular, its rate of formation, distribution through ventricles and the subarachnoid system in the cranium and spine; this complexity may be increased in pathological states, which has implications for how we interpret drug concentrations in different compartments.

Studies have suggested that drug dispersion is enhanced by CSF pulsatility (heart rate and CSF stroke volume) and this leads to a high inter-and intrapatient variability in distribution of the drug in the brain [554,555]. In addition, there is a continuous flow of ECF in the brain and spinal cord towards the CSF space leading to equilibrium of drug concentrations in the ECF and the CSF space by diffusion [237]. However, this could not be the case in an injured brain.

CSF flow and infection/pathology

The pathological decrease in CSF flow rate can result from different sources such as inflammatory diseases which results in reduced CSF flow or tumour blocking the subarachnoid space [121,556]. Simulation findings have shown that a change in CSF dynamics changed the CSF PK profiles but not necessarily the brain ECF profiles regardless of the drug's physiochemical properties [557]. Pathologically, CSF dynamics will be affected by HCP, where CSF volume in the ventricles is larger (which will affect dilution of drug entering through the choroid plexus or brain interstitium) and spinal subarachnoid disease (which will affect circulation between brain and spinal CSF). These findings reiterate that caution must be applied when interpreting LCSF as a proxy for brain ECF concentrations in CNS diseases [557].

Blood-derived vs brain-derived proteins in CSF

In the normal CSF, the main fraction of proteins originate from the blood e.g. albumin 35-80% total protein [556] and about 20% is mostly brain-derived, but rarely brain-specific [558]. Transfer of protein from the brain into CSF and blood into CSF follows the laws of diffusion as a function of molecular size [559]. This results in blood-derived proteins such as albumin equilibrating faster between blood and CSF as compared to larger molecules e.g. Immunoglobulins (IgG, IgA or IgM) [559]. Furthermore, the absolute concentrations of blood-derived proteins would be variable between patients as it depends on individual serum concentrations, site of puncture and volume of extraction as modulated by CSF

flow rate [559]. The brain-derived proteins are distinguished from blood-derived proteins by their higher concentrations in the CSF as compared to serum which leads to a net flux of proteins out of CSF [531]. Furthermore, brain-derived proteins have variable sources which include; brain cells or leptomeningeal cells which influence their dynamics [560]. Blood-derived proteins enter the CSF space via passive diffusion along the concentration gradient [531]. In addition, blood proteins enter into CSF along its way between the ventricles and lumbar subarachnoid space, inducing a 2.5-fold increase in total protein concentration between the two brain compartments [559].

Early ideas described that an increase in protein concentrations in CSF resulted from morphological leakage or breakdown of the BBB [531]. Furthermore, neonates are reported to have an immature choroid plexus, which enables small lipophilic molecules and blood-derived proteins to cross to the CSF through epithelial cells. These have been suggested to lead to higher concentrations of lipophilic anti-infectives as compared to adults and older children [237,513]. However, the idea of the immature barrier has been refuted by a study that showed that it is the slow CSF flow rate that contributes to the high total protein in neonates [531]. Furthermore, development of the spinal canal leads to a slow increase of blood-derived proteins in the CSF [531].

The blood-derived proteins increase non-linearly along the rostro-caudal flow way [531]. Reiber states that these findings give strong evidence for CSF flow rate as the main modulator of protein dynamics in the normal and pathological BCSFB function [121,531]. A case report of a patient who developed post-operative recurrent bacterial meningitis showed differences in the biochemical results (leukocytes, glucose and protein concentrations) of both L-and VCSF compartments [138]. This highlighted the presence of a rostro-caudal gradient of leukocytes and protein and an inverse gradient of glucose, particularly in the acute phase of infection [138]. This highlights the complexity of the dynamics in the injured brain. Other non-bacterial infections also support this increase in protein and leukocytes, greater in LCSF as compared to VCSF [561] which confirms CSF flow rate as the main driver resulting from pathology and not necessarily loss of BBB integrity.

In essence, the transfer of blood-derived proteins can increase non-linearly from reduced CSF flow rate without any change in morphological structures [531]. It has been described that the blood-derived proteins at the LCSF are pooled through different structures and locations [531,549].

The main differences between the brain-derived and the blood-derived proteins have been described as best characterised by two concentration gradients; the CSF/blood concentration ratio (CSF/serum quotients and the V-/CSF concentration gradient (rostro/caudal ratio) [531]. Brain-derived proteins are categorised into 3 groups with differences in consequences for their dynamics: 1) proteins originating from brain cells e.g. *tau* which are mainly released into V- and LCSF, 2) proteins mainly released from

leptomeninges into CSF e.g. β-trace protein and 3) proteins with a non-negligible blood-derived fraction in CSF e.g. angiotensin-converting enzyme [531,560].

Brain ECF

The BBB restricts movement of ions and fluids between the blood and the brain thereby ensuring a brain ECF that provides an optimal medium for neuronal function [562]. The brain ECF provides an environment in which brain cells survive and function [120]. In contrast to plasma, brain ECF has much lower protein content, lower K^+ and Ca^{2+} and higher Mg^{2+} [386].

Distribution of drugs in the brain

Target site kinetics

Various studies have demonstrated that the information on drug concentrations using whole tissue homogenates is limited as it does not account for the compartments such as interstitial fluid, cells and subcellular organelles within a tissue. Concentrations could be underestimated if the drug targets the extracellular compartment and overestimated if the drug is accumulated in the cells [563–565]. Furthermore, drug concentrations in the tissue homogenates would vary depending on how the tissue homogenates were prepared, how the drug of interest was extracted and the method by which the drug was quantified [237].

The CNS cannot be viewed as a single physiological compartment, as it is divided into CSF, extracellular and intracellular spaces of the brain and the spinal cord. Studies have shown that even within one compartment, there would be variability in the concentrations of the drug [547,566]. Research thus far has relied on LCSF, one of the fluid brain compartments, as a surrogate of drug concentrations in the brain tissue following systemic administration [567]. This is not representative of the site of disease and gives very little information about drug distribution within the brain and the larger CNS. Furthermore, a study has shown that there are differences between the V- and LCSF transcriptomic signatures overrepresented by neuronal injury and protein translation plus cytokine signalling respectively in TBM disease, which would influence the penetration of the drug and efficacy [144]. An early study of the drug kinetics of methotrexate found that administration via the Ommaya reservoir resulted in adequate distribution of the drug as compared to administration through LP. This shows differences in the CSF flow dynamics of the two compartments [568]. The findings also highlighted that there is variability in drug concentrations in ventricular, cisternal and lumbar compartments [568].

A more recent cross-species study in TBM corroborates this argument with findings which showed discordant RIF levels in CSF when compared to those in brain parenchyma [343]. This study found higher levels of cytokines in CSF of mice infected with TBM than in brain tissue [343]. As such, these findings support that drug concentrations [343,569], protein expression [144] and inflammation

[241,343] are compartmentalized, reinforcing that the CNS cannot be viewed as a single physiological compartment.

Drug Metabolism in the brain

The brain also has localized metabolic enzymes, many of which have been discussed above. These include oxidoreductases (CYPs and monoamine oxidase), membrane-bound and soluble catechol-o-methyltransferase (COMT), transferases (UGTs) and phenol sulfotransferase (PST) [300]. These enzymes are important in the oxidation or deactivation of endogenous or exogenous compounds [570]. Furthermore, expression of CYPs varies in different regions of the brain [571].

Elimination

The liver and kidneys play a big role in the elimination of unchanged drugs and their metabolites [320]. Renal excretion of drugs involves three processes which include; glomerular filtration, renal tubular secretion and reabsorption from the renal tubular lumen [320]. These processes are affected by development and reach adult levels by 8-12 months postnatal age [572] and during the first year of life for glomerular filtration rate and renal tubular secretion respectively [275].

The basolateral membrane of the renal epithelial cells contains various active transporters responsible for drug uptake. Furthermore, active transporters at the luminal brush border membrane are responsible for the last step of excretion of drug into urine [573]. The pH of urine has been reported to influence the elimination of drugs, which may increase the reabsorption of weakly acidic drugs [574].

It is evident that development has an impact on processes that characterise PK (ADME) which highlights that children cannot be treated as small adults and advocates for age-appropriate dose regimens.

Methods of drug delivery to the brain

Drug delivery to the brain is very challenging owing to various barriers that a therapeutic agent has to overcome until it reaches the target site in the CNS [575]. The main barrier is the BBB, as such, strategies of drug delivery into the CNS need to take the BBB into account during drug development stages [379]. Studies are underway to develop methods that will enhance drug entry into the brain.

The easiest way to increase drug concentrations in the brain is to increase systemic concentrations as advocated in recent studies of increased RIF dosage [237]. However, drugs such as ethambutol (EMB) become toxic at higher concentrations [576,577]. Use of intraventricular administration of drugs to treat CNS infections is to be avoided as findings show that this increased mortality in neonates as compared to IV route [578]. Other approaches have been described that involve in vitro models [579–581], receptor-mediated and adsorptive-mediated transcytosis [582,583], influx transporter [584], inhibition

of efflux transporters [585], modulating the integrity of the BBB and bypassing the barriers by use of convection-enhanced delivery and injection into the CSF [586,587].

Use of Nanotechnology

Another approach currently gaining momentum is nanotechnology. Nanotechnology is a multidisciplinary field that has made an impact on drug delivery and diagnostics through the development of various nanodevices such as liposomes, nanocrystals, nanoparticles and dendrimers [588]. An ideal nanocarrier has been described as constituting the following features; biocompatibility, having the capacity to protect its contents from degradation, the potential to reach its target site in the CNS, and biodegradability [575].

Nanodevices can improve the bioavailability of the drug, reduce the therapeutic dosage by increasing the drug exposure and reduce adverse off-target effects [588]. These nanodevices can either enclose, be conjugated to or complexed at the surface of the therapeutic agent [588]. Strategies that enable efficient drug delivery of anti-TB drugs have been investigated to establish the potential use of biodegradable nanoparticle-based delivery systems for drug therapy against TB [589]. Polymeric nanobeads are preferable as the polymer provides a protective coat for a drug after it is administered as compared to use of liposome [590] and solid-lipid [591] nanoparticles which are less stable [589].

Drug delivery has been investigated for front-line drugs; RIF, INH and PZA in combination with poly(lactic-co-glycolic-acid) (PGLA) *in vitro* [592,593]. In addition, a drug delivery system approach or nano-formulations have been developed to improve drug delivery, particularly in treatment using anti-TB drugs [594].

CHAPTER 4: TREATMENT OF PAEDIATRIC TBM

Regimen in children

Childhood TB represents at least 10-20% of the total TB cases, particularly in endemic areas with poor infection control [595–597]. Children accounted for 11% of all TB cases in 2021[1]. Furthermore, of the 2021 global TB deaths, 14% of these were in HIV negative children and 11% were in HIV positive children [1]. TBM remains one of the most common causes of paediatric bacterial meningitis in the WC, SA [3].

Until recently, WHO recommended that children with drug-susceptible TBM be treated with a 2 months regimen of RIF (10 mg/kg), INH (15 mg/kg), PZA (35 mg/kg) and EMB (20 mg/kg) followed by 10 months of RIF and INH with doses similar to those of PTB [598]. Following findings of similar completion and relapse rates of 6 months regimen vs longer regimens [599], a study in the WC, SA investigated a short-course intensive regimen for 6 months in HIV negative and 9 months in HIV positive children with a combination of RIF (20 mg/kg), INH (15-20 mg/kg), PZA (40 mg/kg) and ETH (20 mg/kg), which proved successful [600]. The findings showed that of 184 children, 147 (80%) had good outcomes and 7 (3.8%) died. TBM therapy should be started as soon as the diagnosis is considered [601].

Most recently, in the 2022 Child and Adolescent Guideline, WHO reviewed existing data relating to the treatment of paediatric TBM. Using a systemic review approach, the WHO-recommended 12-month regimen as described above was compared with a shorter intensive regimen which includes, INH, RIF, PZA at higher dosages combined with ETH for 6 months in HIV negative and 9 months if HIV positive children. Findings showed lower mortality in children treated with an intensive 6-month regimen compared to the WHO recommended 12-month regimen. As such, WHO decided that the intensive 6 months regimen could be used as an alternative to the 12-month regimen [602].

Corticosteroids have been recommended for all children with TBM at a dose of 2 mg/kg (prednisone) for the first month of treatment [75]. This dose is gradually reduced over 1-2 weeks before stopping [220].

System and drug properties which govern anti-TB drugs target site kinetics

For an anti-TB drug to kill the TB bacteria, it must be able to penetrate the complex host lesions and lesion compartments with varying cell types [603–605] at optimal concentrations for the required time as illustrated in Figure 4.1.

This becomes even more challenging for intracellular bacilli as the drug must be able to pass through the cell membrane and organelles, including the intracellular bodies within different cell types [606]. Furthermore, anti-TB drugs targeted to the brain have to overcome the BBB and potential efflux

transporters and drug-metabolizing enzymes prior to entry to the target brain cell types. The idea is that the concentration of the drug within its mycobacterial cell is influenced by multiple factors, including passive and active uptake, pathogen-mediated metabolism, active drug efflux and cell growth [273,607].

As such, plasma and tissue PK analysis may not provide a full picture of the target site kinetics [273]. This has been shown in PK studies that advocate for high dosages of RIF [608–610]. The consequence of suboptimal drug exposure is an increased burden of disease, the development of resistance and the risk of mortality [116,611].

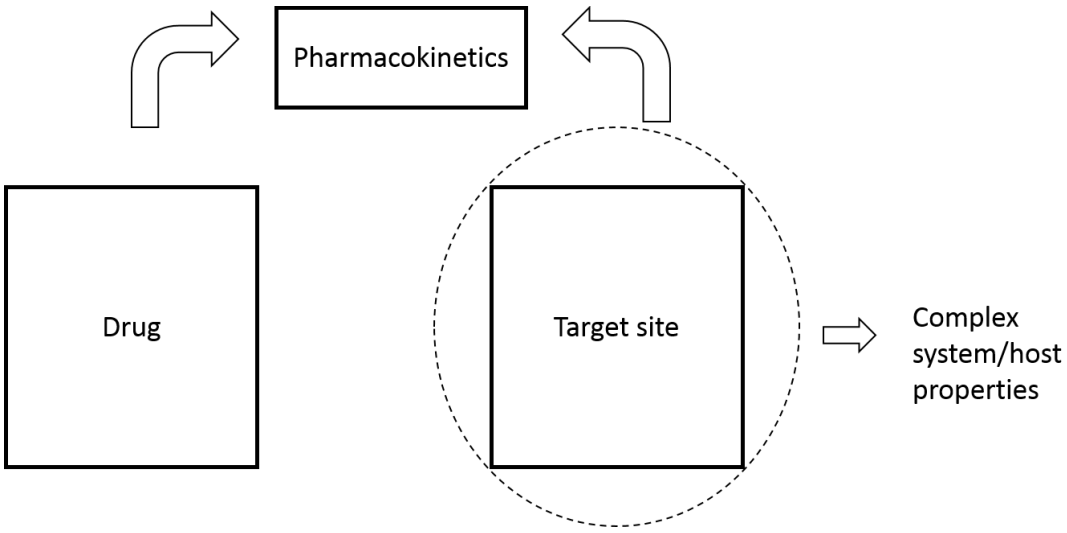

Figure 4.1. host/system and drug properties (adapted from de Lange *et al*. 2013 [298]

Development of Drug resistance

Multidrug resistance (MDR) which is defined as resistance to at least INH and RIF, remains a major public health problem, particularly in TB-endemic geographical settings with poor TB control programmes [612].

DR-TB has been widely reported in children, which is a cause for concern [613–617]. Extensively drug resistance defined as MDR with resistance to fluoroquinolones and 1 second-line injectable agent has also been reported [618].

Drug-resistant TBM

INH monoresistance is seen as the most dominant form of DR-TBM [619,620]. However, TBM patients with HIV-coinfection are at high risk of RIF-resistant TBM [5,620]. Detection of DR-TBM is often challenging owing to low sensitivity of assays in CSF, despite the availability of Xpert and a more recent Ultra assay. Furthermore, DR-TBM is associated with high mortality rates of up to 100% [52]. Therefore, there is a dire need for robust assays for rapid detection of DR-TBM and optimal treatment regimens to treat resistant forms of TBM.

A study in children with CNS-TB in Mumbai reported that previous TB treatment and disseminated TB were independent risk factors for CNS-TB which implies that effective monitoring of patients to ensure adherence and compliance could help prevent the emergence of DR-TB [621].

Treatment and management of drug-resistant TB/TBM

Challenges of administering Second-line drugs to children

Management of children with DR-TB poses a challenge owing to difficulty in diagnosing, limited expertise in dealing with these patients, length of treatment and limited optimal drugs and child-friendly formulations [622].

Formulation

Use of second-line drugs in children is difficult owing to the tablet sizes which have to be subjected to breaking or crushing which may result in suboptimal or toxic levels and potential loss of the active pharmaceutical ingredient [622]. Furthermore, most of the drugs have side effects and often have a horrible taste [623]. In addition, some of the second-line anti-TB drugs are in liquid form or suspension which have their drawbacks including storage and stability [622]. The paediatric formulations problem led to a guideline as outlined by the WHO which favours dispersible tablets [624]. However, second-line anti-TB dispersible tablets are still not available [624].

Regimen in DR-TB

Several factors affect the PK of anti-TB drugs in children such as age [625–627], malabsorption, HIV infection [628,629] poor nutritional status [630] and variable pharmacogenetics [631] which must be taken into consideration. Optimal dosing of second-line drugs has not been established in children [623]. A report by the WHO outlines a programmatic approach to treating DR forms of TB of which 4 to 5 drugs must be included to make a regimen. Drugs are categorised into groups for treatment of DR-TB:

The injectable drugs

The injectables are categorised into group 2 and include aminoglycosides such as kanamycin (KAN), amikacin (AMK), streptomycin (STR) and the cyclic polypeptide, capreomycin (CAP). Cross-resistance has been shown between AMK and KAN in that the *Mtb* strains that are resistant to one of the drugs are also resistant to the other [632]. Furthermore, studies have also shown that if a strain is resistant to an aminoglycoside, it will also be resistant to CAP [633,634].

Fluoroquinolones

Fluoroquinolones (FQs) include ofloxacin (OFX), CPX, levofloxacin (LFX), MOX and gatifloxacin (GFX). A study in adults with PTB found that LFX, GFX and MOX show similar activity to that of INH in a pooled comparison and may exceed activity after several days [635]. FQs show excellent CSF penetration in treatment of patients with TBM against drug-sensitive and DR bacteria [636,637]. However, use of fluoroquinolones has been investigated in various clinical trials and has not shown survival benefit when used in combination with current first-line drugs, particularly for drug-sensitive TB [619,638–641].

Oral bacteriostatic second-line agents

This group consists of thioamides which include ETH and prothionamide (PTH). This class of drugs has been shown to have common biochemical pathways with INH in their activation and demonstrate cross-resistance [642,643]. ETH is 30% protein bound and it readily distributes throughout the body including the CSF [644]. It has been shown that an ETH dose range of 15-20 mg/kg achieves adequate serum concentrations in children [645]. An editorial by Hill *et al*. [646] highlighted the problematic inclusion of ETH in the intensive TBM short-course regimen owing to it being a second-line drug, associated with considerable nausea and vomiting and recommended LFX with its limited adverse effects and no drug-drug interactions with RIF [647].

Other bacteriostatic agents include cycloserine (CS) and terizidone (TRD). The MIC of both agents have been described, with terizidone showing variability [648,649]. In addition, CS has been reported to be widely distributed in the body including the CSF. There remains little data on the PK of CS and TRD in children [650].

In addition to the bacteriostatic agents, para-aminosalicylic acid (PAS) is an old TB drug which is 50-60% protein bound with a half-life ($t_{1/2}$) of 45-60 min and poor CSF penetration [651]. Serum levels of PAS have been investigated in children who were given 300 mg/kg/day, divided into 5 doses of 60 mg/kg. This study showed a T_{max} at 60 min and serum C_{max} was between 6.25 μg/mL and 12 μg/mL. The CSF peak concentrations were found to be generally greater than 1μg/mL [652]. As such PAS concentrations are low in CSF [601].

Repurposed drugs

An increase in *Mtb* strains that are resistant to existing drugs has led to a rethink of old existing drugs that were not included in the first and second-line anti-TB drug regimen. One of these drugs is clofazimine, an old drug that was discovered in 1945 and mostly used to treat *mycobacterium leprae.*

A study has reported the addition of clofazimine (CFZ) in adults diagnosed with MDR-TB which proved effective in most patients as compared to regimens based on OFX and commonly PTH [653]. CFZ has been suggested to concentrate within the macrophages as compared to serum, thereby targeting intracellular bacteria [623,654]. However, CFZ does not penetrate well in CSF but has been shown to widely distribute in brain tissue of mice [655,656].

Other drugs in the group 5 category include thiacetazone (TAZ), clarithromycin, amoxicillin and carbapenems (imipenem and meropenem). TAZ became an unfavourable drug due to severe reactions in HIV patients and its cross-resistance with ETH at 29-79% [657]. Meropenem has been shown to have good CSF penetration and activity against persisters grown in anaerobic media [658].

LZD

LZD is one of the repurposed drugs with a novel mechanism of action. PK clinical trials have been done in children of varying ages which has shown that the drug is cleared faster and has a shorter elimination $t_{1/2}$ as compared to adults [659–661]. A phase III clinical trial comparing oral or intravenously (IV) administered LZD with vancomycin suggested that children younger than 12 should be dosed with 10 mg/kg of LZD every 8 hrs to achieve similar exposures to adults receiving 600 mg/kg twice daily [662,663]. Furthermore, a small retrospective cohort study in children showed improved clinical outcomes in patients who were without clinical improvement after two weeks of a standard regimen, suggesting that LZD may be used as an additional drug in treatment of TBM when given for a short-duration (< 4 weeks) to avoid adverse reactions [664]. LZD has been shown to widely distribute in the body after oral administration and achieves good CSF penetration in treatment of vancomycin-resistant *enterococcus meningitis* [665].

Furthermore, LZD has been used in regimens to treat MDR/extensively drug-resistant (XDR)-TB in adults and children [618,666–671]. However, future studies are required to establish optimal dosing frequency in PTB and TBM.

New drugs

Delamanid

Delamanid (DLM) (OPC-67683), is one of the new TB drugs with a low MIC concentration of 1-12 ng/mL against *Mtb* [672]. DLM has been described for compassionate use in treatment of XDR-TB in a 12-year-old boy through assistance of the ERS/WHO TB consortium in a Milan outbreak [673].

A recent study compared (DLM) concentrations in brain tissue and CSF of 6 rabbits with experimentally induced TBM and steady-state CSF concentrations in 3 humans undergoing treatment of MDR-TB. Their findings in rabbits suggest that DLM reaches adequate concentrations in the brain tissue; mean 518 ng/mL at 9 hrs and 74.0 ng/mL at 24 hrs [672]. This is despite significantly low total CSF concentrations in rabbits (1.26 ng/mL at 9 hrs, 0.47 ng/mL at 24 hrs) and humans (48 ng/mL at 4 hrs) as compared to plasma respectively (124 ng/mL at 9 hrs, 14.5 ng/mL at 24 hrs) vs (726 ng/mL at 4 hrs) [672]. Furthermore, brain tissue DLM concentrations were 5 fold higher than plasma concentrations in rabbits [672]. This study highlights the potential use of DLM in the clinical treatment of TBM to target infected brain tissue.

Bedaquiline and Pretomanid

It has been stated that the high protein binding in the new drugs DLM, bedaquiline (BDQ) and pretomanid (PMD) may limit their penetration into the CSF and increasing in their dose is not a possibility due to potential adverse events [674–676].

There is a need for innovative phase II and phase III clinical trials for new regimens with tools and methods to combat anti-TB DR worldwide [677]. Strides have been made with suggestive drug combinations; one study administered a combination of high-dose RIF with LFX to treat TBM with INH resistance resulting in improved survival [619].

Most recently, a prospective study in adults determined the PK of second-line drugs (LZD, CFZ, CS, DLM and BDQ) in CSF of TBM patients [678]. All CSF measurements of BDQ, DLM and CFZ were below limit of quantification (BLQ) [678]. The high protein binding of these drugs may have hindered transport into the CNS [679–681]. However, a correspondence by Upon *et al.* highlighted that limits of quantification of an assay must be low enough to be able to measure the unbound concentration of a drug (BDQ) that diffuses freely into CSF, which would be roughly 1/1000th of the total drug in plasma [682] which is in contrast to the used lower limit of quantification (0.01 µg/mL) which is argued to be too high for expected CSF concentrations of a plasma range (0.36-3.15 µg/mL) in their study participants. In contrast, Tucker *et al.* were able to detect DLM in CSF at very low concentrations (range 0-33 ng/mL) [672]. Median CSF concentrations of LZD and CS were 0.90 µg/mL and 15.90 µg/mL at

2 hrs and 3.14 µg/mL and 15.10 µg/mL at 6 hrs respectively [678]. As such, CS had higher penetration in CSF and LZD exhibited high concentrations in CSF at 6 hrs post-dose.

Adverse effects in children

Children being a vulnerable population cannot articulate adverse effects that may develop from being administered a cocktail of anti-TB drugs as compared to adults. As such, extra monitoring is crucial during treatment of both PTB and CNS TB. Furthermore, this becomes challenging when treating for co-infection with HIV owing to drug-drug interactions and possible toxicity [683,684]. RIF for example has been shown to lower the concentrations of ARVs [685].

Adverse effects in children have been well documented which include peripheral neuropathy caused by INH and gastrointestinal and rash caused by first-line drugs [686]. FQs have been investigated and considered safe in children but should be given with caution as they may cause neurological problems, peripheral neuropathy and gastrointestinal disturbances [687–692]. Studies have described adverse effects caused by thioamides, including psychiatric disturbances and dose-limiting gastrointestinal toxicities for ETH [52,693,694]. The use of repurposed drug, CFZ, has been found to cause red-brown skin hyperpigmentation which resolves over time [695]. Adverse effects that include headaches and gastrointestinal disturbances have been described in children given short-course LZD [696,697].

Focus on RIF

RIF is an important anti-TB drug which kills bacteria by interfering with the synthesis of mRNA by binding to RNA polymerase [698] and has been included in standard chemotherapy since the 1980s. The inclusion of RIF was critical in the shortening of treatment duration in patients diagnosed with PTB to 6 months when combined with PZA in the first 2 months [609,699–701]. RIF also undergoes deacetylation resulting in its main metabolic derivative, 25-desacetyl-RIF, which is a major contributor to the antibacterial activity in the bile [702].

Use of 600 mg of RIF

Early studies established the use of 600 mg of RIF (8-12 mg/kg/day) daily dose based on the argument of PK data, toxicity and cost [703]. This led to the wide use of 600 mg dose for adults that was eventually included in the TB treatment guidelines [704–706].

It was described that an experience with administration of intermittent high-dose RIF (twice-weekly) at 1,200 mg with 900 mg INH led to the end of the clinical trials with high-dose RIF owing to the high incidence of side effects [707,708]. However, a study that investigated 450 mg, 600 mg and 750 mg of RIF did not find any significant sputum conversion but observed higher treatment failure in patients who received 450 mg of RIF. As such, high-dose RIF should be given daily [709,710].

A rethink of high-dose RIF has led to a resurgence of studies investigating an increase in RIF dosage [641,711–713]. These studies suggest that high dose RIF accelerates bacillary clearance kills persister organisms and a maximum tolerated dose in humans is ~ 40 mg/kg/day [610,714–716].

A recent study in Vietnam administered high dose RIF 15 mg/kg in patients with DR-TBM and there was no overall improvement of the intensified regimen [619]. However, patients who had INH-resistant TBM showed an improvement in survival [619,639]. An increase in the standard-of-care dose of 10 mg/kg showed ~6 and ~8 fold higher exposures when TBM patients are administered with 20 mg/kg IV and 35 mg/kg high dose oral RIF respectively, in a HIV positive Ugandan adult population [717]. Furthermore, increased CSF concentrations above MIC were also observed [717].

Studies have also shown varying improvement in mortality when TBM patients are administered an intensified RIF dose as compared to the standard dose. An Indonesian study showed a 6 months reduction in mortality from 65% to 35 % with a 3 fold increase in CSF concentrations in patients who were administered ~ 13 mg/kg of RIF via IV as compared to ~ 10 mg/kg of RIF [638] vs a Vietnamese study that showed no improvement in mortality in TBM patients who received an oral intensified RIF dose of 15 mg/kg vs standard RIF dose of 10 mg/kg [718].

RIF as an inducer of hepatic drug-metabolizing enzymes

Early studies have shown that RIF is a strong inducer of hepatic drug-metabolizing enzymes [719–721]. This is independent of the route of administration as found in a study done in adults with PTB who underwent oral vs IV dosing [722]. Consequently, blood levels of RIF have been shown to decrease in the early days of treatment through self-induced autoinduction [702,723]. In addition, a South African study investigated RIF serum concentrations at days 1 and 5 of treatment at doses 150, 300 and 600 mg and found a decrease in C_{max} values from 2.53, 3.19 and 13 μg/mL at day 1 to 1.49, 2.89 and 9.53 μg/mL at day 5 respectively [724].

Studies have shown that the maximum induction of drug-metabolizing enzymes is achieved within 24-40 days using RIF PK-enzyme turnover models [723,725]. RIF autoinduction which results from a decrease in RIF exposure with time owing to an increase in elimination by induction of enzymes and/or transporters caused by RIF [702] has also been found to be dose and concentration-dependent [723,726].

RIF resistance

RIF resistance is caused by spontaneous mutations in *rpoB* region, which is a consequence of insufficient intracellular RIF concentrations to bind RNA polymerase [727]. The intracellular concentration of RIF that is available to bind RNA polymerase has been described as a major determinant of developing mutations [728,729]. As such, mutations have been found in the *rpoB* region of *Mtb* in 97% of resistant clinical isolates [727]. This mutation results from single nucleotide

substitution in the *rpoB* region, which is the gene that encodes the β subunit of the deoxyribonucleic acid (DNA)-dependent RNA polymerase [730]. Most of RIF resistant mutations have been found in the 81 bp region of cluster I, also known as the RIF resistance determining region (RRDR) [731,732]. However, RIF mutations have also been found in other *rpoB* regions [733–735]. This RRDR was defined in early studies of *Escherichia* [727,736]. One of the key properties of RIF and drugs such as MOX and BDQ is the ability to retain activity against slow-growing *Mtb*, so-called persisters [737,738]. RIF resistant TBM is 69-100% fatal [619,739–741].

Factors that have an impact on the PK of RIF

Impact of food

The recommended RIF serum concentration 2 hrs post-dose is 8 μg/mL and values lower than this are considered suboptimal [742]. It is suggested that fasting before the administration of RIF could reduce inter-and intraindividual variability [609]. This is owing to findings of reduced absorption of RIF and extended time to C_{max} following ingestion of food as compared to RIF given in a fasted state [743,744]. As such, It has therefore been recommended that RIF be given without food to achieve optimal absorption and also reduce inter-and intra-individual variability [609].

Pharmacogenetics

The SLCO1B1 rs4149032 polymorphism is associated with reduced mean RIF exposures (AUC_{0-24}) [745], which must be taken into consideration when recommending RIF dose in the South African population where it was found to be highly prevalent [745,746]. Furthermore, simulations from a population PK model found that increasing the RIF daily dose to 150 mg in patients with the polymorphism would double the number of patients reaching the C_{max} of ≥ 8 μg/mL [746].

Pathophysiological profile

PK processes can be altered in response to the pathophysiological profile [747]. The impact of malnutrition on the PK of RIF depends on various factors, such as plasma protein binding or absorption which poses a challenge as either one may influence the PK of the drug, e.g. a malnourished patient may exhibit low plasma protein concentrations resulting in increased free drug concentrations in plasma [748]. Other factors that could affect the PK of RIF include, HIV status [749,750] and hepatic impairment [751].

HIV status

A study done in a cohort of Vietnamese patients with HIV-associated TBM showed that TBM/HIV positive patients are prone to lower RIF CSF exposures [752]. However, CSF concentrations were only measured at 2 hrs post-dose and given that there is a delay of drug distribution from systemic to CSF,

subsequent collection of data e.g., at 6 hrs would provide more insight. Furthermore, this has been shown to be independent of time of initiation of ARVs; Immediate vs delayed ARV. The general interaction between ARV treatment in TB-coinfected patients has conflicting results in that there isn't a consensus on whether ARVs reduce RIF exposure [753,754] or affects PK of RIF [755] when compared to HIV negative individuals.

Higher dosage of RIF

Given that RIF is a key drug in treatment of both CNS- and PTB. Studies have been done to investigate the potential use of higher dosages of RIF to aid in shortening the treatment duration, increase concentrations of the drug that will reach the target site of infection in TBM and also reduce the risk of antibiotic resistance emergence [639,714,716,756–765].

Studies have shown that RIF exhibits a dose-dependent increase in serum [724,763,764]. As such, an increase in the dose would result in an increase in RIF exposure over time [714]. This has been suggested to result from saturable biliary excretion or liver transport saturation, increasing the bioavailability of RIF [723,766,767]. The non-linear increase should be taken into consideration when increasing the dose to achieve optimal therapeutic concentrations, particularly in CNS infections [767].

Boeree *et al*, reported that RIF given at 35 mg/kg dose results in a greater than dose-proportional increase in plasma RIF C_{max} and AUC_{24} values and also reduces the time to sputum conversion in liquid media from 62-48 days compared to standard treatment [760]. The findings show the potential to improve treatment outcomes and shorten regimens. Similarly, a higher dose of RIF (35 mg/kg) has been shown to increase RIF exposure and also shorten the time to sputum culture conversion as the time from the start of treatment to the first 2 consecutive cultures in a cohort of patients with PTB [610]. Furthermore, an Indonesian study showed reduced mortality by > 50% when high-dose IV RIF (13 mg/kg) was given [638].

Studies done in murine models suggest that an increase in RIF dosage improves its sterilizing and bactericidal effect, thereby shortening treatment [761,768–770]. Treatment of TBM requires a higher $C_{max} \geq 22$ μg/mL and AUC from time zero to 6 hrs (AUC_6) ≥70 μg.h/mL, this has been associated with reduced mortality [609].

Paediatric clinical trials in TBM

Past reports have shown that there is limited data on safety, dosing and drug-drug interactions of anti-TB drugs in children [694,771,772]. This has resulted in variability of guidelines given the scarcity of clinical trials to inform practice [598,600]. Children, unlike adults, experience changes in the body compartments that influence how they absorb, metabolize and excrete drugs which contributes to the differences in the PK profile as seen in adults [773]. A consensus focusing on the inclusion of children

in TB drug trials reported that there was a lag in several PK studies in children as compared to adults [774]. Furthermore, paediatric phase I and II clinical trials can only be initiated once there is availability of adult safety data [774]. Most recently, there has been a surge of paediatric clinical trials in TBM to optimize treatment and outcomes [775,776] and other studies are underway (e.g. the SURE) study.

PK of anti-TB drugs in treatment of paediatric TBM

Treatment of TBM in children is based on doses tailored for PTB in adults [601]. Although the antibiotics used to treat TBM have been available for more than 60 years, there remains limited PK data in children [7].

RIF has been and still is an important drug in treatment of TBM owing to its sterilizing activity [777]. As mentioned in earlier text; the major factors associated with RIF are protein binding and autoinduction. RIF is approximately 80% protein bound which limits its free concentrations [710,778]. However, for doses $\geq$ 600 mg in adults, the free RIF concentration is usually higher than the MIC [528]. Furthermore, RIF induces drug-metabolizing enzymes that may influence drug transport across biological barriers [779].

Studies have reported that RIF improves treatment outcomes in both PTB and TBM patients [756,780]. However, low LCSF exposures of RIF in patients with TBM have been reported [7,524,528,765]. A study in infants with TB dosed according to revised WHO treatment guidelines reported low RIF exposures in both formulations used (granulate for suspension [100 mg/5 mL; Eramfat manufactured by Riemser Arzneimittel, Germany and registered with a stringent regulatory authority vs R-cin (100 mg/5 mL manufactured by Aspen Pharmacare, SA and registered by the Medicines Council of SA), which may have implications for infants diagnosed with TBM [608]. Studies in adults have found that an increase in the dose of RIF correlates with plasma exposures in patients diagnosed with TBM but this still needs to be further investigated in children [756,765]. Furthermore, there was reduced mortality in the high RIF IV dose group (13 mg/kg) as compared to 10 mg/kg standard dose (64% vs 34%) [756]. Future studies investigating high RIF doses may help improve outcome in TBM.

Nahata and colleagues found mean or individual CSF RIF values of less than 1.0 µg/mL in children receiving dosages of 15-20 mg/kg, which is not optimal for killing bacteria in the brain [525]. However, the children who received dosages of 20 mg/kg reached higher RIF concentrations, which advocates for increased dosages in children [525,781]. These findings only reflect concentrations in the CSF, which may not be the case in the brain tissue. Moreover, studies that have reported on VCSF drug exposures were done on non-TBM patients which is not representative of the TBM disease state [525,526].

INH and PZA

Plasma and CSF exposures of PZA and INH have been reported to be comparable in both adults and children [7,524,601,713,782,783].

PZA has been shown to have limited early bactericidal activity in drug-sensitive PTB in the first 2-4 days of treatment, a period considered critical in treatment of TBM [784,785]. A recent study also reported a decrease in PZA exposure in plasma in the early days of TBM treatment [786]. However, PZA activity seems comparable with RIF and INH from days 4-14 [784,785].

INH is metabolized by genetically polymorphic N-acetyltransferase 2 (NAT2) which results in either fast or slow activity [52]. A study by Donald and colleagues demonstrated that acetylation status of a patient diagnosed with TBM can cause major differences in INH CSF concentrations in dosages of 10 mg/kg and 20 mg/kg, however at approximately 3 hrs, the CSF INH concentrations equilibrate to that of plasma irrespective to the type of dosage and acetylation status [529]. These reports are based on plasma and LCSF exposures and do not provide any data on VCSF and brain ECF exposures.

EMB and ETH

Administration of EMB in TBM has seen a decline owing to toxicity at higher dosages and poor penetration into CSF even in early treatment [524,601,787], while ETH has gained interest owing to its efficacy against *Mtb* and good CSF penetration [576,577]. The distribution of ETH into CSF has been studied in children who after receiving a dosage of 15 mg/kg had mean CSF concentrations varying from 0.85, 1.71, 2.51 to 2.71 µg/mL at 1, 1-2, 2-3 to 3-4.5 hrs post-dose respectively whereas mean CSF concentrations at 20 mg/kg dose achieved at the same times were 1.25 µg/mL, 2.55 µg/mL, 3.24 µg/mL and 2.83 µg/mL. Given the higher achieved concentrations, the study suggested administration of 20 mg/kg dose of ETH in children [788].

Inter- and intraindividual variability

A study by McIlleron *et al*, [789] found that variability in concentrations of anti-TB drugs in patients with TB was attributed to factors which included age, dose per kilogram of weight, HIV status and sex. Variability in penetration of first-line anti-TB drugs in CSF has also been described, which predisposes patients to sub-therapeutic CSF concentrations although drug exposure in plasma reach adequate concentrations [601,790,791]. Pouplin and colleagues reported age-dependent variation in plasma and CSF PK of RIF, INH and PZA in children diagnosed with TBM [7].

L-vs VCSF drug exposures

LCSF has been used as a surrogate for drug concentrations in the brain, but VCSF is closer to the target site of infection. There is a need for optimization of drug exposure at the site of infection to improve patient outcomes [675].

The concentrations of anti-TB drugs in plasma and CSF of patients with TBM may be correlated in the early stages of the disease when the BCSFB is disrupted. A reduction of inflammation as a response to treatment may result in reduced CSF concentrations as the BCSFB is restored [237].

The brain extracellular flow drives the distribution of the drug in the CSF compartments [792]. Literature has shown that RIF CSF concentrations following an oral dose of 17 or 20 mg/kg range from 0.125 mg/L to 1.06 mg/L [765]. This is within the RIF MIC range for susceptible strains which spans from 0.06-0.4 mg/L [648,793].

A study by Nau and colleagues in 7 adults who were undergoing ventriculostomy found median RIF concentrations of 0.73 (range 0.57-1.24) µg/ml in VCSF at 1h after an IV dose of 600 mg [526]. Another study in 8 children undergoing VP shunt surgery found a mean concentration of 1.4 (± 1.0; range 0.12-3.00) at 2 hrs post 20 mg/kg dose [525]. These concentrations are higher than the RIF LCSF concentrations ranges reported above possibly owing to the route of dose administration and compartmental flow dynamics. Furthermore, they do not represent the TBM disease state and requires further exploration. Higher levels of protein in CSF have been found to be linked to higher RIF concentrations [759]. The authors suggest that this may be due to leaky barriers that allow penetration of both proteins in RIF [759].

Target site pharmacokinetics

Sampling the brain ECF

Plasma concentrations of anti-TB drugs do not generally predict drug concentrations at the target site of infection [603]. MD enables sampling of the brain ECF and VCSF and provides detailed information on the drug distribution in the brain [8].

Intraoperative MD was applied to determine RIF concentrations in various compartments in patients undergoing craniotomy for tumour removal. Each patient was given 600 mg of RIF infused over 3 hrs in 500 mL of physiological saline [8]. This study found variations of RIF concentrations in the tissue samples that were taken with the highest RIF concentration within tumours (1.37 ± 1.34 µg/mL; n=8) and cerebellar extracellular space RIF concentrations (0.32 ± 0.11 µg/mL; n=6) were the most reproducible using MD when compared with whole-tissue samples [8].

Another study using MD sampling technique in guinea pigs concluded that blood concentrations did not reflect RIF concentrations in the lung, an organ that is proximal to systemic circulation [794]. Arguably, there is a delay for RIF to distribute to the brain as compared to the lungs which stresses the need for target site concentrations to determine if optimal RIF concentrations are achieved within the infected brain.

In addition, the ECF has been described to exhibit volume fluctuations in the normal brain and a decrease during development and ageing which may influence transport of drugs into the brain cells [795,796]. Application of MD as a technique for sampling brain ECF is discussed in detail in the next chapter.

Other methods

Microdosing is a method that uses a radio-labelled drug and dynamic positron emission tomography to visualise the CNS distribution of drugs in living animals and humans [300]. This was demonstrated by Tucker and colleagues who showed that microdosing ^{11}C-rifampicin is a reliable predictor of the biodistribution of therapeutic doses in animals and humans [569]. Although this method is less invasive than MD, microdosing cannot distinguish between the parent compound and its metabolite and between bound and unbound drug [300].

Summary

A recent review strongly suggests that future combination therapies for TB should be based on multidrug regimens optimised according to specific activities and tissue distributions of each constituent drug [273]. Hill *et al*. [646] stressed the need for bold trials that combine optimal antibiotic treatment with therapy that reduces steroid resistant interferon-α -driven inflammation that underlies many of the devastating complications associated with TBM [647,797–799].

Deductions from a meta-analysis in adults with TBM found that plasma exposure was a better predictor of survival than CSF exposure [759]. This is contrary to the idea that CSF owing to its closeness to the brain would be a better proxy for drug penetration as well as prediction of survival. However, the pooled studies analysed LCSF which is downstream from the target site of infection [759]. As such, further studies are needed closest to the brain tissue using MD to improve understanding of drug penetration in the brain tissue.

CHAPTER 5: USE OF INTRACEREBRAL MICRODIALYSIS AS A DRUG RECOVERY TOOL

Introduction

L- and VCSF have been used as proxies to represent target site drug concentrations in the brain, owing to the rarity and difficulty of sampling the brain tissue and ECF in the clinical setting [299]. However, it is well recognised that CSF concentrations may not reflect regional concentrations within the brain, especially when there are physiological disruptions in injury or disease [299].

MD technique

MD uses a microcatheter that is implanted in tissue, including the brain [800]. It enables measurement of the concentration of molecules in the interstitial compartment of the brain over time in both animal models and human patients [801–824]. Molecules in the ECF cross a semi-permeable membrane at its tip along a concentration gradient into a physiological solution perfused through the catheter [825].

For brain monitoring studies, the flow of the perfusate is usually kept at a constant slow rate between 0.3-0.5 μL/min which enables relative recovery (RR) of various chemicals and metabolites in the ECF as they diffuse across the semi-permeable membrane along a concentration gradient [826]. The returning fluid (dialysate) is collected in vials which are changed hourly [825,827]. It is important to note that the concentration of the substance/molecule to be measured in the dialysate will be different than the concentration in the brain ECF unless there is total equilibration across the dialysis membrane [10]. Therefore, the proportion of the ECF concentration collected in the dialysate is referred to as RR and is influenced by analyte characteristics, membrane pore size, membrane area, rate of flow of perfusate and diffusion speed of the substance [10].

Use of MD in clinical studies

MD was adopted in the 1990s for use in human clinical PK studies [800]. In clinical use, MD has been used to monitor measures of tissue metabolism in patients with acute brain injury, subarachnoid haemorrhage, and meningitis [241,828–830]. Hourly bedside analysis of lactate, pyruvate, glucose, glycerol, and glutamate are analysed on a bedside analyser (Iscus Flex, Microdialysis, Sweden) to track the brain's energy status, cellular damage and excitotoxicity for clinical purposes [828–830].

Over time, wide variations of MD variables have been described following brain injury [803,831,832]. As such, it is suggested that MD must be seen as a trend monitor, with data being interpreted in association with other measured variables [10]. Regional heterogeneity may occur due to injury - a case report found differences in PK patterns of morphine between injured and uninjured parts of the brain [833]. This showed a higher ratio of AUC for unbound morphine between injured brain and blood (1.18)

vs uninjured part of the brain and blood (0.56) [833]. Remnant fluid in the vials after bedside analysis can be stored and analysed offline for various substances including drug concentrations.

Intracerebral MD catheter placement in neurointensive care

In traumatic brain injury (TBI) or stroke there may be wide differences in MD-measured variables close to or further from the focal traumatic lesions or “penumbra zones” compared to mean values found in normal tissue ipsilateral to the parenchymal damage and contralateral normal tissue [834]. One recommendation is to place MD catheters in the non-dominant frontal lobe in cases of traumatic diffuse axonal injuries [10]. To identify the accurate placement, a post-insertion head CT scan will show the gold tip at the end of the catheter [10]. Immediately after insertion, it is recommended that the initial findings are ignored because of the microtrauma effect that settles soon after; a recent review explored the use of dexamethasone to mitigate probe-induced trauma during intracranial MD [835] .

Intracerebral MD markers

Markers of glucose metabolism

The bedside analyser enables determination of concentrations of lactate, pyruvate, glucose, glycerol and glutamate. Glucose serves as the main source of energy to the brain and hence it is important that there is a continuous supply of glucose to maintain the integrity of the cells [10].

Very low MD glucose has been observed in sustained periods of hypoxia/ischaemia after TBI [836,837] and subarachnoid haemorrhage (SAH) [838]. "It has been suggested that low MD glucose concentrations could also result from hyperglycolysis and not solely from a decrease in substrate delivery due to reduced cerebral perfusion [839]."

Glycolysis is a metabolic pathway that involves metabolism of glucose to pyruvate [10]. ATP production occurs through either the aerobic pathway through electron complex mediated reduction of oxygen or via the inefficient anaerobic pathway leading to the formation of lactate [10]. Measurement of the extracellular lactate pyruvate ratio (LPR) therefore reflects the intracellular redox state (a marker for mitochondrial function) [831,840]. Severe hypoxia/ischaemia is associated with marked increases in the LPR, but this may also be caused by mitochondrial dysfunction [841]. An increase of the LPR above established thresholds (20-25) is associated with poor outcomes in TBI [803,842] and SAH [832,843,844].

Glutamate is a marker of excitotoxicity resulting from excessive influx of calcium into brain cells via glutamate-mediated ion channels [10]. Cerebral ischaemia in humans is with an increase in glutamate MD concentration [845] and this increase in glutamate correlates with poor outcomes following TBI [803] and SAH [832,843].

Glycerol is a marker of cell membrane breakdown. This results from failure of cellular metabolism, followed by cell membrane dysfunction which ultimately leads to the breakdown of cell membrane phospholipids and liberation of glycerol into the brain ECF [10]. Elevation of cerebral glycerol has been seen in severe TBI in the first 24 hrs which is likely linked to the primary insult, [846], subsequent increases in MD glycerol are associated with adverse secondary events [847] and seizure activity [848]. Recent data in children with TBI demonstrated an association between increased glycerol from baseline with increasing lesion size on neuroimaging [828]. MD markers are summarised in Table 1.

The primary clinical reason for using MD is the recognition that the use of ICP monitoring alone, which is standard monitoring in TBI, does not detect biochemical and metabolic changes that if detected early, could potentially improve outcomes [849]. MD is therefore used simultaneously with ICP and CPP monitoring in an attempt to obtain more information to direct patient treatment [850,851].

Given that small volumes of dialysate are recovered during MD, the analysis of the concentration of analytes in the brain ECF requires the use of sensitive quantification methods such as LC-MS/MS [852]. For PK studies, there are two key potential advantages in addition to sampling from ECF. First, it enables serial sampling. Second, it enables separate measurement of unbound fraction of the drug at the site of disease, depending on the pore size of the MD catheter membrane (100 kDa and 20 kDa respectively). For samples collected through the 20 kDa catheter, no additional sample preparation measures are required before analysis or unbound drug concentration owing to the absence of interference of macromolecules which are unable to cross the small pore sizes [853,854]. In comparison to the measurement of drugs in tissue biopsies, MD is a preferred technique since it is capable of measuring the unbound fraction of the drug in the ECF (20 kDa) and concentrations attained using tissue biopsies may be an overestimation as it covers multiple compartments [825].

Table 5.1. MD biochemical markers of secondary brain injury [10]

MD Markers	**Underlying mechanism**
Low glucose	reduced cerebral glucose supply Cerebral hyperglycolysis
Increased lactate: pyruvate ratio	Reduced cerebral glucose and oxygen supply Reduction in cellular redox state Mitochondrial dysfunction
Increased glycerol	Cell membrane breakdown
Increased glutamate	Excitotoxicity

Quantitative MD/ MD recovery

Factors that could affect drug recovery

Several factors may affect MD dialysate recovery such as MD perfusion flow rate, characteristics of the perfusion solution, probe membrane area, nature of the dialyzed tissue, physiochemical properties of the analyte of interest and other factors which could alter diffusion characteristics [855,856].

The choice of membrane type and potential non-specific binding to plastic parts could influence recovery of the analyte [857]. Composition and temperature of perfusion solution are also important to consider, as disequilibrium between perfusion fluid and ECF may affect the surrounding ECF composition and consequently MD data. This highlights the importance of using a perfusion medium which resembles the (ion) composition of the brain ECF [857]. It is recommended that MD experiments be performed using perfusion fluids at body temperature [857,858]. Furthermore, the flow rate of the perfusion fluid has been shown to affect RR of a drug [859]. The relationship between flow rate and recovery has been examined [860–864]. Recovery increases linearly with concentration of analyte and dialysis surface (of the catheter) [862] and varies inversely with flow rate [863,865]. Flow rate may also affect the pressure inside the probe [857]. If the pressure is higher inside the probe than in the surrounding ECF, net fluid transport out of the membrane will occur which may affect the diffusion of molecules into the dialysate. It has been suggested that experimental conditions must be chosen where no net fluid transport out of the membrane occurs. Other methodological aspects of MD include: the importance of choosing the right tubing type to regulate the flow rate [865], and the extent of tissue damage induced by insertion of the MD probe [866]. However, in terms of tissue damage, our group and others have extensive experience with MD in TBI and the risk of haematoma formation is exceptionally low [828]. We routinely perform follow-up head scans to check position of the catheter and have not had any visible catheter-related injury. In terms of non-visible microtrauma, the possibility that insertion of the catheter may cause tissue disruption effect was identified many years ago with the introduction of MD into clinical and research monitoring [854,867]. In short, it appears that microtrauma effects likely settle within the first few hrs after insertion as can be measured by glycerol and lactate/pyruvate signalling. After several days, tissue reaction around the catheter may reduce recovery rates; therefore, MD monitoring is seldom continued beyond 4 days. MD as a tool in PK studies of course has limitations like every other tool, but within those limitations, its ability to sample directly from the brain with high frequency has led to it being considered by some to be the gold standard method in animal studies.

Given that there is a constant flow of the perfusate to enable recovery, even at ultra-slow rates, the drug concentration in the microdialysate will be lower than in ECF [868]. As such, if the perfusion fluid does not contain the analyte of interest at baseline, then the brain ECF concentration that is recovered in the

dialysate is the fraction of the analyte in the tissue extracellular compartment, represented as the RR. Determining the RR further allows determination of the true concentration of the analyte concentration in the extracellular tissue when calibration methods are applied [869], which is difficult to do in the clinical situation.

Calibration of MD probes

Ideally, for the concentration of the analyte in the brain ECF to be determined the MD probes should be calibrated [870]. Studies have documented experimental and mathematical approaches to determine the absolute concentration of the compound [864,871–873]. There are several experimental methods that are used to calibrate the MD probes by estimating the RR *in vivo* which include: the flow rate or stop flow method, the zero-net flux or concentration difference also known as the equilibrium method and the retrodialysis or reverse dialysis method [800,874,875].

Zero-net-flux method

The zero-net-flux method initially proposed by Lonroth in 1987 is based on the idea that the concentration of the analyte in the ECF of the tissues should be equal to the concentration of the analyte in the infused dialysate fluid when a net-zero exchange of the analyte occurs between the dialysate in the probe and the ECF outside the probe. The dialysate concentration at the ZNF point C_{ZNF} condition is achieved, that is C_{in}-C_{out}=0 [876].

Retrodialysis

Retrodialysis reflects the loss of a substance from the perfusion solution into the tissue. Two methods of retrodialysis exist which have been redefined by Bouw and colleagues as retrodialysis by drug, when a loss of the drug of interest (which is added to the perfusion fluid) is studied, and retrodialysis by calibrator which involves loss of calibrator from the perfusion fluid [874].

The latter involves use of a calibrator that has a similar permeability-area product to that of a compound of interest. A known concentration of the calibrator (Cic) is added to the perfusion fluid, and then with each brain ECF sample a residual calibrator concentration (Cec) can be measured [875]. The relative loss of the calibrator is 1 minus the ratio of Cec to Cic. Ideally, the loss of calibrator is identical to the recovery of the solute of interest [875]. Bouw *et al.* highlighted that "when retrodialyis by calibrator is to be used for the recovery of >20% is recommended for more reliable estimation of the extracellular unbound concentration [874] Retrodialysis by drug of interest involves adding a known concentration of the drug in the perfusion medium ($C_{perfusate}$) and its disappearance rate across the membrane, designated as recovery, is determined using the following formula: Recovery (%)= 100-($100\times C_{ECF}/C_{perfusate}$) [877].

A study suggested retrodialysis by drug as determined before systemic administration was the best method given that no time-dependent change is observed. This approach would not be ideal for a clinical setting with very ill patients as the first three days of treatment are crucial for obtaining drug PK data. Furthermore, the study suggested the addition of a calibrator as quality control during the experiment [874]. On the contrary, another study used retrodialysis by drug at the end of the experiment which would be more feasible in the clinical setting. *In vivo*, probe recovery was done over 140 min, where a solution with a known concentration of the drug of interest was perfused in the probe to estimate recovery by loss [878].

The Application of MD in PK studies

Human studies

The processes that govern PK are ADME [266] and research to date using MD has mainly focused on drug distribution and metabolism [879].

It has been reported that the actual target space for most infectives is not just tissue but defined compartments within tissues such as ECF [880]. PK studies using MD have been performed in patients with acute brain injury and epilepsy. These studies were done in non-inflamed brain and did not involve anti-TB drugs [853,878,881]. A study using intraoperative MD in epileptic patients showed differences in concentrations of antiepileptic drugs in the CSF and brain ECF [882].

A study of morphine in brain injury found longer half-life of the drug close to the trauma site (169 min) in the brain as compared to blood (64 min) and adipose tissue (63 min) [833]. Minderman and colleagues reported findings of RIF, an important drug in the treatment of TBM, in brain ECF using MD, suggesting that RIF concentrations may be below the MIC in ECF for some infectious microbes [8]. This study was performed not in patients with TB but rather with RIF used as an antistaphylococcal prophylaxis agent in patients who underwent surgery for brain tumours.

Analysis of recovered brain ECF

Since small volumes of brain ECF are recovered, a validated sensitive technique such as LC-MS/MS is used to determine concentrations of the drug of interest. These drug concentrations reflect the average level over the collection interval and the midpoint of the interval is often used as the sample time following correction of the time it takes for the brain ECF to flow from the probe to the vial, this being referred to as lag time [879]. Correction for lag time requires knowledge of the tubing length and dead volume (the volume contained from the membrane to the outlet) [879].

PK analysis of MD data

Evaluation of MD data is usually done via dialysate-corrected mid-interval based non-compartmental analysis (midpoint-NCA) or via nonlinear mixed-effects (NLME) modelling which encompasses dialysate-corrected midpoint-NCA. However, two limitations have been described: 1) data transformation (correction of microdialysate concentrations using RR obtained by calibration methods) before analysis results in loss of valuable information on variability associated with RR. 2) allocation of microdialysate concentration to a specific time point despite origination from a time interval [868]. A dialysate-based integral NLME compartmental analysis approach (Integral-CA) was developed to address the aforementioned limitations [883]. An integral-CA approach acknowledges different sources of variability by considering every measured drug concentration from all individuals simultaneously. Studies have used an integral-CA approach together with NCA and midpoint-CA in analysis of clinical MD data [884–886].

In conclusion, MD is a technique that has been used for clinical and research purposes over many years but has not been applied to CNS TB. The methodological limitations that have implications for how to interpret the resulting data are well established. Nevertheless, given the difficulty of studying drug distribution in the brain and the lack of any other method to study real-time changes in drug distribution in the brain, it is an important technique that could be applied to patients with TBM to study drug PK, in combination with data from other compartments. The results would be valuable because it would be the first data on a drug in the ECF as well as the first demonstration of serial measures of a drug in TBM. Even if only relative values are determined, this could establish baseline drug concentrations to examine the effect of different dosing regimens.

CHAPTER 6: METHODOLOGY

The overarching aim of the study was to examine RIF concentrations in multiple compartments in children with TBM to address gaps in the literature, in particular the lack of data for RIF in VCSF or brain ECF, in patients with TBM. These are considered important because they are closest to the site of disease and because it is unknown whether spinal CSF concentrations reflect exposure in the brain. Given the high rate of poor outcomes in these patients, it is important to optimize our understanding of drug distribution at the site of disease.

The primary objective was:

1. To measure RIF total concentrations in plasma, CSF (LCSF and VCSF) and brain ECF using a validated LC-MS/MS method.

The secondary objectives were:

1. To examine RIF concentrations in time-linked LCSF and VCSF of TBM patients undergoing column tests for the management of HCP.
2. To determine total protein concentrations in time-linked L-and VCSF.

Study design

A descriptive cross-sectional study was performed.

Study location

This study was conducted at RCWMCH, WC, SA, a university-affiliated paediatric hospital.

Scientific and ethics approval

Scientific review and approval were received from the Department of Surgery Research Committee, ethical clearance was obtained from the Human Research Ethics Committee of the University of Cape Town (HREC 564/2012 and HREC 070/2018, Appendix 1 and 2). Hospital clearance was obtained from the WC Department of Health.

Study funding

Funding for the study was provided by the National Research Foundation (NRF) South African Research Chairs Initiative (SARChI) for Clinical Neuroscience.

CHAPTER 7: PATIENT ADMISSION AND CLINICAL CHARACTERISTICS

Methods

Patient selection:

TBM cases

Inclusion criteria:

TBM cases (<13 years) were selected at RCWMCH from children diagnosed with definite or probable TBM between January 2017 and September 2019 based on clinical, bacteriological and radiological criteria consistent with a recent consensus for diagnostic criteria of TBM (Appendix 3) [111]. These TBM cases were categorised into two groups (group 1 and 2) based on how they were treated and managed as described in the patient management section further below.

Group 1: Patients with definite or probable TBM and HCP who underwent neurosurgical procedures to manage TBM HCP (via repeated LPs and/ or continuous EVD or VPS insertion).

Group 2: Patients with definite or probable TBM and HCP who underwent neurosurgical procedures to manage TBM HCP (via repeated LPs and/ or continuous EVD or VPS insertion) in addition to MD monitoring as part of routine neurocritical care.

Exclusion criteria:

The following patients were excluded from the study cohort:

Patients with other systemic or brain infections.

Patients with possible TBM but who do not fulfil the criteria of definite or probable TBM.

Patients with definite or probable TBM who were <3 months of age were excluded from sparse blood sampling.

Sample size

This was a convenience sample of TBM patients to develop pilot data and was based on the expected number of patients we would likely treat over the recruitment period.

Subject recruitment

Parents or legal guardians of patients who meet the selection criteria were asked for consent after the study was fully explained to them. Consent was taken in one of the 3 main languages, namely, English, Afrikaans, and Xhosa as preferred, with the assistance of a hospital translator.

General demographical and clinical data

General demographic and clinical data were collected when available for all patients recruited for the study. These included age, sex, weight, immunization history, TB contacts, previous medical history, other underlying diseases, and HIV status. Clinical data included presenting symptoms, duration of symptoms before admission, clinical and neurological signs. The 'refined' MRC criteria was used to determine TBM severity on admission and after 1 week, as described in chapter 2 (Table 2.1).

In-hospital data

Additional data included details of neurosurgical procedures (EVD placement, VPS insertion and ETV), LPs, Mantoux results (where done) and medication administered.

Laboratory data from CSF included glucose, protein, white cell count and differential, TB culture, ZN staining for AFBs, TB PCR, and drug sensitivity and culture for other bacteria. TB cultured from other sources, which includes tracheal aspirate, gastric wash and sputum, were also documented. Haematological data included sodium levels, liver function tests (where done) and HIV reactivity.

Radiological findings: Imaging data as reviewed by expert paediatric radiologists included Chest X-rays, CT brain scans, and MRI of the brain and spine.

Outcome

Mortality was recorded as deaths within 6 months post-admission.

Data entry

Patient data collection and sample processing was primarily done by the doctoral candidate at RCWMCH with assistance where needed.

Samples from TBM patients were processed and biobanked in secure minus 80-degree Celsius (°C) freezers, and data was stored on secure databases.

Patient management

Management of HCP

The institutional protocol for managing TBM patients with HCP was previously published and is outlined in Appendix 4 [245]. Briefly, suspected TBM patients with HCP are referred to the neurosurgery unit. As described in chapter 2, at the institution HCP is categorised into commHC and NCHC following an AEG based on the previously published experience at Stellenbosch University. Briefly, 5-10 mL of air is injected via LP into subarachnoid space depending on the age and size of a patient after measurement of the opening pressure. The patient is then sat in an upright position for around 30 minutes to allow air to move up the spinal canal into the cranium [244]. A skull radiograph or head CT scan should demonstrate intracranial air [244]. Air located within the ventricles and subarachnoid space suggests CommHC and air in the basal cisterns but not in the ventricular system, suggests NCHC. If no air was seen post-procedure radiographs, either there had been a technical problem, or air was trapped by the spinal arachnoid adhesions [245]. If an inconclusive result is obtained on the first attempt, and the patient is stable enough, the AEG is repeated to exclude possible technical errors. The procedure is performed either by a paediatrician or neurosurgeon treating the patient. However, a neurosurgeon is always informed of the procedure in case NCHC is diagnosed, which requires an immediate EVD or CSF shunt placement. Patients with CommHC are treated medically in the first instance. At our institution, we prefer the protocol suggested by Schoeman *et al.* [248,249] of acetazolamide and furosemide but combined with more frequently repeated LPs. Daily LPs reduce ICP more effectively and also allow more sensitive tracking of ICP using simple CSF manometry to record the opening pressure. As ICP normalises, the frequency of LPs is progressively reduced as long as ICP control is maintained. A head CT scan is usually repeated after 3 weeks of treatment, or earlier when indicated. If there is progression of HCP on head CT, deterioration of the patients, or failure to control ICP by week 3, the patient underwent VPS placement [245].

When NCHC is demonstrated, or in uncertain cases where an AEG cannot be done or has failed to produce a result, the patient is taken to the operating room immediately. At our institution, a selective approach is preferred, as such, VPS was reserved for patients who have failed medical therapy or who have NCHC, for whom endoscopy was also an option.

Patients who were considered clinically too unstable for an initial AEG, who had a significantly depressed LOC on admission, and/or had severe signs of HCP on imaging, typically received an EVD to control raised ICP first, following which an AEG and/or column test could be done in more controlled conditions. The EVD is connected to a transducer and the pressure is monitored to keep the ICP below 10-15 cm of water, depending on age [245]. A control radiograph is taken prior to performing the column test to ensure that the air had not been introduced during the insertion of EVD. Thereafter, a

modified AEG/column test is performed under controlled conditions. Column tests are performed as previously described [887]. Briefly, a post-operative EVD is clamped distally to the drainage system and connected to a monometer at a proximal port. After the patient is sedated and placed in a lateral position, a LP is done, and the opening pressure is measured with a second monometer at the lumbar site without the release of CSF. Thereafter, the two monometer readings are compared, and CSF is then released from the lumbar site. Any corresponding change in the cranial monometer is recorded. Similar monometer readings at the start of the reading and a similar decrease in intracranial CSF pressure upon release of a standard amount of CSF from the lumbar site suggest CommHC. In contrast, lack of correlation between the two compartments implies NCHC. Column test results are considered in combination with AEG results.

Some patients with NCHC are treated with ETV as previously described [250]. Briefly, An ETV is performed by a standard institutional approach from the right coronal burr hole using a rigid endoscope. The anatomy of the floor of the third ventricle is identified and the stoma is made between the mammillary bodies and infundibulum with a balloon catheter. Any additional membranes are sought to ensure that the subarachnoid space has been correctly identified. An EVD is left *in situ* postoperatively (clamped) for 24 hrs, at which time a column test is done to confirm the presence of communication. Thereafter, the EVD is removed, and the patient is medically treated as described above.

Insertion of MD catheter

In selected patients, bedside brain chemistry monitoring was performed using MD. Patients were non-consecutive: patients were selected based on severity of condition (in particular brain ischemia being suspected) and the availability of staff and MD consumables. The primary aim of the monitoring was to detect developing brain ischemia by increased lactate/pyruvate ratios.

MD probe implantation

The MD technique was used primarily for clinical purposes to direct therapy. Patients selected to have a MD catheter were those who presented with a depressed level of consciousness (GCS $\leq$ 8), who also needed placement of EVD for HCP and/or ICP/brain oxygen monitor for brain swelling (group 2). A MD catheter was placed concurrently with the primary ventricular drain into the same region (usually right frontal white matter) or sometimes on the side where hypodensity was more prominent on an initial CT scan.

The MD probe is very thin (<1 mm diameter) as compared to other catheters that are routinely used. As such, this did not increase risk based on reported literature and experiences at the RCWMCH neurosurgery unit.

The MD probe was managed in a standard manner; it was perfused with a physiological solution (CNS Perfusion fluid, MDialysis, Sweden) at a constant flow rate of 0.3 µL/min using an infusion pump (CMA/100 Stockholm, Sweden). A catheter with a 100 kDa cutoff membrane was used. Molecules in the interstitium of the brain diffuse across a semipermeable membrane at the tip of the catheter along their concentration gradient and were collected in the outlet of the catheter into a vial (Figure 7.1). These vials were exchanged hourly and analysed at the bedside on the ISCUSFlex (Mdialysis, Sweden).

Hyponatremia

Hyponatremia was carefully corrected via a fluid management approach using a normotonic or hypertonic fluid.

Antituberculous and adjunctive corticosteroid treatment

All TBM patients were treated with a drug dose regimen consisting of RIF (20 mg/kg), INH (15-20 mg/kg), PZA (40 mg/kg) and ETH (20 mg/kg) for 2 months followed by a 4-month continuation phase of RIF and INH. Prednisone was administered as adjunctive treatment in the first month, according to standard of care.

Antiretroviral treatment

TBM patients who were HIV positive were treated with ART as determined by the infectious disease clinical team.

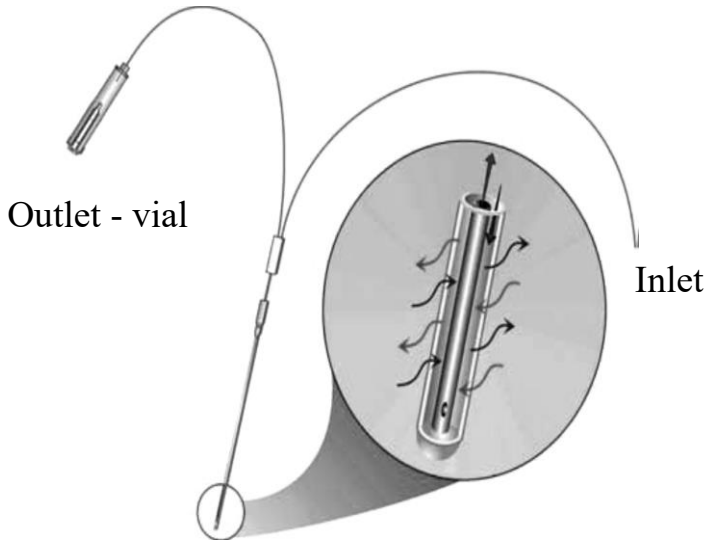

Figure 7.1. CMA brain catheter [829] **.**

CHAPTER 8: PATIENT ADMISSION AND CLINICAL CHARACTERISTICS

Data analysis in this chapter was done using International Business Machines® Statistical Package for the Social Sciences® (IBM® SPSS® Statistics) version 28. Data are presented as median (range or interquartile range) due to non-parametric distribution. Statistical tools used for various analyses are stated in the relevant results sections. The significance level for all analyses in this project was set at 0.05.

Results

Seventy-two patients met the consensus criteria for definite and probable TBM from 16 January 2017 to 26 September 2019 at RCWMCH. In addition, 2 patients who had undergone MD monitoring covered by an existing Human Research Ethics (HREC 200/2014) were included in the final TBM cohort which added to a total of 74 patients that met the consensus criteria. Of these patients, 67 (91%) were diagnosed with HCP and 7 (9%) patients with no HCP. Patients without HCP were not included because no VCSF was available, and no MD was undertaken. Of the patients with HCP who were thought to have TBM, 61 were included in the TBM drug recovery cohort and 6 patients were excluded from analysis for the following reasons: insufficient data owing to discontinuation of MD catheter monitoring (patient deceased) (n=1), pre-dose sample only (no drug) (n=2) and did not fulfil the criteria for definite or probable TBM (n=3). The remaining 61 patients fulfilled the criteria for definite or probable TBM [111].

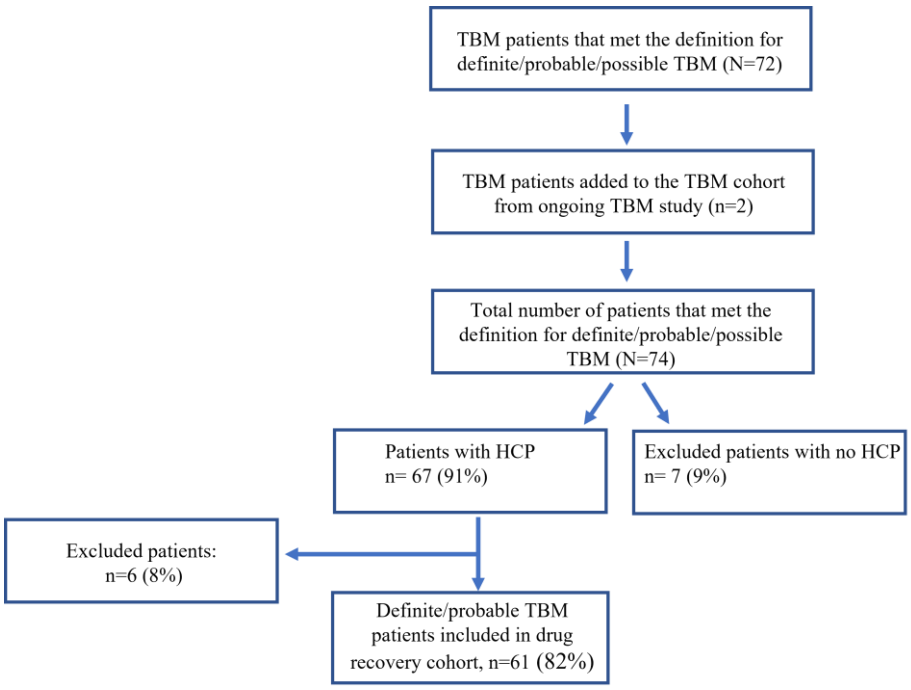

Figure 8.1. Patient selection approach

TBM drug recovery population

From 16 January 2017 to 26 September 2019, 61 patients diagnosed with definite/probable TBM were included in the drug recovery study cohort. These patients had a median age of 2.3 years, a typical age group in our setting [116]. Males and females were equally affected. Most patients presented with MRC stage 2b and 3 of disease. Common non-specific symptoms at admission were present for >1 week and the majority included both systemic and neurological symptoms as shown in Table 8.1. Four patients (7%) tested positive for HIV. A positive CSF result for TB was confirmed in 48% who had a CSF sent for TB culture or Xpert. No cases were drug-resistant. Immunizations were up to date in 60% (34 of 57) of patients and, 4 patients had a missing Road to Health Card. Of the available immunization history cohort (n=57), 8 (14%) patients did not receive the BCG vaccine, owing to missed birth vaccination or shortage in the presenting clinic. Demographic and admission clinical data are shown in Table 8.1.

HCP and imaging features

All TBM study patients had HCP detected on brain CT; 93% of patients had an AEG done which showed that 67% had CommHC, 26% had NCHC and 7% had uncertain communication. An EVD was placed in 66% of patients to temporize the HCP by reducing ICP. HCP was initially treated by VPS or ETV in 21 and 2 patients respectively. Features on contrasted brain CT included basal meningeal enhancement (84%), tuberculomas (20%), and infarcts (75%). Imaging features of TBM with HCP are shown in Table 8.2. The 6-month mortality rate was 13%.

Table 8.1. Demographic and admission clinical data characteristics (N=61)

Characteristic	Value
Demographic characteristics	
Age, years	2.3 (0.3-10.4)
Sex	
Male	29 (48)
Female	32 (52)
Clinical characteristics	
MRC staging	
1	3 (5)
2a	10 (16)
2b	23 (38)
3	25 (41)
Symptom duration (n=60)	7 (2-30 days)
Night sweats	8 (13)
Cough > 2 weeks	9 (15)
Weight loss/failure to thrive	35 (57)
Headache (n=41) [a]	16 (39)
Irritability	25 (41)
Vomiting	35 (57)
Loss of appetite	32 (52)
Fever	37 (61)
Meningism	38 (62)
Altered level of consciousness	47 (77)
Lethargy	54 (89)
Bulging fontanelle (n=9) [b]	7 (78)
Focal neurology [c]	33 (54)
Seizures	32 (52)
HIV infection	4 (7)
TST (n=34)	17 (50)
Recent TB contact	33 (54)
Immunization up to date (n=57) [d]	34 (60)
Diagnostics	
CSF culture/Xpert positive	29 (48)
Outcome	
6 months mortality	8 (13)
Chest X-ray suggestive of PTB	31 (51)

Values are expressed as median (range) or number (percentage). MRC staging refers to the 'refined' MRC for TBM severity staging.
[a] Children <1.5 years of age were excluded (pre-verbal), [b] For children with an open anterior fontanelle, [c] Focal neurology included pupils' response, paresis, aphasia, cranial nerve palsies, [d] Road to Health Card missing.

Table 8.2. Imaging features of TBM with HCP

Characteristic	Value
Hydrocephalus	61 (100)
Non communicating	16 (26)
Communicating	41 (67)
Uncertain	4 (7)
Basal enhancement	51 (84)
Tuberculoma	12 (20)
Infarcts	46 (75)

Values are represented as number (percentage) based on the total number of patients in the TBM drug recovery cohort

Table 8.3. Admission CSF chemistry and cell counts

	LCSF=40	VCSF=26	Differences in LCSF and VCSF
Glucose (mmol/L) (n=39) [a]	1.4 (0.5-3.9)	3.6 (1.8-4.7)	*p*<0.001*
Normal (2.3-3.9)		23 (88)	
Abnormal (<2.3)	13 (33)	3 (12)	
	26 (67)		
Chloride (mmol/L) (n=31) [b] (n=16)[c]	111.0 (93-125)	116.0 (102-130)	*p*=0.044*
Normal (120-130)	5 (16)	5 (31)	
Abnormal (<120)	26 (84)	11 (69)	
Protein (g/L) [d] (n=39) [e]	1.7 (0.54-50.92)	0.6 (0.15-1.72)	*p*<0.001*
Normal (0.2-0.8/0.15-0.45)	0 (0)	7 (27)	
Abnormal (>0.45/>0.8)	39 (100)	19 (73)	
Polymorphonuclear cells (cells/µL) (n=36) [f]	5.0 (0-208)	1.5 (0-51)	*p*=0.068
Lymphocytes (cells/µL) (n=36) [g]	82.0 (0-2800)	20.5 (3-126)	*p*<0.001*
Total WCC (cells/µL) (n=36) [h]	104.5 (0-2812)	26.5 (5-177)	*p*<0.001*
Normal (<10)	3 (8)	5 (19)	
Abnormal (>10)	33 (92)	21 (81)	
Lymphocyte predominance			
>50%	33 (92)	24 (92)	
>90%	21 (58)	14 (56)	

Data reported as median (range) and number (percentage). This table reflects admission CSF values, noting that some patients had LCSF samples, some patients who went directly for EVD placement had either VCSF samples only or VCSF and LCSF. [a] LCSF glucose values were missing for 1 patient (n=39), [b] LCSF chloride values were missing for 9 patients (n=31) and [c] VCSF chloride values were missing from 10 patients (n=16), [d] Protein reference ranges are age dependent >1 year and < 1 year respectively and [e] LCSF protein values were missing for 1 patient (n=39), [f,g,h] LCSF polymorphonuclear cells, lymphocytes and total WCC are missing values from 4 patients (n=36) respectively, * r=statistically significant

Laboratory results

Median protein concentration was significantly higher in LCSF than VCSF (*p<0.001*), as was the lymphocyte count (*p<0.001*) and total WCC (*p<0.001*) (Table 8.3). All LCSF had elevated protein (n=39, 100%) but in 27% of the VCSF samples the protein was in the normal range. Both glucose and chloride were significantly lower in LCSF than in VCSF. Trend differences between L-and VCSF (5 vs 1.5 respectively) were observed in polymorphonuclear cells, but this was not significant.

Table 8.4. Admission blood chemistry

	Values
Sodium (Na) (mmol/L)	128 (115-144)
Creatinine (µmol/L) (n=56)	18 (8-74)
Albumin (g/L) (n=36)	37 (24-45)
Total protein (g/L) (n=15)	80 (68-88)
Aspartate transferase (AST) (n=11)	30 (15-159)
Alanine transaminase (ALT) (n=26)	12 (4-50)

Values are represented as median (range), where values were missing. Total number of patients with available corresponding data is represented (n).

Blood results

The median sodium value was 128 mmol/L (range 115-144); 55 patients had hyponatraemia (normal range 136-145). Of the patients who had liver function tests, 3 patients had elevated ALTs (n=26), and 1 patient had elevated ASTs (n=11). See Table 8.4.

Discussion

TBM drug recovery cohort

The 61 children enrolled in this study demonstrated a fairly typical TBM cohort at our institution, with an obvious bias to HCP by definition of the entry criteria. The overall median age of the TBM study cohort was 2.3 years with most children (77%) below the age of 5 years. Our study is in keeping with other studies demonstrating the young age at which TBM presents in children [7,529,8878]. Our patients were on the more severe end of the spectrum: 3 (5%) were admitted with MRC stage 1 TBM according to 'revised' MRC criteria, 10 (16%) with stage 2a, 23 (38%) stage 2b, and 25 (41%) stage 3. Most patients presented with more severe disease likely because the hospital is a quaternary referral hospital managing ill children, often requiring surgery and advanced paediatric critical care. A local TBM study in children also reported stage 2 and 3 disease severity at admission [529]. Common TBM symptoms were non-specific, as reported elsewhere, including fever, headache, weight loss, and cough

[765,775]. The median duration of symptoms prior to presentation was 7 days (2-30 days). The longer duration of symptoms is typical: an Indonesian phase II clinical trial in adults reported a median duration of symptoms prior to presentation of 14 days (IQR 7-21 days) [756].

Seizures were observed in 32 (52%) of the TBM patients. The cause of seizures in TBM has been described to be multifactorial with varying incidence between populations [889]. Neuro-excitotoxicity which has been implicated in contributing to brain injury may increase the risk of clinical and subclinical seizures in TBM and cortical spreading depression, a secondary injury mechanism known to occur in stroke [144]. Of note, few patients tested positive for HIV (7%), consistent with previous findings at our institution [144]. ARVs were commenced > 2 weeks of anti-TB treatment. One patient had multiple defaults on ARVs prior to first admission and had no treatment for about 6 months. Initiation of ARVs was delayed owing to the risk of IRIS associated with TBM [231]. Twenty-nine (48%) patients tested positive for TBM through TB culture or Xpert. Culture positivity rates are often considerably lower than this, likely due to the paucibacillary nature of *Mtb* [112]. The recent global shortage of BCG vaccine most likely contributed to the 8 (14%) patients who either missed or did not receive BCG vaccine at birth in our TBM cohort [102].

Imaging results

Common features of TBM on CT scan of the brain were HCP (100%) due to the inclusion criteria, basal enhancement (84%), tuberculoma (20%) and infarcts (75%). Meningeal inflammation in TBM and presence of exudate contribute to CT findings of basal enhancement [119]. Same-setting studies have also reported (71.6%-100%) HCP in TBM patients [66,126,144,253,890]. The presence of exudate in TBM blocks the normal flow of CSF resulting in HCP as described in previous text [66,245]. Tuberculomas have previously been described in TBM and may develop early or late during treatment [66,82–85].

In this cohort, 75% of patients had TBM-induced infarction. This is considered a complication of vasculitis caused by the proliferative exudate in the basal subarachnoid space, aggravated by increased ICP. Cerebral infarction is a major cause of long-term morbidity in TBM [891]. The incidence of infarction in TBM has been reported to range from 13 to 53% [53,69,890–892], mostly among children who are young and/or have severe TBM [240]. Basal ganglia infarction has been shown to carry a poor prognosis [890]. As such, follow-up CT scans are important, as new infarcts are known to develop in 22% of cases of acute TBM during the 1st month of anti-TB treatment owing to an ongoing inflammatory response [891].

Laboratory results

We first examined unpaired admission LCSF (n=39) and VCSF (n=26) of patients in the TBM drug recovery cohort. Common LCSF parameters in children with TBM were observed, including raised protein, lymphocyte predominance, and reduced glucose [124,126,262]. Leukocytosis with lymphocyte predominance, elevated protein (>1 g/L) and abnormally decreased CSF glucose (<2.2 mmol/L) are suggestive of TBM [67,133]. These parameters were significantly different in LCSF when compared to VCSF (Table 8.3). Interestingly, all LCSF had elevated protein (>1 g/L) which suggests pooling of CSF in the lumbar region. The decreasing trend of glucose from V-to LCSF has been suggested to be due to consumption by leukocytes and bacteria [136]. Although LCSF had a larger total WCC, lymphocyte predominance >50% was similar. In keeping with these observed differences, previous data from our group has also shown significant differences between VCSF and LCSF for biomarkers of cerebral injury, inflammatory mediators, and gene expression profiles [144, 145]. A study in patients with suspected bacterial CNS infections also showed differences between the two compartments, with ventriculo-lumbar ratios ranging from 0.003 to 10.2 for protein (median 0.42) and 0.002 to 53.5 for leukocytes (median 0.17) in paired L-and VCSF [137]. A case report in a 20-year-old male who had post-surgical meningitis showed increased V-to-LCSF gradients of leukocytes, protein and glucose, particularly during the early acute phase of meningitis [138]. Another case study report also showed differences between L-and VCSF in an adult patient with chronic meningitis [893]. Several reasons may explain these differences, including the sump effect (of CSF cells and proteins in the most dependant part of the spinal axis), meningeal inflammation in the spinal canal, the constant refreshing and clearance of CSF in the ventricles, CSF flow obstructions between the ventricles and the subarachnoid space or within the spinal axis, and different permeabilities of the vessel anatomy and physiology comprising the BBB and BSCBs. In contrast to these observations, Kamat *et al*. reported similar protein concentrations between VCSF (2.471 g/L) and LCSF (2.474 g/L) in adults and children [142]; however, the differences between their data and data from this group have been highlighted [146].

Drug-induced liver injury

In our drug recovery cohort, 2 patients were started on a liver-friendly regimen in response to elevated transaminases: one after 3 months post-admission to treat acute drug-induced liver injury (DILI) and the other re-admitted twice to treat DILI. DILI or Anti-TB drug-induced hepatotoxicity (ADIH) has been defined as an elevation of AST or ALT values to more than X5 normal in those with normal values pre-treatment [894]. A review defined DILI as an elevation of ALT/AST >3X the upper limit of normal (ULN) with symptoms of hepatoxicity e.g., jaundice, vomiting, nausea and abdominal pain) or 5X the ULN without the presence of symptoms [895]. Raised AST and ALT values have previously been reported in children who were treated with an anti-TB regimen for PTB which normalised without treatment adjustment [896]. In a retrospective study of children in Japan who were treated with an anti-

TB regimen (n=99); 22 children (22.2%) had increased AST and ALT values which were <X5 upper limit of normal; 8 (8.1%) children (<5 years) had severe ADIH (>X5 upper limit of normal) which was associated with young age and PZA. Interestingly, only 12 children were administered PZA and 4 of these had TBM. Four patients developed DILI within the first 4 weeks of anti-TB treatment in an Indonesian cohort (n=20) of children and adolescents with TBM [897].

Clinical outcome

At 6 months after admission 8 (13%) patients had died. Other studies at our centre and Tygerberg Hospital (in the same region) have reported mortality rates of 13-16% [67, 145, 253, 888], although case-mix may have differed. Of patients who died, 5 had presented with stage 3 TBM and 3 patients with stage 2b of TBM at admission.

Prompt treatment in the early stages of disease is a critical determinant of outcome, however, patients often present later with advanced disease, and even patients who receive treatment at the early stage of disease may deteriorate [217]. In an Indonesian cohort study of children with TBM (n=20), 7 (35%) died despite only 4 presenting with stage 3 TBM [897]. Despite access to anti-TB drugs and corticosteroids, mortality remains high and most deaths (95%) from TBM occur within 6 months [898]. The use of adjuvant corticosteroids reduces mortality in TBM but its effect on neurodisability in survivors is less clear [218]. In children, Schoeman *et al.* found that use of corticosteroids significantly improved the survival of children with TBM, however, corticosteroids did not significantly affect ICP or the incidence of basal ganglia infarction [252]. In addition, lack of access to supportive care and neurorehabilitation in low-resourced TB endemic settings may further aggravate poor outcomes [899].

A previous study in a cohort of patients with TBM at our institution (n=44) found a 16% mortality rate, but there was also significant disability in survivors: 3 patients (6.8%) were in a persistent vegetative state, two were severely disabled (4.5%), and 11 (25%) suffered mild-moderate disability [253]. A multicentre, retrospective study in a European paediatric cohort reported spasticity of one or more limbs and developmental delay both in 19.2% (20/104), and seizure disorder in 17.3% (18/104) as the main long-term sequelae [776]. A recent systemic review and aggregate level data meta-analysis reported that an intensive 6-month regimen was associated with reduced mortality but more frequent neurological sequelae among survivors of paediatric TBM when compared with a 12-month regimen which includes EMB [900]. A phase II clinical trial reported 50% mortality within 6 months of treatment initiation whilst the cumulative mortality was 65% in patients in the standard dose RIF (450 mg) vs 34% in the high-dose IV administered group (600 mg) [756]. Most patients died within the first weeks of treatment and death was mainly attributed to respiratory failure (n=9), then neurologic deterioration (n=7), sepsis (n=2) and anaphylaxis (n=1) [756].

Poor outcomes have been attributed to factors that include delayed presentation and treatment initiation, severity of disease, and HCP [74,126,256–259]. A previous study in children with TBM showed that the presence of infarction was associated with poor outcomes. Furthermore, lack of association in patients with poor outcomes who had no infarction on initial CT scan was suggested to have resulted from missed infarctions or infarctions that developed during treatment from ongoing inflammation [72]. A retrospective study of children with TBM (n=121) in Ethiopia reported malnutrition, duration of illness, HCP and stage 3 TBM as significant factors associated with poor clinical outcomes [901]. Morbidity after TBM is high, with only about 16% to 20% of children returning to baseline [126,600]. TBM outcomes findings differ depending on the prevalence of risk factors including HIV co-infection, drug resistance [115], severe HCP, cerebral infarct, brainstem dysfunction, raised ICP and malnutrition [67,70,739,902,903].

Limitations

Our TBM cohort patients were treated at a quaternary referral hospital with specialist facilities. As such, most patients presented with more severe disease which could overestimate TBM disease severity at admission. Furthermore, all TBM patients had HCP. Therefore, results could be different in the absence of HCP. Comparison of CSF chemistry between LCSF and VCSF is limited to clinical test requests, therefore, not all patients had time-linked samples for comparison. Blood test results are variable owing to availability of clinically requested test results at admission. MRI of the spine was only available on request and not routine, as such spinal arachnoiditis in TBM may have been missed. Nevertheless, the features are fairly typical of paediatric TBM, and patients on the more severe spectrum of disease represent the group most needing optimised care because of their higher risk for poor outcomes.

CHAPTER 9: RIFAMPICIN ANALYSIS

In this chapter, the relationship between RIF and protein concentrations in samples of blood, VCSF, LCSF and brain ECF from patients treated for TBM at RXWMCH was examined. The patient cohort was divided into 2 groups. Those who received MD monitoring and those who did not. Samples collected from patients who did not undergo MD monitoring include blood and L- and VCSF and for patients who received MD monitoring, ECF was also collected, stored and analysed. RIF and protein concentration were determined in all samples up to 24 hrs after the drug dose was given. Considering samples which were excluded because the results of the analysis were below the LOQ or samples which were taken outside of the recommended sampling time frame, a total of 95 plasma, 75 LCSF, 46 VCSF and 74 brain ECF samples were used for analysis. The results of this analysis are discussed below.

A. SPORADIC MULTICOMPARTMENT SAMPLING AND ANALYSIS

Methods

Pharmacokinetic sampling

A shift hospital nurse administered the anti-TB drugs according to body weight orally or via a nasogastric tube (NGT) based on conventional clinical practice at the hospital and not influenced by this study. Therefore, the results likely represent a 'real world' scenario.

Group 1: patients with TBM HCP (without MD)

PK blood sampling: where possible, three serial blood samples (of 0.6 mL each) per patient were collected on a single day in week 1 or week 2 at 2-, 4-, and 6 hrs post-dose. Whole blood was drawn through an indwelling peripheral venous catheter (long line') in patients who did not have a routine arterial line. The venous line was inserted to coincide with clinically indicated routine sampling to ensure that the patient did not undergo additional veno-punctures. Whole blood samples were collected in a vacutainer ethylenediaminetetraacetic acid (EDTA) blood collection tube and kept on ice until they were processed shortly after collection at 1400 rates per minute (rpm) for 10 min to separate the plasma and biobanked at -80°C within 30 min pending bioanalysis.

PK CSF sampling: CSF was collected from clinically indicated procedures (via neurosurgical procedures or LPs) at different time points up to 24h post-drug dose into sterile 15 mL tubes and kept on ice. In some cases, where procedures such as column tests could be scheduled, these were timed to be performed at 2-, 4- or 6 hrs after the drug was given. Samples were immediately spun at 1400 rpm for 10 min to separate CSF from any tissue pellets or blood and stored at -80°C pending bioanalysis within 30 min of sampling until analysis. Briefly, LCSF was collected from standard diagnostic and/or therapeutic procedures LPs, which are standard at our institution for diagnosis of TBM, for AEG, and for monitoring ICP [245,887,904]. Repeat LPs were performed to monitor the trend in ICP and to reduce

ICP in patients with CommHC. In our institutional protocol, the frequency of LPs depends on the persistence or resolution of raised ICP. VCSF was obtained from, 1) VPS placement (as a definitive treatment for NCHC or failed medical treatment of CommHC), 2) EVD (on insertion, routine testing for bacteriology, and during AEG and/or column tests), or 3) ETV in selected patients with NCHC. Our standard protocol for treating HCP in TBM is previously published [245]. Where blood sampling was planned, we scheduled these for 2-, 4- and 6 hrs post-dose to coincide with clinically indicated neurosurgical procedures as described above where possible.

Appropriate blood, LCSF, VCSF and brain ECF samples which had already been collected as part of our meningitis registry and repository (R026/2014) were also included in the analysis for this study.

Group 2: patients with TBM HCP with MD catheter monitoring

PK sampling of brain ECF: In patients who were undergoing MD monitoring, CSF microdialysate was recovered in microvials (Figure 7.1). These MD vials were changed at hourly intervals and analysed at the bedside (ISCUSFlex, MDialysis) for clinical purposes to observe changes in glucose, pyruvate, lactate, and glycerol (cellular breakdown), and glutamate (excitotoxicity).

Remnant fluid after analysis on the ISCUSFlex was kept on ice and biobanked at -80°C within 6 hrs of collection. Because MD volumes are typically small; hourly samples were pooled over 2-3 hrs epochs to ensure sufficient volumes for LC-MS/MS analysis (>20 µl). Concentrations of substances in the microdialysate are a percentage of the true concentrations in the ECF (RR rate).

PK sampling of blood and CSF: these were sampled and processed as described above. Blood was drawn through an indwelling peripheral venous catheter in patients who did not have a routine arterial line.

Drug quantification

RIF was analysed in all samples: plasma, LCSF, VCSF, and brain ECF. LC-MS/MS assays were developed and validated through collaboration with the Division of Clinical Pharmacology, University of Cape Town. Plasma samples were processed with a protein precipitation extraction method using rifampicin-d3 and 25-desacetyl-rifampicin-d3 as internal standards, followed by high-performance LC-MS/MS detection using an AB SCIEX API 3000 instrument. Isocratic chromatography was performed on a Discovery C18 (5 µm, 50 mm x 4.6 mm) analytical column. The analyte, metabolite and internal standards were monitored at mass transitions of the protonated precursor ions 823.4, 781.5, 826.5, and 784.5 to the product ions 791.4, 749.4, 794.4, and 752.4 for rifampicin, 25-desacetyl-rifampicin, rifampicin-d3 and 25-desacetyl-rifampicin-d3, respectively. The calibration curves both fit a quadratic (weighted by 1/x) regression over the ranges 0.117–30.0 µg/mL for RIF and 0.0391–10.0 µg/mL for 25-desacetyl-rifampicin. The combined accuracy and precision statistics of the limit of quantification,

low, medium, and high-quality controls (three validation batches [n=18]) were between 101% and 107% and between 2.7% and 3.7% for RIF and 25-desacetyl-rifampicin, respectively. CSF samples were processed with a protein precipitation extraction method using acidified acetonitrile and ascorbic acid, followed by LC-MS/MS with detection using an AB SCIEX API 5500Q instrument. Liquid chromatography was performed on a Poroshell 120 EC-C18 (2.7 µm, 4.6 mm x 50 mm) analytical column. RIF and rifampicin-d3 were monitored at mass transitions of the protonated precursor ions 823.1 and 827.3 to the product ions 791.3 and 795.5, respectively. The calibration curve fit a quadratic (weighted by 1/x2) regression over the range of 5 to 2500 ng/mL. The combined accuracy and precision statistics of the limit of quantification, low, medium, and high-quality controls (three validation batches [n=18]) were between 88.9% and 102.9% and between 3.8% and 8.3% for RIF.

Protein quantification

Protein in CSF samples was quantified by National Health Laboratory Services (NHLS) pathologies at Groote Schuur Hospital using the third-generation turbidimetric method, and in-house at RCWMCH using the Pierce BCA protein assay kit (Thermoscientific). Samples tested using the third-generation turbidimetric method were preincubated in an alkaline solution containing EDTA to denature the protein and eliminate any interference from magnesium. Protein was measured following the addition of benzethonium chloride, which produces turbidity proportional to protein concentration. The Pierce BCA protein assay is based on the Biuret reaction where copper is reduced to the cuprous cation by protein in an alkaline medium. Bicinchoninic acid (BCA) reacts with the cuprous cation to form a highly coloured purple complex, the concentration of which proportions to amount of protein present and can be spectroscopically measured at 562 nm [905]. The Pierce BCA protein assay kit was used to determine total protein concentrations in cases where there was insufficient sample volume to use the NHLS third-generation turbidimetric method.

Data preparation

Data clean-up (normalizing data) in preparation for analysis included reducing redundancy and inconsistency of data. This was followed by the process of denormalizing data which included combining data from multiple tables. Data were checked for inaccuracies, missing values (known), and incompleteness, and also to detect any biases, null values, outliers, and duplicates. Furthermore, data were checked for syntax errors (white spaces, typos, extra space, formats that need to be fixed) and outliers that need to be examined for accuracy and inclusion in a data set.

To check for data reliability, summary statistics were performed on individual columns, e.g., minimum, maximum, median, mean etc. Validation was done by verifying consistency, quality and security

(removing patient identifiers) of data prior to sharing (specific to collaborator work). Excel spreadsheets were used for the data-wrangling process. For data visualization, statistical tools were used to interrogate the data e.g., scatter plots to detect outliers.

Sample size and statistical analysis

No sample size calculations were done owing to the explorative nature of the study. Overall, RIF data analysis (n=61) was conducted using GraphPad Prism, Version 4.

Results

Descriptive analysis

A total of 95 plasma, 84 LCSF, 54 VCSF and 79 brain ECF samples were analysed for RIF. Of these, 8 (8.42%) plasma, 13 (14.8 %) LCSF, 8 (16.0%) VCSF and 17 (21.5%) brain ECF were BLQ which was 0.117 µg/mL, 5.00 ng/mL (LCSF and VCSF) and 5.00 ng/mL respectively.

A total of 9 LCSF, 8 VCSF and 5 brain ECF samples were excluded from analysis of RIF because they were either taken pre-daily dose or after 24 hrs post-dose. RIF concentrations were plotted in time epochs as shown in values in Figure 9.1 and Figure 9.2.

RIF concentrations across time epochs are shown in Figures 9.1 and 9.3. Our main findings showed differences in distribution of RIF at the periphery (plasma) and brain compartments (CSF and brain ECF). As expected, plasma RIF concentrations were considerably higher than CSF samples, with a 2 hrs post-dose median value of 5.20 µg/mL (interquartile range, 2.66-10.20 µg/mL) and typically peaked at 2 hrs post-dose (Figures 9.1 and 9.3 and Table 9.1). CSF concentrations were lower, with LCSF and VCSF RIF median concentrations at 2 hrs post-dose of 0.04 and 0.06 µg/mL respectively (Figure 9.3 and values in Table 9.1). Thereafter, LCSF concentrations were higher. At 4 hrs post-dose, RIF concentrations were higher in LCSF with a median value of 0.23 µg/mL (interquartile range, 0.09-0.41) than both VCSF (median: 0.15 µg/mL; interquartile range 0.12-0.32 µg/mL) and brain ECF (median: 0.02 µg/mL; interquartile range 0.01-0.10) (Figures 9.1 and 9.3 and Table 9.1). Brain ECF RIF median concentrations were considerably lower than both CSF compartments (Figure 9.3 and Table 9.1). RIF median concentrations were still detectable in LCSF and VCSF at 10 hrs post-dose at a modest increase of 0.24 µg/mL and 0.15 µg/mL respectively when compared to 6 hrs post-dose (Figure 9.3 and Table 9.1).

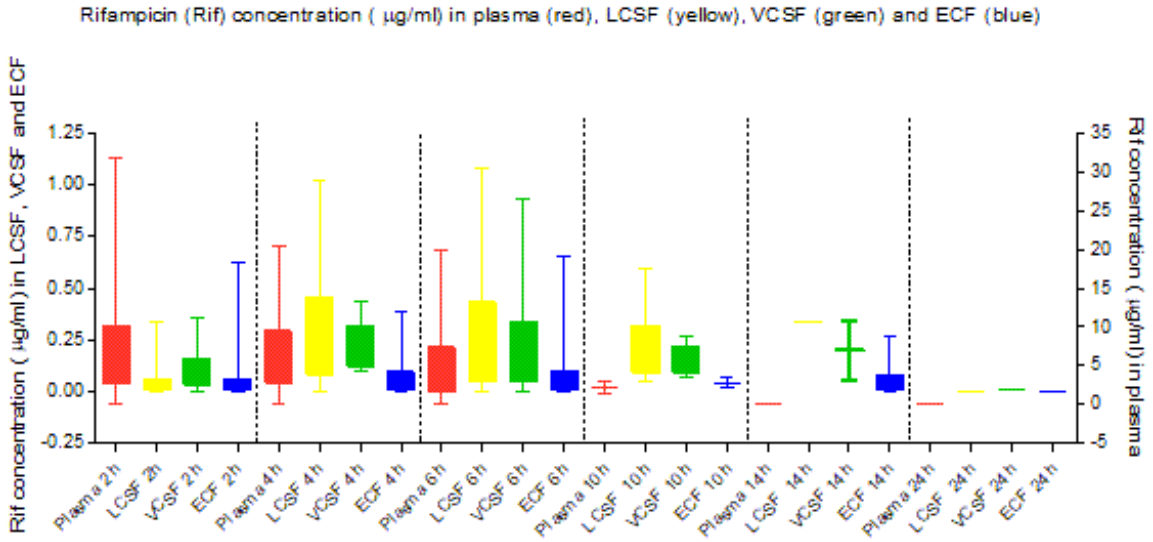

Figure 9.1. demonstrates RIF concentrations across compartments in VCSF (green), LCSF (yellow), brain ECF (blue) and plasma (red) in time epochs, with plasma on the right axis.

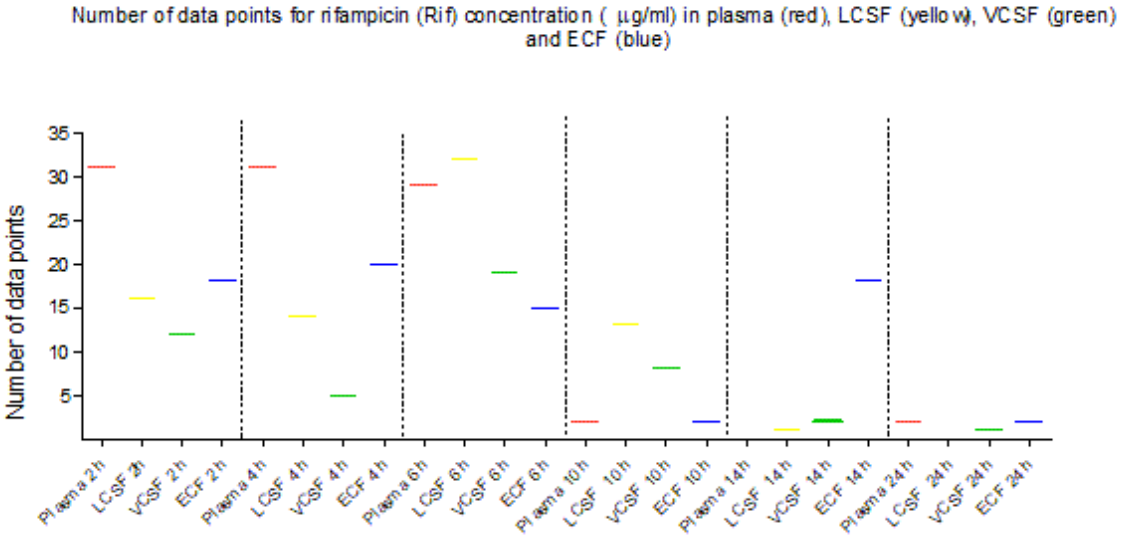

Figure 9.2. demonstrates the number of data points across compartments in VCSF (green), LCSF (yellow), brain ECF (blue) and plasma (red) in time epochs.

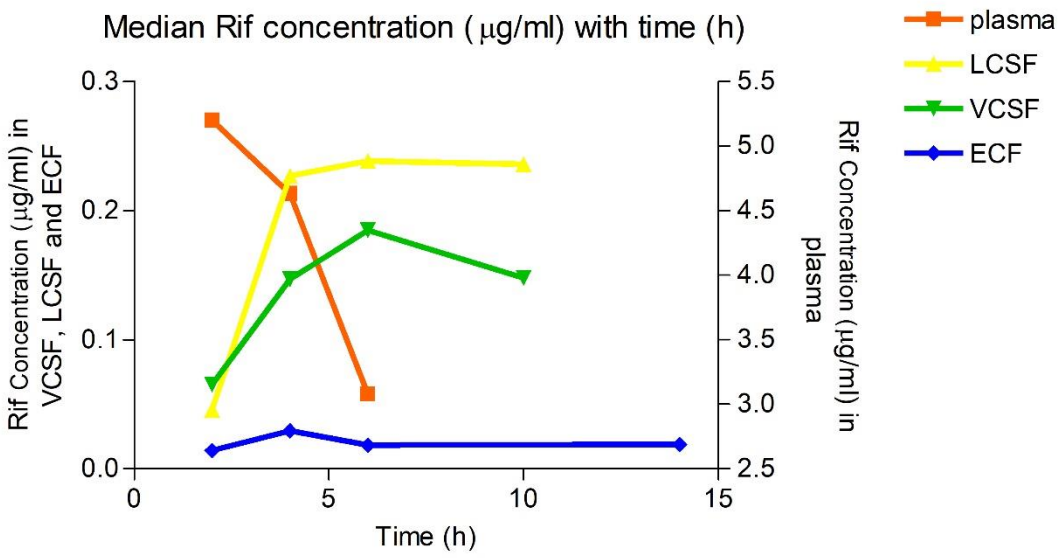

Figure 9.3. Demonstrates median RIF concentrations (µg/mL) versus time epochs at (2,4,6, and 10 hrs) post-dose in VCSF (green triangle), LCSF (yellow triangle), and plasma (orange square), with plasma on the right axis. Brain ECF (blue triangle) includes (2,4,6,10 and14 hrs) time epochs. Timepoints with 2 or fewer samples were excluded from display.

Table 9.1. Median RIF concentrations and interquartile range in plasma, V-and LCSF and brain ECF

Time epoch	Compartments	Median RIF concentrations (μg/mL)	Interquartile range (μg/mL)
2 hrs	Plasma (n=31)	5.20	2.66-10.20
	VCSF (n=12)	0.06	0.02-0.17
	LCSF (n=16)	0.04	0.01-0.06
	ECF (n=18)	0.01	0.01-0.06
4 hrs	Plasma (n=31)	4.63	2.77-9.50
	VCSF (n=5)	0.15	0.12-0.32
	LCSF (n=14)	0.23	0.09-0.41
	ECF (n=20)	0.02	0.01-0.10
6 hrs	Plasma (n=29)	3.08	1.71-7.37
	VCSF (n=19)	0.14	0.05-0.34
	LCSF (n=32)	0.14	0.04-0.44
	ECF (n=15)	0.02	0.01-0.10
10 hrs	Plasma (n=2)	2.28	x
	VCSF (n=7)	0.15	0.09-0.22
	LCSF (n=12)	0.24	0.09-0.32
	ECF (n=2)	0.04	x
11-14 hrs	Plasma (x)	x	x
	VCSF (n=2)	0.02	x
	LCSF (n=1)	0.34	x
	ECF (n=17)	0.01	0.01-0.08
24-31 hrs (pre-dose)	Plasma (n=2)	0.12	x
	VCSF (n=1)	0.01	x
	LCSF (n=0)	x	x
	ECF (n=2)	0.01	x

Data is reported as median and interquartile range. h (hours), x represents no value for the respective compartment and no value for plasma at 14 hours

Discussion

RIF in Plasma

Our findings showed that plasma RIF concentrations were higher than CSF at all time points, with C_{max} recorded at 2 hrs post-dose, with a median value of 5.20 µg/mL (interquartile range 2.66-10.20 µg/mL) (Figure 9.3). It is noted however that samples earlier than 2 hrs were not collected. The RIF concentration range in plasma in our sample cohort was large, but the median values are similar to those published elsewhere. A population PK study in Vietnam reported a steady state plasma C_{max} of RIF (15 mg/kg) with a median value of 4.94 µg/mL (range 2.46-8.37 µg/mL) in children with TBM [906]. A naïve pooled PK non-compartmental analysis in plasma reported a RIF (10 mg/kg) median C_{max} of 4.9 µg/mL and 5.96 µg/mL in children with TBM who were below and above 4 years respectively [7]. Another study reported a plasma median value of 6.3 µg/mL (range 4.9-8.3 µg/mL) at 2 hrs post-dose of RIF (10 mg/kg) vs median value of 22.1 µg/mL (range 19.9-24.6 µg/mL) at 2 hrs post-dose of IV RIF (13 mg/kg) in patients > 14 years with TBM [638]. Our maximum median RIF plasma concentration achieved at 2 hrs post-dose was 5.20 µg/ml, less than the target recommended RIF concentration cited to be ≥8 µg/mL at 2 hrs post-dose in plasma, as was the case in the other studies cited. In most cases, the target concentration was not reached, and the wide interquartile range probably reflects significant inter-and intra-variability in patients [742]. A study by Chigutsa *et al*. [907] found that a RIF C_{max} of >8.2 µg/mL was an independent predictor of RIF's sterilizing activity. However, Te Brake *et al*. cautioned on using the common reference range for RIF (8-24 mg/L) as it represents the 'normal' (population) concentration range that can be expected in adults administered standard doses of TB drugs and not a clinically validated threshold value [713]. It has been recommended that two plasma samples be collected, a 2 hrs post-dose sample will approximate the C_{max} of RIF and a 6 hrs post-dose sample provides information on delayed drug absorption and malabsorption [908]. When 2- and 6 hrs post-dose samples are subtherapeutic, this may imply malabsorption. However, when the 2 hrs post-dose sample is low, but the 6 hrs post-dose sample is therapeutic this implies delayed absorption [609].

RIF in CSF

RIF concentrations overall were higher in LCSF, with a median value of 0.23 µg/mL (interquartile range 0.09- 0.41 µg/mL) compared to VCSF with a median value of 0.15 µg/mL (interquartile range 0.12-0.32 µg/mL) at 4 hrs post-dose (Figure 9.3). It is important to note however that this was an overall analysis, not limited to time-linked samples. Our data also showed that RIF is still detectable above the LOQ at 10 hrs post-dose in LCSF, VCSF and brain ECF possibly owing to CSF dynamics that would influence clearance of the drug. However, caution must be exercised in interpreting samples after 10

hrs as these were few and may be influenced by confounding factors. These samples would typically have been taken at night (given that the usual RIF administration occurs at around 10 am at our institution; therefore, there may have been clinical reasons for these samples to be taken between 6 pm-midnight). Analysis in Section B reports comparisons between time-linked samples.

RIF concentrations in CSF were lower than in plasma and rarely exceeded 1 µg/mL [526,528,601,909], which is slightly above RIF minimum inhibitory concentration (MIC) of *Mtb* for susceptible strains which ranges from 0.06-0.4 µg/mL [648,910]. RIF concentrations in CSF at most were 5% of peak plasma concentrations. In a study of children who had been given RIF for prophylaxis while undergoing shunt surgery, RIF concentrations above MIC were detected at mean concentration of 1.4 (±1.0; range 0.12-3.00) µg/mL 2 hrs post-dose after administration of 20 mg/kg RIF [525]; however, administration in this study was IV and these patients did not have meningeal inflammation, making comparison difficult. A review by Donald *et al.* [601] found the highest CSF RIF concentrations were achieved in most cases in children who were administered RIF dose of 20 mg/kg. A study in an Indonesian cohort (> 14 years) with TBM reported RIF median values in CSF of 0.21 µg/mL (range 0.16-0.27 µg/mL) vs 0.60 µg/mL (0.46-0.78 µg/mL) when patients were administered 10 mg/kg orally and 13 mg/kg IV RIF respectively. A study by Ruslami *et al.* [897] assessed PK and tolerability of TBM treatment in children aged 0-18 years in Indonesia, and reported large interindividual variability in RIF exposure and all patients had very low RIF CSF concentrations when compared to plasma (geometric mean CSF concentration of 0-8 hrs: 0.3 and 0.1 µg/mL on days 2 and 10, respectively). Furthermore, the geometric mean of RIF CSF concentration from 6-8 hrs was 0.4 µg/mL (range 0.1-1.4 µg/mL) and 0.2 µg/mL (range 0.1-0.7 µg/mL) on days 2 and 10 of PK assessment respectively [897].

There are various factors [745,911] to consider which may have contributed to low RIF concentrations in CSF. One factor could be inadequate RIF dosage. A study in 9 children undergoing shunt placement surgery reported CSF concentrations range of 0.12-3.0 (mean: 1.4) µg/mL after an IV dose of RIF (20mg/kg) [525]. Several studies have reported lower mortality in adult TBM patients who were administered high-dose (13 mg/kg) RIF via IV for the first 14 days of treatment compared to standard dose RIF (10 mg/kg) administered orally. High-dose RIF was safe and well tolerated [713,756]. Te Brake *et al.* [713] recommended a minimum target RIF AUC_{24} of at least 116 µg.h /mL and a C_{max} of 22 µg/mL for the first critical days of treatment in patients with TBM. However, RIF MIC was not determined in this study. In contrast, orally administered RIF (15 mg/kg) and LFX (20 mg/kg) did not show mortality benefit when compared with standard-dose RIF (10 mg/kg) (HR 0.94; 95% CI 0.73-1.22) in a Vietnamese adult TBM cohort [639]. Another study in Indonesian adult TBM patients that compared higher oral RIF doses (750 mg and 900 mg, 17 mg/kg and 20 mg/kg) vs IV (600 mg, 13 mg/kg) found that higher oral RIF doses resulted in approximately similar plasma AUC_{0-24} but lower C_{max} values compared with IV over 1.5 hrs [765]. Various studies have shown that the bactericidal

activity of RIF is dose-dependent which advocates for an adequate dose regimen in children with TBM [711,714,724,775,912]. Furthermore, RIF doses of up to 30 mg/kg have been reported to be well-tolerated and safe [758]. A recent phase II clinical trial in paediatric TBM reported higher frequency of adverse events in patients who were administered high-dose RIF (30 mg/kg) compared to standard RIF dose (15 mg/kg) but the former had better neurologic outcomes in fine motor, receptive language and expressive language domains [775].

In our TBM drug recovery cohort, sources of variability within and between patients could be attributed to age, weight and administration route. It is important to note that the nurse administering the drugs was not part of the study and therefore this represents a 'real world' scenario of drug administration. Some patients were administered RIF dose via NGT and some orally after crushing of tablets, and this may affect dissolution characteristics and absorption [913]. Of all the samples that were analysed for RIF (including post-analysis samples that were excluded), plasma samples (n=95), 34% had orally administered RIF vs 66% of samples that had NGT. A hundred percent of brain ECF (n=79) samples had RIF administered via NGT and 20% oral vs 80% NGT for VCSF (n=54) and 45% of LCSF (n=84) samples had RIF administered orally vs 55% NGT. However, studies have shown similar exposures in those receiving crushed tablets as compared to those swallowing whole tablets [758,914]. Food could also be a source of variability. It has been described that ingestion of RIF with food results in delayed absorption and extension of time to C_{max} (t_{max}) [915] to 3-4 hrs as compared to 1.5-2 hrs when administered without food [744,915]. Furthermore, it has been reported that food decreases RIF C_{max} by up to 36-40% [915,916] and decreases the RIF AUC by about 6-26% [915,916]. Physiochemical properties of RIF, which include, high molecular mass, lipophilic nature and 80% plasma protein binding, could also influence the amount of RIF that passes through the BBB when the meninges are uninflamed [8,528,710,778,917,918]. Nau *et al*. reported that in adult patients with uninflamed meninges, the CSF RIF $t_{1/2}$ was significantly longer (9-21 hrs) than in serum [526]. Furthermore, brain barrier efflux pumps may contribute to low CSF RIF concentrations [919]. Various studies have suggested limited strategy options to obtain AUC_{24} [920,921] which was not feasible for this project as in our TBM drug recovery cohort, only 25 patients had more than 1 blood sampled on the same day, at either 2-, 3-, 4-, 5- or 6 hrs post-dose.

RIF in brain ECF microdialysate

Our MD results show the first repeated measures of RIF concentrations in brain ECF in patients with TBM. These are promising because they represent the ability to detect RIF in the interstitium of the brain. Also, it demonstrates a method of repeated sampling that to date has not been possible at such high frequency for CSF studies as we were able to collect in the region of 48 samples over a 4–5-day period of time. More recently our group has refined our method to enable hourly sampling. ECF concentrations ranged from 0.01-0.04 µg/mL. In the first 10 hrs of sampling, brain ECF RIF

concentrations were 13-26% of VCSF concentrations. In interpreting these data, several unknown factors remain; therefore, these data are best viewed as proof of principle. In particular, it is difficult to quantify absolute concentrations of analytes *in vivo,* because the relative recovery rate is unknown. There may also be anatomical heterogeneity, depending on where in the brain the sampling is performed, particularly if there are perfusion differences. As such it is difficult to determine to what extent the lower ECF concentration reflects true or technical differences. However, it is plausible that the concentrations in ECF are lower than in CSF because the passage of drug into brain ECF across the BBB is likely more restricted than its passage into CSF across the BCSFB (through the choroid plexus vessels). That restriction may apply to the overall quantity of drugs crossing the two barriers but also in which form: given that most RIF is protein-bound in plasma, and that the BCSFB is more permeable than the BBB, there may be more protein-bound RIF in CSF than in ECF, which may explain the differences. If 80% of RIF is bound to protein, and macromolecules have limited passage across the BBB, the differences between the two compartments may reflect differences between total and free drug concentrations. With this in mind, if ECF concentrations dominantly reflect free drug concentrations, then the range in ECF 13-26% of the total drug concentration in VCSF may be reasonable considering RIF protein binding is around 80% [710,778].

Population PK analysis

Our collaboration study that applied a population PK analysis approach of RIF data from this project in plasma, CSF (lumbar and ventricular) and brain ECF was recently published [922]. Using a non-linear mixed-effect modelling approach from data collected in children with definite/probable TBM (n=61), the results showed differences in the pseudopartition coefficient between plasma and LCSF/VCSF (4.08%) and ECF (0.459%). Furthermore, the equilibrium half-life between plasma and LCSF/VCSF was ~ 4 hrs and between plasma and ECF ~ 2 hrs [922]. Differences in plasma-CSF equilibration and plasma-brain ECF could be attributed to changes in CSF volume which may affect pressure equilibrium and the concentration gradient between brain and CSF [857]. Our findings support the observation that RIF concentrations are lower in CSF when compared to plasma and provides novel knowledge about RIF in VCSF and brain ECF which are closer to the target site of infection in the brain.

Limitations

In this analysis, sampling was sporadic, including different sites in different patients and at different times. The administration of the drug was part of standard of care and not linked to the study. Therefore, there may have been differences in administration between patients that may affect bioavailability of the drug and therefore variability in the plasma concentrations. However, these differences are likely

true for patients being treated in a 'real world' scenario. As regards the comparison between LCSF and VCSF, these were not time-linked samples and therefore, we cannot control for potential bias introduced by why some patients may have had LPs and others had ventricular samples, i.e. there may be clinical differences between patients that determine the timing and location of the sample taken. For example, LCSF samples are sometimes more difficult to obtain in patients with very high protein values (probably because of arachnoiditis) [66] and patients with NCHC would be more likely to have EVD, shunt placement or endoscopy. Furthermore, our MD samples required pooling for RIF analysis across more than one hour because sample volumes were small (especially after analysing for brain chemistry). More recent improvements in analytical techniques at our institution though have enabled sample volumes as little as 5 µL to be sufficient for analysis. This will enable hourly samples to be analysed.

B. TIME-LINKED SAMPLES OF VCSF AND LCSF

To study TB drug concentrations, samples obtained from the LCSF are usually used to reflect brain concentrations, assuming that it is a reasonable proxy for the brain or VCSF. However, emerging data suggest that transport of substances across capillaries in the brain, choroid plexus and spinal cord may differ. Due to active transport processes at the level of the BBB, BSCB and BCSFB, complex relationships exist between concentrations in blood, VCSF and LCSF, and therefore comparing drug concentrations across these compartments is not always appropriate. Although LCSF is commonly used to study disease and treatment processes in TBM, it may not fully reflect VCSF or the brain. As a second arm of our study, we, therefore, examined paired, time-linked samples of VCSF and LCSF of 28 patients with TBM and analysed these for RIF and total protein concentrations. These samples were VCSF and LCSF taken at the same time in individual patients, either during a column test to determine the level of CSF block, or where a VPS was placed, and a LP was done under the same anaesthetic. Time-linked RIF and protein concentrations ensure each patient is their own control and avoids potential bias from non-matched samples. These time-linked samples afford us the unique opportunity to examine RIF and protein concentration in two different CSF compartments. Total protein concentrations were determined using the BCA or turbidimetry assay, and RIF concentrations were determined using a validated LC-MS/MS method (described above, chapter 9: drug quantification).

TBM drug recovery time-linked population

There were 28 patients diagnosed with definite/probable TBM who had VCSF and LCSF samples taken at the same time and who were included in this study. Of the 28 patients, 9 patients were new additions who were not part of the patient cohort described in section A and were enrolled after the analysis of the samples described in section A was completed. Of the 28 participants, 54% were female and the

median age was 2.6 years (range, 1-12.6 years), with median weight of 11.3 kg (range, 4.8-45 kg). Definite TBM was confirmed in 19 of the 28 cases (68%) who had CSF sent for TB culture or Xpert. A summary of demographic and patient characteristics is shown in Table 9.2. Methods of sample collection and analysis were the same as for the cohort above.

Table 9.2. Demographic and clinical information of time-linked TBM cohort (N=28)

Baseline Characteristics	**Value**
Age, years	2.6 (1-12.6)
Sex	
Female	15 (54)
Body weight	11.3 (4.8-48)
MRC staging admission	
1	2 (7)
2a	3 (11)
2b	5 (18)
3	18 (64)
Immunisations up to date**	18 (64)
HIV infection	1 (4)
Diagnostics	
Positive TB culture, GeneXpert or AFB	19 (68)
CSF characteristics for LCSF (29%)	
Glucose (mmol/L)	1.5 (0.5-2.9)
Chloride (mmol/L)	115 (104-125)
Protein (g/L)**	1.9 (0.5-4.6)
Lymphocytes (/cu mm)	75 (13-190)
Polymorphonuclear cells (/cu mm)	9 (1-88)
CSF characteristics for VCSF (71%)	
Glucose (mmol/L)	3.5 (1.8-4.7)
Chloride (mmol/L)	114 (93-126)
Protein (g/L)	0.6 (0.2-4.5)
Lymphocytes (/cu mm)	13 (3-90)
Polymorphonuclear cells (/cu mm))	1 (0-20)
Mortality	6 (21)

Age, weight and CSF characteristics are reported as median (minimum-maximum) range. Remaining values reported as number (percentage), *Admission CSF given as LCSF unless not available in which case VCSF is given, normal CSF values in paediatrics: glucose 2.3–3.9 mmol/L, chloride 120–130 mmol/L, protein 0.2–0.8 g/L, zero polymorphonuclear cells, <10 lymphocytes/cu mm, not all patience had full biochemistry or cell count profiles because diagnostic procedures had been done on previous specimens. MRC Staging refers to the 'refined' MRC for TBM severity staging, ** Immunization history for 1 patient was not available.

Figure 9.4. Photograph showing VCSF (left) and LCSF (right) taken at the same time from a single patient.

RIF time-linked concentrations

Figure 9.5 shows a longitudinal plot for the RIF concentration of 28 time-linked samples of LCSF and VCSF. Of these samples, 18 (64%) of the pairs showed lower VCSF concentrations compared to LCSF. Median RIF concentrations were lower in VCSF than LCSF: 133.0 ng/mL (range, 7.40-937 ng/mL, interquartile range 61.2-271 ng/mL) versus 299 ng/mL (range, 5-1080 ng/mL, interquartile range, 68.3-634.5 ng/mL) respectively (Figure 9.6). A paired Wilcoxon signed-rank test showed that these differences were significantly different (*P*=0.0046).

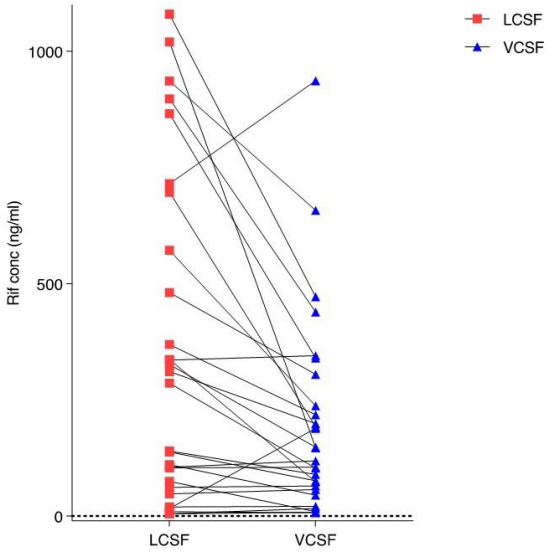

Figure 9.5. Longitudinal plot showing individual patient data comparing their RIF concentrations (ng/mL) LCSF (red square) and VCSF (blue triangle). RIF concentration (ng/mL) is shown on the y-axis. In 64% of the cases, the RIF concentration in LCSF was higher than the concentration in the time-linked VCSF sample.

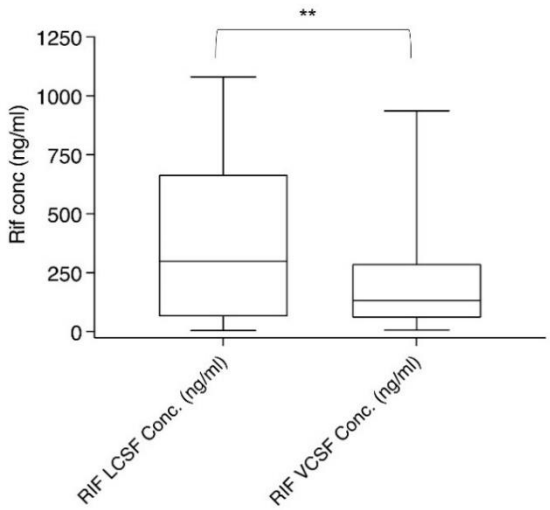

Figure 9.6. Box and Whiskers plot for RIF concentration (ng/mL) for 28 time-linked samples of LCSF and VCSF. The box represents the median and upper and lower quartiles, while the whisker in each plot corresponds to the 5th and 95th percentiles. A paired Wilcoxon signed-rank test was used to determine significance between groups. *P<0.05, **P<0.01; *** P<0.001.

Median RIF concentrations were determined in two hourly epochs. Although the graphs for LCSF and VCSF follow the same trend, reaching similar peaks (t=5 hrs) and troughs (t=2 hrs and 7 hrs) within the same epoch, the RIF concentration in the LCSF was greater than in the VCSF (Figure 9.7).

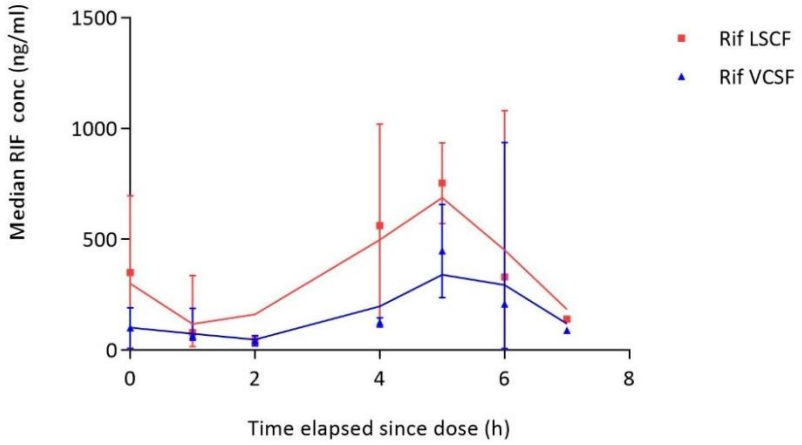

Figure 9.7. RIF concentrations for LCSF in red triangles and VCSF in blue triangles (y-axis) vs time elapsed since dose (x-axis). RIF concentrations are plotted as median with range in the hourly time epoch in which the sample was taken. Time epochs were plotted as follows: time elapsed=0, t=0 (n=2); time elapsed > 0 ≤1, t=1 (n=4); time elapsed > 1 ≤ 2, t=2 (n=2); time elapsed > 2 ≤3, t=3 (n=0); time elapsed > 3 ≤ 4, t=4 (n=2); time elapsed > 4 ≤ 5, t=5 (n=2); time elapsed > 5≤ 6, t=6 (14); time elapsed > 6 ≤ 7, t=7 (n=2).Protein concentrations

Time-linked protein concentrations for 27 samples of LCSF and VCSF were used for analysis (Figures 9.8 and 9.9). Protein concentrations were not available for 1 patient because the sample was not submitted to the laboratory for analysis and insufficient sample volume remained after RIF determination for protein determination at RCWMCH. The Pierce BCA protein assay kit (Thermoscientific) was used to determine protein concentrations in cases where there was insufficient sample volume to use the NHLS third-generation turbidimetric method. The two methods showed good agreement with each other (R^2 = 099).

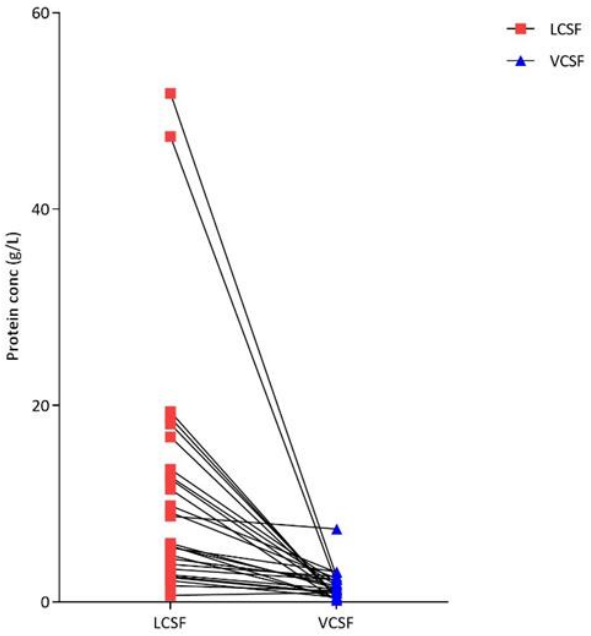

Figure 9.8. Longitudinal plot showing the difference in protein concentration (g/L) between time-linked (n=27) samples of LCSF (red square) and VCSF (blue triangle). Protein concentration (g/L) is shown on the y-axis. In all cases the protein concentration in LCSF was higher than the time-linked concentration in VCSF sample.

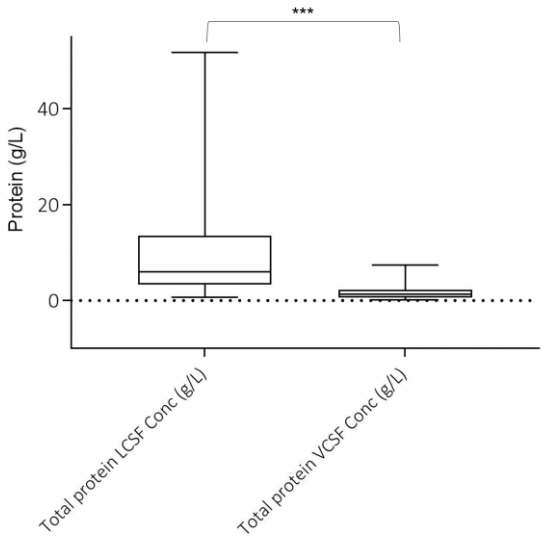

Figure 9.9. Box and Whiskers plot for protein concentration (g/L) for 27 time-linked samples of LCSF and VCSF. The box represents the median and the upper and lower quartiles, while the whisker in each plot corresponds to the 5th and 95th percentiles. A paired Wilcoxon signed-rank test was used to determine significance between groups. *P<0.05; **P<0.01; ***P<0.001.

In all cases, the protein concentration in LCSF was higher than the concentration in the time-linked VCSF sample (Figure 9.8). The median protein concentration in LCSF was 6.0 g/L (range, 0.68-51.8 g/L, interquartile range 3.34-13.5 g/L) and in VCSF 1.3 g/L (range, 0.17-7.44 g/L, interquartile range 0.58-2.25 g/L) (Figure 9.9). A paired Wilcoxon signed-rank test showed that the protein concentrations for LCSF and VCSF were significantly different (p<0.0001).

Discussion (time-linked data)

Knowledge about drug kinetics in the CNS is important, particularly for drugs that act on targets in the CNS such as antibacterials (i.e. RIF) [299]. For an anti-TB drug to be effective in the treatment of TBM, it must be able to penetrate CSF and reach infected tissue in the brain and meninges [636]. Previous studies have not reported VCSF concentrations in TBM patients, and generally have not reported protein concentrations, which may be important given that RIF is a highly protein-bound drug and it is the unbound drug that is active. In our overall cohort, we published for the first time RIF concentrations in VCSF in children, along with an exploratory analysis of RIF in brain ECF [922]. For this current analysis, we selected only patients who had VCSF and LCSF samples taken at the same time to optimize comparison. We determined the RIF (n=28) and protein (n=27) concentrations in time-linked pairs of LCSF and VCSF samples obtained from children who presented to the RCWMCH with definite or probable TBM, all of whom were on a drug dose regimen consisting of RIF (20 mg/kg), INH (15-20 mg/kg), PZA (40 mg/kg) and ETH (20 mg/kg). These data highlight the relevance of careful consideration of the compartments in the CNS, as both RIF and protein concentrations were significantly different between LCSF and VCSF.

A longitudinal plot (Figure 9.5) showed that LCSF RIF concentrations were higher in almost two-thirds of samples. Median values for RIF were 133.0 ng/mL (interquartile range 61.2-271 ng/mL) versus 299 ng/mL (interquartile range, 68.3-634.5 ng/mL) for VCSF and LCSF respectively. It is unlikely that these differences are explained only by a delay in drug appearing in LCSF as the peak and troughs are similar and there is no pattern of a delayed peak in LCSF. Similarly, we would have expected concentrations in VCSF then to be higher in the earlier samples. There did not appear to be a significant delay between the peak in LCSF and VCSF. Given the observation that the BSCB is more permeable than BBB, it is possible that the drug concentrations in the LCSF may cross from the systemic circulation directly into spinal CSF [923], rather than the traditional bulk flow theory of CSF circulation in which the drug first appears in the ventricles of the brain and moves in a slow rostro-caudal direction out of the ventricular system and down the spinal subarachnoid space. The peak RIF concentration was 0.745 mg/L in LCSF and 0.447 mg/mL VCSF. Although both values are above the MIC for *Mtb* (0.2 – 0.4 mg/L), [648] the peak concentration of RIF in LCSF was 1.7 times greater than in VCSF.

The results were similar for protein concentrations in LCSF and VCSF. In 27 time-linked samples, the protein concentrations were significantly greater in LCSF compared to VCSF, and values were higher in all samples (27/27) (Figure 9.8). These findings may be particularly important if results reported for LCSF are used to infer the drug concentrations in the brain, in particular because RIF is highly protein-

bound. Consequently, the significantly lower protein concentration in VCSF (median 1.3g/L, range 0.17-7.4 g/L) compared to LCSF (median 6.0 g/L, range 0.68-51.8 g/L) may influence the availability of the unbound pharmacologically active fraction of RIF [702]. To date, this has not been examined yet because unbound drug concentrations in CSF of TBM patients have not been determined. The CSF protein compartment differences are likely an exacerbation of normal physiology due to reduced flow in the spinal canal, possibly increased by arachnoiditis associated with TBM. Still, even in the healthy brain with no restriction to CSF movement, LCSF total protein concentration may be 3 times higher than VCSF owing to equilibration of CSF with plasma through meningeal capillary walls during the passage through the spinal canal [924,925]. As such, reduction of CSF flow owing to CNS pathology affecting the spine may result in pooling of CSF and an exaggeration of total protein levels which progressively mimics that of plasma in total protein concentration and patterns of proteins present [926]. This could add to the increase in LCSF total protein in TBM in which spinal disease has been reported [66]. Panjasawatwong *et al.* found that protein was significantly associated with RIF concentrations in Vietnamese children with TBM [906]. Furthermore, based on their modelling with a presumed 80% protein binding in the plasma from reported literature, only 16.9% (14.5%-19.6%, 95% C.I) of the total drug penetrated the BBB (or, was assumed to, given that these were spinal CSF samples), which rose to 27.8% when the protein content in the CSF increased by 1g/L [906]. CSF protein has been described as a known marker of CNS inflammation and is thought to correlate with the function of the BBB, resulting in higher protein content in CSF because of severe inflammation and a leaky BBB [237,918]. As a result, RIF penetrates the BBB better at high protein concentrations. However, there may be other factors that influence protein concentrations in spinal CSF which may confound its role (or that of albumin) as a marker of BBB permeability. For example, it is possible that a reduced CSF flow rate in the spinal canal leads to an increase in CSF protein concentrations due to decreased volume exchange. This may result in a subsequent change in BCSFB concentration gradients with an initial increase in molecular net flux of proteins into CSF without changes in BCSFB-related structures [121]. The argument therefore suggests that regardless of BBB integrity, a reduction in CSF flow (due to relative obstruction for instance) results in an increase in spinal CSF protein, implying a change in CSF flow rate to be a main driver/determinant of change in protein dynamics within and between CSF compartments. Recently, Reiber has shown that there is a nonlinear increase in blood proteins in CSF between the ventricles and lumbar subarachnoid space [927]. Relative barriers to CSF flow in the spinal canal increases the flux of molecules from the systemic circulation. This has been shown experimentally, in animals, and is thought to be the cause of the high protein concentrations seen in Froin's syndrome [927–929]. Spinal parenchymal and subarachnoid space involvement, including exudate and extramedullary lesions, appear on MRI spine imaging in most children with TBM, possibly adding to the disturbed circulation of spinal CSF [66]. Finally, entry into LCSF may also occur via the vessels surrounding the spinal cord, and the barrier in these vessels (BSCB) have been shown to be

somewhat different to the vessels comprising the BBB. In particular, the BSCB has been shown to be more permeable than the BBB. Experiments in rabbit models showed increased uptake of both [3H]-D-mannitol and [14C]-carboxyl-inulin in the spine compared to the brain [930]. Using radiolabelled interferons, Pan *et al.* demonstrated that in mouse models the spinal cord had the highest permeability while the brain was least permeable to interferons of similar chemical structure and molecular weight [923]. Therefore, CSF protein concentrations may be affected by increased permeability of the BBB, reduced flow in the spinal canal, and differential permeability of the BSCB, potentially leading to higher concentrations both of blood-derived proteins as well as drug concentrations in the LCSF. Variability in total protein within CSF compartments could also be influenced by age which would in turn influence the composition of proteins that make up the total protein concentrations [926].

Consistent with these observations, differences in concentrations of molecules between LCSF and VCSF have been shown in several published studies, from physiological to pathological conditions. CSF rostro-caudal gradients are reported in dogs, neurologically normal humans, and increasingly in several conditions such as Parkinson's disease and idiopathic normal pressure HCP [928,931–933]. When infants with CommHC were administered radiolabeled serum albumin through IV, it was found that radioactivity was highest in the LCSF and lowest in the VCSF [934]. Previous work in our group in TBM patients is in keeping with these observations. First, VCSF and LCSF have different protein biomarker profiles, with significantly higher concentrations of proteins of cerebral origin in VCSF and higher concentrations of inflammatory mediators in LCSF [888]. Second, RNA sequencing showed significantly different gene expression profiles between the LCSF and VCSF, with the ventricular signature demonstrating pathways associated with brain injury and the lumbar signature demonstrating protein translation and cytokine signalling [144].

It is interesting to note that the peak RIF concentration in both the LCSF and VCSF compartments occurred 5 hrs after the RIF dose was given (Figure 9.7). Given the expectation that substances in the LCSF depend on passage from the ventricular compartment to the lumbar compartment, this is unanticipated. However, based on the potential that substances enter LCSF also directly from the systemic circulation, could contribute to this finding. Also, in critically ill patients who present with TBM, the increased permeability of the BSCB means that molecules may freely flow directly from the blood vessels which supply the spinal cord into the LCSF [935,936]. Molecules may therefore enter VCSF and LCSF through different routes but at similar times. In this case, the LCSF and VCSF compartments may be comparable in terms of timing but do not reflect each other in terms of composition.

Additionally, experiments by Klarica *et al.* have challenged the classical theory of unidirectional CSF movement as previously described in chapter 3. They have postulated instead that CSF is being permanently produced and absorbed inside the entire CSF system and that there is an influx and exchange of fluid at the capillary level in the CNS, thereby explaining how peak concentration can simultaneously be reached in the LCSF and VCSF as seen in Figure 9.7 [534,535,543]. All the above may help explain the observations of differences in drug and protein concentrations demonstrated in our results.

Since LCSF total protein concentrations are said to pool from various sources [924,925], a question arises if free RIF concentrations follow a similar pattern in LCSF which could therefore overestimate RIF concentrations in brain tissue. Di Paolo *et al.* stated that studies of the distribution of antibacterials from systemic circulation into the CSF should only consider free fraction of drugs in plasma, which is responsible for the pharmacological effect in tissues [937]. Collective literature has shown that RIF has limited penetration into the CNS with current regimens and has been shown to decrease rapidly as early as two weeks after treatment initiation [569,756]. Whilst LCSF has been widely accepted as a surrogate for target site drug concentrations, a rethink may be needed. Furthermore, Shen *et al.* highlighted the fact that the presence of a drug in CSF only reflects extracellular drug availability and does not reveal access of drugs to the intracellular sites within the brain parenchyma [548].

Limitations

Although significant differences were shown, the study sample size is small, and the results need to be replicated in a larger study. Still, this is the first study of its kind that performed time-linked comparison of brain and spinal CSF, and the results are informative for further studies. Patients were on the more severe end of the spectrum compared to many other cohorts given that they had HCP that required intervention and because of referral patterns to our hospital. However, these are patients that are at the highest risk of poor outcomes and the group for which an accurate understanding of drug concentrations is of greatest value. The study also relied on diagnostic and clinical procedures and therefore sampling was sporadic and timing varied. This is unfortunately true for most studies because sampling is invasive, and therefore this is a difficult limitation to overcome. Higher frequency sampling may yield different results. Finally, like other studies, these results reflect total concentrations of the drug, whereas it is the free drug concentration that is active. This is particularly relevant given the differences between protein concentrations in blood compared to CSF, between CSF compartments as demonstrated here, and between patients. Despite these limitations, these are the first data that compare drug concentrations in paired samples of VCSF and LCSF in TBM patients.

Conclusion

This study is the first to report and compare RIF and protein concentrations in time-linked, paired samples of LCSF and VCSF. It showed significant differences for both RIF concentrations and CSF protein concentrations between compartments. Interpreted in conjunction with previous work showing other differences between the compartments in TBM patients, and emerging data on anatomical and physiological reasons why LCSF and VCSF may differ in various constituents, it is important that we consider these differences in interpreting PK data for drugs targeted at neurological disorders. Emerging data from studies such as this could inform models to more accurately predict drug action at the critical sites of disease. Our conclusions are based on a limited number of paired LCSF and VCSF samples and further analysis with a larger sample size is needed to confirm the results seen in this exploratory study.

FINAL THESIS SUMMARY

The overarching aim of this study was to describe RIF concentrations in multiple compartments, and over time (where possible), in children with TBM. RIF remains one of the crucial first-line drugs in TBM management, yet our understanding of its distribution and dynamics between the periphery and within the CNS remains limited. This study's access to unique, high-frequency site-of-disease samples contributes important novel insights to this domain of TBM research.

Our results showed that plasma concentrations were lower than the suggested target concentration of ≥8 µg/mL at 2 hrs post-dose. Although this concentration is yet to be validated in children, these real-world data highlight the value of an updated higher paediatric dosing regimen.

In this work, we report, for the first time, RIF concentrations in VCSF in TBM patients, RIF concentrations in brain tissue ECF, and time-linked paired samples of VCSF and LCSF. Whilst site-of-disease sampling was sporadic, our data provides novel knowledge about RIF in VCSF and brain ECF which are closer to the target site of infection in the brain.

VCSF RIF concentrations were low. Intriguingly, the paired sample analysis shows higher RIF concentrations in LCSF, which may reflect a sump effect, different protein-binding characteristics (because LCSF protein concentrations were also higher), or differential permeability of the spinal blood vessels. This work raises important discussion points about the different barriers that may influence the drug concentrations in a compartment and the interpretation thereof, namely the BBB, the BCSFB, and the BSCB. Given that the current knowledge of RIF in TBM patients is largely based on spinal CSF studies, it is important to note the potential differences as reported in this work, and therefore that LCSF concentrations may overestimate concentrations in VCSF.

We also demonstrated for the first time the capacity to serially sample RIF directly from brain ECF, where concentrations were considerably lower than in VCSF. This may be technical but also may reflect a difference between total and free drug concentrations, given the differential barrier properties of the BBB (determining ECF concentrations) and BCSFB (determining VCSF concentrations).

Overall, these studies contribute timely and important data in an era of focus on maximising RIF exposure by increasing drug dosing. Our findings are important as TBM affects children during critical brain development and there is an urgency to optimize antimicrobial therapy that reaches the target site of infection in the brain.

RECOMMENDATION OF FUTURE WORK

These findings highlight the importance of target site PK studies (CNS compartments) when feasible. Recommendations for future work include considering variability in drug exposure from decreased or delayed absorption due to critical illness, trialling alternative regimens /novel anti-TB drugs to optimize dosing in children with TBM, examining the impact of IV RIF, especially in critically ill patients, in whom drug availability from oral administration may not be the same as in less ill patients, and measuring free drug in CSF along with total drug to further our understanding of protein-drug binding in CSF and the availability of active drug. To overcome some methodological limitations of MD, further *in vitro* experiments to determine the RR in tissue would be valuable, and the Paediatric Neurosurgery Unit at RCWMCH has developed a novel approach to performing MD in CSF, where RR can be determined and the impact of drugs on target pathways can be evaluated.

REFERENCES

1. World Health Organization. Annual Report of Tuberculosis. Annu Glob TB Rep WHO. 2022 [cited 2023 Jun 1];8(1):1–68.

2. Bagcchi S. WHO's Global Tuberculosis Report 2022. 2023 [cited 2023 Jun 19].

3. Wolzak NK, Cooke ML, Orth H, Van Toorn R. The Changing Profile of Pediatric Meningitis at a Referral Centre in Cape Town, South Africa. Journal of tropical pediatrics. 2012 Dec 1 ; [cited 2019 Dec 5]58(6):491-5.

4. Donald PR, Schoeman JF. Tuberculous meningitis. N Engl J Med. 2004 Oct 21;351(17):1719-20.

5. Thwaites GE, Duc Bang N, Huy Dung N, Thi Quy H, Thi Tuong Oanh D, Thi Cam Thoa N, et al. The Influence of HIV Infection on Clinical Presentation, Response to Treatment, and Outcome in Adults with Tuberculous Meningitis. J Infect Dis. 2005 Dec 15 [cited 2020 May 19];192(12):2134–41.

6. Wilkinson RJ, Rohlwink U, Misra UK, Van Crevel R, Mai NTH, Dooley KE, et al. Tuberculous meningitis. Vol. 13, Nature Reviews Neurology. Nature Publishing Group; 2017 Oct [cited 2020 Sep 30];13(10):581-98.

7. Pouplin T, Bang ND, Toi P Van, Phuong PN, Dung NH, Duong TN, et al. Naïve-pooled pharmacokinetic analysis of pyrazinamide, isoniazid and rifampicin in plasma and cerebrospinal fluid of Vietnamese children with tuberculous meningitis. BMC Infect Dis. 2016 Apr 2 [cited 2017 Feb 20];16(1):144.

8. Mindermann T, Zimmerli W, Gratzl O. Rifampin concentrations in various compartments of the human brain: A novel method for determining drug levels in the cerebral extracellular space. Antimicrob Agents Chemother. 1998;42(10):2626–9.

9. Ederoth P, Tunblad K, Bouw R, Lundberg CJ, Ungerstedt U, Nordstrom CH, et al. Blood-brain barrier transport of morphine in patients with severe brain trauma. Br J Clin Pharmacol. 2004;57(4):427–35.

10. Tisdall MM, Smith M. Cerebral microdialysis: research technique or clinical tool. Br J Anaesth. 2006 Jul 1 [cited 2021 Feb 2];97(1):18–25.

11. Rock RB, Olin M, Baker CA, Molitor TW, Peterson PK. Central nervous system tuberculosis: Pathogenesis and clinical aspects. Vol. 21, Clinical Microbiology Reviews. American Society for Microbiology Journals; 2008 Apr [cited 2021 Feb 7;21(2):243-61.

12. Eruslanov EB, Lyadova I V., Kondratieva TK, Majorov KB, Scheglov I V., Orlova MO, et al. Neutrophil responses to Mycobacterium tuberculosis infection in genetically susceptible and resistant mice. Infect Immun. 2005 Mar 1 [cited 2021 Feb 2];73(3):1744–53.

13. Eum SY, Kong JH, Hong MS, Lee YJ, Kim JH, Hwang SH, et al. Neutrophils are the predominant infected phagocytic cells in the airways of patients with active pulmonary TB. Chest. 2010 Jan 1;137(1):122–8.

14. Davis AG, Rohlwink UK, Proust A, Figaji AA, Wilkinson RJ. The pathogenesis of tuberculous meningitis. J Leukoc Biol. 2019 Feb 15 [cited 2021 Feb 3];105(2):267–80.

15. Wolf AJ, Linas B, Trevejo-Nuñez GJ, Kincaid E, Tamura T, Takatsu K, et al. Mycobacterium tuberculosis Infects Dendritic Cells with High Frequency and Impairs Their Function In Vivo . J Immunol. 2007 Aug 15 [cited 2021 Feb 3];179(4):2509–19.

16. Kleinnijenhuis J, Oosting M, Joosten LA, Netea MG, Van Crevel R . Innate immune recognition of mycobacterium tuberculosis. Clinical and Developmental Immunology. 2011;2011:405310.

17. Akira S, Takeda K, Kaisho T. Toll-like receptors: Critical proteins linking innate and acquired immunity. Nature Immunology. 2001 Aug 2 [cited 2021 Jun 9];2(8):675-80.

18. Kindler V, Sappino AP, Grau GE, Piguet PF, Vassalli P. The inducing role of tumor necrosis factor in the development of bactericidal granulomas during BCG infection. Cell. 1989 Mar 10 [cited 2020 Apr 20];56(5):731–40.

19. Flynn JAL, Goldstein MM, Chan J, Triebold KJ, Pfeffer K, Lowenstein CJ, et al. Tumor necrosis factor-α is required in the protective immune response against mycobacterium tuberculosis in mice. Immunity. 1995 Jun 1;2(6):561–72.

20. Fremond CM, Togbe D, Doz E, Rose S, Vasseur V, Maillet I, et al. IL-1 Receptor-Mediated Signal Is an Essential Component of MyD88-Dependent Innate Response to Mycobacterium tuberculosis Infection . J Immunol. 2007 Jul 15 [cited 2021 Jun 9];179(2):1178–89.

21. Juffermans NP, Florquin S, Camoglio L, Verbon A, Kolk AH, Speelman P, et al. Interleukin-1 signaling is essential for host defense during murine pulmonary tuberculosis. J Infect Dis. 2000 Sep 1 [cited 2021 Jun 9];182(3):902–8.

22. Yamada H, Mizumo S, Horai R, Iwakura Y, Sugawara I. Protective role of interleukin-1 in mycobacterial infection in IL-1 α/β double-knockout mice. Lab Investig. 2000 May 1 [cited 2021 Jun 9];80(5):759–67.

23. Stout RD. Macrophage activation by T cells: cognate and non-cognate signals. Curr Opin Immunol. 1993;5(3):398–403.

24. Bhatt K, Salgame P. Host Innate Immune Response to Mycobacterium tuberculosis. J Clin Immunol. 2007 Jun 11 [cited 2019 Oct 7];27(4):347–62.

25. Russell DG, Barry CE, Flynn JL. Tuberculosis: what we don't know can, and does, hurt us. Science. 2010 May 14 [cited 2019 Oct 7];328(5980):852–6.

26. Delogu G, Provvedi R, Sali M, Manganelli R. Mycobacterium tuberculosis virulence: Insights and impact on vaccine development. Vol. 10, Future Microbiology. Future Medicine Ltd. 2015 Jul 1;10(7):117-94.

27. Singh M, Mynak ML, Kumar L, Mathew JL, Jindal SK. Prevalence and risk factors for transmission of infection among children in household contact with adults having pulmonary tuberculosis. Arch Dis Child. 2005 Jun 1;90(6):624–8.

28. Drain PK, Bajema KL, Dowdy D, Dheda K, Naidoo K, Schumacher SG, et al. Incipient and subclinical tuberculosis: A clinical review of early stages and progression of infection. Vol. 31, Clinical Microbiology Reviews. American Society for Microbiology; 2018 Oct [cited 2020 Nov 4];31(4):10-128.

29. Wolf AJ, Desvignes L, Linas B, Banaiee N, Tamura T, Takatsu K, et al. Initiation of the adaptive immune response to Mycobacterium tuberculosis depends on antigen production in the local lymph node, not the lungs. J Exp Med. 2008 Jan 21;205(1):105–15.

30. Gallegos AM, Pamer EG, Glickman MS. Delayed protection by ESAT-6-specific effector CD4+ T cells after airborne M. tuberculosis infection. J Exp Med. 2008 Sep 29;205(10):2359–68.

31. Pando RH, Aguilar LD, Smith I, Manganelli R. Immunogenicity and Protection Induced by a Mycobacterium tuberculosis sigE Mutant in a BALB/c Mouse Model of Progressive Pulmonary Tuberculosis. Infect Immun. 2010 [cited 2019 Mar 27];78(7):3168–76.

32. Aguilo JI, Alonso H, Uranga S, Marinova D, Arbués A, de Martino A, et al. ESX-1-induced apoptosis is involved in cell-to-cell spread of Mycobacterium tuberculosis. Cell Microbiol. 2013 Dec [cited 2020 Apr 20];15(12):1994–2005.

33. Gröschel MI, Sayes F, Simeone R, Majlessi L, Brosch R. ESX secretion systems: mycobacterial evolution to counter host immunity. Nat Publ Gr. 2016 Nov;14(11):677-91.

34. Houben ENG, Korotkov K V., Bitter W. Take five - Type VII secretion systems of Mycobacteria. Biochim Biophys Acta - Mol Cell Res. 2014 Aug 1;1843(8):1707–16.

35. Begley DJ. Delivery of therapeutic agents to the central nervous system: the problems and the possibilities. Pharmacol Ther. 2004 Oct [cited 2017 Sep 14];104(1):29–45.

36. Serlin Y, Shelef I, Knyazer B, Friedman A. Anatomy and physiology of the blood–brain barrier. Semin Cell Dev Biol. 2015;38:2–6.

37. Pulzova L, Bhide MR, Andrej K. Pathogen translocation across the blood-brain barrier. FEMS Immunology and Medical Microbiology. Oxford Academic; 2009 [cited 2021 Feb 3];57:203-13.

38. Be N a, Kim KS, Bishai WR, Jain SK. Pathogenesis of central nervous system tuberculosis. Curr Mol Med. 2009;9(2):94–9.

39. Milhorat TH. Structure and Function of the Choroid Plexus and Other Sites of Cerebrospinal Fluid Formation. Int Rev Cytol. 1976 Jan 1;47:225-88.

40. Van Der Flier M, Hoppenreijs S, Van Rensburg AJ, Ruyken M, Kolk AHJ, Springer P, et al. Vascular endothelial growth factor and blood-brain barrier disruption in tuberculous meningitis. Pediatr Infect Dis J. 2004 Jul [cited 2021 Feb 4];23(7):608–13.

41. Kim H, Lee JM, Park JS, Jo SA, Kim YO, Kim CW, et al. Dexamethasone coordinately regulates angiopoietin-1 and VEGF: A mechanism of glucocorticoid-induced stabilization of blood-brain barrier. Biochem Biophys Res Commun. 2008 Jul 18 [cited 2021 Feb 4];372(1):243–8.

42. Lee KY, Kim EH, Yang WS, Ryu H, Cho S-N, Lee BI, et al. Persistent increase of matrix metalloproteinases in cerebrospinal fluid of tuberculous meningitis. Journal of the neurological sciences.2004 May 15 [cited 2022 Jul 21];220(1-2):73-8..

43. Yong VW. Metalloproteinases: Mediators of pathology and regeneration in the CNS. Nat Rev Neurosci. 2005 Dec;6(12):931–44.

44. David Y, Cacheaux LP, Ivens S, Lapilover E, Heinemann U, Kaufer D, et al. Astrocytic Dysfunction in Epileptogenesis: Consequence of Altered Potassium and Glutamate Homeostasis? J Neurosci. 2009 Aug 26;29(34):10588-99.

45. Lapilover EG, Lippmann K, Salar S, Maslarova A, Dreier JP, Heinemann U, et al. Peri-infarct blood-brain barrier dysfunction facilitates induction of spreading depolarization associated with epileptiform discharges. Neurobiol Dis. 2012 Dec 1;48(3):495-506.

46. Ivens S, Kaufer D, Flores LP, Bechmann I, Zumsteg D, Tomkins O, et al. TGF-β receptor-mediated albumin uptake into astrocytes is involved in neocortical epileptogenesis. Brain. 2007 Feb 1;130(2):535-47.

47. Nadal A, Fuentes E, Pastor J, McNaughton PA. Plasma albumin is a potent trigger of calcium signals and DNA synthesis in astrocytes. Proc Natl Acad Sci. 1995 Feb 28;92(5):1426-30.

48. RICH, AR. The pathogenesis of tuberculous meningitis. Bull John Hopkins Hosp. 1933;52:5.

49. Donald PR, Schaaf HS, Schoeman JF. Tuberculous meningitis and miliary tuberculosis: The Rich focus revisited. J Infect. 2005;50(3):193–5.

50. Jain SK, Tobin DM, Tucker EW, Venketaraman V, Ordonez AA, Jayashankar L, et al. Tuberculous meningitis: A roadmap for advancing basic and translational research. In: Nature Immunology. 2018 Jun;19(6):521-5.

51. Al-Deeb SM, Yaqub BA, Sharif HS, Motaery KR. Neurotuberculosis: a review. Clin Neurol Neurosurg. 1992;94(SUPPL.):30–3.

52. Cresswell F V., Te Brake L, Atherton R, Ruslami R, Dooley KE, Aarnoutse R, et al. Intensified antibiotic treatment of tuberculosis meningitis. Vol. 12, Expert Review of Clinical Pharmacology. Taylor and Francis Ltd; 2019 Mar 4;12(3):267-88.

53. Thwaites G, Chau T, Mai N, Drobniewski F, McAdam K, Farrar J. Tuberculous meningitis. J Neurol Neurosurg Psychiatry. 2000 Mar 1;68(3):289-99.

54. Nguyen L, Pieters J. The Trojan horse: Survival tactics of pathogenic mycobacteria in macrophages. Vol. 15, Trends in Cell Biology. Elsevier Ltd; 2005 May 1;15(5):269-76.

55. Ginhoux F, Greter M, Leboeuf M, Nandi S, See P, Gokhan S, et al. Fate mapping analysis reveals that adult microglia derive from primitive macrophages. Science. 2010 Nov 5 [cited 2019 Jul 4];330(6005):841–5.

56. Peterson PK, Gekker G, Hu S, Sheng WS, Anderson WR, Ulevitch RJ, et al. CD14 receptor-mediated uptake of nonopsonized Mycobacterium tuberculosis by human microglia. Infect Immun. 1995 [cited 2021 Feb 3];63(4):1598–602.

57. Rock RB, Hu S, Gekker G, Sheng WS, May B, Kapur V, et al. Mycobacterium tuberculosis-induced cytokine and chemokine expression by human microglia and astrocytes: Effects of dexamethasone. J Infect Dis. 2005 Dec 15 [cited 2021 Feb 3];192(12):2054–8.

58. Rock RB, Gekker G, Hu S, Sheng WS, Cheeran M, Lokensgard JR, et al. Role of microglia in central nervous system infections]. Vol. 17, Clinical Microbiology Reviews. 2004 Oct [cited 2021 Jun 18];17(4):942-64.

59. Kreutzberg GW. Microglia: a sensor for pathological events in the CNS. Trends Neurosci. 1996 Aug 1 [cited 2019 Jul 18];19(8):312–8.

60. Tsenova L, Bergtold A, Freedman VH, Young RA, Kaplan G. Tumor necrosis factor α is a determinant of pathogenesis and disease progression in mycobacterial infection in the central

nervous system. Proc Natl Acad Sci U S A. 1999 May 11 [cited 2021 Feb 4];96(10):5657–62.

61. Curto M, Reali C, Palmieri G, Scintu F, Schivo ML, Sogos V, et al. Inhibition of cytokines expression in human microglia infected by virulent and non-virulent mycobacteria. Neurochem Int. 2004 [cited 2021 Feb 3];44(6):381–92.

62. Yang CS, Lee HM, Lee JY, Kim JA, Lee SJ, Shin DM, et al. Reactive oxygen species and p47phox activation are essential for the Mycobacterium tuberculosis-induced pro-inflammatory response in murine microglia. J Neuroinflammation. 2007 Dec 4 [cited 2021 Feb 3];4:1-6.

63. Katti MK. Pathogenesis, diagnosis, treatment, and outcome aspects of cerebral tuberculosis. Medical Science Monitor. International journal of experimental and clinical research 2004 Aug 20;10(9):RA215-29.

64. Dastur DK, Manghani DK, Udani PM. Pathology and pathogenetic mechanisms in neurotuberculosis. Radiologic Clinics of North America. 1995 Jul 1;33(4):733-52.

65. Daniel PM. Gross Morbid Anatomy of the Central Nervous System of Cases of Tuberculous Meningitis Treated with Streptomycin. J R Soc Med. 1949 [cited 2021 Feb 5];42(3):169–74.

66. Rohlwink UK, Kilborn T, Wieselthaler N, Banderker E, Zwane E, Figaji AA. Imaging Features of the Brain, Cerebral Vessels and Spine in Pediatric Tuberculous Meningitis With Associated Hydrocephalus. Pediatr Infect Dis J. 2016 Oct 1;35(10):e310-10.

67. J van Well GT, Paes BF, Terwee CB, Springer P, Roord JJ, Donald PR, et al. Twenty Years of Pediatric Tuberculous Meningitis: A Retrospective Cohort Study in the Western Cape of South Africa. *Pediatrics* (2009)123(1):e1-e8

68. Thwaites GE, Macmullen-Price J, Chau TTH, Phuong Mai P, Dung NT, Simmons CP, et al. Serial MRI to determine the effect of dexamethasone on the cerebral pathology of tuberculous meningitis: an observational study. Lancet Neurol. 2007;6(3):230–6.

69. Hsieh FY, Chia LG, Shen WC. Locations of cerebral infarctions in tuberculous meningitis. Neuroradiology. 1992 May;34(3):197–9.

70. Springer P, Swanevelder S, van Toorn R, van Rensburg AJ, Schoeman J. Cerebral infarction and neurodevelopmental outcome in childhood tuberculous meningitis. Eur J Paediatr Neurol. 2009 Jul 1;13(4):343–9.

71. Garg RK. Tuberculosis of the central nervous system. [cited 2021 Jun 13]. *Posgraduate Medical Journal*, 1999 March;75(881):133-140.

72. Andronikou S, Wilmshurst J, Hatherill M, VanToorn R. Distribution of brain infarction in

children with tuberculous meningitis and correlation with outcome score at 6 months. Pediatr Radiol. 2006 Dec 10 [cited 2021 Jun 15];36(12):1289–94.

73. Pienaar M, Andronikou S, Van Toorn R. MRI to demonstrate diagnostic features and complications of TBM not seen with CT. Child's Nerv Syst. 2009 Aug 24 [cited 2020 Oct 8];25(8):941–7.

74. Ramzan A, Nayil K, Asimi R, Wani A, Makhdoomi R, Jain A. Childhood tubercular meningitis: An institutional experience and analysis of predictors of outcome. Pediatr Neurol. 2013 Jan;48(1):30–5.

75. Schoeman JF, Donald PR. Tuberculous meningitis. In: Handbook of Clinical Neurology. Elsevier B.V.; 2013. p. 1135–8.

76. Chambers ST, Record C, Hendrickse WA, Rudge P, Smith H. Paradoxical expansion of intracranial tuberculomas during chemotherapy. Lancet. 1984 Jul 28;324(8396):181–4.

77. Thonell L, Pendle S, Sacks L. Clinical and radiological features of South African patients with tuberculomas of the brain. Clin Infect Dis. 2000 Aug 1 [cited 2021 Jun 27];31(2):619–20.

78. Dubé MP, Holtom PD, Larsen RA. Tuberculous meningitis in patients with and without human immunodeficiency virus infection. Am J Med. 1992 Nov 1;93(5):520–4.

79. Martínez-Vázquez C, Bordón J, Rodríguez-González A, de la J, Sopeña B, Gallego-Rivera A, et al. Cerebral tuberculoma - A comparative study in patients with and without HIV infection. Infection. 1995 May [cited 2021 Jun 27];23(3):149–53.

80. Welchman JM. Computerised tomography of intracranial tuberculomata. Clin Radiol. 1979;30(5):567–73.

81. Bhargava S, Tandon PN. Intracranial tuberculomas: A CT study. Br J Radiol. 1980 Jan 28 [cited 2021 Jun 27];53(634):935–45.

82. Lees AJ, Macleod AF, Marshall J. Cerebral tuberculomas developing during treatment of tuberculous meningitis. Lancet. 1980 Jun 7;315(8180):1208–11.

83. Teoh R, Humphries MJ, O'Mahony G. Symptomatic intracranial tuberculoma developing during treatment of tuberculosis: A report of 10 patients and review of the literature. Q J Med. 1987 May 1 [cited 2021 Jun 27];63(241):449–60.

84. Ravenscroft A, Schoeman JF, Donald PR. Tuberculous granulomas in childhood tuberculous meningitis: Radiological features and course. J Trop Pediatr. 2001 Feb 1 [cited 2021 Jun 27];47(1):5–12.

85. Farinha NJ, Razali KA, Holzel H, Morgan G, Novelli VM. Tuberculosis of the central nervous system in children: A 20-year survey. J Infect. 2000;41(1):61–8.

86. Shah I, Borse S. Paradoxical tuberculomas after completion of antituberculous treatment. Trop Med Health. 2012 [cited 2021 Jun 27];40(1):15–7.

87. Kumar R, Pandey CK, Rose N, Sahay S. Tuberculous brain abscess: Clinical presentation, pathophysiology and treatment (in children). Child's Nerv Syst. 2002 Apr 22 [cited 2021 Feb 7];18(3–4):118–23.

88. Kumar R, Singhi V. Tuberculous brain stem abscesses in children. J Pediatr Neurol. 2004;2(2):101–6.

89. Schoeman JF, Fieggen G, Seller N, Mendelson M, Hartzenberg B. Intractable intracranial tuberculous infection responsive to thalidomide: Report of four cases. J Child Neurol. 2006 Apr 2 [cited 2021 Feb 7];21(4):301–8.

90. Saini AG, Dogra S, Kumar R, Nada R, Singh M. Primary tuberculous cerebellar abscess: case report. Ann Trop Paediatr. 2011 Nov 22 [cited 2021 Feb 7];31(4):367–9.

91. Schoeman JF, Morkel A, Seifart HI, Parkin DP, van Helden PD, Hewlett RH, et al. Massive Posterior Fossa Tuberculous Abscess Developing in a Young Child Treated for Miliary Tuberculosis. Pediatr Neurosurg. 1998 [cited 2021 Feb 7];29(2):64–8.

92. Moghtaderi A, Alavi Naini R. Tuberculous radiculomyelitis: review and presentation of five patients. The International Journal of Tuberculosis and Lung Disease. 2003 Dec 1;7(12):1186-90.

93. Hernandez Pando R, Aguilar D, Cohen I, Guerrero M, Ribon W, Acosta P, et al. Specific bacterial genotypes of Mycobacterium tuberculosis cause extensive dissemination and brain infection in an experimental model. Tuberculosis. 2010 Jul;90(4):268–77.

94. Srivastava T, Kochar DK. Asymptomatic spinal arachnoiditis in patients with tuberculous meningitis. Neuroradiology. 2003 Oct 20 [cited 2021 Feb 7];45(10):727–9.

95. Lim YS, Kim SB, Kim MK, Lim YJ. Disseminated tuberculosis of central nervous system : spinal intramedullary and intracranial tuberculomas. J Korean Neurosurg Soc. 2013 Jul [cited 2021 Feb 7];54(1):61–4.

96. Skendros P, Kamaria F, Kontopoulos V, Tsitouridis I, Sidiropoulos L. Intradural, eextramedullary tuberculoma of the spinal cord as a complication of tuberculous meningitis. Infection. 2003 Mar [cited 2021 Feb 7];31(2):115–7.

97. FareR LS, Lowell AM, meador mp. Extrapulmonary tuberculosis in the united states1. Am J Epidemiol. 1979 Feb 1 [cited 2020 Apr 20];109(2):205–17.

98. Dodd PJ, Gardiner E, Coghlan R, Seddon JA. Burden of childhood tuberculosis in 22 high-burden countries: A mathematical modelling study. Lancet Glob Heal. 2014 [cited 2021 Feb 4];2(8).

99. Colditz GA, Berkey CS, Mosteller F, Brewer TF, Wilson ME, Burdick E, et al. The efficacy of bacillus Calmette-Guérin vaccination of newborns and infants in the prevention of tuberculosis: meta-analyses of the published literature. Pediatrics. 1995 July 1;96(1):29-35.

100. WHO | Global tuberculosis report 2016. WHO 2017 [cited 2017 Mar 30].

101. Bacillus Calmette-Guérin Vaccine Supply & Demand Outlook UNICEF Supply Division. 2015 [cited 2019 Mar 27].

102. du Preez K, Seddon JA, Schaaf HS, Hesseling AC, Starke JR, Osman M, et al. Global shortages of BCG vaccine and tuberculous meningitis in children. The Lancet Global Health. 2019 Jan 1;7(1):e28-9.

103. Arbues A, Aguilo JI, Gonzalo-Asensio J, Marinova D, Uranga S, Puentes E, et al. Construction, characterization and preclinical evaluation of MTBVAC, the first live-attenuated M. tuberculosis-based vaccine to enter clinical trials. Vaccine. 2013 Oct 1;31(42):4867-73.

104. Hinchey J, Jeon BY, Alley H, Chen B, Goldberg M, Derrick S, et al. Lysine auxotrophy combined with deletion of the secA2 gene results in a safe and highly immunogenic candidate live attenuated vaccine for tuberculosis. PLoS One. 2011 Jan 10;6(1):e15857.

105. Grode L, Ganoza CA, Brohm C, Weiner J, Eisele B, Kaufmann SHE. Safety and immunogenicity of the recombinant BCG vaccine VPM1002 in a phase 1 open-label randomized clinical trial. Vaccine. 2013 Feb 18;31(9):1340-8.

106. Sali M, Di Sante G, Cascioferro A, Zumbo A, Nicolò C, Donà V, et al. Surface expression of MPT64 as a fusion with the PE domain of PE-PGRS33 enhances Mycobacterium bovis BCG protective activity against Mycobacterium tuberculosis in mice. Infect Immun.2010 Dec;78(12):5202-13.

107. Sweeney KA, Dao DN, Goldberg MF, Hsu T, Venkataswamy MM, Henao-Tamayo M, et al. A recombinant Mycobacterium smegmatis induces potent bactericidal immunity against Mycobacterium tuberculosis. Nat Med. 2011 Oct;17(10):1261-8.

108. Nemes E, Geldenhuys H, Rozot V, Rutkowski KT, Ratangee F, Bilek N, et al. Prevention of M. tuberculosis Infection with H4:IC31 Vaccine or BCG Revaccination. N Engl J Med. 2018 Jul

12;379(2):138-49.

109. Van Der Meeren O, Hatherill M, Nduba V, Wilkinson RJ, Muyoyeta M, Van Brakel E, et al. Phase 2b Controlled Trial of M72/AS01E Vaccine to Prevent Tuberculosis. N Engl J Med. 2018 [cited 2019 Mar 27];379(17):1621–34.

110. Tait DR, Hatherill M, Van Der Meeren O, Ginsberg AM, Van Brakel E, Salaun B, et al. Final Analysis of a Trial of M72/AS01 E Vaccine to Prevent Tuberculosis . N Engl J Med. 2019 Dec 19 [cited 2021 Jun 28];381(25):2429–39.

111. Marais S, Thwaites G, Schoeman JF, TÖrÖk ME, Misra UK, Prasad K, et al. Tuberculous meningitis: a uniform case definition for use in clinical research. Lancet Infect Dis. 2010;10(11):803–12.

112. Philip N, William T, John DV. Diagnosis of tuberculous meningitis: Challenges and promises. Malays J Pathol. 2015;37(1):1–9.

113. Thwaites GE, Tran TH. Tuberculous meningitis: many questions, too few answers. Lancet Neurol. 2005 Mar 1;4(3):160–70.

114. Thwaites GE, van Toorn R, Schoeman J. Tuberculous meningitis: More questions, still too few answers. The Lancet Neurology. 2013 Oct 1;12(10):999-1010.

115. Daniel B, Grace G, Natrajan M. Tuberculous meningitis in children: Clinical management & outcome. Indian Journal of Medical Research. 2019 Aug 1;150:117-30.

116. Seddon JA, Schaaf HS. Drug-resistant tuberculosis and advances in the treatment of childhood tuberculosis. Pneumonia. 2016 Dec 24;8(1):1–13.

117. Van Toorn R, Springer P, Laubscher JA, Schoeman JF. Value of different staging systems for predicting neurological outcome in childhood tuberculous meningitis. Int J Tuberc Lung Dis. 2012 May 1;16(5):628–32.

118. Alarcón F, Moreira J, Rivera J, Salinas R, Dueñas G, Van den Ende J. Tuberculous meningitis: Do modern diagnostic tools offer better prognosis prediction? Indian J Tuberc. 2013;60(1):5–14.

119. Andronikou S, Smith B, Hatherhill M, Douis H, Wilmshurst J. Definitive neuroradiological diagnostic features of tuberculous meningitis in children. Pediatr Radiol. 2004 Nov 17 [cited 2021 Jun 15];34(11):876–85.

120. Hladky SB, Barrand MA. Mechanisms of fluid movement into, through and out of the brain: Evaluation of the evidence. Fluids Barriers CNS. 2014 Dec 2 [cited 2022 Aug 3];11(1):1–32.

121. Reiber H. Flow rate of cerebrospinal fluid (CSF) — A concept common to normal blood-CSF barrier function and to dysfunction in neurological diseases. J Neurol Sci. 1994 Apr 1 [cited 2019 Sep 12];122(2):189–203.

122. Verdon R, Chevret S, Laissy JP, Wolff M. Tuberculous meningitis in adults: review of 48 cases. Clin Infect Dis. 1996 Jun [cited 2020 Apr 21];22(6):982–8.

123. Jeren T, Beus I. Characteristics of cerebrospinal fluid in tuberculous meningitis. Acta Cytol. 1982;26(5):678–80.

124. Principi N, Esposito S. Diagnosis and therapy of tuberculous meningitis in children. Tuberculosis. 2012 Sep 1 [cited 2020 May 25];92(5):377-83.

125. Yaramis A, Gurkan F, Elevli M, So M, Haspolat K, Tas MA. Central Nervous System Tuberculosis in Children : A Review of 214. 1998;102(5).

126. Van Well GTJ, Paes BF, Terwee CB, Springer P, Roord JJ, Donald PR, et al. Twenty years of pediatric tuberculous meningitis: a retrospective cohort study in the western cape of South Africa. Pediatrics. 2009;123(1):e1–8.

127. Kent SJ, Crowe SM, Yung A, Lucas CR, Mijch AM. Tuberculous meningitis: A 30-year review. Clin Infect Dis. 1993 [cited 2021 Feb 25];17(6):987–94.

128. Thwaites GE, Simmons CP, Quyen NTH, Chau TTH, Mai PP, Dung NT, et al. Pathophysiology and Prognosis in Vietnamese Adults with Tuberculous Meningitis. J Infect Dis. 2003 Oct 15 [cited 2021 Feb 25];188(8):1105–15.

129. Grobbelaar M, van Toorn R, Solomons R. Lumbar Cerebrospinal Fluid Evolution in Childhood Tuberculous Meningitis. J Child Neurol. 2018 Oct 1 [cited 2021 Feb 3];33(11):700–7.

130. Marais S, Pepper DJ, Schutz C, Wilkinson RJ, Meintjes G. Presentation and Outcome of Tuberculous Meningitis in a High HIV Prevalence Setting. Plos one. 2011 May 19 [cited 2021 Jul 2];6(5):e20077.

131. Cecchini D, Ambrosioni J, Brezzo C, Corti M, Rybko A, Perez M, et al. Tuberculous meningitis in HIV-infected and non-infected patients: comparison of cerebrospinal fluid findings. ingentaconnect.com. 2009 [cited 2021 Nov 22];13(2):269–71.

132. Katrak SM, Shembalkar PK, Bijwe SR, Bhandarkar LD. The clinical, radiological and pathological profile of tuberculous meningitis in patients with and without human immunodeficiency virus infection. J Neurol Sci. 2000 Dec 1;181(1–2):118–26.

133. Torok ME, Chau T, Mai PP, Phong ND, Dung NT. Clinical and Microbiological Features of

HIV-Associated Tuberculous Meningitis in Vietnamese Adults. PLoS One. 2008 [cited 2021 Nov 22];3(3):1772.

134. Kumar R, Singh SN, Kohli N. A diagnostic rule for tuberculous meningitis. Arch Dis Child. 1999 Sep 1;81(3)221-4.

135. Yechoor VK, Shandera WX, Rodriguez P, Cate TR. Tuberculous Meningitis Among Adults With and Without HIV Infection: Experience in an Urban Public Hospital. Arch Intern Med. 1996 Aug 12 [cited 2021 Nov 22];156(15):1710–6.

136. Sommer JB, Gaul C, Heckmann J, Neundörfer B, Erbguth FJ. Does lumbar cerebrospinal fluid reflect ventricular cerebrospinal fluid? A prospective study in patients with external ventricular drainage. Eur Neurol. 2002 [cited 2020 Nov 3];47(4):224–32.

137. Gerber J, Tumani H, Kolenda H, Nau R. Lumbar and ventricular CSF protein, leukocytes, and lactate in suspected bacterial CNS infections. Neurology. 1998 [cited 2020 Nov 3];51(6):1710–4.

138. Naija W, Matéo J, Raskine L, Timsit JF, Lukascewicz AC, George B, et al. Case report: greater meningeal inflammation in lumbar than in ventricular region in human bacterial meningitis. Crit Care. 2004 [cited 2020 Nov 3];8(6).

139. Ernst JD, Decazes JM, Sande MA. Experimental pneumococcal meningitis: Role of leukocytes in pathogenesis. Infect Immun. 1983 [cited 2020 Nov 3];41(1):275–9.

140. Said M, Uppal P, Bye A, Palasanthiran P. Unusual case of tuberculous meningitis with discordant ventricular and lumbar cerebrospinal fluid; lessons in the era of world-wide migration. J Paediatr Child Health. 2018 Jan 1 [cited 2020 Nov 11];54(1):93–5.

141. Alfayate S, García Martinez S. Normal ventricular-CSF may confound the diagnosis of tuberculous meningitis hydrocephalus. Artic Neurocir. 2011 [cited 2020 Nov 11];22:157–61.

142. Kamat AS, Gretschel A, Vlok AJ, Solomons R. CSF protein concentration associated with ventriculoperitoneal shunt obstruction in tuberculous meningitis. Int J Tuberc Lung Dis. 2018 Jul 1;22(7):788–92.

143. Figaji A, Fieggen G, Enslin N, Taylor A, Rohlwink U. Cerebrospinal fluid protein and shunt obstruction in tuberculous meningitis. International Journal of Tuberculosis and Lung Disease. International Union against Tubercul. and Lung Dis.; 2019 Jun 1;23(6):765.

144. Rohlwink UK, Figaji A, Wilkinson KA, Horswell S, Sesay AK, Deffur A, et al. Tuberculous meningitis in children is characterized by compartmentalized immune responses and neural excitotoxicity. Nat Commun. 2019 Dec 21 [cited 2019 Sep 10];10(1):3767.

145. Rohlwink UK, Figaji AA. Biomarkers of brain injury in cerebral infections. Clin Chem. 2014;60(6):823–34.

146. Chaidir L, Annisa J, Dian S, Parwati I, Alisjahbana A, Purnama F, et al. Microbiological diagnosis of adult tuberculous meningitis in a ten-year cohort in Indonesia. Diagn Microbiol Infect Dis. 2018 May 1;91(1):42–6.

147. Cresswell F V., Tugume L, Bahr NC, Kwizera R, Bangdiwala AS, Musubire AK, et al. Xpert MTB/RIF Ultra for the diagnosis of HIV-associated tuberculous meningitis: a prospective validation study. Lancet Infect Dis. 2020 Mar 1;20(3):308–17.

148. Thwaites GE, Chau TTH, Stepniewska K, Phu NH, Chuong L V., Sinh DX, et al. Diagnosis of adult tuberculous meningitis by use of clinical and laboratory features. Lancet. 2002;360(9342):1287–92.

149. Bahr NC, Tugume L, Rajasingham R, Kiggundu R, Williams DA, Morawski B, et al. Improved diagnostic sensitivity for tuberculous meningitis with Xpert® MTB/RIF of centrifuged CSF. Int J Tuberc Lung Dis. 2015 Oct 1;19(10):1209–15.

150. Bahr NC, Meintjes G, Boulware DR. Inadequate diagnostics: the case to move beyond the bacilli for detection of meningitis due to Mycobacterium tuberculosis. J Med Microbiol. 2019;68:755–60.

151. Thakur R, Goyal R, Sarma S. Laboratory Diagnosis of Tuberculous Meningitis – Is There a Scope for Further Improvement? J Lab Physicians. 2010 Jan [cited 2022 Jul 25];2(01):021–4.

152. Caws M, Ha DTM, Torok E, Campbell J, Thu DDA, Chau TTH, et al. Evaluation of the MODS Culture Technique for the Diagnosis of Tuberculous Meningitis. PLoS One. 2007 Nov 14 [cited 2022 Mar 30];2(11):e1173.

153. Heemskerk AD, Donovan J, Thu DDA, Marais S, Chaidir L, Dung VTM, et al. Improving the microbiological diagnosis of tuberculous meningitis: A prospective, international, multicentre comparison of conventional and modified Ziehl–Neelsen stain, GeneXpert, and culture of cerebrospinal fluid. J Infect. 2018 Dec 1;77(6):509–15.

154. STEWART SM. The bacteriological diagnosis of tuberculous meningitis. J Clin Pathol. 1953 [cited 2021 Jul 5];6(3):241–2.

155. Kennedy DH, Fallon RJ. Tuberculous Meningitis. JAMA J Am Med Assoc. 1979 Jan 19;241(3):264-8.

156. Thwaites GE, Chau TTH, Farrar JJ. Improving the Bacteriological Diagnosis of Tuberculous Meningitis. J Clin Microbiol. 2004 [cited 2021 Jul 5];42(1):378–9.

157. Pai M, Flores LL, Pai N, Hubbard A, Riley LW, Colford JM. Diagnostic accuracy of nucleic acid amplification tests for tuberculous meningitis: a systematic review and meta-analysis. Lancet Infect Dis. 2003;3(10):633–43.

158. Shankar P, Manjunath N, Mohan K, lancet KP-T. Rapid diagnosis of tuberculous meningitis by polymerase chain reaction. academia.edu. 1991 Jan 5 [cited 2020 Apr 21]; 337(8732):5-7.

159. Kox LFF, Kuijper SI, Kolk AHJ. Early diagnosis of tuberculous meningitis by polymerase chain reaction. Neurology. 1995;45(12):2228–32.

160. Pormohammad A, Nasiri MJ, McHugh TD, Riahi SM, Bahr NC. A systematic review and meta-analysis of the diagnostic accuracy of nucleic acid amplification tests for tuberculous meningitis. J Clin Microbiol. 2019 Jun 1 [cited 2022 Jul 25];57(6).

161. Nagdev KJ, Kashyap RS, Parida MM, Kapgate RC, Purohit HJ, Taori GM, et al. Loop-mediated isothermal amplification for rapid and reliable diagnosis of tuberculous meningitis. J Clin Microbiol. 2011 May [cited 2022 Aug 4];49(5):1861–5.

162. Modi M, Sharma K, Sharma M, Sharma A, Sharma N, Sharma S, et al. Multitargeted loop-mediated isothermal amplification for rapid diagnosis of tuberculous meningitis. The International Journal of Tuberculosis and Lung Disease. 2016 May 1 [cited 2022 Aug 4]; 20(5):625-30.

163. Poplin V, Boulware DR, Bahr NC. Methods for rapid diagnosis of meningitis etiology in adults. Biomark Med. 2020 Apr 1 [cited 2022 Aug 4];14(6):459.

164. Manyelo CM, Solomons RS, Walzl G, Chegou NN. Tuberculous Meningitis: Pathogenesis, Immune Responses, Diagnostic Challenges, and the Potential of Biomarker-Based Approaches. 2021 Feb 18 [cited 2022 Jul 19];59(3):10-128.

165. Patel VB, Theron G, Lenders L, Matinyena B, Connolly C, Singh R, et al. Diagnostic Accuracy of Quantitative PCR (Xpert MTB/RIF) for Tuberculous Meningitis in a High Burden Setting: A Prospective Study. PLoS Med. 2013 [cited 2021 Jul 5];10(10):e1001536.

166. Nhu NTQ, Heemskerk D, Thu DDA, Chau TTH, Mai NTH, Nghia HDT, et al. Evaluation of genexpert MTB/RIF for diagnosis of tuberculous meningitis. J Clin Microbiol. 2014;52(1):226–33.

167. Denkinger CM, Schumacher SG, Boehme CC, Dendukuri N, Pai M, Steingart KR. Xpert MTB/RIF assay for the diagnosis of extrapulmonary tuberculosis: A systematic review and meta-analysis. Eur Respir J. 2014 Aug 1 [cited 2021 Jul 1];44(2):435–46.

168. World Health Organization. Automated real-time nucleic acid amplification technology for rapid

and simultaneous detection of tuberculosis and rifampicin resistance: Xpert MTB/RIF assay for the diagnosis of pulmonary and extrapulmonary TB in adults and children. WHO 2013 [cited 2021 Jul 1].

169. Bahr NC, Nuwagira E, Evans EE, Cresswell F V., Bystrom P V., Byamukama A, et al. Diagnostic accuracy of Xpert MTB/RIF Ultra for tuberculous meningitis in HIV-infected adults: a prospective cohort study. Lancet Infect Dis. 2018 Jan 1;18(1):68–75.

170. Chakravorty S, Simmons AM, Rowneki M, Parmar H, Cao Y, Ryan J, et al. The new Xpert MTB/RIF ultra: Improving detection of Mycobacterium tuberculosis and resistance to Rifampin in an assay suitable for point-of-care testing. MBio. 2017 Jul 1;8(4).

171. Donovan J, Thu DDA, Phu NH, Dung VTM, Quang TP, Nghia HDT, et al. Xpert MTB/RIF Ultra versus Xpert MTB/RIF for the diagnosis of tuberculous meningitis: a prospective, randomised, diagnostic accuracy study. Lancet Infect Dis. 2020 Jan [cited 2020 Jan 22];20(30):299-307.

172. Pradhan NN, Paradkar MS, Kagal A, Valvi C, Kinikar A, Khwaja S, et al. Performance of Xpert® MTB/RIF and Xpert® Ultra for the diagnosis of tuberculous meningitis in children. Int J Tuberc Lung Dis. 2022 Apr 1;26(4):317–25.

173. WHO Meeting Report of a Technical Expert Consultation: Non-inferiority analysis of Xpert MTB/RIF Ultra compared to Xpert MTB/RIF. WHO 2017 [cited 2022 Jul 25].

174. Bahr NC, Marais S, Caws M, Van Crevel R, Wilkinson RJ, Tyagi JS, et al. GeneXpert MTB/Rif to Diagnose Tuberculous Meningitis: Perhaps the First Test but not the Last. Clinical Infectious Diseases. Oxford University Press; 2016 [cited 2021 Jul 5;62(9):113-5.

175. Sharma K, Sharma M, Modi M, Singla N, Sharma A, Sharma N, et al. Comparative analysis of TruenatE MTB plus and XpertW Ultra in diagnosing tuberculous meningitis. Int J Tuberc Lung Dis. 2021 Aug 1;25(8):626–31.

176. Jeyashree K, Shanmugasundaram D, Rade K, Gangakhedkar RR, Murhekar M V. Public Health Action Impact and operational feasibility of TrueNat™ MTB/Rif under India's RNTCP. 2020 Sep 21 [cited 2022 Jul 21];10(3):87-91.

177. Katti MK. Immunodiagnosis of tuberculous meningitis: rapid detection of mycobacterial antigens in cerebrospinal fluid by reverse passive hemagglutination assay and their characterization by Western blotting. FEMS Immunol Med Microbiol. 2001 Jul;31(1):59–64.

178. Kashyap RS, Kainthla RP, Biswas SK, Agarwal N, Chandak N, Purohit HJ, et al. Rapid diagnosis of tuberculous meningitis using the Simple Dot ELISA method. Med Sci Monit. 2003

Nov 1 [cited 2022 Aug 4];9(11):MT123-6.

179. Yu J, Wang ZJ, Chen LH, Li HH. Diagnostic accuracy of interferon-gamma release assays for tuberculous meningitis: A meta-Analysis. Int J Tuberc Lung Dis. 2016 Apr 1;20(4):494–9.

180. Wen A, Leng EL, Liu SM, Zhou YL, Cao WF, Yao DY, et al. Diagnostic Accuracy of Interferon-Gamma Release Assays for Tuberculous Meningitis: A Systematic Review and Meta-Analysis. Front Cell Infect Microbiol. 2022 Apr 22;12:455.

181. Siddiqi OK, Birbeck GL, Ghebremichael M, Mubanga E, Love S, Buback C, et al. Prospective cohort study on performance of cerebrospinal fluid (CSF) Xpert MTB/RIF, CSF lipoarabinomannan (LAM) lateral flow assay (LFA), and urine LAM LFA for diagnosis of tuberculous meningitis in Zambia. J Clin Microbiol. 2019 [cited 2021 Jun 8];57(8).

182. Cox JA, Lukande RL, Kalungi S, Van Marck E, Lammens M, Van De Vijver K, et al. Accuracy of lipoarabinomannan and xpert MTB/RIF testing in cerebrospinal fluid to diagnose tuberculous meningitis in an autopsy cohort of HIV-infected adults. J Clin Microbiol. 2015 Aug 1 [cited 2022 Mar 31];53(8):2667–73.

193. Manyelo CM, Solomons RS, Snyders CI, Mutavhatsindi H, Manngo PM, Stanley K, et al. Potential of host serum protein biomarkers in the diagnosis of tuberculous meningitis in children. Front Pediatr. 2019;7(SEP):376.

194. Sameer Kumar GS, Venuaopal AK, Kashvap MK, Raiu R, Marimuthu A, Palapetta SM, et al. Gene Expression Profiling of Tuberculous Meningitis Co-infected with HIV. J Proteomics Bioinform. 2012 [cited 2022 Jul 26];5(9):235.

195. Sutherland JS, van der Spuy G, Gindeh A, Thuong NTT, Namuganga A, Owolabi O, et al. Diagnostic Accuracy of the Cepheid 3-gene Host Response Fingerstick Blood Test in a Prospective, Multi-site Study: Interim Results. Clin Infect Dis. 2022 Jul 6 [cited 2022 Jul 28];74(12):2136–41.

196. Sweeney TE, Braviak L, Tato CM, Khatri P, Khatri and P. Genome-wide expression for diagnosis of pulmonary tuberculosis: a multicohort analysis. 2016 Mar 1;4(3):213-24.

197. Warsinske HC, Rao AM, Moreira FMF, Santos PCP, Liu AB, Scott M, et al. Assessment of Validity of a Blood-Based 3-Gene Signature Score for Progression and Diagnosis of Tuberculosis, Disease Severity, and Treatment Response. JAMA Netw Open. 2018 Oct 5 [cited 2022 Jul 28];1(6):e183779–e183779.

198. Södersten E, Ongarello S, Mantsoki A, Wyss R, Persing DH, Banderby S, et al. Diagnostic accuracy study of a novel blood-based assay for identification of tuberculosis in people living

with HIV. J Clin Microbiol. 2021 Mar 1 [cited 2022 Jul 28];59(3).

199. Moreira FMF, Verma R, Pereira dos Santos PC, Leite A, da Silva Santos A, de Araujo RCP, et al. Blood-based host biomarker diagnostics in active case finding for pulmonary tuberculosis: A diagnostic case-control study. EClinicalMedicine. 2021 Mar 1;33:100776.

200. Sabir N, Hussain T, Shah SZA, Peramo A, Zhao D, Zhou X. miRNAs in tuberculosis: New avenues for diagnosis and host-directed therapy. Front Microbiol. 2018 Mar 29;9(MAR):602.

201. O'connell RM, Rao DS, Chaudhuri AA. Physiological and pathological roles of microRNAs in the immune system Noncoding RNA Regulation of B-cell Development View project. Nat Rev Immunol. 2010 [cited 2022 Aug 1];10.

202. Watanabe Y, Kanai A. Systems biology reveals microRNA-mediated gene regulation. Front Genet. 2011;2(JUNE):29.

203. Fu Y, Yi Z, Wu X, Li J, Xu F. Circulating microRNAs in patients with active pulmonary tuberculosis. J Clin Microbiol. 2011 Dec [cited 2022 Aug 2];49(12):4246–51.

204. Ambros V. The functions of animal microRNAs. Nat 2004 4317006. 2004 Sep 15 [cited 2022 Aug 2];431(7006):350–5.

205. Stefani G, biology FS-N reviews M cell, 2008. Small non-coding RNAs in animal development. nature.com. 2008 Mar [cited 2022 Aug 2];9(3):219-30.

206. Qi Y, Cui L, Ge Y, Shi Z, Zhao K, Guo X, et al. Altered serum microRNAs as biomarkers for the early diagnosis of pulmonary tuberculosis infection. BMC Infect Dis. 2012 Dec 28 [cited 2022 Aug 1];12(1):1–9.

207. Zhou M, Yu G, Yang X, Zhu C, Zhang Z, Zhan X. Circulating microRNAs as biomarkers for the early diagnosis of childhood tuberculosis infection. Mol Med Rep. 2016 Jun 1 [cited 2022 Aug 2];13(6):4620–6.

208. Wang J, Xu J, Han Y, Zhu Y, Zhang W. Diagnostic values of microRNA-31 in peripheral blood mononuclear cells for pediatric pulmonary tuberculosis in Chinese patients. Genet Mol Res. 2015 [cited 2022 Aug 2];14(4):17235–43.

209. Pan D, Pan M, Xu Y-M. Mir-29a expressions in peripheral blood mononuclear cell and cerebrospinal fluid: Diagnostic value in patients with pediatric tuberculous meningitis. Brain Res Bull. 2017 [cited 2022 Aug 2];130:231–5.

210. Pan L, Liu F, Zhang J, Li J, Jia H, Huang M, et al. Genome-Wide miRNA Analysis Identifies Potential Biomarkers in Distinguishing Tuberculous and Viral Meningitis. Front Cell Infect

Microbiol. 2019 Sep 10;9:323.

211. Hu X, Liao S, Bai H, Wu L, Wang M, Wu Q, et al. Integrating exosomal microRNAs and electronic health data improved tuberculosis diagnosis. EBioMedicine. 2019 Feb 1;40:564–73.

212. Kaddurah-Daouk R, Kristal BS, Weinshilboum RM. Metabolomics: A Global Biochemical Approach to Drug Response and Disease. 2007 Feb 10 [cited 2022 Aug 1];48(1):653-83.

213. Kumar GSS, Venugopal AK, Mahadevan A, Renuse S, Harsha HC, Sahasrabuddhe NA, et al. Quantitative proteomics for identifying biomarkers for tuberculous meningitis. Clin Proteomics. 2012 Nov 30 [cited 2022 Aug 3];9(1):1–13.

214. Li Z, Du B, Li J, Zhang J, Zheng X, Jia H, et al. Cerebrospinal fluid metabolomic profiling in tuberculous and viral meningitis: Screening potential markers for differential diagnosis. 2017 Mar 1 [cited 2022 Aug 3];466:38-45.

215. Mason S, Tutu Van Furth • A Marceline, Solomons • Regan, Wevers RA, Van Reenen M, Carolus •, et al. A putative urinary biosignature for diagnosis and follow-up of tuberculous meningitis in children: outcome of a metabolomics study disclosing host-pathogen responses. Metabolomics. 2016 Jul;12:1-6.

216. Donovan J, Rohlwink UK, Tucker EW, Hiep NTT, Thwaites GE, Figaji AA, et al. Checklists to guide the supportive and critical care of tuberculous meningitis. Wellcome Open Res. 2019 [cited 2021 Jul 19];4.

217. Thwaites GE, Bang ND, Dung NH, Quy HT, Oanh DTT, Thoa NTC, et al. Dexamethasone for the Treatment of Tuberculous Meningitis in Adolescents and Adults. N Engl J Med. 2004 Oct 21 [cited 2021 Jun 7];351(17):1741–51.

218. Prasad K, Singh MB, Ryan H. Corticosteroids for managing tuberculous meningitis. Cochrane Database of Systematic Reviews. 2016 (4).

219. Dooley DP, Carpenter JL, Rademacher S. Adjunctive Corticosteroid Therapy for Tuberculosis: A Critical Reappraisal of the Literature. Clin Infect Dis. 1997 Oct 1 [cited 2020 Apr 21];25(4):872–87.

220. Schoeman JF, Van Zyl LE, Laubscher JA, Donald PR. Effect of corticosteroids on intracranial pressure, computed tomographic findings, and clinical outcome in young children with tuberculous meningitis. Pediatrics. 1997 Feb 1 [cited 2020 Oct 8];99(2):226–31.

221. Wasserman S, Davis A, Wilkinson RJ, Meintjes G. Key considerations in the pharmacotherapy of tuberculous meningitis. Expert Opin Pharmacother. 2019 Oct 13 [cited 2020 May 20];20(15):1791–5.

222. Mai NT, Dobbs N, Phu NH, Colas RA, Thao LT, Thuong NT, et al. A randomised double blind placebo controlled phase 2 trial of adjunctive aspirin for tuberculous meningitis in HIV-uninfected adults. Elife. 2018 Feb 27;7.

223. Schoeman JF, Janse Van Rensburg A, Laubscher JA, Springer P. The role of aspirin in childhood tuberculous meningitis. J Child Neurol. 2011 Aug 31 [cited 2020 Oct 8];26(8):956–62.

224. Misra UK, Kalita J, Nair PP. Role of aspirin in tuberculous meningitis: A randomized open label placebo controlled trial. J Neurol Sci. 2010 Jun 15;293(1–2):12–7.

225. Huang SM, Chen CC, Chiu PC, Cheng MF, Chiu CL, Hsieh KS. Tuberculous meningitis complicated with hydrocephalus and cerebral salt wasting syndrome in a three-year-old boy. Pediatr Infect Dis J. 2004 Sep [cited 2020 Oct 8];23(9):884–6.

226. Cotton MF, Donald PR, Schoeman JF, Van Zyl LE, Aalbers C, Lombard CJ. Raised intracranial pressure, the syndrome of inappropriate antidiuretic hormone secretion, and arginine vasopressin in tuberculous meningitis. Child's Nerv Syst. 1993 Feb [cited 2020 Oct 8];9(1):10–5.

227. Seddon JA, Wilkinson R, van Crevel R, Figaji A, Thwaites GE. Knowledge gaps and research priorities in tuberculous meningitis. Wellcome Open Res. 2019 Nov 28 [cited 2020 Jan 15];4:188.

228. Cotton MF, Donald PR, Schoeman JF, Aalbers C, Van Zyl LE, Lombard C. Plasma arginine vasopressin and the syndrome of inappropriate antidiuretic hormone secretion in tuberculous meningitis. Pediatr Infect Dis J. 1991;10(11):837–42.

229. Singh BS, Patwari AK, Deb M. Serum sodium and osmolal changes in tuberculous meningitis. Indian pediatrics. 1994 Nov 1;31(11):1345-80.

230. Misra UK, Kalita J, Kumar M, Neyaz Z. Hypovolemia due to cerebral salt wasting may contribute to stroke in tuberculous meningitis. QJM. 2018 Jul 1 [cited 2021 Jun 7];111(7):455–60.

231. Torok ME, Yen NTB, Chau TTH, Mai NTH, Phu NH, Mai PP, et al. Timing of Initiation of Antiretroviral Therapy in Human Immunodeficiency Virus (HIV)-Associated Tuberculous Meningitis. Clin Infect Dis. 2011 Jun 1 [cited 2021 Feb 4];52(11):1374–83.

232. Marais S, Meintjes G, Pepper DJ, Dodd LE, Schutz C, Ismail Z, et al. Frequency, severity, and prediction of tuberculous meningitis immune reconstitution inflammatory syndrome. Clin Infect Dis. 2013 Feb [cited 2021 Feb 4];56(3):450–60.

233. Meintjes G, Lynen L. Prevention and treatment of the immune reconstitution inflammatory

syndrome. Vol. 3, Current Opinion in HIV and AIDS. 2008. p. 468–76.

234. Cresswell F V, Bangdiwala AS, Meya DB, Bahr NC, Vidal JE, Estée Török M, et al. Absence of cerebrospinal fluid pleocytosis in tuberculous meningitis is a common occurrence in HIV co-infection and a predictor of poor outcomes. International Journal of Infectious Diseases. 2018 Mar 1 [cited 2021 Feb 4];68:77-8.

235. Cecchini D, Ambrosioni J, Brezzo C, Corti M, Rybko A, Perez M, et al. Tuberculous meningitis in HIV-infected patients: drug susceptibility and clinical outcome. AIDS. 2007 Jan 30 [cited 2021 Feb 4];21(3):373–4.

236. Thwaites G. E, Chau T. T. H, Caws M, Phu N. H, Chuong L. V, Sinh D. X, et al. Isoniazid resistance, mycobacterial genotype and outcome in Vietnamese adults with tuberculous meningitis. The International Journal of Tuberculosis and Lung Disease. 2002 Oct 1;6(10):865-71.

237. Nau R, Sörgel F, Eiffert H. Penetration of drugs through the blood-cerebrospinal fluid/blood-brain barrier for treatment of central nervous system infections. Clin Microbiol Rev. 2010 Oct 1 [cited 2019 Aug 15];23(4):858–83.

238. Marais S, Lai RPJ, Wilkinson KA, Meintjes G, O'Garra A, Wilkinson RJ. Inflammasome activation underlying central nervous system deterioration in HIV-associated tuberculosis. J Infect Dis. 2017 [cited 2021 Feb 4];215(5):677–86.

239. van Laarhoven A, Dian S, Aguirre-Gamboa R, Avila-Pacheco J, Ricaño-Ponce I, Ruesen C, et al. Cerebral tryptophan metabolism and outcome of tuberculous meningitis: an observational cohort study. Lancet Infect Dis. 2018 May 1;18(5):526–35.

240. Ozates M, Kemaloglu S, Gurkan F, Ozkan U, Hosoglu S, Simsek MM. CT of the brain in tuberculous meningitis. A review of 289 patients. Acta radiol. 2000 Jan 1 [cited2021 Jun 8];41(1):13–7. 241.

241. Loxton NW, Rohlwink UK, Tshavhungwe M, Dlamini L, Shey M, Enslin N, et al. A pilot study of inflammatory mediators in brain extracellular fluid in paediatric TBM. Mink RB, editor. PLoS One. 2021 Mar 12 [cited 2021 Mar 13];16(3):e0246997.

242. Kukreti V, Mohseni-Bod H, Drake J. Management of raised intracranial pressure in children with traumatic brain injury. J Pediatr Neurosci. 2014 Oct 1 [cited 2021 Jul 19];9(3):207.

243. Stocchetti N, Maas AIR. Traumatic Intracranial Hypertension. 2014 May 28 [cited 2021 Jul 19];370(22):2121–30.

244. Figaji AA, Fieggen AG, Peter JC. Air encephalography for hydrocephalus in the era of

neuroendoscopy. Childs Nerv Syst. 2005;21:559–65.

245. Figaji AA, Fieggen AG. The neurosurgical and acute care management of tuberculous meningitis: Evidence and current practice. Tuberculosis. 2010;90(6):393–400.

246. Figaji AA, Fieggen AG. Endoscopic Challenges and Applications in Tuberculous Meningitis. World Neurosurg. 2013 Feb 1;79(2):S24.e9-S24.e14.

247. Avery RA, Shah SS, Licht DJ, Seiden JA, Huh JW, Boswinkel J, et al. Reference Range for Cerebrospinal Fluid Opening Pressure in Children. N Engl J Med. 2010 Aug 26 [cited 2021 Jun 15];363(9):891–3.

248. Lamprecht D, Schoeman J, Donald P, Hartzenberg H. Ventriculoperitoneal shunting in childhood tuberculous meningitis. Br J Neurosurg. 2001;15(2):119–25.

249. Schoeman J, Donald P, Zyl L van, Keet M, Wait J. Tuberculous Hydrocephalus: Comparison of Different Treatments With Regard to Icp, Ventricular Size and Clinical Outcome. Dev Med Child Neurol. 1991 May 1 [cited 2021 Aug 24];33(5):396–405.

250. Figaji a a, Fieggen a G, Peter JC. Endoscopic third ventriculostomy in tuberculous meningitis. Childs Nerv Syst. 2003;19(4):217–25.

251. Wait JW, Schoeman JF. Behaviour Profiles After Tuberculous Meningitis. J Trop Pediatr. 2010 Jun 1 [cited 2021 Feb 4];56(3):166–71.

252. Schoeman CJ, Herbst I, Nienkemper DC. The effect of tuberculous meningitis on the cognitive and motor development of children. South African Med J. 1997;87(1):70–2.

253. Rohlwink UK, Donald K, Gavine B, Padayachy L, Wilmshurst JM, Fieggen GA, et al. Clinical characteristics and neurodevelopmental outcomes of children with tuberculous meningitis and hydrocephalus. Dev Med Child Neurol. 2016 May 1;58(5):461–8.

254. Sinha MK, Garg RK, Anuradha HK, Agarwal A, Singh MK, Verma R, et al. Vision impairment in tuberculous meningitis: Predictors and prognosis. J Neurol Sci. 2010 Mar 15;290(1–2):27–32.

255. Peloquin C. What is the 'right' dose of rifampin? [Editorial]. International Journal of Tuberculosis and Lung Disease. 2003 Jan 1[cited 2019 Oct 3];7(1):3-5.

256. Raut T, Garg RK, Jain A, Verma R, Singh MK, Malhotra HS, et al. Hydrocephalus in tuberculous meningitis: Incidence, its predictive factors and impact on the prognosis. J Infect. 2013 Apr;66(4):330–7.

257. Chan KH, Cheung RTF, Fong CY, Tsang KL, Mak W, Ho SL. Clinical relevance of

hydrocephalus as a presenting feature of tuberculous meningitis. Q J Med. 2003 [cited 2020 May 25];96:643–8.

258. Karande S, Gupta V, Kulkarni M, Joshi A. Prognostic clinical variables in childhood tuberculous meningitis: An experience from Mumbai, India. Neurol India. 2005;53(2):191–5.

259. Chiang SS, Khan FA, Milstein MB, Tolman AW, Benedetti A, Starke JR, et al. Treatment outcomes of childhood tuberculous meningitis: a systematic review and meta-analysis. Lancet Infect Dis. 2014 Oct 1;14(10):947-57.

260. Kalita J, Misra UK. Outcome of tuberculous meningitis at 6 and 12 months: a multiple regression analysis. INT J TUBERC LUNG DIS. 1999 Mar 1; 3(3):261-265

261. Sheu JJ, Yuan RY, Yang CC. Predictors for outcome and treatment delay in patients with tuberculous meningitis. Am J Med Sci. 2009 Aug 1;338(2):134–9.

262. Bang ND, Caws M, Truc TT, Duong TN, Dung NH, Ha DTM, et al. Clinical presentations, diagnosis, mortality and prognostic markers of tuberculous meningitis in Vietnamese children: A prospective descriptive study. BMC Infect Dis. 2016 Oct 18 [cited 2021 Feb 4];16(1):1–10.

263. Simmons CP, Thwaites GE, Quyen NTH, Torok E, Hoang DM, Chau TTH, et al. Pretreatment Intracerebral and Peripheral Blood Immune Responses in Vietnamese Adults with Tuberculous Meningitis: Diagnostic Value and Relationship to Disease Severity and Outcome. J Immunol. 2006 Feb 1 [cited 2021 Feb 4];176(3):2007–14.

264. Green JA, Tran CTH, Farrar JJ, Nguyen MTH, Nguyen PH, Dinh SX, et al. Dexamethasone, Cerebrospinal Fluid Matrix Metalloproteinase Concentrations and Clinical Outcomes in Tuberculous Meningitis. PLoS One. 2009 Sep 30 [cited 2022 Jul 22];4(9):e7277.

265. Li YJ, Wilkinson KA, Wilkinson RJ, Figaji AA, Rohlwink UK. Elevated Matrix Metalloproteinase Concentrations Offer Novel Insight Into Their Role in Pediatric Tuberculous Meningitis. J Pediatric Infect Dis Soc. 2020 Feb 28 [cited 2022 Jul 22];9(1):82–6.

266. Batchelor HK, Marriott JF. Paediatric pharmacokinetics: key considerations. Br J Clin Pharmacol. 2015 Mar 1 [cited 2018 Nov 23];79(3):395–404.

267. Tanaka H, Mizojiri K. Drug-Protein Binding and Blood-Brain Barrier Permeability. J Pharmacol Exp Ther. 1999;288(3).

268. Hammarlund-Udenaes M, Paalzow LK, De Lange ECM. Drug equilibration across the blood-brain barrier - Pharmacokinetic considerations based on the microdialysis method. Pharmaceutical Research. 1997 Feb;14:128-34.

269. Kola I, Landis J. Can the pharmaceutical industry reduce attrition rates? Nat Rev Drug Discov. 2004;3(8):711–5.

270. Peck CC, Barr WH, Benet LZ, Collins J, Desjardins RE, Furst DE, et al. Opportunities for Integration of Pharmacokinetics, Pharmacodynamics, and Toxicokinetics in Rational Drug Development. J Pharm Sci . 1992 Jun 1 [cited 2019 Jan 28];81(6):605–10.

271. Medicines Agency E. Committee for Medicinal Products for Human Use (CHMP) Guideline on strategies to identify and mitigate risks for first-in-human and early clinical trials with investigational medicinal products. 2017 [cited 2019 Jun 21].

272. Suvarna DV. Phase IV of Drug Development. Perspect Clin Res. 2010 Apr [cited 2023 Nov 14];1(2):57.

273. Tanner L, Denti P, Wiesner L, Warner DF. Drug permeation and metabolism in *Mycobacterium tuberculosis* : Prioritising local exposure as essential criterion in new TB drug development. IUBMB Life. 2018 Sep 1 [cited 2020 Feb 18];70(9):926–37.

274. Daemmrich A. A tale of two experts: thalidomide and political engagement in the United States and West Germany. Soc Hist Med J Soc Soc Hist Med. 2002 Apr 1 [cited 2019 Jun 5];15(1):137–58.

275. Jones BL, Van Den Anker JN, Kearns GL. Pediatric Clinical Pharmacology and Therapeutics. Princ Clin Pharmacol. 2012 Jan 1 [cited 2019 Jan 28];417–36.

276. Sutherland JM. Fatal cardiovascular collapse of infants receiving large amounts of chloramphenicol. AMA J Dis Child. 1959 Jun [cited 2019 Jun 5];97(6):761–7.

277. Krekels EHJ, Calvier EAM, Graaf PH, Knibbe CAJ. Children Are Not Small Adults, but Can We Treat Them As Such? CPT Pharmacometrics Syst Pharmacol. 2019 Jan 28 [cited 2019 Jun 5];8(1):34–8.

278. Shirkey H. Editorial comment: Therapeutic orphans. The Journal of Pediatrics. 1968;73;119-20.

279. Kimland E, Nydert P, Odlind V, Böttiger Y, Lindemalm S. Paediatric drug use with focus on off-label prescriptions at Swedish hospitals - a nationwide study. Acta Paediatr. 2012 Jul [cited 2020 Jan 31];101(7):772–8.

280. Cuzzolin L, Atzei A, Fanos V. Off-label and unlicensed prescribing for newborns and children in different settings: A review of the literature and a consideration about drug safety. Vol. 5, Expert Opinion on Drug Safety. 2006. p. 703–18.

281. Pandolfini C, Bonati M. A literature review on off-label drug use in children. Vol. 164, European

Journal of Pediatrics. 2005. p. 552–8.

282. Santos DB, Clavenna A, Bonati M, Coelho HLL. Off-label and unlicensed drug utilization in hospitalized children in Fortaleza, Brazil. Eur J Clin Pharmacol. 2008;64(11):1111–8.

283. Figaji AA. Anatomical and physiological differences between children and adults relevant to traumatic brain injury and the implications for clinical assessment and care. Vol. 8, Frontiers in Neurology. Frontiers Media S.A.; 2017 [cited 2021 Feb 2]. p. 1.

284. Melmon KL, Parris EE, Melmon KL. Preventable drug reactions--causes and cures. N Engl J Med. 1971 Jun 17 [cited 2019 Jan 31];284(24):1361–8.

285. Kearns GL, Abdel-Rahman SM, Alander SW, Blowey DL, Leeder JS, Kauffman RE. Developmental Pharmacology — Drug Disposition, Action, and Therapy in Infants and Children. Wood AJJ, editor. N Engl J Med. 2003 Sep 18 [cited 2018 Nov 23];349(12):1157–67.

286. Le J, Bradley JS. Optimizing Antibiotic Drug Therapy in Pediatrics: Current State and Future Needs. J Clin Pharmacol. 2018 Oct;58:S108-22.

287. Anderson BJ, Holford NHG. Mechanism-Based Concepts of Size and Maturity in Pharmacokinetics. Annu Rev Pharmacol Toxicol. 2008 Feb 9 [cited 2019 May 6];48(1):303–32.

288. Edginton AN, Schmitt W, Voith B, Willmann S. A Mechanistic Approach for the Scaling of Clearance in Children. Clin Pharmacokinet. 2006 [cited 2019 Jun 6];45(7):683–704.

289. Mahmood I, Staschen C-M, Goteti K. Prediction of Drug Clearance in Children: an Evaluation of the Predictive Performance of Several Models. AAPS J. 2014 Nov [cited 2019 Jun 6];16(6):1334.

290. Calvier EAM, Krekels EHJ, Välitalo PAJ, Rostami-Hodjegan A, Tibboel D, Danhof M, et al. Allometric Scaling of Clearance in Paediatric Patients: When Does the Magic of 0.75 Fade? Clin Pharmacokinet. 2017 Mar 10 [cited 2019 Jun 6];56(3):273–85.

291. Mahmood I. Prediction of Drug Clearance in Premature and Mature Neonates, Infants, and Children ≤2 Years of Age: A Comparison of the Predictive Performance of 4 Allometric Models. J Clin Pharmacol. 2016 Jun [cited 2019 Jun 6];56(6):733–9.

292. Strougo A, Yassen A, Monnereau C, Danhof M, Freijer J. Predicting the “First dose in children” of CYP3A-metabolized drugs: Evaluation of scaling approaches and insights into the CYP3A7-CYP3A4 switch at young ages. J Clin Pharmacol. 2014 Sep [cited 2019 Jun 6];54(9):1006–15.

293. Mahmood I, Tegenge MA. A Comparative Study Between Allometric Scaling and Physiologically Based Pharmacokinetic Modeling for the Prediction of Drug Clearance From

Neonates to Adolescents. J Clin Pharmacol. 2019 Feb [cited 2019 Jun 6];59(2):189–97.

294. Wang C, Peeters MYM, Allegaert K, Blussé van Oud-Alblas HJ, Krekels EHJ, Tibboel D, et al. A bodyweight-dependent allometric exponent for scaling clearance across the human life-span. Pharm Res. 2012 Jun 28 [cited 2019 Jun 6];29(6):1570–81.

295. Wang C, Allegaert K, Peeters MYM, Tibboel D, Danhof M, Knibbe CAJ. The allometric exponent for scaling clearance varies with age: a study on seven propofol datasets ranging from preterm neonates to adults. Br J Clin Pharmacol. 2014 Jan [cited 2019 Jun 6];77(1):149–59.

296. Bartelink IH, Boelens JJ, Bredius RGM, Egberts ACG, Wang C, Bierings MB, et al. Body weight-dependent pharmacokinetics of busulfan in paediatric haematopoietic stem cell transplantation patients: towards individualized dosing. Clin Pharmacokinet. 2012 May 1 [cited 2019 Jun 6];51(5):331–45.

297. Wang C, Sadhavisvam S, Krekels EHJ, Dahan A, Tibboel D, Danhof M, et al. Developmental changes in morphine clearance across the entire paediatric age range are best described by a bodyweight-dependent exponent model. Clin Drug Investig. 2013 Jul 11 [cited 2019 Jun 6];33(7):523–34.

298. de Lange EC. The mastermind approach to CNS drug therapy: translational prediction of human brain distribution, target site kinetics, and therapeutic effects. Fluids Barriers CNS. 2013 Dec;10:1-6.

299. de Lange ECM, Danhof M. Considerations in the use of cerebrospinal fluid pharmacokinetics to predict brain target concentrations in the clinical setting: implications of the barriers between blood and brain. Clin Pharmacokinet. 2002;41(10):691–703.

300. Yamamoto Y, Danhof M, de Lange ECM. Microdialysis: the Key to Physiologically Based Model Prediction of Human CNS Target Site Concentrations. AAPS J. 2017;19;891-909.

301. Aungst BJ. Novel Formulation Strategies for Improving Oral Bioavailability of Drugs with Poor Membrane Permeation or Presystemic Metabolism. J Pharm Sci. 1993 Oct 1 [cited 2019 Sep 18];82(10):979–87.

302. Ho N, Park J, Ni P, Higuchi W. Advancing quantitative and mechanistic approaches in interfacing gastrointestinal drug absorption studies in animals and humans. 1983 [cited 2019 Sep 18].

303. Atkinson AJ. Drug Absorption and Bioavailability. Princ Clin Pharmacol 2007 Jan 1 [cited 2019 May 6];37–49.

304. Nicolas J-M, Bouzom F, Hugues C, Ungell A-L. Oral drug absorption in pediatrics: the intestinal

wall, its developmental changes and current tools for predictions. Biopharm Drug Dispos. 2017 Apr 1 [cited 2019 Jun 18];38(3):209–30.

305. Mooij MG, de Koning BA, Huijsman ML, de Wildt SN. Ontogeny of oral drug absorption processes in children. Expert Opin Drug Metab Toxicol. 2012 Oct 11 [cited 2019 Jun 19];8(10):1293–303.

306. Kenyon CJ, Brown F, McClelland GR, Wilding IR. The Use of Pharmacoscintigraphy to Elucidate Food Effects Observed with a Novel Protease Inhibitor (Saquinavir). Pharm Res. 1998 [cited 2019 May 6];15(3):417–22.

307. Sousa T, Paterson R, Moore V, Carlsson A, Abrahamsson B, Basit AW. The gastrointestinal microbiota as a site for the biotransformation of drugs. Int J Pharm. 2008 Nov 3 [cited 2019 Aug 22];363(1–2):1–25.

308. Smith DA, Di L, Kerns EH. The effect of plasma protein binding on in vivo efficacy: misconceptions in drug discovery. Nat Rev Drug Discov. 2010 Dec 1 [cited 2019 Jan 31];9(12):929–39.

309. Bowles A, Keane J, Ernest T, Clapham D, Tuleu C. Specific aspects of gastro-intestinal transit in children for drug delivery design. Int J Pharm. 2010 Aug 16 [cited 2019 Jun 19];395(1–2):37–43. Available from:

310. Yu G, Zheng Q-S, Li G-F. Similarities and Differences in Gastrointestinal Physiology Between Neonates and Adults: a Physiologically Based Pharmacokinetic Modeling Perspective. AAPS J. 2014 Nov 3 [cited 2019 Jun 19];16(6):1162–6.

311. Riezzo G, Indrio F, Montagna O, Tripaldi C, Laforgia N, Chiloiro M, et al. Gastric electrical activity and gastric emptying in term and preterm newborns. Neurogastroenterol Motil. 2000 Jun 1 [cited 2019 Jun 19];12(3):223–9.

312. Bonner JJ, Vajjah P, Abduljalil K, Jamei M, Rostami-Hodjegan A, Tucker GT, et al. Does age affect gastric emptying time? A model-based meta-analysis of data from premature neonates through to adults. Biopharm Drug Dispos. 2015 May 1 [cited 2019 Jun 19];36(4):245–57.

313. Maharaj AR, Edginton AN. Examining Small Intestinal Transit Time as a Function of Age: Is There Evidence to Support Age-Dependent Differences among Children? Drug Metab Dispos. 2016 Jul 1 [cited 2019 Jun 19];44(7):1080–9.

314. van Elburg RM. Intestinal permeability in relation to birth weight and gestational and postnatal age. Arch Dis Child - Fetal Neonatal Ed. 2003 Jan 1;88(1):F52-5

315. Fakhoury M, Litalien C, Medard Y, Cavé H, Ezzahir N, Peuchmaur M, et al. Localization and

mRNA expression of CYP3A and P-glycoprotein in human duodenum as a function of age. Drug Metab Dispos. 2005 Nov;33(11):1603-7.

316. Wilson ID, Nicholson JK. Gut microbiome interactions with drug metabolism, efficacy, and toxicity. Transl Res 2017 Jan 1 [cited 2019 Aug 22];179:204–22.

317. Okuda H, Ogura K, Kato A, Takubo H, Watabe T. A Possible Mechanism of Eighteen Patient Deaths Caused by Interactions of Sorivudine, a New Antiviral Drug, with Oral 5-Fluorouracil Prodrugs. J Pharmacol Exp Ther. 1998;287(2).

318. Johnson TN, Thomson M. Intestinal Metabolism and Transport of Drugs in Children: The Effects of Age and Disease. J Pediatr Gastroenterol Nutr. 2008 Jul [cited 2019 Feb 1];47(1):3–10.

319. Takano M, Yumoto R, Murakami T. Expression and function of efflux drug transporters in the intestine. Pharmacology and Therapeutics. 2006 Jan 1; 109(1-2):137-61.

320. Lin JH, Yamazaki M. Role of P-Glycoprotein in Pharmacokinetics. Clin Pharmacokinet. 2003 [cited 2019 Sep 17];42(1):59–98.

321. Mayer U, Wagenaar E, Beijnen JH, Smit JW, Meijer DKF, Asperen J, et al. Substantial excretion of digoxin via the intestinal mucosa and prevention of long-term digoxin accumulation in the brain by the mdrla P-glycoprotein. Br J Pharmacol. 1996 Nov 1 [cited 2019 Sep 19];119(5):1038–44.

322. Sparreboom A, van Asperen J, Mayer U, Schinkel AH, Smit JW, Meijer DK, et al. Limited oral bioavailability and active epithelial excretion of paclitaxel (Taxol) caused by P-glycoprotein in the intestine. Proc Natl Acad Sci U S A. 1997 Mar 4 [cited 2019 Sep 19];94(5):2031–5.

323. Golden PL, Pardridge WM. Brain Microvascular P-Glycoprotein and a Revised Model of Multidrug Resistance in Brain. Cell Mol Neurobiol. 2000 [cited 2019 Sep 19];20(2):165–81.

324. Stephens RH, O'Neill CA, Warhurst A, Carlson GL, Rowland M, Warhurst G. Kinetic Profiling of P-glycoprotein-Mediated Drug Efflux in Rat and Human Intestinal Epithelia. J Pharmacol Exp Ther. 2001;296(2).

325. Schinkel AH. The physiological function of drug-transporting P-glycoproteins. Semin Cancer Biol. 1997 Jun 1 [cited 2019 Sep 17];8(3):161–70.

326. Gottesman MM, Pastan I. Biochemistry of Multidrug Resistance Mediated by the Multidrug Transporter. Annu Rev Biochem. 1993 Jun 28 [cited 2019 Sep 17];62(1):385–427.

327. van Helvoort A, Smith AJ, Sprong H, Fritzsche I, Schinkel AH, Borst P, et al. MDR1 P-

Glycoprotein Is a Lipid Translocase of Broad Specificity, While MDR3 P-Glycoprotein Specifically Translocates Phosphatidylcholine. Cell. 1996 Nov 1 [cited 2019 Sep 17];87(3):507–17.

328. Pan B, Dutt A, Experimental JN-J of P and, 1994. Enhanced transepithelial flux of cimetidine by Madin-Darby canine kidney cells overexpressing human P-glycoprotein. ASPET. 1994 Jul [cited 2019 Sep 18]; 270(1):1-7.

329. Wu C-Y, Benet LZ, Hebert MF, Gupta SK, Rowland M, Gomez DY, et al. Differentiation of absorption and first-pass gut and hepatic metabolism in humans: Studies with cyclosporine*. Clin Pharmacol Ther. 1995 Nov 1 [cited 2019 Sep 18];58(5):492–7.

330. Peter Chiba, Wolfgang Holzer, Marion Landau, Gerhard Bechmann, Karin Lorenz, Brigitte Plagens, et al. Substituted 4-Acylpyrazoles and 4-Acylpyrazolones: Synthesis and Multidrug Resistance-Modulating Activity. Journal of Medicinal Chemistry. 1998 Oct [cited 2019 Sep 18];41(21):4001-11.

331. Seelig A, Landwojtowicz E. Structure–activity relationship of P-glycoprotein substrates and modifiers. Eur J Pharm Sci. 2000 Nov 1 [cited 2019 Sep 18];12(1):31–40.

332. Ecker G, Huber M, Schmid D, Chiba P. The Importance of a Nitrogen Atom in Modulators of Multidrug Resistance. Mol Pharmacol. 1999;56(4).

333. Thiebaut F, Tsuruo T, Hamada H, Gottesman MM, Pastan I, Willingham MC. Cellular localization of the multidrug-resistance gene product P-glycoprotein in normal human tissues. Proc Natl Acad Sci U S A. 1987 Nov 1 [cited 2019 Sep 17];84(21):7735–8.

334. Cordon-Cardo C, O'Brien JP, Boccia J, Casals D, Bertino JR, Melamed MR. Expression of the multidrug resistance gene product (P-glycoprotein) in human normal and tumor tissues. J Histochem Cytochem. 1990 Sep 5 [cited 2019 Sep 17];38(9):1277–87.

335. Schinkel AH, Smit JJM, van Tellingen O, Beijnen JH, Wagenaar E, van Deemter L, et al. Disruption of the mouse mdr1a P-glycoprotein gene leads to a deficiency in the blood-brain barrier and to increased sensitivity to drugs. Cell. 1994 May 20 [cited 2019 Sep 17];77(4):491–502.

336. Schinkel AH, Mayer U, Wagenaar E, Mol CA, van Deemter L, Smit JJ, et al. Normal viability and altered pharmacokinetics in mice lacking mdr1-type (drug-transporting) P-glycoproteins. Proc Natl Acad Sci U S A. 1997 Apr 15 [cited 2019 Sep 17];94(8):4028–33.

337. Lown KS, Mayo RR, Leichtman AB, Hsiao H, Turgeon DK, Schmiedlin-Ren P, et al. Role of intestinal P-glycoprotein (mdr1) in interpatient variation in the oral bioavailability of

cyclosporine*. Clin Pharmacol Ther. 1997 Sep 1 [cited 2019 Sep 18];62(3):248–60.

338. Masuda S, Uemoto S, Hashida T, Inomata Y, Tanaka K, Inui K. Effect of intestinal P-glycoprotein on daily tacrolimus trough level in a living-donor small bowel recipient. Clin Pharmacol Ther. 2000 Jul 1 [cited 2019 Sep 18];68(1):98–103.

339. Fardel O, Lecureur V, Guillouzo A. Regulation by dexamethasone of P-glycoprotein expression in cultured rat hepatocytes. FEBS Lett. 1993 Jul 26 [cited 2019 Sep 20];327(2):189–93.

340. Zhao JY, Ikeguchi M, Eckersberg T, Kuo MT. Modulation of multidrug resistance gene expression by dexamethasone in cultured hepatoma cells. Endocrinology. 1993 Aug 1 [cited 2019 Sep 20];133(2):521–8.

341. Lin JH, Chiba M, Chen I-W, Nishime JA, deLuna FA, Yamazaki M, et al. Effect of Dexamethasone on the Intestinal First-Pass Metabolism of Indinavir in Rats: Evidence of Cytochrome P-450 A and p-Glycoprotein Induction. Drug Metab Dispos. 1999;27(10).

342. Greiner B, Eichelbaum M, Fritz P, Kreichgauer HP, von Richter O, Zundler J, et al. The role of intestinal P-glycoprotein in the interaction of digoxin and rifampin. J Clin Invest. 1999 Jul 15 [cited 2019 Sep 20];104(2):147–53.

352. Satyanarayana U, and CR-A of M, 2017. Developmental Pattern of Hepatic Drug-Metabolizing Enzymes in Pediatric Population and its Role in Optimal Drug Treatment. archive-ouverte.unige.ch. 2017 Jan [cited 2019 Aug 14];5(1):115-22.

353. Lin JH, Lu AY. Interindividual variability in inhibition and induction of cytochrome p450 enzymes. Annu Rev Pharmacol Toxicol. 2001 Apr 28 [cited 2019 Sep 18];41(1):535–67.

354. Blum M, Demierre A,Grant DM, Heim M, Meyer UA.. Molecular mechanism of slow acetylation of drugs and carcinogens in humans. Natl Acad Sci. 1991 Jun [cited 2019 Aug 14];88(12):5237-41.

355. Rakhmanina N, reviews J van den A-A drug delivery, 2006. Pharmacological research in pediatrics: from neonates to adolescents. Advanced drug delivery reviews [cited 2019 Aug 14]; 2006 Apr 20;58(1):4-14.

356. Pariente-Khayat A, Rey E, Gendrel D, Vauzelle-Kervroëdan F, Crémier O, d'Athis P, et al. Isoniazid acetylation metabolic ratio during maturation in children. Clin Pharmacol Ther. 1997 Oct [cited 2019 Aug 14];62(4):377–83.

357. Chignell CF, Vesell ES, Starkweather DK, Berlin CM. The binding of sulfaphenazole to fetal, neonatal, and adult human plasma albumin. Clin Pharmacol Ther. [cited 2019 Feb 1];12(6):897–901.

358. Ehrnebo M, Agurell S, Jalling B, Boréus LO. Age differences in drug binding by plasma proteins: Studies on human foetuses, neonates and adults. Eur J Clin Pharmacol. 1971 Sep;3:189-93.

359. Milsap RL, Jusko WJ. Pharmacokinetics in the infant. In: Environmental Health Perspectives. 1994 Dec;102(suppl 11)107-10)

360. Mouritsen O, … KJ-P and stability, 1995. Permeability of lipid bilayers near the phase transition. books.google.com].

361. Derendorf H, Hochhaus G, Mölimann H, Barth J, Krieg M, Tunn S, et al. Receptor-Based Pharmacokinetic-Pharmacodynamic Analysis of Corticosteroids. J Clin Pharmacol. 1993 Feb 1 [cited 2018 Oct 29];33(2):115–23.

362. Lin JH. CSF as a Surrogate for Assessing CNS Exposure: An Industrial Perspective. Curr Drug Metab. 2008 Jan;9(1)46-59

363. Day RO, Francis H, Vial J, Geisslinger G, Williams KM. Naproxen concentrations in plasma and synovial fluid and effects on prostanoid concentrations. J Rheumatol. 1995 Dec 1;22(12):2295-303.

364. Debruyne D. Clinical pharmacokinetics of fluconazole in superficial and systemic mycoses. Clinical Pharmacokinetics. 1997 Jul;33:52-77.

365. Schramm P, Wildfeuer A, Sarnow E. Determination of fluconazole concentrations in the prostatic and seminal vesicle fluid (split ejaculate). Mycoses. 1994 Nov;37(11-12):417-20.

366. Hammarlund-Udenaes M. Active-Site Concentrations of Chemicals-Are They a Better Predictor of Effect than Plasma ⁄Organ ⁄ Tissue Concentrations? Basic & clinical phramacology & toxicology. 2010 Mar;106(3):215-20.

367. Avdeef A. Physicochemical profiling (solubility, permeability and charge state). Curr Top Med Chem. 2001 Sep [cited 2019 Feb 1];1(4):277–351.

368. Di L, Kerns EH, Carter GT. Strategies to assess blood–brain barrier penetration. Expert Opin Drug Discov. 2008 Jun 22 [cited 2019 Feb 1];3(6):677–87.

369. Liu X, Tu M, Kelly RS, Chen C, Smith BJ. Development of a computational approach to predict blood-brain barrier permeability. Drug Metab Dispos. 2004 Jan 1 [cited 2019 Feb 1];32(1):132–9.

370. Lau YY, Huang Y, Frassetto L, Benet LZ. Effect of OATP1B transporter inhibition on the pharmacokinetics of atorvastatin in healthy volunteers. Clin Pharmacol Ther. 2007

Feb;81(2):194-204.

371. Minchinton AI, Tannock IF. Drug penetration in solid tumours. Nature Reviews Cancer. 2006 Aug1;6(8):583-92.

372. Liu X, Smith BJ, Chen C, Callegari E, Becker SL, Chen X, et al. Evaluation of cerebrospinal fluid concentration and plasma free concentration as a surrogate measurement for brain free concentration. Drug Metab Dispos. 2006 Sep 1;34(9):1443-7.

373. Kalvass JC, Olson ER, Cassidy MP, Selley DE, Pollack GM. Pharmacokinetics and pharmacodynamics of seven opioids in P-glycoprotein-competent mice: assessment of unbound brain EC50,u and correlation of in vitro, preclinical, and clinical data. J Pharmacol Exp Ther. 2007 Oct 1;323(1):346-55.

374. Maurer TS, DeBartolo DB, Tess DA, Scott DO. Relationship between exposure and nonspecific binding of thirty-three central nervous system drugs in mice. Drug Metab Dispos. 2005 Jan 1;33(1):175-81.

375. Miyazaki M, Maekawa C, Iwanaga K, Morimoto K, Kakemi M. Bioavailability assessment of disopyramide using pharmacokinetic-pharmacodynamic (PK-PD) modeling in the rat. Biol Pharm Bull. 2000 Nov 1;23(11):1363-9.

376. Hammarlund-Udenaes M, Fridén M, Syvänen S, Gupta A. On the rate and extent of drug delivery to the brain. Pharmaceutical Research. 2008 Aug;25:1737-50.

377. Van der Graaf PH, Van Schaick EA, Visser SA, De Greef HJ, Ijzerman AP, Danhof M. Mechanism-based pharmacokinetic-pharmacodynamic modeling of antilipolytic effects of adenosine A(1) receptor agonists in rats: prediction of tissue-dependent efficacy in vivo. J Pharmacol Exp Ther. 1999 Aug [cited 2018 Oct 29];290(2):702–9.

378. Keaney J, Campbell M. The dynamic blood-brain barrier. FEBS J. 2015 Nov;282(21):4067-79.

379. Abbott NJ, Rönnbäck L, Hansson E. Astrocyte-endothelial interactions at the blood-brain barrier. Nature Reviews Neuroscience. 2006 Jan 1;7(1):41-53.

380. Bartanusz V, Jezova D, Alajajian B, Digicaylioglu M. The blood–spinal cord barrier: Morphology and Clinical Implications. Ann Neurol. 2011 Aug 1 [cited 2023 Jan 18];70(2):194–206.

381. Huss A, Bachhuber F. The cerebrospinal fluid and barriers – anatomic and physiologic considerations. Handb Clin Neurol. 2018 Jan 1 [cited 2019 Aug 29];146:21–32.

382. Obermeier B, Daneman R, Ransohoff RM. Development, maintenance and disruption of the

blood-brain barrier. Nat Med. 2013;19(12):1584–96.

383. Pardridge WM. Drug Delivery to the Brain. J Cereb Blood Flow Metab. 1997 Jul 31 [cited 2018 Oct 29];713–31.

384. Moos T, Mollgard K. Cerebrovascular permeability to azo dyes and plasma proteins in rodents of different ages. Neuropathol Appl Neurobiol. 1993 Apr;19(2):120-7.

385. Daneman R, Zhou L, Kebede AA, Barres BA. Pericytes are required for blood?????"brain barrier integrity during embryogenesis. Nature. 2010 Nov 25;468(7323):562-6.

386. Abbott NJ, Rönnbäck L, Hansson E. Astrocyte–endothelial interactions at the blood–brain barrier. Nat Rev Neurosci. 2006 Jan [cited 2019 Jul 3];7(1):41–53.

387. Abbott NJ, Patabendige AAK, Dolman DEM, Yusof SR, Begley DJ. Structure and function of the blood-brain barrier. Neurobiology of Disease. 2010 Jan 1;37(1):13-25.

388. Hawkins BT. The Blood-Brain Barrier/Neurovascular Unit in Health and Disease. Pharmacol Rev. 2005 Jun 1;57(2)173-85.

389. Daneman R. The blood-brain barrier in health and disease. Ann Neurol. 2012 Nov;72(5):648-72.

390. Wong AD, Ye M, Levy AF, Rothstein JD, Bergles DE, Searson PC. The blood-brain barrier: an engineering perspective. Front Neuroeng. 2013 Aug 30;6:7.

391. Cserr HF, Bundgaard M. Blood-brain interfaces in vertebrates: a comparative approach. Am J Physiol. 1984 Mar [cited 2019 Jul 3];246(3 Pt 2):R277-88.

392. Henderson JT, Piquette-Miller M. Blood-Brain Barrier: An Impediment to Neuropharmaceuticals. 2015 [cited 2019 Jun 24];97:308.

393. Risau W, Hallmann R, Albrecht U. Differentiation-dependent expression of proteins in brain endothelium during development of the blood-brain barrier. Dev Biol. 1986 Oct 1 [cited 2019 Jun 25];117(2):537–45.

394. Hartz A, Bauer B. ABC transporters in the CNS - an inventory. Curr Pharm Biotechnol. 2011 Apr 1;12(4):656-73.

395. Ueno M. Mechanisms of the Penetration of Blood-Borne Substances into the Brain. Curr Neuropharmacol. 2009 Jun 1 [cited 2018 Nov 23];7(2):142–9.

396. Benarroch EE. Circumventricular organs: Receptive and homeostatic functions and clinical implications. Neurology. 2011 Sep 20;77(12):1198-204.

397. Duvernoy HM, Risold PY. The circumventricular organs: An atlas of comparative anatomy and vascularization. Brain Research Reviews. 2007 Nov 1;56(1):119-47.

398. Ganong WF. Circumventricular organs: Definition and role in the regulation of endocrine and autonomic function. In: Clinical and Experimental Pharmacology and Physiology. 2000 May;27(5-6):422-7.

399. Nag S. Ultracytochemical Studies of the Compromised Blood–Brain Barrier. In: Blood-Brain Barrier. New Jersey: Humana Press; 2003 [cited 2019 Jun 24]. p. 145–60.

400. Vorbrodt AW, Dobrogowska DH, Lossinsky AS, Wisniewski HM. Ultrastructural localization of lectin receptors on the luminal and abluminal aspects of brain micro-blood vessels. J Histochem Cytochem. 1986 Feb 5 [cited 2019 Jun 24];34(2):251–61.

401. Nag S. Morphology and Molecular Properties of Cellular Components of Normal Cerebral Vessels. In: Blood-Brain Barrier. New Jersey: Humana Press; 2003 [cited 2019 Jun 24]. p. 3–36.

402. Wolburg H, Noell S, Mack A, Wolburg-Buchholz K, Fallier-Becker P. Brain endothelial cells and the glio-vascular complex. Cell Tissue Res. 2009 Jan 16 [cited 2019 Jun 24];335(1):75–96.

403. El-Bachá R, (Noisy-le AM-C and molecular biology. Drug metabolizing enzymes in cerebrovascular endothelial cells afford a metabolic protection to the brain. 1999 Feb 1 [cited 2019 Jul 3];45(1):15-23.

404. Abbott NJ, Patabendige AAK, Dolman DEM, Yusof SR, Begley DJ. Structure and function of the blood–brain barrier. Neurobiol Dis. 2010 Jan [cited 2018 Nov 29];37(1):13–25.

405. Saunders NR, Liddelow SA, Dziegielewska KM. Barrier mechanisms in the developing brain. Front Pharmacol. 2012 Mar 29;3:46.

406. Lee H, Pienaar IS. Disruption of the blood-brain barrier in Parkinson's disease: curse or route to a cure? Front Biosci (Landmark Ed. 2014 Jan 1 [cited 2019 Jun 24];19:272–80.

407. Nag S. Morphology and Properties of Brain Endothelial Cells. In: Methods in molecular biology (Clifton, NJ). 2011 [cited 2019 Jun 24]. p. 3–47.

408. Oldendorf WH, Cornford ME, Brown WJ. The large apparent work capability of the blood-brain barrier: A study of the mitochondrial content of capillary endothelial cells in brain and other tissues of the rat. Ann Neurol. 1977 May 1 [cited 2019 Jul 13];1(5):409–17.

409. Simionescu M, Simionescu N, Palade GE. Morphometric data on the endothelium of blood capillaries. J Cell Biol. 1974 Jan 1 [cited 2019 Jun 24];60(1):128–52.

410. Simionescu M, Simionescu N. Endothelial transport of macromolecules: transcytosis and endocytosis. A look from cell biology. Cell Biol Rev. 1991 [cited 2019 Jul 16];25(1):1–78.

411. Simionescu M, Popov D, Sima A. Endothelial transcytosis in health and disease. Cell Tissue Res. 2009 Jan 3 [cited 2019 Jul 16];335(1):27–40.

412. Schnitzer JE. Caveolae: from basic trafficking mechanisms to targeting transcytosis for tissue-specific drug and gene delivery in vivo. Adv Drug Deliv Rev. 2001 Jul 28 [cited 2019 Jul 16];49(3):265–80.

413. Schulze C, Firth JA. Immunohistochemical localization of adherens junction components in blood-brain barrier microvessels of the rat. Journal of cell science. 1993 Mar 1 [cited 2023 Aug 15];104(3):773-82.

414. Brown RC, Davis TP. Calcium Modulation of Adherens and Tight Junction Function. Stroke. 2002 Jun 1 [cited 2019 Jul 4];33(6):1706–11.

415. Bazzoni G, Dejana E. Endothelial Cell-to-Cell Junctions: Molecular Organization and Role in Vascular Homeostasis. Physiol Rev. 2004 Jul [cited 2019 Jul 4];84(3):869–901.

416. Bazzoni G. Endothelial tight junctions: Permeable barriers of the vessel wall. Thromb Haemost. 2006;95(01):36-42.

417. Vorbrodt A, Reviews DD-BR, 2003. Molecular anatomy of intercellular junctions in brain endothelial and epithelial barriers: electron microscopist's view. Brain Research Reviews. 2003 Jun 1 [cited 2019 Jul 13];42(3):221-42.

418. Stevenson BR, Siliciano JD, Mooseker MS, Goodenough DA. Identification of ZO-1: a high molecular weight polypeptide associated with the tight junction (zonula occludens) in a variety of epithelia. J Cell Biol. 1986 Sep 1 [cited 2019 Jul 15];103(3):755–66.

419. Fanning AS, Jameson BJ, Jesaitis LA, Anderson JM. The tight junction protein ZO-1 establishes a link between the transmembrane protein occludin and the actin cytoskeleton. J Biol Chem. 1998 Nov 6 [cited 2019 Jul 15];273(45):29745–53.

420. Gumbiner B, Lowenkopf T, Apatira D. Identification of a 160-kDa polypeptide that binds to the tight junction protein ZO-1. Proc Natl Acad Sci U S A. 1991 Apr 15 [cited 2019 Jul 15];88(8):3460–4.

421. Citi S, Sabanay H, Kendrick-Jones J, Geiger B. Cingulin: characterization and localization. J Cell Sci. 1989;93(1).

422. Bauer H-C, traweger A, bauer H. Proteins of the Tight Junction in the Blood-Brain Barrier.

Blood-Spinal Cord Brain Barriers Heal Dis. 2004 Jan 1 [cited 2019 Jul 13];1–10.

423. Yu ASL, McCarthy KM, Francis SA, McCormack JM, Lai J, Rogers RA, et al. Knockdown of occludin expression leads to diverse phenotypic alterations in epithelial cells. Am J Physiol Physiol. 2005 Jun [cited 2019 Jul 3];288(6):C1231–41.

424. Furuse M, Hirase T, Itoh M, Nagafuchi A, Yonemura S, Tsukita S, et al. Occludin: a novel integral membrane protein localizing at tight junctions. J Cell Biol. 1993 Dec 15 [cited 2019 Jul 13];123(6 Pt 2):1777–88.

425. Liebner S, Kniesel U, Kalbacher H, Wolburg H. Correlation of tight junction morphology with the expression of tight junction proteins in blood-brain barrier endothelial cells. E journal of cell. 2000 Oct [cited 2019 Jul 3];79(10):707-17.

426. Wolburg H, pharmacology AL-V, 2002. Tight junctions of the blood–brain barrier: development, composition and regulation. Elsevier. [cited 2019 Jul 3]; Available from: https://www.sciencedirect.com/science/article/pii/S1537189102002008

427. Tsukita S, Tanaka H, Tamura A. The Claudins: From Tight Junctions to Biological Systems. Vol. 44, Trends in Biochemical Sciences. Elsevier Ltd; 2019. p. 141–52.

428. Furuse M, Fujita K, Hiiragi T, Fujimoto K, Tsukita S. Claudin-1 and -2: novel integral membrane proteins localizing at tight junctions with no sequence similarity to occludin. J Cell Biol. 1998 Jun 29 [cited 2019 Jul 13];141(7):1539–50.

429. Huber JD, Egleton RD, Davis TP. Molecular physiology and pathophysiology of tight junctions in the blood–brain barrier. Trends Neurosci. 2001 Dec 1 [cited 2019 Jul 16];24(12):719–25.

430. Volterra A, Meldolesi J. Astrocytes, from brain glue to communication elements: The revolution continues. Nature Reviews Neuroscience. 2005 Aug 1;6(8):626-40.

431. Halassa MM, Haydon PG. Integrated Brain Circuits: Astrocytic Networks Modulate Neuronal Activity and Behavior. Annu Rev Physiol. 2010 Mar 17;72(1):335-55.

432. Freeman MR. Specification and morphogenesis of astrocytes. Science. 2010 Nov 5;330(6005):774-8.

433. Mulligan SJ, MacVicar BA. Calcium transients in astrocyte endfeet cause cerebrovascular constrictions. Nature. 2004 Sep [cited 2019 Jun 25];431(7005):195–9.

434. Takano T, Tian G-F, Peng W, Lou N, Libionka W, Han X, et al. Astrocyte-mediated control of cerebral blood flow. Nat Neurosci. 2006 Feb 25 [cited 2019 Jun 25];9(2):260–7.

435. Alvarez JI, Dodelet-Devillers A, Kebir H, Ifergan I, Fabre PJ, Terouz S, et al. The hedgehog

pathway promotes blood-brain barrier integrity and CNS immune quiescence. Science. 2011 Dec 23;334(6063):1727-31.

436. Wosik K, Cayrol R, Dodelet-Devillers A, Berthelet F, Bernard M, Moumdjian R, et al. Angiotensin II Controls Occludin Function and Is Required for Blood Brain Barrier Maintenance: Relevance to Multiple Sclerosis. J Neurosci. 2007 Aug 22;27(34):9032-42.

437. Bell RD, Winkler EA, Singh I, Sagare AP, Deane R, Wu Z, et al. Apolipoprotein e controls cerebrovascular integrity via cyclophilin A. Nature. 2012 May 24;485(7399):512-6.

438. Winkler EA, Bell RD, Zlokovic B V. Central nervous system pericytes in health and disease. Nature Neuroscience. 2011 Nov;14(11):1398-405.

439. Lindahl P, Johansson BR, Levéen P, Betsholtz C. Pericyte loss and microaneurysm formation in PDGF-B-deficient mice. Science. 1997 Jul;227(5323):242-5.

440. Bell RD, Winkler EA, Sagare AP, Singh I, LaRue B, Deane R, et al. Pericytes Control Key Neurovascular Functions and Neuronal Phenotype in the Adult Brain and during Brain Aging. Neuron. 2010 Nov 4;68(3):409-27.

441. Armulik A, Genové G, Mäe M, Nisancioglu MH, Wallgard E, Niaudet C, et al. Pericytes regulate the blood-brain barrier. Nature. 2010 Nov 25;468(7323):557-61.

442. Farkas E, Luiten PG. Cerebral microvascular pathology in aging and Alzheimers disease neurobiology. 2001 Aug;64(6):575-611.

443. Rascher G, Fischmann A, Kröger S, Duffner F, Grote E-H, Wolburg H. Extracellular matrix and the blood-brain barrier in glioblastoma multiforme: spatial segregation of tenascin and agrin. Acta Neuropathol. 2002 Jul 28 [cited 2019 Jul 3];104(1):85–91.

444. Rosenberg GA, Estrada E, Kelley RO, Kornfeld M. Bacterial collagenase disrupts extracellular matrix and opens blood-brain barrier in rat. Neurosci Lett. 1993 Sep 17 [cited 2019 Jul 3];160(1):117–9.

445. Tilling T, Korte D, Hoheisel D, Galla H-J. Basement Membrane Proteins Influence Brain Capillary Endothelial Barrier Function In Vitro. J Neurochem. 2002 Nov 13 [cited 2019 Jul 3];71(3):1151–7.

446. Savettieri G, Di Liegro I, Catania C, Licata L, Pitarresi GL, D'Agostino S, Shiera G, De Caro V, Giandalia G, Giannola LI, Cestelli A. Neurons and ECM regulate occludin localization in brain endothelial cells. Neuroreport. 2000 Apr 7;11(5):1081-4.

447. Abbott NJ. Anatomy and Physiology of the Blood–Brain Barriers. In Springer, New York, NY;

2014 [cited 2018 Nov 29]. p. 3–21.

448. Erdő F, Denes L, de Lange E. Age-associated physiological and pathological changes at the blood–brain barrier: A review. J Cereb Blood Flow Metab. 2017 Jan 13 [cited 2019 Sep 3];37(1):4–24.

449. Segal MB. The choroid plexuses and the barriers between the blood and the cerebrospinal fluid. Vol. 20, Cellular and Molecular Neurobiology. 2000 Apr;20:183-96.

450. Brightman MW, Reese TS. Junctions between intimately apposed cell membranes in the vertebrate brain. J Cell Biol. 1969 Mar 1;40(3):648-77.

451. Kusuhara H, Sugiyama Y. Active efflux across the blood-brain barrier: Role of the solute carrier family. NeuroRx. 2005 Jan 1;2(1):73-85.

452. de Lange EC, de Bock G, Schinkel AH, de Boer AG, Breimer DD. BBB transport and P-glycoprotein functionality using MDR1A (-/-) and wild-type mice. Total brain versus microdialysis concentration profiles of rhodamine-123. Pharm Res. 1998 Nov [cited 2018 Oct 26];15(11):1657–65.

453. Schinkel AH, Jonker JW. Mammalian drug efflux transporters of the ATP binding cassette (ABC) family: An overview. Advanced Drug Delivery Reviews. 2012 Dec 1;64;138-53.

454. Löscher W, Potschka H. Role of drug efflux transporters in the brain for drug disposition and treatment of brain diseases. Progress in Neurobiology. 2005 May 1; 76(1):22-76.

455. Rao V V, Dahlheimer JL, Bardgett ME, Snyder AZ, Finch RA, Sartorelli AC, et al. Choroid plexus epithelial expression of MDR1 P glycoprotein and multidrug resistance-associated protein contribute to the blood-cerebrospinal-fluid drug-permeability barrier. Proc Natl Acad Sci U S A. 1999 Mar 30 [cited 2018 Oct 26];96(7):3900–5.

456. Nies AT, Jedlitschky G, König J, Herold-Mende C, Steiner HH, Schmitt H-P, et al. Expression and immunolocalization of the multidrug resistance proteins, MRP1-MRP6 (ABCC1-ABCC6), in human brain. Neuroscience 2004 Jan [cited 2018 Oct 26];129(2):349–60.

457. Schinkel AH. P-Glycoprotein, a gatekeeper in the blood-brain barrier. Advanced Drug Delivery Reviews. 1999 Apr 5;36(2-3):179-94.

458. Löscher W, Potschka H. Blood-brain barrier active efflux transporters: ATP-binding cassette gene family. NeuroRx. 2005 Jan 1;2(1):86-98.

459. Spector R. Nature and consequences of mammalian brain and CSF efflux transporters: four decades of progress. J Neurochem. 2010 Jan 1 [cited 2019 Aug 16];112(1):13–23.

460. Schumacher U, Mollgård K. The multidrug-resistance P-glycoprotein (Pgp, MDR1) is an early marker of blood-brain barrier development in the microvessels of the developing human brain. Histochem Cell Biol. 1997 Aug [cited 2019 Feb 1];108(2):179–82.

461. Virgintino D, Errede M, Girolamo F, Capobianco C, Robertson D, Vimercati A, et al. Fetal blood-brain barrier P-glycoprotein contributes to brain protection during human development. J Neuropathol Exp Neurol. 2008 Jan 1 [cited 2019 Feb 1];67(1):50–61.

462. Miller DS. Regulation of ABC transporters at the blood-brain barrier. Clinical pharmacology and therapeutics. 2015 Apr;97(4):395-403.

463. Campos CR, Schröter C, Wang X, Miller DS. ABC transporter function and regulation at the blood-spinal cord barrier. J Cereb Blood Flow Metab. 2012 Aug;32(8):1559–66.

464. Cartwright TA, Campos CR, Cannon RE, Miller DS. Mrp1 is essential for sphingolipid signaling to p-glycoprotein in mouse blood-brain and blood-spinal cord barriers. J Cereb Blood Flow Metab. 2013 Mar;33(3):381–8.

465. Wang X, Campos CR, Peart JC, Smith LK, Boni JL, Cannon RE, et al. Nrf2 upregulates ATP binding cassette transporter expression and activity at the blood-brain and blood-spinal cord barriers. J Neurosci. 2014;34(25):8585–93.

466. Zlokovic B V. The Blood-Brain Barrier in Health and Chronic Neurodegenerative Disorders. Neuron. 2008 Jan 24;57(2):178-201.

467. Abuznait AH, Kaddoumi A. Role of ABC transporters in the pathogenesis of Alzheimers disease. Vol. 3, ACS Chemical Neuroscience. 2012 Nov 21;3(11):820-31.

468. Dutheil F, Jacob A, Dauchy S, Beaune P, Scherrmann JM, Declves X, et al. ABC transporters and cytochromes P450 in the human central nervous system: Influence on brain pharmacokinetics and contribution to neurodegenerative disorders. Expert Opinion on Drug Metabolism and Toxicology. 2010 Oct 1;6(10):1161-74.

469. Miller DS, Bauer B, Hartz AMS. Modulation of P-glycoprotein at the blood-brain barrier: opportunities to improve central nervous system pharmacotherapy. Pharmacol Rev. 2008 Jun 1 [cited 2019 Aug 16];60(2):196–209.

470. Beaulieu E, Demeule M, Ghitescu L, Béliveau R. P-glycoprotein is strongly expressed in the luminal membranes of the endothelium of blood vessels in the brain. Biochem J. 1997 Sep 1 [cited 2019 Sep 19];326 (Pt 2)(2):539–44.

471. Pardridge W, Golden PL, Kang YS, Bickel U. Brain microvascular and astrocyte localization of P-glycoprotein. Wiley Online Libr. 1996 Mar [cited 2019 Sep 19];68(3):1278-85

472. Bendayan R, Ronaldson PT, Gingras D, Bendayan M. In situ localization of P-glycoprotein (ABCB1) in human and rat brain. J Histochem Cytochem. 2006 Oct;54(10):1159–67.

473. Kemper EM, Verheij M, Boogerd W, Beijnen JH, van Tellingen O. Improved penetration of docetaxel into the brain by co-administration of inhibitors of P-glycoprotein. Eur J Cancer. 2004 May 1 [cited 2019 Aug 18];40(8):1269–74.

474. Kemper EM, van Zandbergen AE, Cleypool C, Mos HA, Boogerd W, Beijnen JH, et al. Increased Penetration of Paclitaxel into the Brain by Inhibition of P-Glycoprotein. Clin Cancer Res. 2003 Jul 1;9(7):2849-55.

475. Wang Q, Yang H, Miller DW, Elmquist WF. Effect of the p-glycoprotein inhibitor, cyclosporin A, on the distribution of rhodamine-123 to the brain: an in vivo microdialysis study in freely moving rats. Biochem Biophys Res Commun. 1995 Jun 26 [cited 2020 Feb 5];211(3):719–26.

476. Kruh GD, Belinsky MG. The MRP family of drug efflux pumps. Oncogene. 2003 Oct;22(47):7537-52.

477. König J, Nies AT, Cui Y, Leier I, Keppler D. Conjugate export pumps of the multidrug resistance protein (MRP) family: Localization, substrate specificity, and MRP2-mediated drug resistance. Biochimica et Biophysica Acta - Biomembranes. 1999 Dec 6;1461(2):377-94.

478. Leslie EM, Deeley RG, Cole SPC. Toxicological relevance of the multidrug resistance protein 1, MRP1 (ABCC1) and related transporters. Toxicology. 2001 Oct 5;167(1):3-23.

479. Strazielle N, Ghersi-Egea JF. Efflux transporters in blood-brain interfaces of the developing brain. Frontiers in Neuroscience. 2015 Feb 5;9:21.

480. Kwan P, Li HM, Al-Jufairi E, Abdulla R, Gonzales M, Kaye AH, et al. Association between temporal lobe P-glycoprotein expression and seizure recurrence after surgery for pharmacoresistant temporal lobe epilepsy. Neurobiol Dis. 2010 Aug 1;39(2):192-7.

481. Potschka H. Transporter hypothesis of drug-resistant epilepsy: Challenges for pharmacogenetic approaches. Pharmacogenomics. 2010 Oct 1;11(10):1427-38.

482. Hesselink MB, Smolders H, Eilbacher B, De Boer AG, Breimer DD, Danysz W. The Role of Probenecid-Sensitive Organic Acid Transport in the Pharmacokinetics of N-Methyl-d-Aspartate Receptor Antagonists Acting at the GlycineB-Site: Microdialysis and Maximum Electroshock Seizures Studies. J Pharmacol Exp Ther. 1999;290(2).

483. Engelhardt B. The blood-central nervous system barriers actively control immune cell entry into the central nervous system. Curr Pharm Des. 2008 [cited 2018 Nov 29];14(16):1555–65.

484. Neuwelt EA, Bauer B, Fahlke C, Fricker G, Iadecola C, Janigro D, et al. Engaging neuroscience to advance translational research in brain barrier biology. Nat Rev Neurosci. 2011 Mar [cited 2018 Nov 29];12(3):169–82.

485. Bronger H, König J, Kopplow K, Steiner HH, Ahmadi R, Herold-Mende C, et al. ABCC drug efflux pumps and organic anion uptake transporters in human gliomas and the blood-tumor barrier. Cancer Res. 2005 Dec 15;65(24):11419-28.

486. Ivey NS, MacLean AG, Lackner AA. Acquired immunodeficiency syndrome and the blood-brain barrier. Journal of NeuroVirology. 2009 Jan 1;15(2):111-22.

487. Hartz AMS, Miller DS, Bauer B. Restoring Blood-Brain Barrier P-Glycoprotein Reduces Brain Amyloid- in a Mouse Model of Alzheimer's Disease. Mol Pharmacol. 2010 May 1;77(5):715-23.

488. Moskowitz MA, Lo EH, Iadecola C. The science of stroke: Mechanisms in search of treatments. Neuron. 2010 Jul 29;67(2):181-98.

489. McQuaid S, Cunnea P, McMahon J, Fitzgerald U. The effects of blood-brain barrier disruption on glial cell function in multiple sclerosis. Biochem Soc Trans. 2009 Feb 1;329-31

490. Remy S, Beck H. Molecular and cellular mechanisms of pharmacoresistance in epilepsy. Brain. 2006 Jan 1;129(1)18-35.

491. Uchiyama S, Carlin AF, Khosravi A, Weiman S, Banerjee A, Quach D, et al. The surface-anchored NanA protein promotes pneumococcal brain endothelial cell invasion. J Exp Med. 2009 Aug 31;206(9):1845-52.

492. Petty MA, Lo EH. Junctional complexes of the blood–brain barrier: permeability changes in neuroinflammation. Prog Neurobiol. 2002 Dec 1 [cited 2019 Jul 16];68(5):311–23.

493. Plumb J, McQuaid S, Mirakhur M, Kirk J. Abnormal Endothelial Tight Junctions in Active Lesions and Normal-appearing White Matter in Multiple Sclerosis. Brain Pathol. 2006 Apr 5 [cited 2019 Jul 16];12(2):154–69.

494. Kirk J, Plumb J, Mirakhur M, McQuaid S. Tight junctional abnormality in multiple sclerosis white matter affects all calibres of vessel and is associated with blood-brain barrier leakage and active demyelination. J Pathol. 2003 Oct 1 [cited 2019 Jul 16];201(2):319–27.

495. Minagar A, Alexander JS. Blood-brain barrier disruption in multiple sclerosis. Mult Scler J. 2003 Dec 2 [cited 2019 Jul 16];9(6):540–9.

496. Dallasta LM, Pisarov LA, Esplen JE, Werley J V., Moses A V., Nelson JA, et al. Blood-Brain

Barrier Tight Junction Disruption in Human Immunodeficiency Virus-1 Encephalitis. Am J Pathol. 1999 Dec 1 [cited 2019 Jul 16];155(6):1915–27.

497. Fiala M, Liu QN, Sayre J, Pop V, Brahmandam V, Graves MC, et al. Cyclooxygenase-2-positive macrophages infiltrate the Alzheimer's disease brain and damage the blood-brain barrier. Eur J Clin Invest. 2002 May 1 [cited 2019 Jul 16];32(5):360–71.

498. Kim BJ, Hancock BM, Bermudez A, Cid N Del, Reyes E, Van Sorge NM, et al. Bacterial induction of Snail1 contributes to blood-brain barrier disruption. J Clin Invest. 2015 Jun 1;125(6):2473-83.

499. Roe K, Kumar M, Lum S, Orillo B, Nerurkar VR, Verma S. West nile virus-induced disruption of the blood-brain barrier in mice is characterized by the degradation of the junctional complex proteins and increase in multiple matrix metalloproteinases. J Gen Virol. 2012 Jun;93(6):1193-203.

500. Greenwood J, Wang Y, Calder VL. Lymphocyte adhesion and transendothelial migration in the central nervous system: the role of LFA-1, ICAM-1, VLA-4 and VCAM-1. off. Immunology. 1995 Nov [cited 2019 Feb 1];86(3):408–15.

501. Munji RN, Soung AL, Weiner GA, Sohet F, Semple BD, Trivedi A, et al. Profiling the mouse brain endothelial transcriptome in health and disease models reveals a core blood-brain barrier dysfunction module. Nat Neurosci. 2019 Oct 14 [cited 2019 Nov 21];22(11):1892-902.

502. Liu X, Chen C. Strategies to optimize brain penetration in drug discovery. Curr Opin Drug Discov Devel. 2005 Jul 1;8(4):505-12

503. Liu X, Smith BJ, Chen C, Callegari E, Becker SL, Chen X, et al. Use of physiologically based pharmacokinetic model to study the time to reach brain equilibrium: an experimental analysis of the role of blood-brain barrier permeability, plasma protein binding, and brain tissue binding . J Pharmacol Exp Tech. 2005 Jun;313(3):1254-62.

504. Hammarlund-Udenaes M. The use of microdialysis in CNS drug delivery studies: Pharmacokinetic perspectives and results with analgesics and antiepileptics. Advanced Drug Delivery Reviews. 2000 Dec 15;45(2-3):283-94.

505. Tan K, Purcell W, Heales SJ, McLeod JD, Hurst RD. Evaluation of the role of P-glycoprotein in inflammation induced blood–brain barrier damage. Neuroreport. 2002 Dec 20 [cited 2019 Aug 18];13(18):2593-7.

506. Théron D, Barraud de Lagerie S, Tardivel S, Pélerin H, Demeuse P, Mercier C, et al. Influence of tumor necrosis factor-α on the expression and function of P-glycoprotein in an immortalised

rat brain capillary endothelial cell line, GPNT. Biochem Pharmacol. 2003 Aug 15 [cited 2019 Aug 18];66(4):579–87.

507. Seelbach MJ, Brooks TA, Egleton RD, Davis TP. Peripheral inflammatory hyperalgesia modulates morphine delivery to the brain: a role for P-glycoprotein. J Neurochem. 2007 Sep 1 [cited 2019 Aug 18];102(5):1677–90.

508. Scheld WM, Dacey RG, Winn HR, Welsh JE, Jane JA, Sande MA. Cerebrospinal fluid outflow resistance in rabbits with experimental meningitis. Alterations with penicillin and methylprednisolone. J Clin Invest . 1980 Aug 1 [cited 2019 Aug 15];66(2):243–53.

509. Yamamoto Y, Välitalo PA, van den Berg DJ, Hartman R, van den Brink W, Wong YC, et al. A Generic Multi-Compartmental CNS Distribution Model Structure for 9 Drugs Allows Prediction of Human Brain Target Site Concentrations. Pharm Res. 2017;34(2).

510. Levin VA. Relationship of octanol/water partition coefficient and molecular weight to rat brain capillary permeability. J Med Chem. 1980 Jun [cited 2019 Aug 16];23(6):682–4.

511. Lipinski CA, Lombardo F, Dominy BW, Feeney PJ. Experimental and computational approaches to estimate solubility and permeability in drug discovery and development settings. Advanced Drug Delivery Reviews.1997 Jan 15;23(1-3):3-25.

512. Avdeef A. Physicochemical Profiling (Solubility, Permeability and Charge State). Curr Top Med Chem. 2001 Sep 1;1(4):277-351.

513. Saunders N, Habgood M, Dziegielewska K. Barrier mechanisms in the brain, ii. Immature brain. Clin Exp Pharmacol Physiol. 1999 Feb 1 [cited 2019 Aug 18];26(2):85–91.

514. Nau R, Sörgel F, Prange HW. Lipophilicity at pH 7.4 and molecular size govern the entry of the free serum fraction of drugs into the cerebrospinal fluid in humans with uninflamed meninges. J Neurol Sci. 1994 Mar 1 [cited 2019 Aug 15];122(1):61–5.

515. Lin TH, Lin JH. Effects of protein binding and experimental disease states on brain uptake of benzodiazepines in rats. J Pharmacol Exp Ther. 1990;253(1).

516. Thea D, Barza M. Use of antibacterial agents in infections of the central nervous system. Infect Dis Clin North Am. 1989 Sep [cited 2019 Aug 16];3(3):553–70.

517. Pajouhesh H, Lenz GR. Medicinal chemical properties of successful central nervous system drugs. NeuroRx. 2005 [cited 2020 Oct 2];2(4):541–53.

518. Wager TT, Chandrasekaran RY, Hou X, Troutman MD, Verhoest PR, Villalobos A, et al. Defining desirable central nervous system drug space through the alignment of molecular

properties, in vitro ADME, and safety attributes. ACS Chem Neurosci. 2010 Jun 16 [cited 2020 Oct 2];1(6):420–34.

519. Wager TT, Hou X, Verhoest PR, Villalobos A. Moving beyond rules: The development of a central nervous system multiparameter optimization (CNS MPO) approach to enable alignment of druglike properties. ACS Chem Neurosci. 2010 Jun 16 [cited 2020 Oct 2];1(6):435–49.

520. Alffenaar JWC, De Vries PM, Luijckx GJ, Van Soolingen D, Van Der Werf TS, Van Altena R. Plasma and cerebrospinal fluid pharmacokinetics of moxifloxacin in a patient with tuberculous meningitis. Antimicrobial Agents and Chemotherapy. 2008 Jun;52(6):2293-5.

521. Beer R, Engelhardt KW, Pfausler B, Broessner G, Helbok R, Lackner P, et al. Pharmacokinetics of intravenous linezolid in cerebrospinal fluid and plasma in neurointensive care patients with staphylococcal ventriculitis associated with external ventricular drains. Antimicrob Agents Chemother. 2007 Jan 1 [cited 2019 Aug 18];51(1):379–82.

522. Villani P, Regazzi MB, Marubbi F, Viale P, Pagani L, Cristini F, et al. Cerebrospinal fluid linezolid concentrations in postneurosurgical central nervous system infections. Antimicrob Agents Chemother. 2002 Mar 1 [cited 2019 Aug 18];46(3):936–7.

523. Rupprecht TA, Pfister H-W. Clinical experience with linezolid for the treatment of central nervous system infections. Eur J Neurol. 2005 Jul 1 [cited 2019 Aug 18];12(7):536–42.

524. Ellard G a, Humphries MJ, Allen BW. Cerebrospinal fluid drug concentrations and the treatment of tuberculous meningitis. Am Rev Respir Dis. 1993;148(3):650–5.

525. Nahata MC, Fan-Havard P, Barson WJ, Bartkowski HM, Kosnik EJ. Pharmacokinetics, cerebrospinal fluid concentration, and safety of intravenous rifampin in pediatric patients undergoing shunt placements. Eur J Clin Pharmacol. 1990 [cited 2017 Feb 20];38(5):515–7.

526. Nau R, Prange HW, Menck S, Kolenda H, Visser K, Seydel JK. Penetration of rifampicin into the cerebrospinal fluid of adults with uninflamed meninges. J Antimicrob Chemother. 1992 Jun [cited 2017 Feb 20];29(6):719–24.

527. Kaojarern S, Supmonchai K, Phuapradit P, Mokkhavesa C, Krittiyanunt S. Effect of steroids on cerebrospinal fluid penetration of antituberculous drugs in tuberculous meningitis. Clin Pharmacol Ther. 1991 Jan [cited 2016 Jun 2];49(1):6–12.

528. D'Oliveira JJG. Cerebrospinal Fluid Concentrations of Rifampin in Meningeal Tuberculosis [1, 2]. Am Rev Respir Dis. 1972 Sep 4 [cited 2019 Aug 20];106(3):432–7.

529. Donald PR, Gent WL, Seifart HI, Lamprecht JH, Parkin DP. Cerebrospinal fluid isoniazid concentrations in children with tuberculous meningitis: the influence of dosage and acetylation

status. Pediatrics. 1992 Feb 1;89(2):247-50.

530. Donald PR, Seifart H. Cerebrospinal fluid pyrazinamide concentrations in children with tuberculous meningitis. Pediatr Infect Dis J. 1988 Jul [cited 2019 Aug 20];7(7):469–71.

531. Reiber H. Proteins in cerebrospinal fluid and blood: Barriers, CSF flow rate and source-related dynamics. In: Restorative Neurology and Neuroscience. 2003 Jan 1;21(3-4):79-96.

532. Oreškovi D, Klarica M, Vuki M. The formation and circulation of cerebrospinal fluid inside the cat brain ventricles: a fact or an illusion? Neurosci Lett. 2002 Jul 19;327(2):103–6.

533. Klarica M, Oreškovic´, D, Oreškovic´, O, Božic´, B, Božic´, B, Vukic´, M, et al. NEW experimental model of acute aqueductal blockage in cats: effects on cerebrospinal fluid pressure and the size of brain ventricles. Nsc. 2009;158:1397–405.

534. Bulat M, Lupret V, Ore{kovi} D, Klarica M. Transventricular and Transpial Absorption of Cerebrospinal Fluid into Cerebral Microvessels. Coll Antropol. 2008;32:43–50.

535. Orešković D, Klarica M. The formation of cerebrospinal fluid: Nearly a hundred years of interpretations and misinterpretations. 2010 Sep 24;64(2):241-62.

536. Oreskovic D, Klarica M, Vukic M. Does the secretion and circulation of the cerebrospinal fluid really exist? Med Hypotheses. 2001 May 1;56(5):622–4.

537. Zmajevicá MZ, Klarica M, Varda R, Kudelicá K, Bulat M. Elimination of phenolsulfonphthalein from the cerebrospinal fluid via capillaries in central nervous system in cats by active transport. Neurosci Lett. 2002 [cited 2022 Nov 14];321:123–5.

538. Klarica M, Miš E B, Vladic´, A, Vladic´, V, Radoš M, Oreš Kovic´d AD, et al. "'Compensated hyperosmolarity'" of cerebrospinal fluid and the development of hydrocephalus. Neuroscience. 2013 Sep 17[cited 2022 Nov 14];248:278-89.

539. Casal JA, Corzo MD, Pérez LF, Alvarez JA, Aldegunde M, Tutor JC. Homeostatic role of the active transport in elimination of [3H]benzylpenicillin out of the cerebrospinal fluid system. Life Sci. 2000 Sep 29;67(19):2375–85.

540. Hutton D, Fadelalla MG, Kanodia AK, Hossain-Ibrahim K. Choroid plexus and CSF: an updated review. https://doi.org/101080/0268869720211903390. 2021 [cited 2022 Nov 8];36(3):307–15.

541. Thomale UW. Integrated understanding of hydrocephalus — a practical approach for a complex disease. Child's Nervous System. 2021 Nov [cited 2022 Nov 8];37(11):3313-24.

542. Oreškovicoreškovicá D, Klarica M. Development of hydrocephalus and classical hypothesis of cerebrospinal fluid hydrodynamics: Facts and illusions. Progress in neurobiology. 2011 Aug

1;94(3)238-58.

543. Bulat M, Klarica M. Recent insights into a new hydrodynamics of the cerebrospinal fluid. 2011 Jan 1;65(2):99-112.

544. Oreš Kovic D, Radoš M, Klarica M. Review role of choroid plexus in cerebrospinal fluid hydrodynamics.Neuroscience. 2017 Jun 23[cited 2022 Nov 8] ;354:69-87.

545. Davson, H., Segal MB. Physiology of the CSF and blood-brain-barriers. Diabetes Care. 1995.

546. Brinker T, Stopa E, Morrison J, Klinge P. A new look at cerebrospinal fluid circulation. Fluids Barriers CNS. 2014 May 1 [cited 2019 Aug 29];11(1):10.

547. Welch K, Segal M. Physiology and pathophysiology of the cerebrospinal fluid. 1987.

548. Shen DD, Artru AA, Adkison KK. Principles and applicability of CSF sampling for the assessment of CNS drug delivery and pharmacodynamics. Adv Drug Deliv Rev. 2004 [cited 2022 Oct 11];56:1825–57.

549. Herndon R, Brumback R. The cerebrospinal fluid. 2012 [cited 2019 Oct 22].

550. Orešković D, Klarica M. A new look at cerebrospinal fluid movement. 2014 Dec [cited 2022 Nov 16];11:1-3.

551. Klarica M, Radoš M, Erceg G, Petošić A, Jurjević I, Orešković D. The Influence of Body Position on Cerebrospinal Fluid Pressure Gradient and Movement in Cats with Normal and Impaired Craniospinal Communication. PLoS One. 2014 Apr 18 [cited 2022 Nov 16];9(4):e95229.

552. Alperin N, Lee SH, Sivaramakrishnan A, Hushek SG. Quantifying the effect of posture on intracranial physiology in humans by MRI flow studies. J Magn Reson Imaging. 2005 Nov 1 [cited 2022 Nov 16];22(5):591–6.

553. Martins AN, Wiley JK, Myers PW. Dynamics of the cerebrospinal fluid and the spinal dura mater. J Neurol Neurosurg Psychiatry. 1972 Aug 1 [cited 2022 Nov 16];35(4):468–73.

554. Hettiarachchi HDM, Hsu Y, Harris TJ, Linninger AA. The Effect of Pulsatile Flow on Intrathecal Drug Delivery in the Spinal Canal. Ann Biomed Eng. 2011 Oct 13 [cited 2019 Sep 11];39(10):2592–602.

555. Hsu Y, Hettiarachchi HDM, Zhu DC, Linninger AA. The Frequency and Magnitude of Cerebrospinal Fluid Pulsations Influence Intrathecal Drug Distribution. Anesth Analg. 2012 Aug [cited 2019 Sep 11];115(2):386–94.

556. Reiber H, Peter JB. Cerebrospinal fluid analysis: Disease-related data patterns and evaluation programs. Journal of the Neurological Sciences. 2001 Mar 1;184(2):101-22.

557. Saleh MAA, Loo CF, Elassaiss-Schaap J, De Lange ECM. Lumbar cerebrospinal fluid-to-brain extracellular fluid surrogacy is context-specific: insights from LeiCNS-PK3.0 simulations. J Pharmacokinet Pharmacodyn. 2021 Oct 1 [cited 2021 Dec 8];48(5):725–41.

558. Thompson E. The CSF proteins: a biochemical approach. 1988.

559. Reiber H. Cerebrospinal fluid - physiology, analysis and interpretation of protein patterns for diagnosis of neurological diseases. Mult Scler J . 1998 Jun 2 [cited 2019 Oct 24];4(3):99–107.

560. Reiber H. Dynamics of brain-derived proteins in cerebrospinal fluid. Clin Chim Acta. 2001 Aug 20;310(2):173–86.

561. Torres-Corzo JG, Tapia-Pérez JH, Sánchez-Aguilar M, Della Vecchia RR, Chalita Williams JC, Cerda-Gutiérrez R. Comparison of cerebrospinal fluid obtained by ventricular endoscopy and by lumbar puncture in patients with hydrocephalus secondary to neurocysticercosis. Surg Neurol. 2009 Mar 1;71(3):376–9.

562. Abbott NJ. Evidence for bulk flow of brain interstitial fluid: significance for physiology and pathology. Neurochem Int. 2004 [cited 2019 Jul 3];45:545–52.

563. Stein GE, Schooley S, Peloquin CA, Missavage A, Havlichek DH. Linezolid tissue penetration and serum activity against strains of methicillin-resistant Staphylococcus aureus with reduced vancomycin susceptibility in diabetic patients with foot infections. J Antimicrob Chemother. 2007 Jul 10 [cited 2019 Apr 29];60(4):819–23.

564. Ryan DM, Carst O. A problem in the interpretation of β-lactam antibiotic levels in tissues. J Antimicrob Chemother. 1983 Sep 1 [cited 2019 Apr 29];12(3):281–4.

565. Mouton JW, Theuretzbacher U, Craig WA, Tulkens PM, Derendorf H, Cars O. Tissue concentrations: do we ever learn? J Antimicrob Chemother. 2007 Dec 19 [cited 2019 Apr 29];61(2):235–7.

566. Davson H. Physiology of the cerebrospinal fluid. 1970 [cited 2019 Aug 15].

567. Liu X, Van Natta K, Yeo H, Vilenski O, Weller PE, Worboys PD, et al. Unbound drug concentration in brain homogenate and cerebral spinal fluid at steady state as a surrogate for unbound concentration in brain interstitial fluid. Drug Metab Dispos. 2009 Apr 1 [cited 2019 Aug 15];37(4):787–93.

568. Shapiro WR, Young DF, Mehta BM. Methotrexate: distribution in cerebrospinal fluid after

intravenous, ventricular and lumbar injections. N Engl J Med. 1975 Jul 24;293(4):161-6.

569. Tucker EW, Guglieri-Lopez B, Ordonez AA, Ritchie B, Klunk MH, Sharma R, et al. Noninvasive 11C-rifampin positron emission tomography reveals drug biodistribution in tuberculous meningitis. Sci Transl Med. 2018 Dec 5 [cited 2020 Oct 2];10(470):965.

570. Miksys SL, Tyndale RF. Drug-metabolizing cytochrome P450s in the brain. Journal of psychiatry and Neuroscience. 2002 Nov;27(6):406.

571. Strobel HW, Thompson CM, Antonovic L. Cytochromes P450 in brain: function and significance. Current drug metabolism. 2001 Jun 1 [cited 2019 Aug 14]; 2(2):199-214.

572. Arant BS. Developmental patterns of renal functional maturation compared in the human neonate. J Pediatr. 1978 May 1;92(5):705–12.

573. Koepsell H, Gorboulev V, Biology PA-J of M, 1999. Molecular pharmacology of organic cation transporters in kidney. 1999 Jan [cited 2019 Sep 19];167(2):103-17.

574. Alcorn J, McNamara PJ. Using ontogeny information to build predictive models for drug elimination. Drug Discovery Today. 2008 Jun 1;13(11-12):507-12.

575. Leiro V, Duque Santos S, Lopes CDF, Paula Pêgo A. Dendrimers as Powerful Building Blocks in Central Nervous System Disease: Headed for Successful Nanomedicine. Adv Funct Mater. 2018 Mar [cited 2020 Jan 23];28(12):1700313.

576. Chan RYC, Kwok AKH. Ocular toxicity of ethambutol. Hong Kong Medical Journal. 2006 Feb 1;12(1):56.

577. Pilheu JA, Maglio F, Cetrangolo R, Pleus AD. Concentrations of ethambutol in the cerebrospinal fluid after oral administration. Tubercle. 1971 Jun 1;52(2):117-22.

578. Shah SS, Ohlsson A, Shah VS. Intraventricular antibiotics for bacterial meningitis in neonates. Cochrane Database Syst Rev. 2012 Jul 11 [cited 2019 Aug 20];(7).

579. Stanimirovic DB, Bani-Yaghoub M, Perkins M, Haqqani AS. Blood–brain barrier models: *in vitro* to *in vivo* translation in preclinical development of CNS-targeting biotherapeutics. Expert Opin Drug Discov. 2015 Feb 1;10(2):141-55.

580. Wolff A, Antfolk M, Brodin B, Tenje M. In Vitro Blood-Brain Barrier Models - An Overview of Established Models and New Microfluidic Approaches. Journal of Pharmaceutical Sciences. 2015 Sep 1;104(9):2727-46.

581. Wilhelm I, Krizbai IA. In vitro models of the blood-brain barrier for the study of drug delivery to the brain. Molecular Pharmaceutics. 2014 Jul 7;11(7):1949-63.

582. Pardridge WM. Drug transport across the blood-brain barrier. Journal of Cerebral Blood Flow and Metabolism. 2012 Nov;32(11):1959-72.

583. Palmiotti CA, Prasad S, Naik P, Abul KMD, Sajja RK, Achyuta AH, et al. In vitro cerebrovascular modeling in the 21st century: Current and prospective technologies. Pharmaceutical Research. 2014 Dec;31:3229-50.

584. Liang Y, Li S, Chen L. The physiological role of drug transporters. Protein and Cell. 2015 May;6(5):334-50.

585. Bauer B, Hartz AMS, Fricker G, Miller DS. Modulation of p-Glycoprotein Transport Function at the Blood-Brain Barrier. Exp Biol Med. 2005 Feb [cited 2019 Feb 1];230(2):118–27.

586. Abbott NJ. Blood–brain barrier structure and function and the challenges for CNS drug delivery. J Inherit Metab Dis. 2013 May 23 [cited 2019 Feb 1];36(3):437–49.

587. Kantorovich S, Astary GW, King MA, Mareci TH, Sarntinoranont M, Carney PR. Influence of neuropathology on convection-enhanced delivery in the rat hippocampus. PLoS One. 2013 Nov 8;8(11):e80606

588. Mignani S, Tripathi R, Chen L, Caminade A-M, Shi X, Majoral J-P. New Ways to Treat Tuberculosis Using Dendrimers as Nanocarriers. Pharmaceutics. 2018 Jul 26 [cited 2019 Sep 25];10(3):105.

589. Griffiths G, Nyström B, Sable SB, Khuller GK. Nanobead-based interventions for the treatment and prevention of tuberculosis. Nature Reviews Microbiology. 2010 Nov [cited 2019 Oct 7];827-34.

590. Khuller G, Kapur M, Sharma S. Liposome Technology for Drug Delivery Against Mycobacterial Infections. Curr Pharm Des. 2004 Oct 1 [cited 2019 Oct 7];10(26):3263–74.

591. Pandey R, Khuller GK. Solid lipid particle-based inhalable sustained drug delivery system against experimental tuberculosis. Tuberculosis. 2005 Jul 1[cited 2019 Oct 7];85(4)227-34.

592. Sharma A, Sharma S, Khuller GK. Lectin-functionalized poly (lactide-co-glycolide) nanoparticles as oral/aerosolized antitubercular drug carriers for treatment of tuberculosis. J Antimicrob Chemother. 2004 Oct 1 [cited 2019 Oct 7];54(4):761–6.

593. Pandey R, Sharma A, Zahoor A, Sharma S, Khuller GK, Prasad B. Poly (DL-lactide-co-glycolide) nanoparticle-based inhalable sustained drug delivery system for experimental tuberculosis. J Antimicrob Chemother. 2003 Nov 12 [cited 2019 Oct 7];52(6):981–6.

594. Nabi B, Rehman S, Khan S, Baboota S, Ali J. Ligand conjugation: An emerging platform for

enhanced brain drug delivery. Brain Research Bulletin. 2018 Sep 1;142:384-93.

595. Marais BJ, Obihara CC, Warren RM, Schaaf HS, Gie RP, Donald PR. The burden of childhood tuberculosis: A public health perspective. International Journal of Tuberculosis and Lung Disease. 2005 Dec 1;9(12):1305-13.

596. Marais BJ, Hesseling AC, Gie RP, Schaaf HS, Beyers N. The burden of childhood tuberculosis and the accuracy of community-based surveillance data. Int J Tuberc Lung Dis. 2006 Mar 1;10(3):259-63.

597. Walls T, Shingadia D. Global epidemiology of paediatric tuberculosis. J Infect. 2004 Jan 1 [cited 2019 Mar 27];48(1):13–22.

598. Rapid Advice: Treatment of Tuberculosis in Children. 2010 [cited 2023 Nov 14].

599. Woodfield J, Argent A. Evidence Behind the WHO Guidelines: Hospital Care for Children: What is the Most Appropriate Anti-microbial Treatment for Tuberculous Meningitis? J Trop Pediatr. 2008 Mar 13 [cited 2019 Nov 21];54(4):220–4.

600. van Toorn R, Schaaf HS, Laubscher JA, van Elsland SL, Donald PR, Schoeman JF. Short Intensified Treatment in Children with Drug-susceptible Tuberculous Meningitis. Pediatr Infect Dis J. 2014 Mar [cited 2019 Nov 21];33(3):248–52.

601. Donald PR. Cerebrospinal fluid concentrations of antituberculosis agents in adults and children. Tuberculosis. 2010;90(5):279–92.

602. WHO consolidated guidelines on tuberculosis Module 5: Management of tuberculosis in children and adolescents. World Health Organization. 2022 [cited 2022 Apr 20].

603. Dartois V. The path of anti-tuberculosis drugs: From blood to lesions to mycobacterial cells. Nat Rev Microbiol. 2014 Mar 3;12(3):159–67.

604. Dartois V, Barry CE. A medicinal chemists' guide to the unique difficulties of lead optimization for tuberculosis. Bioorganic and Medicinal Chemistry Letters. 2013 Sep 1;23(17):4741-50.

605. Lenaerts A, Barry CE, Dartois V. Heterogeneity in tuberculosis pathology, microenvironments and therapeutic responses. Immunol Rev. 2015 Mar 1 [cited 2020 Feb 21];264(1):288–307.

606. Sarathy JP, Zuccotto F, Hsinpin H, Sandberg L, Via LE, Marriner GA, et al. Prediction of Drug Penetration in Tuberculosis Lesions. ACS Infect Dis. 2016 Aug 12;2(8):552–63.

607. Fange D, Nilsson K, Tenson T, Ehrenberg M. Drug efflux pump deficiency and drug target resistance masking in growing bacteria. Proc Natl Acad Sci U S A. 2009 May 19;106(20):8215–20.

608. Bekker A, Schaaf HS, Draper HR, Van Ser Laan L, Murray S, Wiesner L, et al. Pharmacokinetics of rifampin, isoniazid, pyrazinamide, and ethambutol in infants dosed according to revised whorecommended treatment guidelines. Antimicrob Agents Chemother. 2016 Apr;60(4):2171-9..

609. Abulfathi AA, Decloedt EH, Svensson EM, Diacon AH, Donald P, Reuter H. Clinical Pharmacokinetics and Pharmacodynamics of Rifampicin in Human Tuberculosis. Clin Pharmacokinet. 2019 May 3 [cited 2019 May 24];1–27.

610. Svensson EM, Svensson RJ, te Brake LHM, Boeree MJ, Heinrich N, Konsten S, et al. The Potential for Treatment Shortening With Higher Rifampicin Doses: Relating Drug Exposure to Treatment Response in Patients With Pulmonary Tuberculosis. Clin Infect Dis. 2018 Jun 18 [cited 2019 Oct 3];67(1):34–41.

611. Thee S, Seddon JA, Donald PR, Seifart HI, Werely CJ, Hesseling AC, et al. Pharmacokinetics of isoniazid, rifampin,and pyrazinamide in children younger than two years of age with tuberculosis: Evidence for implementation of revised World Health Organization recommendations. Antimicrob Agents Chemother. 2011 Dec 1;55(12):5560–7.

612. Pooran A, Pieterson E, Davids M, Theron G, Dheda K. What is the Cost of Diagnosis and Management of Drug Resistant Tuberculosis in South Africa? PLoS One. 2013 Jan 18;8(1):e54587.

613. Simon Schaaf H, Paed Mm, Moll AP, Dheda K. Multidrug- and Extensively Drug-resistant Tuberculosis in Africa and South America: Epidemiology, Diagnosis and Management in Adults and Children. Clinics in chest medicine. 2009 Dec 1[cited 2019 Feb 9];30(4):667-83.

614. Schaaf HS, Marais BJ, Hesseling AC, Brittle W, Donald PR. Surveillance of antituberculosis drug resistance among children from the Western Cape Province of South Africa - An upward trend. Am J Public Health. 2009 Dec 1;30(4):667-83.

615. Mukinda FK, Theron D, Van Der Spuy GD, Jacobson KR, Roscher M, Streicher EM, et al. Rise in rifampicin-monoresistant tuberculosis in Western Cape, South Africa. Int J Tuberc Lung Dis. 2012 Feb 1;16(2):196-202.

616. Dramowski A, Morsheimer MM, Jordaan AM, Victor TC, Donald PR, Schaaf HS. Rifampicin-monoresistant Mycobacterium tuberculosis disease among children in Cape Town, South Africa. Int J Tuberc Lung Dis. 2012 Jan 1;16(1):76-81.

617. Zignol M, Sismanidis C, Falzon D, Glaziou P, Dara M, Floyd K. Multidrug-resistant tuberculosis in children: evidence from global surveillance. Eur Respir J. 2013 Sep 6 [cited 2019

Feb 9];42(3):701–7.

618. Schaaf HS, Willemse M, Donald PR. Long-term linezolid treatment in a young child with extensively drug-resistant tuberculosis. Pediatr Infect Dis J. 2009 Aug [cited 2019 Nov 11];28(8):748–50.

619. Heemskerk AD, Nguyen MTH, Dang HTM, Vinh Nguyen C Van, Nguyen LH, Do TDA, et al. Clinical Outcomes of Patients With Drug-Resistant Tuberculous Meningitis Treated With an Intensified Antituberculosis Regimen. Clin Infect Dis. 2017 [cited 2020 Mar 16];65(1):20–8.

620. Vinnard C, King L, Munsiff S, Crossa A, Iwata K, Pasipanodya J, et al. Clinical Infectious Diseases Long-term Mortality of Patients With TBM in New York City Long-term Mortality of Patients With Tuberculous Meningitis in New York City: A Cohort Study. Clin Infect Dis ®. 2017 [cited 2020 May 19];401(4):401–8.

621. SS M, J J, M P, MK A, GI K. Drug Resistance in Children with Central Nervous System Tuberculosis from a Tertiary Care Center in Mumbai. J Trop Pediatr. 2021 Dec 8 [cited 2022 Jan 10];67(6).

622. Taneja R, Garcia-Prats AJ, Furin J, Maheshwari HK. Paediatric formulations of second-line anti-tuberculosis medications: challenges and considerations. Int J Tuberc Lung Dis. 2015 Dec 1 [cited 2019 Feb 8];19(12):61–8.

623. Seddon JA, Hesseling AC, Marais BJ, McIlleron H, Peloquin CA, Donald PR, et al. Paediatric use of second-line anti-tuberculosis agents: A review. Tuberculosis. 2012 Jan 1 [cited 2019 Feb 8];92(1):9–17.

624. World Health Organization, UNICEF. Sources and prices of selected medicines for children including therapeutic food , dietary vitamin and mineral supplementation. 2009;(January).

625. Schaaf HS, Willemse M, Cilliers K, Labadarios D, Maritz JS, Hussey GD, et al. Rifampin pharmacokinetics in children, with and without human immunodeficiency virus infection, hospitalized for the management of severe forms of tuberculosis. BMC Med. 2009 Dec 22 [cited 2019 Feb 19];7(1):19.

626. Schaaf HS, Parkin DP, Seifart HI, Werely CJ, Hesseling PB, Van Helden PD, et al. Isoniazid pharmacokinetics in children treated for respiratory tuberculosis. Archives of disease in childhood. 2005 Jun 1 [cited 2019 Feb 19];90(6):614-8.

627. McIlleron H, Willemse M, Werely CJ, Hussey GD, Schaaf HS, Smith PJ, et al. Isoniazid Plasma Concentrations in a Cohort of South African Children with Tuberculosis: Implications for International Pediatric Dosing Guidelines. Clin Infect Dis. 2009 Jun 1 [cited 2019 Feb

19];48(11):1547–53.

628. Graham SM, Bell DJ, Nyirongo S, Hartkoorn R, Ward SA, Molyneux EM. Low levels of pyrazinamide and ethambutol in children with tuberculosis and impact of age, nutritional status, and human immunodeficiency virus infection. Antimicrob Agents Chemother. 2006 Feb;50(2):407-13.

629. Peloquin CA, Nitta AT, Burman WJ, Brudney KF, Miranda-Massari JR, McGuinness ME, et al. Low Antituberculosis Drug Concentrations in Patients with AIDS. Ann Pharmacother. 1996 Sep 28 [cited 2019 Feb 19];30(9):919–25.

630. Roy V, Gupta D, Gupta P, Sethi GR, Mishra TK. Pharmacokinetics of isoniazid in moderately malnourished children with tuberculosis. Int J Tuberc Lung Dis. 2010 Mar 1;14(3):374.

631. Donald PR, Parkin DP, Seifart HI, Schaaf HS, Van Helden PD, Werely CJ, et al. The influence of dose and N-acetyltransferase-2 (NAT2) genotype and phenotype on the pharmacokinetics and pharmacodynamics of isoniazid. Eur J Clin Pharmacol. 2007 Jul;63(7):633-9.

632. Allen BW, Mitchison DA, Chan YC, Yew WW, Allan WGL, Girling DJ. Amikacin in the treatment of pulmonary tuberculosis. Tubercle. 1983 Jun 1 [cited 2019 Feb 19];64(2):111–8.

633. Caminero JA, Sotgiu G, Zumla A, Migliori GB. Best drug treatment for multidrug-resistant and extensively drug-resistant tuberculosis. Lancet Infect Dis. 2010 Sep 1 [cited 2019 Feb 19];10(9):621–9.

634. Maus CE, Plikaytis BB, Shinnick TM. Molecular analysis of cross-resistance to capreomycin, kanamycin, amikacin, and viomycin in Mycobacterium tuberculosis. Antimicrob Agents Chemother. 2005 Aug 1 [cited 2019 Feb 19];49(8):3192–7.

635. Johnson JL, Hadad DJ, Boom WH, Daley CL, Peloquin CA, Eisenach K D, et al. Early and extended early bactericidal activity of levofloxacin, gatifloxacin and moxifloxacin in pulmonary tuberculosis. INT J TUBERC LUNG DIS. 2006 Jun 1 [cited 2019 Feb 19];10(6):605-12.

636. Donald PR. The chemotherapy of tuberculous meningitis in children and adults. Tuberculosis. 2010 Nov 1;90(6):375-92.

637. Alffenaar JWC, van Altena R, Bökkerink HJ, Luijckx GJ, van Soolingen D, Aarnoutse RE, et al. Pharmacokinetics of Moxifloxacin in Cerebrospinal Fluid and Plasma in Patients with Tuberculous Meningitis. Clin Infect Dis. 2009 Oct 1 [cited 2020 May 18];49(7):1080–2.

638. Ruslami R, Ganiem AR, Dian S, Apriani L, Achmad TH, van der Ven AJ, et al. Intensified regimen containing rifampicin and moxifloxacin for tuberculous meningitis: an open-label, randomised controlled phase 2 trial. Lancet Infect Dis. 2013 Jan 1 [cited 2019 Oct 3];13(1):27–

35.

639. Heemskerk AD, Bang ND, Mai NTH, Chau TTH, Phu NH, Loc PP, et al. Intensified Antituberculosis Therapy in Adults with Tuberculous Meningitis. N Engl J Med. 2016 Jan 14 [cited 2019 Oct 3];374(2):124–34.

640. Rizvi I, Malhotra HS, Garg RK, Kumar N, Uniyal R, Pandey S. Fluoroquinolones in the management of tuberculous meningitis: Systematic review and meta-analysis. Journal of Infection. 2018 Oct 1:77(4):261-75.

641. Ruslami R, Ganiem AR, Aarnoutse RE, Van Crevel R. Rifampicin and moxifloxacin for tuberculous meningitis. The Lancet Infectious Diseases. 2013 Jul 1;13(7):570.

642. Banerjee A, Dubnau E, Quemard A, Balasubramanian V, Um KS, Wilson T, et al. inhA, a gene encoding a target for isoniazid and ethionamide in Mycobacterium tuberculosis. Science. 1994 Jan 14;263(5144):227-30.

643. Schaaf HS, Victor TC, Venter A, Brittle W, Jordaan AM, Hesseling AC, et al. Ethionamide cross-and co-resistance in children with isoniazid-resistant tuberculosis. Int J Tuberc Lung Dis. 2009 Nov 1;13(11):1355-9.

644. Dover LG, Corsino PE, Daniels IR, Cocklin SL, Tatituri V, Besra GS, et al. Crystal structure of the TetR/CamR family repressor Mycobacterium tuberculosis EthR implicated in ethionamide resistance. J Mol Biol. 2004 Jul 23;340(5):1095–105.

645. Thee S, Seifart HI, Rosenkranz B, Hesseling AC, Magdorf K, Donald PR, et al. Pharmacokinetics of ethionamide in children. Antimicrob Agents Chemother. 2011 Oct;55(10):4594–600.

646. Hill J, Marais B. Arch Dis Child. Drug Ther Editor. 2022 [cited 2021 Dec 18];107(1).

647. Huynh J, Thwaites G, Marais BJ, Simon Schaaf H. Tuberculosis treatment in children: the changing landscape. Paediatr Respir Rev. 2020 Feb 26 [cited 2020 Mar 2];36:33-43.

648. Rastogi N, Labrousse V, Goh KS. In vitro activities of fourteen antimicrobial agents against drug susceptible and resistant clinical isolates of Mycobacterium tuberculosis and comparative intracellular activities against the virulent H37Rv strain in human macrophages. Curr Microbiol. 1996;33(3):167–75.

649. Vora A. Terizidone. Vol. 58, Journal of Association of Physicians of India. 2010 Apr;58:267-8.

650. Zhu M, Nix DE, Adam RD, Childs JM, Peloquin CA. Pharmacokinetics of Cycloserine under Fasting Conditions and with High-Fat Meal, Orange Juice, and Antacids. Pharmacotherapy.

2001 Aug [cited 2019 Nov 11];21(8):891–7.

651. Global Alliance for TB Drug Development. Handbook of Anti-Tuberculosis Agents. Tuberculosis. 2008;88-85-170.

652. Söderhjelm L. Serum Para-Aminosalicylic Acid (PAS) following Oral Ingestion in Children. Tex Rep Biol Med. 1949 [cited 2019 Feb 27];7(3):471–9.

653. Van Deun A, Maug AKJ, Salim MAH, Das PK, Sarker MR, Daru P, et al. Short, highly effective, and inexpensive standardized treatment of multidrug-resistant tuberculosis. Am J Respir Crit Care Med. 2010 Sep 1;182(5):684-92

654. Nix DE, Adam RD, Auclair B, Krueger TS, Godo PG, Peloquin CA. Pharmacokinetics and relative bioavailability of clofazimine in relation to food, orange juice and antacid. Tuberculosis. 2004;84(6):365–73.

655. Holdiness MR. Clinical Pharmacokinetics of Clofazimine: A Review. Clinical Pharmacokinetics. 1989 Feb;16(2):74-85.

656. Baijnath S, Naiker S, Shobo A, Moodley C, Adamson J, Ngcobo B, et al. Evidence for the presence of clofazimine and its distribution in the healthy mouse brain. J Mol Histol. 2015 Oct 19;46(4–5):439–42.

657. Ellard GA, Dickinson JM, Gammon PT, Mitchison DA. Serum concentrations and antituberculosis activity of thiacetazone. Tubercle. 1974;55(1):41–54.

658. Hugonnet JE, Tremblay LW, Boshoff HI, Barry CE, Blanchard JS. Meropenem-clavulanate is effective against extensively drug-resistant Mycobacterium tuberculosis. Science (80-). 2009 Feb 27;323(5918):1215–8.

659. Kearns G, Abdel-Rahman SM, Blumer JL, Reed MD, James LP, Jacobs RF, Welshman IR, Jungbluth GL, Stalker DJ. Single dose pharmacokinetics of linezolid in infants and children. Pediatric infectious disease journal. 2000 Dec 1;19(12):1178-84.

660. Jungbluth GL, Welshman IR, Hopkins NK. Linezolid pharmacokinetics in pediatric patients: an overview. Pediatr Infect Dis J. 2003 Sep [cited 2019 Feb 28];22(9):S153–7.

661. Chiappini E, Conti C, Galli L, de Martino M. Clinical efficacy and tolerability of linezolid in pediatric patients: a systematic review. Clinical therapeutics. 2010 Jan 1;32(1):66-88..

662. Vo M, Rubino CM, Cirincione BB, Bruss J, Jungbluth GL. Pharmacokinetic-pharmacodynamic analysis of data from a phase III trial of linezolid IV/PO for the treatment of resistant gram-positive bacterial infections in children. Clin Pharmacol Ther. 2003 Feb;73(2):74–74.

663. Rubino CM, McPhee M, Vo M, Jungbluth GL. Application of real-time data assembly (RTDA) to a pivotal phase III pediatric trial: A proactive approach to population pharmacokinetic/pharmacodynamic (PK/PD) dataset creation. Clin Pharmacol Ther. 2003 Feb;73(2):P65–P65.

664. Sun F, Ruan Q, Wang J, Chen S, Jin J, Shao L, et al. Linezolid manifests a rapid and dramatic therapeutic effect for patients with life-threatening tuberculous meningitis. Antimicrob Agents Chemother. 2014 Oct 1;58(10):6297–301.

665. Hachem R, Afif C, Gokaslan Z, Raad I. Successful Treatment of Vancomycin-Resistant Enterococcus Meningitis with Linezolid. Eur J Clin Microbiol Infect Dis. 2001 Jun [cited 2019 Nov 14];20(6):432–4.

666. Fortún J, Martín-Dávila P, Navas E, Pérez-Elías MJ, Cobo J, Tato M, et al. Linezolid for the treatment of multidrug-resistant tuberculosis. J Antimicrob Chemother. 2005 Jul 1 [cited 2019 Nov 14];56(1):180–5.

667. Park I-N. Efficacy and tolerability of daily-half dose linezolid in patients with intractable multidrug-resistant tuberculosis. J Antimicrob Chemother. 2006 Jul 1 [cited 2019 Nov 14];58(3):701–4.

668. Condos R, Hadgiangelis N, Leibert E, Jacquette G, Harkin T, Rom WN. Case series report of a linezolid-containing regimen for extensively drug-resistant tuberculosis. Chest. 2008;134(1):187–92.

669. Agyeman AA, Ofori-Asenso R. Efficacy and safety profile of linezolid in the treatment of multidrug-resistant (MDR) and extensively drug-resistant (XDR) tuberculosis: a systematic review and meta-analysis. Ann Clin Microbiol Antimicrob. 2016 Dec 22 [cited 2020 May 19];15(1):41.

670. Zhang X, Falagas ME, Vardakas KZ, Wang R, Qin R, Wang J, et al. Systematic review and meta-analysis of the efficacy and safety of therapy with linezolid containing regimens in the treatment of multidrug-resistant and extensively drug-resistant tuberculosis. J Thorac Dis. 2015;7(4):603–15.

671. Alffenaar JWC, Van Altena R, Harmelink IM, Filguera P, Molenaar E, Wessels AMA, et al. Comparison of the pharmacokinetics of two dosage regimens of linezolid in multidrug-resistant and extensively drug-resistant tuberculosis patients. Clin Pharmacokinet. 2010 Sep 30;49(8):559–65.

672. Tucker EW, Pieterse L, Zimmerman MD, Udwadia ZF, Peloquin CA, Gler MT, et al. Delamanid

Central Nervous System Pharmacokinetics in Tuberculous Meningitis in Rabbits and Humans. Antimicrob Agents Chemother. 2019 Aug 5 [cited 2019 Aug 13];AAC.00913-19.

673. Esposito S, D'Ambrosio L, Tadolini M, Schaaf HS, Caminero Luna J, Marais B, et al. ERS/WHO Tuberculosis Consilium assistance with extensively drug-resistant tuberculosis management in a child: case study of compassionate delamanid use. Eur Respir J. 2014 Sep 15 [cited 2019 Feb 12];44(3):811–5.

674. Donald PR. Chemotherapy for Tuberculous Meningitis. N Engl J Med. 2016 Jan 14 [cited 2019 Feb 8];374(2):179–81.

675. Onno W. Akkerman, Omar F.F. Odish, Mathieu S. Bolhuis, Wiel C.M. de Lange, Hubertus P.H. Kremer, Gert-Jan R. Luijckx, Tjip S. van der werf, Jan-Willem Allfenaar. Pharmacokinetics of Bedaquiline in Cerebrospinal Fluid and Serum in Multidrug-Resistant Tuberculous Meningitis. 2015 Feb 15 [cited 2020 May 19]; 523-524

676. Keam SJ. Pretomanid: First Approval. Drugs. 2019 [cited 2023 Feb 27];79:1797–803.

677. Thwaites G, Nahid P. Triumph and Tragedy of 21st Century Tuberculosis Drug Development. N Engl J Med. 2020 Mar 5 [cited 2020 Mar 5];382(10):959–60.

678. Kempker RR, Smith AGC, Avaliani T, Gujabidze M, Bakuradze T, Sabanadze S, et al. Cycloserine and Linezolid for Tuberculosis Meningitis: Pharmacokinetic Evidence of Potential Usefulness. Clin Infect Dis. 2022 Sep 10 [cited 2023 Apr 5];75(4):682–9.

679. Sasahara K, Shimokawa Y, Hirao Y, Koyama N, Kitano K, Shibata M, et al. Pharmacokinetics and Metabolism of Delamanid, a Novel Anti-Tuberculosis Drug, in Animals and Humans: Importance of Albumin Metabolism In Vivo. Drug Metab Dispos. 2015 Aug 1 [cited 2023 Apr 5];43(8):1267–76.

680. Swanson R V., Adamson J, Moodley C, Ngcobo B, Ammerman NC, Dorasamy A, et al. Pharmacokinetics and pharmacodynamics of clofazimine in a mouse model of tuberculosis. Antimicrob Agents Chemother. 2015 Jun 1 [cited 2023 Apr 5];59(6):3042–51.

681. van Heeswijk RPG, Dannemann B, Hoetelmans RMW. Bedaquiline: a review of human pharmacokinetics and drug–drug interactions. J Antimicrob Chemother. 2014 Sep 1 [cited 2023 Apr 5];69(9):2310–8.

682. Upton CM, Wiesner L, Dooley KE, Maartens G. Cerebrospinal Fluid and Tuberculous Meningitis. Clin Infect Dis. 2023 Jul 5 [cited 2023 Oct 23];77(1):158–158.

683. Coyne KM, Pozniak AL, Lamorde M, Boffito M. Pharmacology of second-line antituberculosis drugs and potential for interactions with antiretroviral agents. AIDS. 2009 Feb [cited 2019 Nov

14];23(4):437–46.

684. Scano F, Vitoria M, Burman W, Harries AD, Gilks CF, Havlir D. Management of HIV-infected patients with MDR- and XDR-TB in resource-limited settings. The international journal of tuberculosis and lung disease. 2008 Dec 1;12(12):1370-5.

685. McIlleron H, Khoo SH. Interactions between antituberculosis and antiretroviral agents. Antituberculosis and antiretroviral agents. 2011 [cited 2019 Nov 14];191-202.

686. Van Der Watt JJ, Harrison TB, Benatar M, Heckmann JM. Polyneuropathy, anti-tuberculosis treatment and the role of pyridoxine in the HIV/AIDS era: A systematic review.The International Journal of Tuberculosis and Lung Disease. 2011 Jun 1;15(6):722-8.

687. Hampel B, Hullmann R, Schmidt H. Ciprofloxacin in pediatrics: worldwide clinical experience based on compassionate use-safety report. The Pediatric infectious disease journal. 1997 Jan 1; 16(1):127-9.

688. Berning SE, Madsen L, Iseman MD, Peloquin CA. Long-term safety of ofloxacin and ciprofloxacin in the treatment of mycobacterial infections. Am J Respir Crit Care Med. 1995;151(6):2006–9.

689. Kubin R. Safety and efficacy of ciprofloxacin in paediatric patients. Infection. 1993 Nov;21(6):413-21.

690. Schaad UB. Fluoroquinolone antibiotics in infants and children. Infectious Disease Clinics. 2005 Sep 1;19(3):617-28. p. 617–28.

691. Leibovitz E. The use of fluoroquinolones in children. Current opinion in pediatrics. 2006 Feb 1;18(1):64-70.

703. van Ingen J, Aarnoutse RE, Donald PR, Diacon AH, Dawson R, Plemper van Balen G, et al. Why Do We Use 600 mg of Rifampicin in Tuberculosis Treatment? Clin Infect Dis. 2011 May [cited 2020 Mar 16];52(9):e194-9.

704. Newman R, Doster B, Murray FJ, Ferebee S. Rifampin in initial treatment of pulmonary tuberculosis. A U.S. Public Health Service tuberculosis therapy trial. Am Rev Respir Dis. 1971 Apr;103(4):461–76.

705. Corpe RF, Sanchez ES. Rifampin in initial treatment of advanced pulmonary tuberculosis. Chest. 1972 Jun [cited 2020 Mar 16];61(6):564–7.

706. Davidson PT, Goble M, Lester W. The antituberculosis efficacy of rifampin in 136 patients. Chest. 1972 Jun [cited 2020 Mar 16];61(6):574–8.

707. Poole G, Stradling P, Worlledge S. Potentially Serious Side Effects of High-Dose Twice-Weekly Rifampicin. Br Med J. 1971 Aug 7;3(5770):343–7.

708. Van Ingen J, Aarnoutse RE, Donald PR, Diacon AH, Dawson R, Plemper van Balen G, Gillespie SH, Boeree MJ. Why do we use 600 mg of rifampicin in tuberculosis treatment? Clinical Infectious Diseases. 2011 May 1 [cited 2020 Mar 5];52(9):e194-9.

709. Steingart KR, Jotblad S, Robsky K, Deck D, Hopewell PC, Huang D, et al. Higher-dose rifampin for the treatment of pulmonary tuberculosis: a systematic review. The International journal of tuberculosis and lung disease. 2011 Mar 1;15(3):305-16.

710. Burman, W.J.Gallicano, K.Peloquin C. Comparative pharmacokinetics and pharmacodynamics of the rifamycin antibacterials. Clin Pharmacokinetics. 2001 May;40:327-41.

711. Diacon AH, Patientia RF, Venter A, van Helden PD, Smith PJ, McIlleron H, et al. Early bactericidal activity of high-dose rifampin in patients with pulmonary tuberculosis evidenced by positive sputum smears. Antimicrob Agents Chemother. 2007 Aug 1 [cited 2019 Oct 3];51(8):2994–6.

712. Mezochow A, Thakur KT, Zentner I, Subbian S, Kagan L, Vinnard C. Attainment of target rifampicin concentrations in cerebrospinal fluid during treatment of tuberculous meningitis. Int J Infect Dis. 2019 Jul [cited 2019 Aug 15];84:15–21.

713. Te Brake L, Dian S, Ganiem AR, Ruesen C, Burger D, Donders R, et al. Pharmacokinetic/pharmacodynamic analysis of an intensified regimen containing rifampicin and moxifloxacin for tuberculous meningitis. Int J Antimicrob Agents. 2015 May 1;45(5):496–503.

714. Boeree MJ, Diacon AH, Dawson R, Narunsky K, du Bois J, Venter A, et al. A Dose-Ranging Trial to Optimize the Dose of Rifampin in the Treatment of Tuberculosis. Am J Respir Crit Care Med. 2015 May 1 [cited 2019 Oct 3];191(9):1058–65.

715. Hu Y, Liu A, Ortega-Muro F, Alameda-Martin L, Mitchison D, Coates A. High-dose rifampicin kills persisters, shortens treatment duration, and reduces relapse rate in vitro and in vivo. Front Microbiol. 2015 Jun 23 [cited 2019 Oct 3];6:641.

716. Svensson RJ, Svensson EM, Aarnoutse RE, Diacon AH, Dawson R, Gillespie SH, et al. Greater Early Bactericidal Activity at Higher Rifampicin Doses Revealed by Modeling and Clinical Trial Simulations. J Infect Dis. 2018 Aug 14 [cited 2019 Oct 3];218(6):991–9.

717. Cresswell F V, Meya DB, Kagimu E, Grint D, te Brake L, Kasibante J, et al. High-dose oral and intravenous rifampicin for the treatment of tuberculous meningitis in predominantly HIV-

positive Ugandan adults: a phase II open-label randomised controlled trial. Clin Infect Dis. 2021 Sep 1 [cited 2021 Apr 6];73(5):876-84.

718. Heemskerk D, Day J, Chau TT, Dung NH, Yen NT, Bang ND, et al. Intensified treatment with high dose rifampicin and levofloxacin compared to standard treatment for adult patients with tuberculous meningitis (TBM-IT): protocol for a randomized controlled trial. Trials. 2011;12:25.

719. Kenny MT, Strates B. Metabolism and Pharmacokinetics of the Antibiotic Rifampin. Drug Metab Rev. 1981 Jan 22 [cited 2019 Jun 12];12(1):159–218.

720. Remmer H, Schoene B, Fleischmann RA. Induction of the unspecific microsomal hydroxylase in the human liver. Drug Metab Dispos. 1973;1(1).

721. Breimer DD, Zilly W, Richter E. Influence of rifampicin on drug metabolism: Differences between hexobarbital and antipyrine. Clin Pharmacol Ther. 1977 Apr [cited 2019 Nov 11];21(4):470–81.

722. Loos U, Musch E, Jensen JC, Mikus G, Schwabe HK, Eichelbaum M. Pharmacokinetics of oral and intravenous rifampicin during chronic administration. Klin Wochenschr. 1985;63(23):1205–11.

723. Svensson RJ, Aarnoutse RE, Diacon AH, Dawson R, Gillespie SH, Boeree MJ, et al. A Population Pharmacokinetic Model Incorporating Saturable Pharmacokinetics and Autoinduction for High Rifampicin Doses. Clin Pharmacol Ther. 2018 Apr 7 [cited 2019 Oct 3];103(4):674–83.

724. Sirgel FA, Fourie PB, Donald PR, Padayatchi N, Rustomjee R, Levin J, et al. The Early Bactericidal Activities of Rifampin and Rifapentine in Pulmonary Tuberculosis. Am J Respir Crit Care Med. 2005 Jul [cited 2019 Nov 15];172(1):128–35.

725. Smythe W, Khandelwal A, Merle C, Rustomjee R, Gninafon M, Lo MB, et al. A semimechanistic pharmacokinetic-enzyme turnover model for rifampin autoinduction in adult tuberculosis patients. Antimicrob Agents Chemother. 2012 Apr;56(4):2091–8.

726. Clewe O, Goutelle S, Conte JE, Simonsson USH. A pharmacometric pulmonary model predicting the extent and rate of distribution from plasma to epithelial lining fluid and alveolar cells - Using rifampicin as an example. Eur J Clin Pharmacol. 2015;71(3):313–9.

727. Telenti A, Imboden P, Marchesi F, Matter L, Schopfer K, Bodmer T, et al. Detection of rifampicin-resistance mutations in Mycobacterium tuberculosis. Lancet. 1993 Mar 13;341(8846):647-51.

728. Fange D, Nilsson K, Tenson T, Ehrenberg M. Drug efflux pump deficiency and drug target

resistance masking in growing bacteria. Proc Natl Acad Sci. 2009 May 19;106(20):8215-20.

729. Bhat J, Narayan A, Venkatraman J, Chatterji M. LC-MS based assay to measure intracellular compound levels in Mycobacterium smegmatis: Linking compound levels to cellular potency. J Microbiol Methods. 2013 Aug 1;94(2):152-8.

730. Koch A, Mizrahi V, Warner DF. The impact of drug resistance on Mycobacterium tuberculosis physiology: What can we learn from rifampicin? Emerging Microbes and Infections. 2014 Jan 1;3(1):1-1.

731. Zhang Y, Telenti A. Molecular genetics of mycobacteria. Eds Hatfull G, William R. Jacobs Jr. AMS Press DC. 2000.

732. Ramaswamy S, Musser JM. Molecular genetic basis of antimicrobial agent resistance in Mycobacterium tuberculosis: 1998 update. Tubercle and Lung Disease. 1998 Jan 1;79(1):3-29.

733. Siu GKH, Zhang Y, Lau TCK, Lau RWT, Ho PL, Yew WW, et al. Mutations outside the rifampicin resistance-determining region associated with rifampicin resistance in Mycobacterium tuberculosis. J Antimicrob Chemother. 2011 Apr 1;66(4):730-3.

734. Heep M, Brandstätter B, Rieger U, Lehn N, Richter E, Rüsch-Gerdes S, et al. Frequency of rpoB mutations inside and outside the cluster I region in rifampin-resistant clinical Mycobacterium tuberculosis isolates. J Clin Microbiol. 2001 Jan 1;39(1):107-10.

735. Heep M, Odenbreit S, Beck D, Decker J, Prohaska E, Rieger U, et al. Mutations at four distinct regions of the rpoB gene can reduce the susceptibility of Helicobacter pylori to rifamycins. Antimicrob Agents Chemother. 2000 Jun 1;44(6):1713-5.

736. Campbell EA, Korzheva N, Mustaev A, Murakami K, Nair S, Goldfarb A, et al. Structural mechanism for rifampicin inhibition of bacterial RNA polymerase. Cell. 2001 Mar 23;104(6):901-12.

737. Connolly LE, Edelstein PH, Ramakrishnan L. Why Is Long-Term Therapy Required to Cure Tuberculosis? PLoS Med. 2007 Mar;4(3):e120.

738. Piccaro G, Giannoni F, Filippini P, Mustazzolu A, Fattorini L. Activities of drug combinations against mycobacterium tuberculosis grown in aerobic and hypoxic acidic conditions. Antimicrob Agents Chemother. 2013 Mar;57(3):1428-33.

739. Seddon JA, Visser DH, Bartens M, Jordaan AM, Victor TC, van Furth AM, et al. Impact of drug resistance on clinical outcome in children with tuberculous meningitis. Pediatr Infect Dis J. 2012 Jul [cited 2017 Sep 14];31(7):711–6.

740. Thwaites GE, Lan NTN, Dung NH, Quy HT, Oanh DTT, Thoa NTC, et al. Effect of antituberculosis drug resistance on response to treatment and outcome in adults with tuberculous meningitis. J Infect Dis. 2005 Jul 1 [cited 2017 Sep 14];192(1):79–88.

741. Tho DQ, Török ME, Thi N, Yen B, Duc Bang N, Lan N, et al. Influence of Antituberculosis Drug Resistance and Mycobacterium tuberculosis Lineage on Outcome in HIV-Associated Tuberculous Meningitis. Antimicrobial agents and chemotherapy. 2012 Jun [cited 2020 May 19];56(6):3074-9.

742. Donald PR, Maritz JS, Diacon AH. The pharmacokinetics and pharmacodynamics of rifampicin in adults and children in relation to the dosage recommended for children. Tuberculosis. 2011 May 1; 91(3):196-207.

743. Peloquin C, Namdar R, Singleton M, Chest DN-, 1999. Pharmacokinetics of rifampin under fasting conditions, with food, and with antacids. Chest. 1999 Jan 1[cited 2019 Nov 18];115(1):12-8.

744. Zent C, Smith P. Study of the effect of concomitant food on the bioavailability of rifampicin, isoniazid and pyrazinamide. Tuber Lung Dis. 1995;76(2):109–13.

745. Weiner M, Peloquin C, Burman W, Luo CC, Engle M, Prihoda TJ, et al. Effects of tuberculosis, race, and human gene SLCO1B1 polymorphisms on rifampin concentrations. Antimicrob Agents Chemother. 2010 Oct;54(10):4192–200.

746. Chigutsa E, Visser ME, Swart EC, Denti P, Pushpakom S, Egan D, et al. The SLCO1B1 rs4149032 polymorphism is highly prevalent in South Africans and is associated with reduced rifampin concentrations: Dosing implications. Antimicrob Agents Chemother. 2011 Sep;55(9):4122–7.

747. Krishnaswamy K. Drug Metabolism and Pharmacokinetics in Malnourished Children. Clin Pharmacokinet. 1989;17(1):68–88.

748. Polasa K, Murthy K, Krishnaswamy K. Rifampicin kinetics in undernutrition. Br J Clin Pharmacol. 1984 Apr [cited 2019 Nov 18];17(4):481–4.

749. Peloquin CA, MacPhee AA, Berning SE. Malabsorption of Antimycobacterial Medications. N Engl J Med. 1993 Oct 7 [cited 2019 Nov 20];329(15):1122–3.

750. Patel KB, Belmonte R, Crowe HM. Drug Malabsorption and Resistant Tuberculosis in HIV-Infected Patients. N Engl J Med. 1995 Feb 2 [cited 2019 Nov 20];332(5):336–7.

751. Kumar N, Kedarishetty CK, Kumar S, Khillan V, Sarin SK. Antitubercular therapy in patients with cirrhosis: Challenges and options. World J Gastroenterol. 2014;20(19):5760–72.

752. Török M, Aljayyoussi G, Waterhouse D, Chau T, Mai N, Phu N, et al. Suboptimal Exposure to Anti-TB Drugs in a TBM/HIV+ Population Is Not Related to Antiretroviral Therapy. Clin Pharmacol Ther. 2018 Mar [cited 2019 Dec 6];103(3):449–57.

753. Chideya S, Winston CA, Peloquin CA, Bradford WZ, Hopewell PC, Wells CD, et al. Isoniazid, Rifampin, Ethambutol, and Pyrazinamide Pharmacokinetics and Treatment Outcomes among a Predominantly HIV-Infected Cohort of Adults with Tuberculosis from Botswana. Clin Infect Dis. 2009 Jun 15 [cited 2019 Dec 6];48(12):1685–94.

754. Perlman DC, Segal Y, Rosenkranz S, Rainey PM, Remmel RP, Salomon N, et al. The Clinical Pharmacokinetics of Rifampin and Ethambutol in HIV-Infected Persons with Tuberculosis. Clin Infect Dis. 2005 Dec 1 [cited 2019 Dec 6];41(11):1638–47.

755. Bhatt NB, Barau C, Amin A, Baudin E, Meggi B, Silva C, et al. Pharmacokinetics of rifampin and isoniazid in tuberculosis-hivcoinfected patients receiving nevirapine-or efavirenz-based antiretroviral treatment. Antimicrob Agents Chemother. 2014;58(6):3182–90.

756. Ruslami R, Ganiem AR, Dian S, Apriani L, Achmad TH, van der Ven AJ, et al. Intensified regimen containing rifampicin and moxifloxacin for tuberculous meningitis: An open-label, randomised controlled phase 2 trial. Lancet Infect Dis. 2013;13(1):27–35.

757. Aarnoutse RE, Kibiki GS, Reither K, Semvua HH, Haraka F, Mtabho CM, et al. Pharmacokinetics, Tolerability, and Bacteriological Response of Rifampin Administered at 600, 900, and 1,200 Milligrams Daily in Patients with Pulmonary Tuberculosis. Antimicrob Agents Chemother. 2017 Nov 1 [cited 2019 Oct 3];61(11):e01054-17.

758. Dian S, Yunivita V, Ganiem AR, Pramaesya T, Chaidir L, Wahyudi K, et al. Double-blind, randomized, placebo-controlled phase II dose-finding study to evaluate high-dose rifampin for tuberculous meningitis. Antimicrob Agents Chemother. 2018 Dec 1;62(12).

759. Svensson EM, Dian S, te Brake L, Ganiem AR, Yunivita V, van Laarhoven A, et al. Model-based meta-analysis of rifampicin exposure and mortality in Indonesian tuberculosis meningitis trials. Clin Infect Dis. 2019 Oct 30 [cited 2020 Nov 15];2020(8):1817–40.

760. Boeree MJ, Heinrich N, Aarnoutse R, Diacon AH, Dawson R, Rehal S, et al. High-dose rifampicin, moxifloxacin, and SQ109 for treating tuberculosis: a multi-arm, multi-stage randomised controlled trial. Lancet Infect Dis. 2017 Jan 1 [cited 2019 Oct 3];17(1):39–49.

761. Hu Y, Liu A, Ortega-Muro F, Alameda-Martin L, Mitchison D, Coates A. High-dose rifampicin kills persisters, shortens treatment duration, and reduces relapse rate in vitro and in vivo. Front Microbiol. 2015 Jun 23;6:641.

762. Diacon AH, Patientia RF, Venter A, Van Helden PD, Smith PJ, McIlleron H, et al. Early bactericidal activity of high-dose rifampin in patients with pulmonary tuberculosis evidenced by positive sputum smears. Antimicrob Agents Chemother. 2007;51(8):2994–6.

763. Ruslami R, Nijland HMJ, Alisjahbana B, Parwati I, van Crevel R, Aarnoutse RE. Pharmacokinetics and tolerability of a higher rifampin dose versus the standard dose in pulmonary tuberculosis patients. Antimicrob Agents Chemother. 2007 Jul 1 [cited 2019 Oct 3];51(7):2546–51.

764. Milstein M, Lecca L, Peloquin C, Mitchison D, Seung K, Pagano M, et al. Evaluation of high-dose rifampin in patients with new, smear-positive tuberculosis (HIRIF): study protocol for a randomized controlled trial. BMC Infect Dis. 2016 Dec 27 [cited 2019 Oct 3];16(1):453.

765. Yunivita V, Dian S, Ganiem AR, Hayati E, Hanggono Achmad T, Purnama Dewi A, et al. Pharmacokinetics and safety/tolerability of higher oral and intravenous doses of rifampicin in adult tuberculous meningitis patients. Int J Antimicrob Agents. 2016;48(4):415–21.

766. Acocella G, Pagani V, Marchetti M, Baroni GC, Nicolis FB. Kinetic Studies on Rifampicin. Chemotherapy. 1971 [cited 2019 Nov 18];16(6):356–70.

767. Chirehwa MT, Rustomjee R, Mthiyane T, Onyebujoh P, Smith P, McIlleron H, et al. Model-based evaluation of higher doses of rifampin using a semimechanistic model incorporating autoinduction and saturation of hepatic extraction. Antimicrob Agents Chemother. 2016 Jan 1;60(1):487–94.

768. Rosenthal IM, Tasneen R, Peloquin CA, Zhang M, Almeida D, Mdluli KE, et al. Dose-ranging comparison of rifampin and rifapentine in two pathologically distinct murine models of tuberculosis. Antimicrob Agents Chemother. 2012 Aug 1 [cited 2019 Oct 3];56(8):4331–40.

769. de Steenwinkel JEM, Aarnoutse RE, de Knegt GJ, ten Kate MT, Teulen M, Verbrugh HA, et al. Optimization of the Rifampin Dosage to Improve the Therapeutic Efficacy in Tuberculosis Treatment Using a Murine Model. Am J Respir Crit Care Med. 2013 May 15 [cited 2019 Oct 3];187(10):1127–34.

770. Jayaram R, Gaonkar S, Kaur P, Suresh BL, Mahesh BN, Jayashree R, et al. Pharmacokinetics-pharmacodynamics of rifampin in an aerosol infection model of tuberculosis. Antimicrob Agents Chemother. 2003;47(7):2118–24.

771. Seddon JA, Godfrey-Faussett P, Jacobs K, Ebrahim A, Hesseling AC, Schaaf HS. Hearing loss in patients on treatment for drug-resistant tuberculosis. European Respiratory Journal. 2012 Nov 1;40(5):1277-86.

772. Dooley KE, Mitnick CD, DeGroote MA, Obuku E, Belitsky V, Hamilton CD, et al. Old drugs, new purpose: Retooling existing drugs for optimized treatment of resistant tuberculosis. Clinical Infectious Diseases. 2012 Aug 15;55(4):572-81.

773. Thee S, Detjen A, Wahn U, Magdorf K, Magdorf K. Rifampicin serum levels in childhood tuberculosis. Int J Tuberc Lung Dis. 2009 Sep 1;13(9):1106-11.

774. Nachman S, Ahmed A, Amanullah F, Becerra MC, Botgros R, Brigden G, et al. Towards early inclusion of children in tuberculosis drugs trials: A consensus statement. The Lancet Infectious Diseases. 2015 Jun 1;15(6):711-20.

775. Paradkar MS, Devaleenal D B, Mvalo T, Arenivas A, Thakur KT, Wolf L, et al. Randomized Clinical Trial of High-Dose Rifampicin With or Without Levofloxacin Versus Standard of Care for Pediatric Tuberculous Meningitis: The TBM-KIDS Trial. Clin Infect Dis]. 2022 Mar 15 [cited 2022 May 2];75(9):1594-601.

776. Thee S, Basu Roy R, Blázquez-Gamero D, Falcón-Neyra L, Neth O, Noguera-Julian A, et al. Treatment and Outcome in Children With Tuberculous Meningitis: A Multicenter Pediatric Tuberculosis Network European Trials Group Study. Clin Infect Dis]. 2022 Aug 31 [cited 2023 Jan 30];75(3):372–81.

777. Gumbo T, Louie A, Deziel MR, Liu W, Parsons LM, Salfinger M, et al. Concentration-dependent Mycobacterium tuberculosis killing and prevention of resistance by rifampin. Antimicrob Agents Chemother. 2007;51(11):3781–8.

778. Woo J, Cheung W, Chan R, Chan HS, Cheng A, Chan K. In vitro protein binding characteristics of isoniazid, rifampicin, and pyrazinamide to whole plasma, albumin, and α-1-acid glycoprotein. Clin Biochem. 1996;29(2):175–7.

779. Chen J, Raymond K. Roles of rifampicin in drug-drug interactions: underlying molecular mechanisms involving the nuclear pregnane X receptor. Ann Clin Microbiol Antimicrob. 2006.

780. Boeree MJ, Plemper van Balen G, Aarnoutse RA. High-dose rifampicin: how do we proceed? [Correspondence]. Int J Tuberc Lung Dis. 2011 Aug 1 [cited 2016 Oct 12];15(8):1133–1133.

781. Mahajan M, Rohatgi D, Talwar V, Patni SK, Mahajan P, Agarwal DS. Serum and cerebrospinal fluid concentrations of rifampicin at two dose levels in children with tuberculous meningitis. J Commun Dis. 1997 Sep 1;29(3):269-74.

782. Phuapradit P, Supmonchai K, Kaojarern S, Mokkhavesa C. The blood/cerebrospinal fluid partitioning of pyrazinamide: a study during the course of treatment of tuberculous meningitis. J Neurol Neurosurg Psychiatry. 1990 Jan 1;53(1):81-2.

783. Alvarez-Uria G, Midde M, Pakam R, Naik PK. Clinical Study Initial Antituberculous Regimen with Better Drug Penetration into Cerebrospinal Fluid Reduces Mortality in HIV Infected Patients with Tuberculous Meningitis: Data from an HIV Observational Cohort Study. Tuberc Res Treat. 2013 [cited 2020 May 19];2013(1):242604.

784. Botha FJH, Sirgel FA, Parkin DP, Van De Wal BW, Donald PR, Mitchison DA, et al. Early bactericidal activity of ethambutol, pyrazinamide and the fixed combination of isoniazid, rifampicin and pyrazinamide (Rifater) in patients with pulmonary tuberculosis. South African Medical Journal. 1996;86(2).

785. Jindani A, Aber VR, Edwards EA, Mitchison DA. The early bactericidal activity of drugs in patients with pulmonary tuberculosis. Am Rev Respir Dis. 1980;121(6):939–49.

786. Stemkens R, Litjens CHC, Dian S, Ganiem AR, Yunivita V, van Crevel R, et al. Pharmacokinetics of pyrazinamide during the initial phase of tuberculous meningitis treatment. Int J Antimicrob Agents. 2019 Sep 1;54(3):371–4.

787. Gundert-Remy U, Klett M, Weber E. Concentration of Ethambutol in Cerebrospinal Fluid in Man as a Function of the Non-Protein-Bound Drug Fraction in Serum. Vol. 6, Europ. J. clin. Pharmacol. 1973 Aug;6:133-6.

788. Donald PR, Seifart HI. Cerebrospinal fluid concentrations of ethionamide in children with tuberculous meningitis. J Pediatr. 1989 Sep 1;115(3):483-6.

789. McIlleron H, Wash P, Burger A, Norman J, Folb PI, Smith P. Determinants of rifampin, isoniazid, pyrazinamide, and ethambutol pharmacokinetics in a cohort of tuberculosis patients. Antimicrob Agents Chemother. 2006 Apr;50(4):1170-7.

790. Peloquin CA, Jaresko GS, Yong CL, Keung ACF, Bulpitt AE, Jelliffe RW. Population pharmacokinetic modeling of isoniazid, rifampin, and pyrazinamide. Antimicrob Agents Chemother. 1997;41(12):2670–9.

791. Ellard GA, Humphries MJ, Gabriel M, Teoh R. Penetration of pyrazinamide into the cerebrospinal fluid in tuberculous meningitis. Br Med J (Clin Res Ed). 1987 Jan 31 [cited 2017 Apr 13];294(6567):284–5.

792. Lee G, Dallas S, Hong M, Bendayan R. Drug transporters in the central nervous system: brain barriers and brain parenchyma considerations. Pharmacological reviews. 2001 Dec 1:53(4):569-96.

793. Bemer-Melchior P, Bryskier A, Drugeon HB. Comparison of the in vitro activities of rifapentine and rifampicin against Mycobacterium tuberculosis complex. Journal of Antimicrobial

Chemotherapy. 2000 Oct 1 [cited 2020 May 19]; 46(4):571-6.

794. Lanni FR. Determination of Organ Specific Pharmacokinetic Data for the Anti-Tuberculosis Drugs in Guinea Pigs Using Microdialysis. Open University (United Kingdom) 2019 Sep 17.

795. Kroeger D, Tamburri A, Amzica F, Sík A. Activity-Dependent Layer-Specific Changes in the Extracellular Chloride Concentration and Chloride Driving Force in the Rat Hippocampus. J Neurophysiol. 2010 Apr [cited 2019 Nov 14];103(4):1905–14.

796. Syková E, Nicholson C. Diffusion in brain extracellular space. Physiological Reviews. 2008 Oct;88(4):1277-340.

797. Van Toorn R, Solomons RS, Seddon JA, Schoeman JF. Thalidomide Use for Complicated Central Nervous System Tuberculosis in Children: Insights From an Observational Cohort. Clin Infect Dis. 2021 Mar 1 [cited 2022 Sep 27];72(5):e136–45.

798. Marais BJ, Cheong E, Fernando S, Daniel S, Watts MR, Berglund LJ, et al. Use of Infliximab to Treat Paradoxical Tuberculous Meningitis Reactions.InOpen forum infectious diseases. 2021 Jan 1;8(1):ofaa604.

799. Abo YN, Curtis N, Osowicki J, Haeusler G, Purcell R, Kadambari S, et al. Infliximab for Paradoxical Reactions in Pediatric Central Nervous System Tuberculosis. J Pediatric Infect Dis Soc. 2021 Dec 31 [cited 2022 Sep 27];10(12):1087–91.

800. Ungerstedt U. Microdialysis--principles and applications for studies in animals and man. J Intern Med. 1991 Oct [cited 2016 Oct 12];230(4):365–73.

801. Bourne JA. Intracerebral microdialysis: 30 years as a tool for the neuroscientist. Clin Exp Pharmacol Physiol. [cited 2016 Oct 12];30(1–2):16–24.

802. Roberts PJ, Anderson SD. Stimulatory effect of L-glutamate and related amino acids on [^{3}H] dopamine release from rat striatum: an invitro model for glutamate actions. S. J Neurochem. 1979 May 1 [cited 2021 Feb 18];32(5):1539–45.

803. Hutchinson PJ, al-Rawi PG, O'Connell MT, Gupta AK, Maskell LB, Hutchinson DB, et al. On-line monitoring of substrate delivery and brain metabolism in head injury. Acta Neurochir Suppl. 2000 [cited 2021 Feb 10];76:431–5.

804. Chefer VI, Thompson AC, Zapata A, Shippenberg TS. Overview of brain microdialysis. Current Protocols in Neuroscience. 2009 Apr [cited 2021 Feb 18];47(1):7-1.

805. Stenken JA, Church MK, Gill CA, Clough GF. How minimally invasive is microdialysis sampling? A cautionary note for cytokine collection in human skin and other clinical studies.

AAPS Journal. 2010 Mar [cited 2021 Feb 18];12:73-8.

806. Stenken JA, Chen R, Yuan X. Influence of geometry and equilibrium chemistry on relative recovery during enhanced microdialysis. Anal Chim Acta. 2001 Jun 1;436(1):21–9.

807. Bosche B, Dohmen C, Graf R, Neveling M, Staub F, Kracht L, et al. Extracellular Concentrations of Non-Transmitter Amino Acids in Peri-Infarct Tissue of Patients Predict Malignant Middle Cerebral Artery Infarction. Stroke. 2003;34(12):2908–13.

808. Schuck VJA, Rinas I, Derendorf H. In vitro microdialysis sampling of docetaxel. J Pharm Biomed Anal. 2004 Nov 19 [cited 2021 Feb 18];36(4):807–13.

809. Ungerstedt U, Rostami E. Microdialysis in neurointensive care. Curr Pharm Des. 2004 Jul 1;10(18):2145-52.

810. Parkin MC, Hopwood SE, Jones DA, Hashemi P, Landolt H, Fabricius M, et al. Dynamic changes in brain glucose and lactate in pericontusional areas of the human cerebral cortex, monitored with rapid sampling on-line microdialysis: Relationship with depolarisation-like events. J Cereb Blood Flow Metab. 2005 Mar [cited 2021 Feb 18];25(3):402–13.

811. Shou M, Ferrario CR, Schultz KN, Robinson TE, Kennedy RT. Monitoring dopamine in vivo by microdialysis sampling and on-line CE-laser-induced fluorescence. Anal Chem. 2006 Oct 1 [cited 2021 Feb 18];78(19):6717–25.

812. Mitala CM, Wang Y, Borland LM, Jung M, Shand S, Watkins S, et al. Impact of microdialysis probes on vasculature and dopamine in the rat striatum: A combined fluorescence and voltammetric study. J Neurosci Methods. 2008 Sep 30 [cited 2021 Feb 18];174(2):177–85.

813. Ungerstedt U. Microdialysis—principles and applications for studies in animals and man. J Intern Med. 1991 [cited 2021 Feb 18];230(4):365–73.

814. Jaquins-Gerstl A, Shu Z, Zhang J, Liu Y, Weber SG, Michael AC. Effect of dexamethasone on gliosis, ischemia, and dopamine extraction during microdialysis sampling in brain tissue. Anal Chem. 2011 Oct 15 [cited 2021 Feb 18];83(20):7662–7.

815. Wang Y, Michael AC. Microdialysis probes alter presynaptic regulation of dopamine terminals in rat striatum. J Neurosci Methods. 2012 Jun 30 [cited 2021 Feb 18];208(1):34–9.

816. Zhang J, Jaquins-Gerstl A, Nesbitt KM, Rutan SC, Michael AC, Weber SG. In vivo monitoring of serotonin in the striatum of freely moving rats with one minute temporal resolution by online microdialysis-capillary high-performance liquid chromatography at elevated temperature and pressure. Anal Chem. 2013 Oct 15 [cited 2021 Feb 18];85(20):9889–97.

817. Nesbitt KM, Varner EL, Jaquins-Gerstl A, Michael AC. Microdialysis in the rat striatum: Effects of 24 h dexamethasone retrodialysis on evoked dopamine release and penetration injury. ACS Chem Neurosci. 2015 Jan 21 [cited 2021 Feb 18];6(1):163–73.

818. Benveniste H, Drejer J, Schousboe A, Diemer NH. Regional Cerebral Glucose Phosphorylation and Blood Flow After Insertion of a Microdialysis Fiber Through the Dorsal Hippocampus in the Rat. J Neurochem. 1987 [cited 2021 Feb 18];49(3):729–34.

819. Benveniste H, Hansen AJ, Ottosen NS. Determination of Brain Interstitial Concentrations by Microdialysis. J Neurochem. 1989 [cited 2021 Feb 18];52(6):1741–50.

820. Santiago M, Westerink BHC. Characterization of the in vivo release of dopamine as recorded by different types of intracerebral microdialysis probes. Naunyn Schmiedebergs Arch Pharmacol. 1990 Oct [cited 2021 Feb 18];342(4):407–14.

821. Carneheim C, Ståhle L. Microdialysis of Lipophilic Compounds: A Methodological Study. Pharmacol Toxicol. 1991 [cited 2021 Feb 18];69(5):378–80.

822. Parsons LH, Smith AD, Justice JB. The in vivo microdialysis recovery of dopamine is altered independently of basal level by 6-hydroxydopamine lesions to the nucleus accumbens. J Neurosci Methods. 1991 [cited 2021 Feb 18];40(2–3):139–47.

823. Dykstra KH, Hsiao JK, Morrison PF, Bungay PM, MefFord IN, Scully MM, et al. Quantitative Examination of Tissue Concentration Profiles Associated with Microdialysis. J Neurochem. 1992 [cited 2021 Feb 18];58(3):931–40.

824. Stenken JA. Methods and issues in microdialysis calibration. Anal Chim Acta. 1999 Jan 18;379(3):337–58.

825. Brunner M, Langer O. Microdialysis versus other techniques for the clinical assessment of in vivo tissue drug distribution. AAPS J. 2006 Apr 14 [cited 2017 Jul 24];8(2):E263-71.

826. de Lange EC, de Boer BA, Breimer D. Microdialysis for pharmacokinetic analysis of drug transport to the brain. Adv Drug Deliv Rev. 1999;36(2–3):211–27.

827. Hillered L, Persson L, Pontén U, Ungerstedt U. Neurometabolic monitoring of the ischaemic human brain using microdialysis. Acta Neurochir (Wien). 1990 Sep [cited 2017 Aug 31];102(3–4):91–7.

828. Thango NS, Rohlwink UK, Dlamini L, Tshavhungwe MP, Banderker E, Salie S, et al. Brain interstitial glycerol correlates with evolving brain injury in paediatric traumatic brain injury. Childs Nerv Syst. 2021 May [cited 2021 Feb 17];1713-21.

829. Hillered L, Vespa PM, Hovda D a. Translational neurochemical research in acute human brain injury: the current status and potential future for cerebral microdialysis. J Neurotrauma. 2005;22(1):3–41.

830. Hutchinson PJ, Jalloh I, Helmy A, Carpenter KLH, Rostami E, Bellander B-M, et al. Consensus statement from the 2014 International Microdialysis Forum. Intensive Care Med. 2015 Sep 21 [cited 2019 Sep 5];41(9):1517–28.

831. Persson L, Hillered L. Chemical monitoring of neurosurgical intensive care patients using intracerebral microdialysis. Journal of Neurosurgery. 1992 Jan 1 [cited 2021 Feb 10];76(1):72-80.

832. Persson L, Valtysson J, Enblad P, Wärme PE, Cesarini K, Lewén A, et al. Neurochemical monitoring using intracerebral microdialysis in patients with subarachnoid hemorrhage. J Neurosurg. 1996 [cited 2021 Feb 10];84(4):606–16.

833. Bouw R, Ederoth P, Lundberg J, Ungerstedt U, Nordström CH, Hammarlund-Udenaes M. Increased blood-brain barrier permeability of morphine in a patient with severe brain lesions as determined by microdialysis. Acta Anaesthesiol Scand. 2001 Mar [cited 2017 Jul 26];45(3):390–2.

834. Engström M, Polito A, Reinstrup P, Romner B, Ryding E, Ungerstedt U, et al. Intracerebral microdialysis in severe brain trauma: The importance of catheter location. Journal of Neurosurgery. 2005 Mar 1 [cited 2021 Feb 9];102(3):460-9.

835. Jaquins-Gerstl A, Michael AC. Dexamethasone-Enhanced Microdialysis and Penetration Injury. Frontiers in Bioengineering and Biotechnology. 2020 Dec 8[cited 2021 Feb 18];8:602266.

836. Goodman JC, Valadka AB, Gopinath SP, Uzura M, Robertson CS. Extracellular lactate and glucose alterations in the brain after head injury measured by microdialysis. Crit Care Med. 1999 [cited 2021 Feb 10];27(9):1965–73.

837. Langemann H, Mendelowitsch A, Landolt H, Alessandri B, Gratzl O. Experimental and clinical monitoring of glucose by microdialysis. Clin Neurol Neurosurg. 1995 May 1;97(2):149-55.

838. Unterberg AW, Sakowitz OW, Sarrafzadeh AS, Benndorf G, Lanksch WR. Role of bedside microdialysis in the diagnosis of cerebral vasospasm following aneurysmal subarachnoid hemorrhage. J Neurosurg. 2001 [cited 2021 Feb 10];94(5):740–9.

839. Vespa P, Bergsneider M, Hattori N, Wu H-M, Huang S-C, Martin N a, et al. Metabolic crisis without brain ischemia is common after traumatic brain injury: a combined microdialysis and positron emission tomography study. J Cereb Blood Flow Metab. 2005;25(6):763–74.

840. Siesjo BK. Cerebral circulation and metabolism. Journal of Neurosurgery. 1984 May 1 [cited 2021 Feb 10];883-908.

841. Ståhl N, Mellergård P, Hallström A, Ungerstedt U, Nordström CH. Intracerebral microdialysis and bedside biochemical analysis in patients with fatal traumatic brain lesions. Acta Anaesthesiol Scand. 2001 [cited 2021 Feb 10];45(8):977–85.

842. Zauner A, Doppenberg EMR, Woodward JJ, Choi SC, Young HF, Bullock R. Continuous monitoring of cerebral substrate delivery and clearance: Initial experience in 24 patients with severe acute brain injuries. Neurosurgery. 1997 Nov [cited 2021 Feb 10];41(5):1082–93.

843. Kett-White R, Hutchinson PJ, Al-Rawi PG, Gupta AK, Pickard JD, Kirkpatrick PJ, et al. Adverse cerebral events detected after subarachnoid hemorrhage using brain oxygen and microdialysis probes. Neurosurgery 2002 Jun 1 [cited 2021 Feb 10];50(6):1213–22.

844. Sarrafzadeh A, Haux D, Küchler I, Lanksch WR, Unterberg AW. Poor-grade aneurysmal subarachnoid hemorrhage: Relationship of cerebral metabolism to outcome. J Neurosurg. 2004 [cited 2021 Feb 10];100(3):400–6.

845. Hutchinson PJ, Gupta AK, Fryer TF, Al-Rawi PG, Chatfield DA, Coles JP, et al. Correlation between cerebral blood flow, substrate delivery, and metabolism in head injury: A combined microdialysis and triple oxygen positron emission tomography study. J Cereb Blood Flow Metab. 2002 Jun [cited 2021 Feb 17];22(6):735–45.

846. Clausen T, Alves OL, Reinert M, Doppenberg E, Zauner A, Bullock R. Association between elevated brain tissue glycerol levels and poor outcome following severe traumatic brain injury. J Neurosurg. 2005 Aug [cited 2021 Feb 17];103(2):233–8.

847. Reinstrup P, Ståhl N, Mellergård P, Uski T, Ungerstedt U, Nordström CH. Intracerebral microdialysis in clinical practice: Baseline values for chemical markers during wakefulness, anesthesia, and neurosurgery. Neurosurgery. 2000 [cited 2021 Feb 17];47(3):701–10.

848. Vespa P, Martin NA, Nenov V, Glenn T, Bergsneider M, Kelly D, et al. Delayed increase in extracellular glycerol with post-traumatic electrographic epileptic activity: Support for the theory that seizures induce secondary injury. In: Acta Neurochirurgica, Supplement. Springer Vienna; 2002 [cited 2021 Feb 17]; 355–7.

849. Chesnut RM, Bleck TP, Citerio G, Classen J, Cooper DJ, Coplin WM, et al. A Consensus-Based Interpretation of the Benchmark Evidence from South American Trials: Treatment of Intracranial Pressure Trial. J Neurotrauma. 2015 Nov 15 [cited 2019 Sep 5];32(22):1722–4.

850. Oddo M, Hutchinson PJ. Understanding and monitoring brain injury: the role of cerebral

microdialysis. Intensive Care Med. 2018 Nov 23 [cited 2019 Sep 5];44(11):1945–8.

851. Le Roux P, Menon DK, Citerio G, Vespa P, Bader MK, Brophy GM, et al. Consensus Summary Statement of the International Multidisciplinary Consensus Conference on Multimodality Monitoring in Neurocritical Care. Neurocrit Care. 2014 Dec 11 [cited 2019 Sep 5];21(S2):1–26.

852. Kissinger PT, Shoup RE. Optimization of LC apparatus for determinations in neurochemistry with an emphasis on microdialysis samples. J Neurosci Methods. 1990 Sep 1;34(1-3):3-10.

853. Dahyot-Fizelier C, Frasca D, Grégoire N, Adier C, Mimoz O, Debaene B, et al. Microdialysis study of cefotaxime cerebral distribution in patients with acute brain injury. Antimicrob Agents Chemother. 2013 Jun 1 [cited 2017 Jul 26];57(6):2738–42.

854. Allen DD, Crooks PA, Yokel RA. 4-trimethylammonium antipyrine: A quaternary ammonium nonradionuclide marker for blood-brain barrier integrity during in vivo microdialysis. J Pharmacol Toxicol Methods. 1992 Nov 1;28(3):129-35.

855. Sawchuk RJ, Cheung BWY. Chapter 6.7 Application of microdialysis in pharmacokinetic studies. Handbook od Behavioral Neuroscience. 2006 [cited 2017 Aug 31]: 601-22.

856. Torto N, Gorton L, Laurell T, Marko-Varga G. Technical issues of in vitro microdialysis sampling in bioprocess monitoring. TrAC - Trends Anal Chem. 1999 Apr 1;18(4):252–60.

857. de Lange EC, Danhof M, de Boer a G, Breimer DD. Methodological considerations of intracerebral microdialysis in pharmacokinetic studies on drug transport across the blood-brain barrier. Brain Res Brain Res Rev. 1997;25(1):27–49.

858. de Lange ECM, Danhof M, de Boer AG, Breimer DD. Critical factors of intracerebral microdialysis as a technique to determined the pharmacokinetics of drugs in rat brain. Brain Res. 1994;666(1):1–8.

859. Schroepf S, Burau D, Muench H-G, Derendorf H, Zeitlinger M, Genzel-Boroviczény O, et al. Microdialysis sampling to monitor target-site vancomycin concentrations in septic infants: a feasible way to close the knowledge gap. Int J Antimicrob Agents. 2021 [cited 2023 May 10];58:106405.

860. Johnson RD, Justice JB. Model studies for brain dialysis. Brain Res Bull. 1983 Apr 1;10(4):567–71.

861. Jacobson I, Hamberger A. Kainic acid-induced changes of extracellular amino acid levels, evoked potentials and EEG activity in the rabbit olfactory bulb. Brain Res. 1985 Dec 2 [cited 2023 Oct 9];348(2):289–96.

862. Tossman U, Ungerstedt U. Microdialysis in the study of extracellular levels of amino acids in the rat brain. Acta Physiol Scand. 1986 Sep 1 [cited 2023 Oct 9];128(1):9–14.

863. Levine JE, Powell KD. Microdialysis for measurement of neuroendocrine peptides. Methods Enzymol. 1989 Jan 1;168(C):166–81.

864. Amberg G, Lindefors N. Intracerebral microdialysis: II. mathematical studies of diffusion kinetics. J Pharmacol Methods. 1989 Nov 1;22(3):157-83.

865. Lindefors N, Amberg G, Ungerstedt U. Intracerebral microdialysis: I. Experimental studies of diffusion kinetics. J Pharmacol Methods. 1989 [cited 2023 Oct 9];22(3):141–56.

866. Ruggeri M, Zoli M, Grimaldi R, Ungerstedt U, Eliasson A, Agnati LF, et al. Aspects of neural plasticity in the central nervous system—III. Methodological studies on the microdialysis technique. Neurochem Int. 1990 Jan 1;16(4):427–35.

867. Westergren I, Nyström B, Hamberger A, Johansson BB. Intracerebral dialysis and the blood-brain barrier. J Neurochem. 1995;64(1):229–34.

868. Busse D, Schaeftlein A, Solms A, Ilia L, Michelet R, Zeitlinger M, et al. Which Analysis Approach Is Adequate to Leverage Clinical Microdialysis Data? A Quantitative Comparison to Investigate Exposure and Reponse Exemplified by Levofloxacin. Pharm Res. 2021 Mar 1 [cited 2023 Feb 28];38(3):381–95.

869. Chaurasia CS, Müller M, Bashaw ED, Benfeldt E, Bolinder J, Bullock R, et al. AAPS-FDA workshop white paper: Microdialysis principles, application and regulatory perspectives. In: Pharmaceutical Research. 2007 May;24(5):1014-25

870. Brunner M, Langer O. Microdialysis versus other techniques for the clinical assessment of in vivo tissue drug distribution. AAPS J. 2006;8(2):E263–71.

871. Lönnroth P, Jansson PA, Smith U. A microdialysis method allowing characterization of intercellular water space in humans. Am J Physiol. 1987 Aug [cited 2017 Jul 26];253(2):E228-31.

872. Lerma J, Herranz AS, Herreras O, Abraira V, del Rio RM. In vivo determination of extracellular concentration of amino acids in the rat hippocampus. A method based on brain dialysis and computerized analysis. Brain Res. 1986 Oct 1;384(1):145-55.

873. Morrison PF, Bungay PM, Hsiao JK, Ball BA, Mefford IN, Dedrick RL. Quantitative Microdialysis: Analysis of Transients and Application to Pharmacokinetics in Brain. J Neurochem. 1991 Jul;57(1):103-19.

874. Bouw MR, Hammarlund-Udenaes M. Methodological aspects of the use of a calibrator in in vivo microdialysis-further development of the retrodialysis method. Pharm Res. 1998 Nov [cited 2017 Jul 26];15(11):1673–9.

875. Wang Y, Wong S.L SR. Comparison of in vitro and in vivo calibration of microdialysis probes using retrodialysis. Curr Separarations. 1991;10:87.

876. Chen KC. Chapter 1.4 The validity of intracerebral microdialysis. Handbook of Behavioral Neuroscience. 2006 Jan 1;16:47-70.

877. Müller M. Microdialysis in clinical drug delivery studies. Adv Drug Deliv Rev. 2000 Dec 15;45(2-3):255-69.

878. Dahyot-Fizelier C, Timofeev I, Marchand S, Hutchinson P, Debaene B, Menon D, et al. Brain microdialysis study of meropenem in two patients with acute brain injury. Antimicrob Agents Chemother. 2010 Aug 1 [cited 2017 Jul 26];54(8):3502–4.

879. Sawchuk RJ, Cheung BW. Application of microdialysis in pharmacokinetic studies. 2006 Jan 1;16:601-22.

880. Brunner M, Muller M. Microdiaysis in clinical drug delivery studies. 2006 Jan 1;16:625-44.

881. Frasca D, Dahyot-Fizelier C, Adier C, Mimoz O, Debaene B, Couet W, et al. Metronidazole and Hydroxymetronidazole Central Nervous System Distribution: 2. Cerebrospinal Fluid Concentration Measurements in Patients with External Ventricular Drain. Antimicrobial agents and chemotherapy. 2014 Feb[cited 2017 Jul 26] ;58(2):1024-7.

882. Rambeck B, Jurgens UH, May TW, Wolfgang Pannek H, Behne F, Ebner A, et al. Comparison of Brain Extracellular Fluid, Brain Tissue, Cerebrospinal Fluid, and Serum Concentrations of Antiepileptic Drugs Measured Intraoperatively in Patients with Intractable Epilepsy. Epilepsia. 2006 Apr 1 [cited 2017 Jul 26];47(4):681–94.

883. Tunblad K, Hammarlund-Udenaes M, Jonsson EN. An integrated model for the analysis of pharmacokinetic data from microdialysis experiments. Pharm Res. 2004 Sep [cited 2023 Feb 17];21(9):1698–707.

884. Ehmann L, Simon P, Busse D, Petroff D, Dorn C, Huisinga W, et al. Risk of target non-attainment in obese compared to non-obese patients in calculated linezolid therapy. Clin Microbiol Infect. 2020 Sep 1;26(9):1222–8.

885. Ullah S, Matzneller P, Zeitlinger M, Fuhr U, Taubert M. A population pharmacokinetic model of intravenous telavancin in healthy individuals to assess tissue exposure. Naunyn Schmiedebergs Arch Pharmacol. 2019 Sep 5 [cited 2023 Feb 28];392(9):1097–106.

886. Minichmayr IK, Schaeftlein A, Kuti JL, Zeitlinger M, Kloft C. Clinical Determinants of Target Non-Attainment of Linezolid in Plasma and Interstitial Space Fluid: A Pooled Population Pharmacokinetic Analysis with Focus on Critically Ill Patients. Clin Pharmacokinet. 2017 Jun 1 [cited 2023 Feb 28];56(6):617–33.

887. Figaji AA, Fieggen AG, Peter JC. Endoscopic third ventriculostomy in tuberculous meningitis. Childs Nerv Syst. 2003;19(4):217–25.

888. Rohlwink UK, Mauff K, Wilkinson KA, Enslin N, Wegoye E, Wilkinson RJ, et al. Biomarkers of Cerebral Injury and Inflammation in Pediatric Tuberculous Meningitis. Clinical Infectious Diseases. 2017 Oct 15;65(8):1298-307.

889. Donovan J, Figaji A, Imran D, Phu NH, Rohlwink U, Thwaites GE. The neurocritical care of tuberculous meningitis. Lancet Neurol. 2019 Aug 1 [cited 2023 Aug 23];18(8):771–83.

890. Schoeman JF, Van Zyl LE, Laubscher JA. Serial CT Scanning in Childhood Tuberculous Meningitis: Prognostic Features in 198 Cases. 1995 Jul 1 [cited 2023 Aug 2];10(4):320–9.

891. Semlali S, El Kharras A, Mahi M, Hsaini Y, Benameur M, Aziz N, et al. [Imaging features of CNS tuberculosis]. J Radiol. 2008 Feb 1 [cited 2023 Aug 2];89(2):209–20.

892. Leiguarda R, Berthier M, Starkstein S, Nogués M, Lylyk P. Ischemic infarction in 25 children with tuberculous meningitis. Stroke. 1988 Feb;19(2):200-4.

893. Patel B, Sardana V. Discrepancy between ventricular and lumbar CSF in chronic meningitis. 2020 Apr 1 [cited 2023 Jan 30];67(2):277-80.

894. Donald PR. Antituberculosis Drug-Induced Hepatotoxicity in Children. Pediatr Reports 2011, Vol 3, Page e16. 2011 Jun 20 [cited 2022 Jul 4];3(2):e16.

895. Saukkonen JJ, Cohn DL, Jasmer RM, Schenker S, Jereb JA, Nolan CM, et al. An official ATS statement: Hepatotoxicity of antituberculosis therapy. Am J Respir Crit Care Med. 2006 Oct 15 [cited 2023 Nov 21];174(8):935–52.

896. le Bourgeois M, de Blic J, Paupe J, Scheinmann P. Good tolerance of pyrazinamide in children with pulmonary tuberculosis. Arch Dis Child. 1989 [cited 2023 Mar 22];64(1):177.

897. Ruslami R, Gafar F, Yunivita V, Parwati I, Ganiem AR, Aarnoutse RE, et al. Pharmacokinetics and safety/tolerability of isoniazid, rifampicin and pyrazinamide in children and adolescents treated for tuberculous meningitis. Arch Dis Child. 2022 Jan 1 [cited 2022 Jul 4];107(1):70–7.

898. Marais S, Cresswell F V, Hamers RL, te Brake LHM, Ganiem AR, Imran D, et al. High dose oral rifampicin to improve survival from adult tuberculous meningitis: A randomised placebo-

controlled double-blinded phase III trial (the HARVEST study). Wellcome Open Res. 2019 Dec 2 [cited 2020 Jan 15];4:190.

899. Tucker EW, Marais S, Seddon JA, van Crevel R, Ganiem AR, Ruslami R, et al. International Survey Reveals Opportunities to Improve Tuberculous Meningitis Management and the Need for Standardized Guidelines. Open Forum Infect Dis. 2020 Nov 1 [cited 2023 Jun 29];7(11).

900. Sulis G, Tavaziva G, Gore G, Benedetti A, Solomons R, van Toorn R, et al. Comparative effectiveness of regimens for drug-susceptible tuberculous meningitis in children and adolescents: a systematic review and aggregate-level data meta-analysis. Open Forum Infect Dis. 2022 Apr 9 [cited 2022 Apr 14];9(6):ofac108.

901. Abdella A, Deginet E, Weldegebreal F, Eshetu B, Desalew A, Ketema I. Tuberculous Meningitis in Children: Treatment Outcomes at Discharge and Its Associated Factors in Eastern Ethiopia: A Five Years Retrospective Study. Infect Drug Resist. 2022 May 31 [cited 2023 Aug 2];15:2743–51.

902. Schoeman J, Wait J, Burger M, van Zyl F, Fertig G, van Rensburg a J, et al. Long-term follow up of childhood tuberculous meningitis. Dev Med Child Neurol. 2002 Aug;44(8):522-6.

903. Nataprawira HM, Ruslianti V, Solek P, Hawani D, Milanti M, Anggraeni R, et al. Outcome of tuberculous meningitis in children: the first comprehensive retrospective cohort study in Indonesia. Int J Tuberc Lung Dis. 2016 Jul 1;20(7):909–14.

904. Figaji AA, Fieggen AG, Peter JC. Endoscopy for tuberculous hydrocephalus. Child's Nerv Syst. 2007 Jan;23:79-84.

905. Smith PK, Krohn RI, Hermanson GT, Mallia AK, Gartner FH, Provenzano MD, et al. Measurement of protein using bicinchoninic acid. Anal Biochem. 1985 Oct 1;150(1):76–85.

906. Panjasawatwong N, Wattanakul T, Hoglund RM, Bang ND, Pouplin T, Nosoongnoen W, et al. Population pharmacokinetic properties of anti-tuberculosis drugs in Vietnamese children with tuberculous meningitis. Antimicrob Agents Chemother. 2020 Nov 2 [cited 2020 Nov 8];5.

907. Chigutsa E, Pasipanodya JG, Visser ME, Van Helden PD, Smith PJ, Sirgel FA, et al. Impact of nonlinear interactions of pharmacokinetics and mics on sputum bacillary kill rates as a marker of sterilizing effect in tuberculosis. Antimicrob Agents Chemother. 2015 Jan 1 [cited 2022 Sep 8];59(1):38–45.

908. Alsultan A, Peloquin CA. Therapeutic Drug Monitoring in the Treatment of Tuberculosis: An Update. Drugs. 2014 Jun;74:839-54.

909. Ellard GA, Humphries MJ, Allen BW. Cerebrospinal Fluid Drug Concentrations and the

Treatment of Tuberculous Meningitis. Am Rev Respir Dis. 1993 Sep [cited 2017 Feb 20];148(3):650–5.

910. Bemer-Melchior P, Bryskier A, Drugeon HB. Comparison of the in vitro activities of rifapentine and rifampicin against Mycobacterium tuberculosis complex. Journal of Antimicrobial Chemotherapy. 2000 Oct 1;46(4):571-6.

911. Gengiah TN, Botha JH, Soowamber D, Naidoo K, Abdool Karim SS. Low rifampicin concentrations in tuberculosis patients with HIV infection. J Infect Dev Ctries. 2014 Aug 13;8(08):987-93.

912. Chan SL, Yew WW, Ma WK, Girling DJ, Aber VR, Felmingham D, et al. The early bactericidal activity of rifabutin measured by sputum viable counts in Hong Kong patients with pulmonary tuberculosis. Tuber Lung Dis. 1992;73(1):33–8.

913. Wilkins JJ, Savic RM, Karlsson MO, Langdon G, McIlleron H, Pillai G, et al. Population pharmacokinetics of rifampin in pulmonary tuberculosis patients, including a semimechanistic model to describe variable absorption. Antimicrob Agents Chemother. 2008 Jun [cited 2022 Oct 4];52(6):2138–48.

914. Wasserman S, Davis A, Stek C, Chirehwa M, Botha S, Daroowala R, et al. Plasma pharmacokinetics of high-dose oral versus intravenous rifampicin in patients with tuberculous meningitis: a randomized controlled trial. Antimicrob Agents Chemother. 2021 Aug 1 [cited 2022 Oct 4];65(8).

915. Pcloquin CA, Namdar R, Singleton MD, Nix DE. Pharmacokinetics of Rifampin Under Fasting Conditions, With Food, and With Antacids. Chest. 1999 Jan 1;115(1):12–8.

916. Lin HC, Yu MC, Liu HJ, Bai KJ. Impact of food intake on the pharmacokinetics of first-line antituberculosis drugs in Taiwanese tuberculosis patients. J Formos Med Assoc. 2014;113(5):291–7.

917. Kaojarern S, Supmonchai K, Phuapradit P, Mokkhavesa C, Krittiyanunt S. Effect of steroids on cerebrospinal fluid penetration of antituberculous drugs in tuberculous meningitis. Clin Pharmacol Ther. 1991;49(1):6–12.

918. Germovsek E, Lutsar I, Kipper K, Karlsson MO, Planche T, Chazallon C, et al. Plasma and CSF pharmacokinetics of meropenem in neonates and young infants: results from the NeoMero studies. J Antimicrob Chemother]. 2018 Jul 1 [cited 2022 Oct 4];73(7):1908–16.

919. Te Brake LHM, De Knegt GJ, De Steenwinkel JE, Van Dam TJP, Burger DM, Russel FGM, et al. The Role of Efflux Pumps in Tuberculosis Treatment and Their Promise as a Target in Drug

Development: Unraveling the Black Box. Annu Rev Pharmacol Toxicol. 2018 Jan 6 [cited 2022 Jul 4];58:271–91.

920. Magis-Escurra C, Later-Nijland HMJ, Alffenaar JWC, Broeders J, Burger DM, van Crevel R, et al. Population pharmacokinetics and limited sampling strategy for first-line tuberculosis drugs and moxifloxacin. Int J Antimicrob Agents. 2014 Sep [cited 2017 Jul 26];44(3):229–34.

921. Srivastava S, Journal TG-ER, 2014. Integrating drug concentrations and minimum inhibitory concentrations with Bayesian-dose optimisation for multidrug-resistant tuberculosis. Eur Respir Soc. 2014 Jan 1 [cited 2022 Sep 8];43(1):312-3.

922. Abdelgawad N, Tshavhungwe M (Phophi), Rohlwink U, McIlleron H, Abdelwahab MT, Wiesner L, et al. Population Pharmacokinetic Analysis of Rifampicin in Plasma, Cerebrospinal Fluid, and Brain Extracellular Fluid in South African Children with Tuberculous Meningitis. Antimicrob Agents Chemother. 2023 Mar 16 [cited 2023 Apr 3];67(3):e01474-22.

923. Pan W, Banks WA, Kastin AJ. Permeability of the blood–brain and blood–spinal cord barriers to interferons. J Neuroimmunol. 1997 Jun 1;76(1–2):105–11.

924. Schliep G, Felgenhauer K. Serum-CSF protein gradients, the blood-CSF barrier and the local immune response. J Neurol 1978 2182. 1978 May [cited 2022 Nov 2];218(2):77–96.

925. Cutler RWP, Deuel RK, Barlow CF, Cutler RWP. Albumin exchange between plasma and cerebrospinal fluid. Arch Neurol. 1967 [cited 2022 Nov 2];17(3):261–70.

926. Thompson EJ. Immunochemistry of CSF proteins. In Immunichemistry in Clinical Laboratory Medicine. Proceedings of a symposium held at the University of Lancaster, March, 1979 Feb 28[cited 2021 Jul 17] : 229-236. Dordrecht: Springer Netherlands.

927. Reiber H. Non-linear ventriculo – Lumbar protein gradients validate the diffusion-flow model for the blood-CSF barrier. Clin Chim Acta. 2021 Feb 1;513:64–7.

928. Galan A, Seisdedos-Benzal A, Carletti BE, Quiros S, Martin EM, Menor D, et al. Cisternal versus lumbar cerebrospinal fluid lactate concentration in healthy dogs. J Vet Intern Med. 2020 [cited 2023 May 25];65(7):297–300.

929. Garispe A, Naji H, Dong F, Arabian S, Neeki M. Froin's Syndrome Secondary to Traumatic and Infectious Etiology. Cureus. 2019 Dec;11(12).

930. Prockop LD, Naidu KA, Binard JE, Ransohoff J. Selective Permeability of [3H]-D-Mannitol and [l4C]-Carboxyl-lnulin Across the Blood-Brain Barrier and Blood-Spinal Cord Barrier in the Rabbit. The journal of spinal cord medicine.1995 Jan 1;18(4):221-6.

931. Tigchelaar C, Muller WD, Atmosoerodjo SD, Wardenaar KJ, Kema IP, Absalom AR, et al. Concentration gradients of monoamines, their precursors and metabolites in serial lumbar cerebrospinal fluid of neurologically healthy patients determined with a novel LC–MS/MS technique. Fluids Barriers CNS. 2023 Dec 1 [cited 2023 May 30];20(1):1–12.

932. Mollenhauer B, Trautmann E, Otte B, Ng J, Spreer A, Lange P, et al. α-Synuclein in human cerebrospinal fluid is principally derived from neurons of the central nervous system. J Neural Transm. 2012 Jul 18 [cited 2023 May 30];119(7):739–46.

933. Rostgaard N, Olsen MH, Ottenheijm M, Drici L, Simonsen AH, Plomgaard P, et al. Differential proteomic profile of lumbar and ventricular cerebrospinal fluid. Fluids Barriers CNS. 2023 Dec 1 [cited 2023 May 30];20(1):1–13.

934. Fishman RA, Ransohoff J, Osserman EF. Factors influencing the concentration gradient of protein in cerebrospinal fluid. The Journal of clinical investigation. 1958 Oct 1;37(10):1419-24.

935. Kaur C, Ling EA. Blood Brain Barrier in Hypoxic-Ischemic Conditions. Curr Neurovasc Res. 2008 Feb 12;5(1):71–81.

936. Jacobs TP, Kempski O, McKinley D, Dutka AJ, Hallenbeck JM, Feuerstein G. Blood flow and vascular permeability during motor dysfunction in a rabbit model of spinal cord ischemia. Stroke. 1992 [cited 2022 Dec 2];23(3):367–73.

937. Di Paolo A, Gori G, Tascini C, Danesi R, Del Tacca M. Clinical pharmacokinetics of antibacterials in cerebrospinal fluid. Clinical Pharmacokinetics. 2013 Jul;52:511-42.

Appendix 1: Human Research Ethics Approval

UNIVERSITY OF CAPE TOWN
Faculty of Health Sciences
Human Research Ethics Committee

Room E52-24 Old Main Building
Groote Schuur Hospital
Observatory 7925
Telephone [021] 404 7682
Email: nosi.tsama@uct.ac.za
Website: www.health.uct.ac.za/fhs/research/humanethics/forms

12 February 2018

HREC REF: 070/2018

Prof A Figaji
Neurosurgery
Room 617, ICH
Red Cross Children's Hospital

Dear Prof Figaji

PROJECT TITLE: DRUG RECOVERY AND BIOMARKERS IN TUBERCULOUS MENINGITIS (PHD CANDIDATE - MS M TSHAVHUNGWE) SUB-STUDY LINKED TO 564/2012

Thank you for submitting your study to the Faculty of Health Sciences Human Research Ethics Committee for review.

It is a pleasure to inform you that the HREC has **formally approved** the above-mentioned study. This is subject to the following:

1. Please expand on the role of the HREC, and please remove board and call it Human Research Ethics Committee.
2. Please add that all future research on the stored samples will be approved by the HREC.
3. Please supply the MTA for transferred samples.

Approval is granted for one year until the 28th February 2019.

Please submit a progress form, using the standardised Annual Report Form if the study continues beyond the approval period. Please submit a Standard Closure form if the study is completed within the approval period.
(Forms can be found on our website: www.health.uct.ac.za/fhs/research/humanethics/forms)

We acknowledge that the student Ms M Tshavhungwe will be involved in this study.

Please note that for all studies approved by the HREC, the principal investigator **must** obtain appropriate institutional approval before the research may occur.

Please quote the HREC REF in all your correspondence.

Please note that the ongoing ethical conduct of the study remains the responsibility of the principal investigator.

Yours sincerely

PROFESSOR M BLOCKMAN
CHAIRPERSON, FHS HUMAN RESEARCH ETHICS COMMITTEE

Appendix 2: Human Research Ethics Approval

UNIVERSITY OF CAPE TOWN

FACULTY OF HEALTH SCIENCES
Human Research Ethics Committee

FHS016: Annual Progress Report / Renewal

HREC office use only (FWA00001637; IRB00001938) This serves as notification of annual approval, including any documentation described below.			
☑ Approved	Annual progress report	Approved until/next renewal date	30/04/24
☐ Not approved	See attached comments		
Signature Chairperson of the HREC/ Designee		Date Signed	13/3/2023

Note: Please note that incomplete submissions will not be reviewed.
Please email this form and supporting documents (if applicable) in a combined pdf-file to hrec-enquiries@uct.ac.za.
Please clarify your plan for research-related activities during COVID-19 lockdown

Comments to PI from the HREC

Principal Investigator to complete the following:

1. Protocol information

Date (when submitting this form)	10/03/2023		
HREC REF Number	564/2012	Current Ethics Approval was granted until	30/03/2023
Protocol title	Microdialysis in Meningitis		
Protocol number (if applicable)			
Are there any sub-studies linked to this study?	☐ Yes ✓ No		
If yes, could you please provide the HREC Ref's for all sub-studies? **Note:** A separate FHS016 must be submitted for each sub-study.			
Principal Investigator	Prof. Anthony Figaji		

HUMAN RESEARCH ETHICS COMMITTEE
13 MAR 2023
FHS016
HEALTH SCIENCES FACULTY
UNIVERSITY OF CAPE TOWN

(Note: Please complete the Closure form (FHS010) if the study is completed within the approval period)

Appendix 3: TBM case definition criteria (adapted from Marais *et al.* 2010 [111]**)**

TBM diagnostic criteria

Clinical criteria

Symptoms and signs of meningitis including one if the following: headache, irritability, vomiting, fever, neck stiffness, convulsions, focal neurological deficits, altered consciousness, or lethargy.

Definite TBM

Clinical criteria plus acid-fast bacilli seen in CSF and Mycobacterium tuberculosis culture-positive in CSF or CSF positive in molecular based test.

Probable TBM

Clinical criteria plus a total diagnostic score of 10 or more points (when cerebral imaging is not available) or 12 or more points (when cerebral imaging is available) plus exclusion of alternative diagnoses.

Possible TBM

Clinical criteria plus a total diagnostic score of 6-9 points (when cerebral imaging is not available or 6-11 points (when cerebral imaging is available) plus exclusion of alternative diagnoses.

Not TBM

Alternative diagnosis established, without a definitive diagnosis of TBM or other convincing signs of dual disease.

Clinical Criteria	**Maximum category score=6**
Symptom duration of more than 5 days	4
Systemic symptoms suggestive of tuberculosis (one or more of the following): weight loss (or poor weight gain in children), night sweats, or persistent cough for more than 2 weeks	2
History of recent (within past year) close contact with an individual with pulmonary tuberculosis or a positive TST or interferon gamma release assay (only in children <10	2

years of age)	
Focal neurological deficit (excluding cranial nerve palsies)	1
Cranial nerve palsy	1
Altered consciousness	1
CSF criteria	**Maximum category score =4**
Clear appearance	1
Cells 10-500/μL	1
Lymphocyte predominance (>50%)	1
Protein concentration > 1g/L	1
CSF to plasma glucose ratio of <50% or an absolute CSF glucose concentration <2.2 mmol/L	1
Cerebral imaging criteria	**Maximum category score=6**
Hydrocephalus	1
Basal meningeal enhancement	2
Tuberculoma	2
infarct	1
Pre-contrast basal hyperdensity	2
Evidence of tuberculosis elsewhere	**Maximum category score=4**
Chest radiography suggestive of active tuberculosis: signs of tuberculosis=2; miliary tuberculosis=4	2/4
CT/MRI/ultrasound evidence for tuberculosis outside the CNS	2
AFB identified or Mycobacterium tuberculosis cultured from another source- ie, sputum, lymph node, gastric washing, urine, blood culture	4
Positive commercial M tuberculosis NAAT from extra-neural specimen	4

Exclusion of alternative diagnoses An alternative diagnosis must be confirmed microbiologically (by stain, culture, or NAAT when appropriate), serologically (e.g., syphilis), or histopathologically (eg,lymphoma). The list of alternative diagnosis that should be considered, dependent upon age, immune status, and geographical region, include: • Pyogenic bacterial meningitis • Cryptococcal meningitis • Syphilitic meningitis • Viral meningo-encephalitis • Cerebral malaria Parasitic or eosinophilic meningitis (Angiostrongylus cantonesis, Gnathostoma spinigerum, toxocariasis, cysticercosis) • Cerebral toxoplasmosis • Bacterial brain abscess (space-occupying lesion on cerebral imaging) and malignancy (eg, lymphoma)	

Appendix 4: TBM patient management institutional Protocol

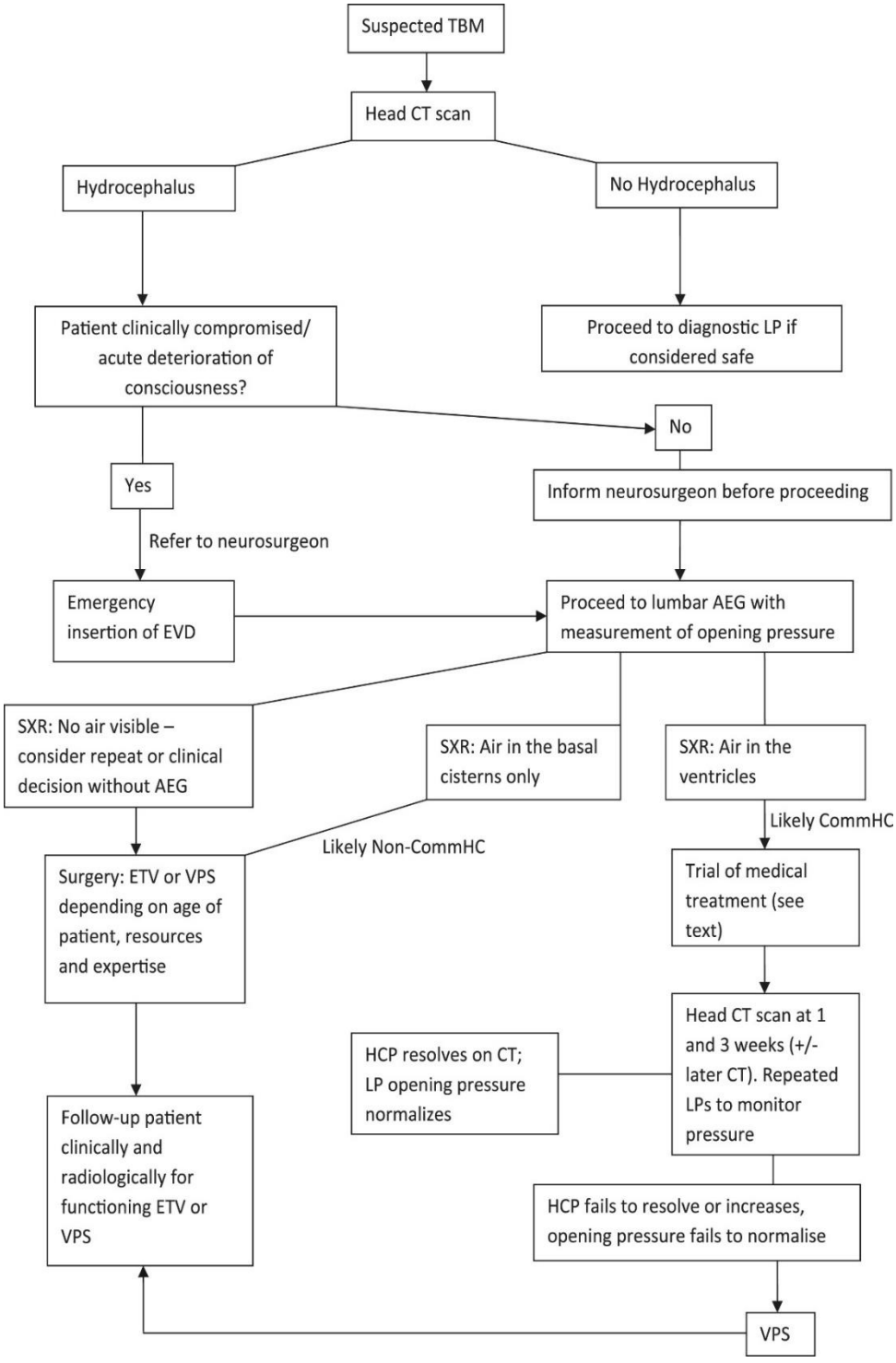

TBM patient management institutional protocol. [245]. Abbreviations: lumbar (L), Ventricular (V), Computed tomography (CT), external ventricular drain (EVD), endoscopic third ventriculostomy (EVD), ventriculoperitoneal shunt (VPS), Skull X-ray (SXR), Non-commHC, non-communicating hydrocephalus; CommHC, communicating hydrocephalus.